PROCEEDINGS OF

THE NATIONAL CONFERENCE ON

EARTHQUAKE AND ENVIRONMENTAL DISASTER

December 17, 2015

Chittagong University of Engineering and Technology (CUET), Chittagong

EDITED BY

Md. Abdur Rahman Bhuiyan

Sudip Kumar Pal

Maruful Hasan Mazumder

Ram Krishna Mazumder

Farah Rahman Omi

Published by

Department of Disaster and Environmental Engineering (CUET)

Institute of Earthquake Engineering Research (CUET)

PREFACE

Bangladesh is highly vulnerable to earthquake and other natural disasters because of her proximity to one of the tectonic plates, high population density, illiteracy, lack of resources etc. The country has also started to suffer as one of the worst victims of the growing impacts of the global climate change. Natural disasters like earthquake, cyclone, storm surge, floods etc. frequently occur in this region and the country will be highly vulnerable to increased risks and hazards of these disasters due to the growing impacts of global climate change.

It is unfortunate that our nation will be one of the worst sufferers of the associated disastrous phenomena due to the global climate change. The effects of global climate change have complex and interrelated phenomena that need to be addressed in an integrated manner. The effects of global rise of temperature is not only linked to greenhouse gas emissions, but also is affecting the biological cycle causing depletion of natural oxygen level that is crucial for our existence on earth. Hence, the appropriate measure to mitigate the hazards of any natural disaster is indeed very challenging and needs addressing several other interrelated issues addressing properly the causes and effects of the disaster. The scientists, engineers, managers and other professionals working in relevant areas need to act in an integrated manner to help mitigate the risks and hazards of natural disasters in Bangladesh. A good interaction and cooperation among the professionals of different disciplines is a key to address these issues in a comprehensive way.

Against these backdrops, it is important to aggregate and foster the research activities on natural disasters in Bangladesh through a national conference. The Department of Disaster and Environmental Engineering (DEE) and the Institute of Earthquake Engineering Research (IEER) of CUET, therefore, initiated for the first time to arrange a day-long conference named as NCEED 2015. The keynote speeches and technical discussions of the conference were chosen to cover a wide range of issues of earthquake engineering, disaster risk management, waste management, structural and environmental engineering and other relevant disciplines of science and engineering. Professionals of different relevant fields of researches were engaged in vigorous discussions regarding major concerns of natural and human-induced disasters in Bangladesh. I believe that the NCEED 2015 conference marks a milestone to identify effective ways and means to limit the risk or vulnerability of civil infrastructures and the environment to socio-economically acceptable levels in Bangladesh.

Prof. Dr. Md. A. R. Bhuiyan
Conference Chair
(& Director of IEER, CUET)

CONTENTS

NCEED 2015 -National Conference on Earthquake and Environmental Disaster; December 17, 2015; CUET, Chittagong, Bangladesh
Bhuiyan M. A. R., Pal S. K., Mazumder M. H., Mazumder R. K., Omi F. R. (eds.)

Use of NiTi Shape Memory Alloy Bars in Seismic Retrofit of Multi-span Elevated Highway

A.K.M. Thohidul Alam Khan
Institute of Earthquake Engineering Research, Chittagong University of Engineering & Technology, Chittagong, Bangladesh

M. A. Rahman Bhuiyan
Department of Civil Engineering, Chittagong University of Engineering & Technology, Chittagong, Bangladesh

M. Shahria Alam
School of Engineering, University of British Columbia, Okanagan Campus, Kelowna, BC Canada

ABSTRACT: Shape memory alloy (SMA) bars are known for their super-elastic properties, which have been utilized in various applications in the fields of engineering and science. More recently, these materials have been evaluated for applications in the area of earthquake engineering. This study investigates the effectiveness of shape memory alloy based rubber bearing system to reduce the seismic vulnerability of an elevated highway against near-field earthquakes by performing a nonlinear dynamic analysis. The isolation system considered in this study consists of a laminated rubber bearing providing lateral flexibility and an auxiliary device made of SMA bars. The dynamic analysis of the elevated highway is conducted for various near-field ground motions that are spectrally matched to a target design spectrum. The seismic response quantities of the elevated highway as evaluated in the analysis include the absolute maximum values of deck drift, deck acceleration, pier displacement and normalized base shear. The numerical results show that the SMA bars are effective in limiting the pier displacement and pounding effect of the girders.

1 INTRODUCTION

Seismic isolation has been considered to be an efficient technology to provide mitigation of seismic damages to highway bridges, and has proven to be reliable and cost effective. In order to improve the seismic performance both for new and retrofitting applications, different forms of seismic isolation devices have been widely employed for the last few decades (Naeim and Kelly, 1996; Skinner et al., 1993). Field evidence on the seismic response of isolated bridges during recent earthquakes (Chaudhary et al., 2000, 2001), experimental research (Hwang et al., 2002; Kelly et al., 1985; Kikuchi and Aiken, 1997) as well as analytical studies (Dicleli and Buddaram, 2006; Ghobarah and Ali, 1988; Karim and Yamazaki, 2007; Ozbulut and Hurlebaus, 2010, 2011; Wilde et al., 2000; Zhang and Huo, 2009; Zhang et al., 2009) have shown applicability of isolation devices in order to improve the seismic resistance and consequently reduce the cost for repair and rehabilitation after earthquakes.

Laminated rubber bearings are one of widely used devices in seismic isolation of bridges and buildings. They have revealed the ability to carry vertical loads in compression and to accommodate shear deformations. The rubber layers, reinforced with steel shims, reduce the freedom to bulge by increasing the vertical stiffness of the bearing. Three types of laminated rubber bearings are widely used as seismic isolation devices: natural rubber bearing (NRB), lead rubber bearing (LRB), and high damping rubber bearing (HDRB). Natural rubber bearing occupies flexibility property and small damping and hence it has been used to accommodate the thermal movement, the effects of pre-stressing, creep, and shrinkage of superstructure of highway bridges or it has been used in seismic isolation by combining with other energy dissipation devices, such as lead, steel and viscous damper, etc. (Skinner et al., 1993 and Kelly, 1997). Other two types of bearings possess high damping which are developed and widely used in various civil structures including bridges in many countries, especial-

ly in Japan and USA (Naeim and Kelly, 1996; Skinner et al., 1993). High damping rubber bearing possess a variety of mechanical properties, which are influenced by their compounding effect (Hwang et al., 2002), non-linear elasto-plastic behavior (Abe et al., 2004; Bhuiyan, 2009) and temperature and strain-rate dependent viscosity property (Bhuiyan, 2009; Bhuiyan et al., 2009; Dall'Asta and Ragni, 2006). Lead rubber bearings also acquire all the mechanical properties of HDRB with reduced extent (Bhuiyan, 2009; Robinson, 1982). LRB experiences some consequence-problems when subjected to strong earthquake excitations, especially the near field earthquake ground motions (Ozubulut and Hurlebaus, 2011). The unfortunate coincidence of the natural period of the seismically isolated bridge with that of the near field earthquakes amplifies the seismic responses of isolation system. In particular, LRB experiences large horizontal deformation under near field earthquakes which cause detrimental problems, such as instability of the bearings, pounding and unseating problems of the bridge deck (Choi, 2005; Dev, 2004). In recent years, a number of attempts are reported, by combining LBBs and shape memory alloy (SMA) in seismic isolation of highway bridges, to partially solve the above mentioned limitations (Choi, 2005, 2006; DesRoches and Delemont, 2002; Ozbulut and Hurlebaus, 2010, 2011; Wilde et al., 2000). The super-elasticity accompanied by hysteresis property of the SMA allows it to fabricate with LRBs to reduce the residual deformation of the bridge system. Considering the restoration and energy dissipation capacity of SMAs, its use is gaining acceptance widely in seismic protection of highway bridges.

The objective of this work is to carry out seismic performance analysis of a bridge acted upon by far field earthquake ground accelerations in longitudinal direction. In this regard, nonlinear dynamic analysis of a bridge pier using a direct time integration approach is carried out. Two types of isolation bearings are employed in the analysis: laminated rubber bearing (LRB) and smart material based laminated rubber bearing (SRB). The LRB (Fig. 1a) is manufactured by alternating rubber layers with steel shims along with lead plugs to be inserted through bearing while the SRB (Fig. 1b) comprises Ni-Ti based shape memory alloy wire plus natural rubber bearing. In nonlinear dynamic analysis the force-displacement behaviors of LRB and SRB are evaluated using visco-elasto-plastic models. In addition, bilinear and linear elastic models are used for the bridge pier and deck, respectively. The variation of seismic responses of the bridge due to the use of LRB and SRBs is explored in the study. The bridge responses considered in the exploration include the peak values of deck displacement, pier top displacement, deck acceleration and bearing's displacement. The comparison shows that the seismic responses of the bridge are affected by the use of two types of isolation bearings; more specifically, the residual displacements of the bridge pier are distinctly reduced in the case of SRB if compared to LRB for all earthquakes considered in the analysis.

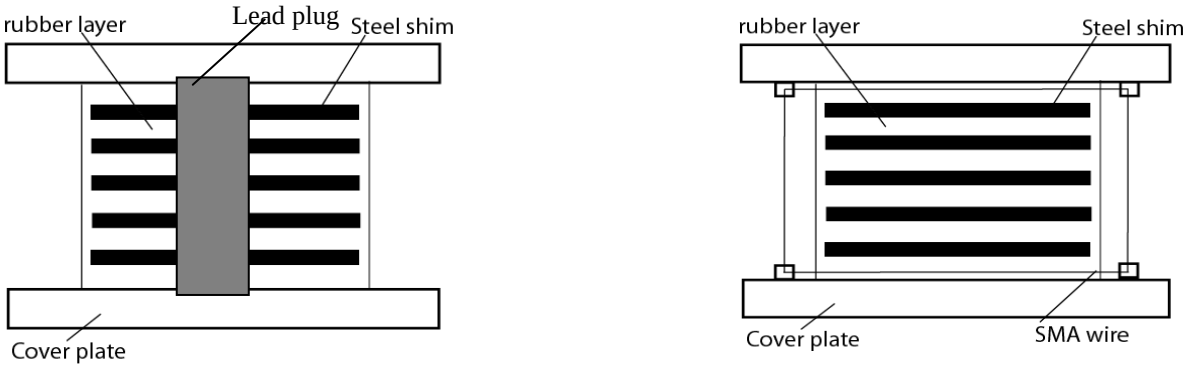

(a) (b)

Figure 1. Description of the isolation bearing (a) LRB; the rubber layers with high damping properties are vulcanized by steel shims, (b) SRB in un-deformed condition; the rubber layers with low damping properties are vulcanized by steel shim and (c) SRB in deformed condition; the rubber layers with low damping properties are vulcanized by steel shims.

2 ANALYSIS MODELS

2.1 *Physical Model*

A typical three-span continuous highway bridge, isolated by LRBs and SRBs, is used in the current study. The bridge consists of continuous reinforced concrete (RC) deck-steel girder isolated by LRBs and SRBs installed below the steel girder supported on RC piers. The superstructure consists of 260 mm RC slab covered by 80 mm of asphalt layer. The height of the continuous steel girder is 1800 mm. The mass of a single span bridge deck is 600×10^3 kg and that of a pier is 240×10^3 kg. The substructure consists of RC piers and footings supported on shallow foundation. The dimensions and material properties of the bridge deck, piers with footings are given in Table 1.

2.2 *Modeling of the Bridge System*

2.2.1 *Modeling of the Bridge*

The bridge model is simplified into a two-degree of freedom (2-DOF) system: one at the bridge deck level and the other at the bridge pier top level. This simplification holds true only when the bridge superstructure is assumed to be rigid in its own plane which shows no significant structural effects on the seismic performance of the bridge system when subjected to earthquake ground acceleration in longitudinal direction. The mass proportional damping of the bridge pier is considered in the analysis. Equations that govern the dynamic responses of the 2-DOF system can be derived by considering the equilibrium of all forces acting on it using the d'Alermbert's principle. In this case, the internal forces are the inertia forces and the restoring forces, while the external forces are the earthquake induced forces. Equations of motion are given as:

$$m_p\ddot{u}_p(t)+F_p(u_p,t)-F_{is}(t)=-m_p\ddot{u}_g(t), \quad (1a)$$

$$m_d\ddot{u}_d(t)+F_{is}(t)=-m_d\ddot{u}_g(t), \quad (1b)$$

where m_p, m_d, u_p and u_d are the masses and displacements of pier and deck, respectively. $\ddot{u}_p$ and $\ddot{u}_d$ are the accelerations of pier and deck, respectively. $\ddot{u}_g$ is the ground acceleration. F_p is the internal restoring force of the pier. F_{is} is the restoring force of the isolation bearings (LRB and SRB). The unconditionally stable Runge Kutta 4th order method is used in the direct time integration of the equations of motion (Eqs. (1)).

Table 1. Geometries and material properties of the bridge.

Properties	Specifications
Cross-section area of the pier cap (mm^2)	2000x12000
Cross-section area of the pier body (mm^2)	2000x9000
Height of the pier (mm)	15000
Young's modulus of elasticity of concrete (N/mm^2)	25000
Young's modulus of elasticity of steel (N/mm^2)	200000

2.2.2 *Modeling of the bridge pier*

The bridge pier is restricted to participate in energy absorption in the bridge system in addition to the isolation bearing. The secondary plastic behavior was expected to be lumped at bottom of the pier where plastic hinge is occurred. The plastic hinge of the pier is modeled by nonlinear spring element. Four hysteresis models for the nonlinear spring are usually used in the nonlinear dynamic analysis of a bridge structure: elasto-plastic model, bilinear model, Clough degradation model, and tri-linear Takeda model. In the current study, the nonlinear spring element is modeled using the bilinear model. The ratio of the post yield stiffness to the elastic stiffness is considered to be 0.1.

2.2.3 *Modeling of LRB and SRB*

The experimental investigations of laminated rubber bearings have revealed the four different basic properties, which together characterize the typical overall response: (i) a dominating elastic ground stress response, which is characterized by large elastic strains (ii) a finite elasto-plastic response associated with relaxed equilibrium states (iii) a finite strain-rate dependent viscosity induced overstress, which is portrayed by relaxation tests, and finally (iv) a damage response within the first cycles, which induces considerable stress softening in the subsequent cycles. Considering the first three properties, a strain-rate dependent constitutive model for the LRB is developed by Bhuiyan (2009) which is verified for sinusoidal excitations and subsequently implemented in seismic analysis of highway bridges carried out using professional software (Resp-T, 2006).

The shape memory based natural rubber bearing (SRB) comprise natural rubber bearing and NiTi SMA bar. The constitutive model of SMA is very complicated in a sense that it depends upon many factors, such as strain rates, strain magnitude and strain history. Three categories of constitutive models are used for characterizing the superelasticity and damping properties of NiTi SMA, such as parametric, nonparametric and differential equation-based models. However, the differential equation-based constitutive model is widely used for SMAs since it is capable of using in continuum mechanics based FE algorithms considering small and finite deformations and subsequently in finite element based professional software packages, such as ANSYS, 2010) and SeismoStruct (2011), etc. In realization, the complexity of replicating the mechanical behavior of SMAs by the use of phenomenological models, three versions of the models are used in seismic applications. The models include a simplified model, which is constructed based on experimentally obtained data; a thermo-

mechanical model, which considers the stress-strain-temperature relationship in SMAs; and a thermo-mechanical model, which also takes into account the cyclic loading effects in SMAs. In recognizing the intricacy of the phenomenological models considering the thermo-mechanical behavior of SMAs, a simplified model (Bhuiyan and Alam, 2013) is used in the current study to model the SRB.

3 SEISMIC GROUND ACCELERATIONS

Most of the seismic design guidelines are developed based on the characteristics of far-field ground motions. One of the characteristic features is the epicentral distance from building site to the rupturing fault to separate the near field from the far field ground accelerations. According to Caltrans (2004), if the structure under consideration is within 10 miles (approx. 15 km) of a fault can be classified as near-fault. Ground motions outside this range are classified as far-field motions. The current study considers a suite of five far-field earthquake ground motion records, of medium to strong earthquakes with PGA values ranging from 0.24g to 0.73g. The characteristics of the earthquake ground motion records are presented in Figs. 2(a) and (b). Fig. 2(a) shows ground motion histories and Fig.2 (b) presents the acceleration response spectra with 5% damping ratio of the ground motions. From Fig.2 (b), it is seen that the dominant periods of the seismic ground motion records from 0.2 sec to less than 1.0 sec which cover the wide range of natural periods of simple bridge structures.

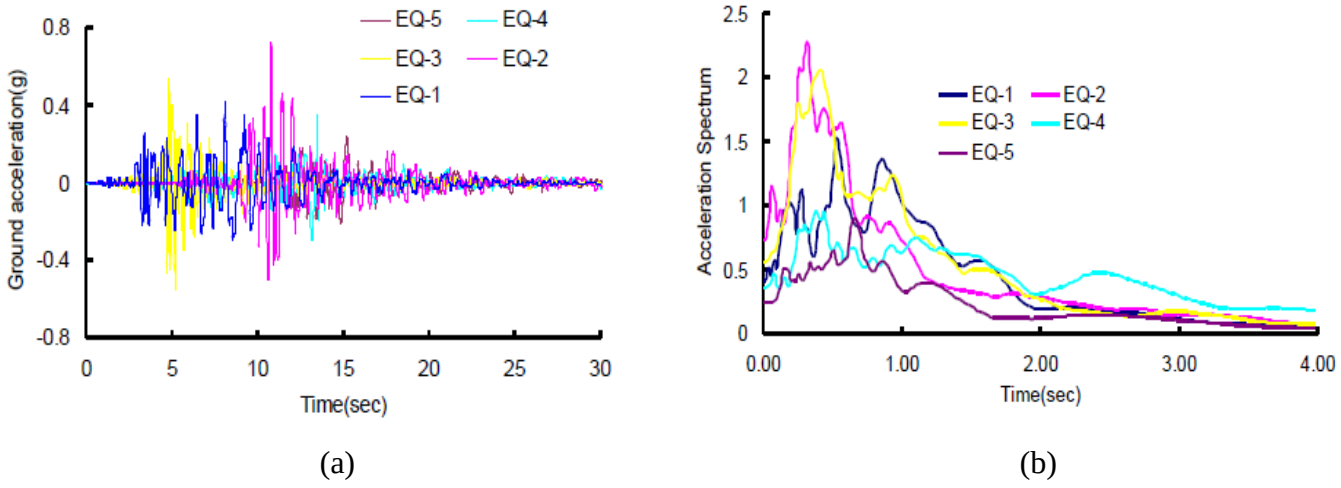

Figure 2. (a) acceleration-time histories and (b) acceleration response spectra of earthquake ground motions.

4 NUMERICAL RESULTS AND DISCUSSION

Seismic performance of the bridge system modeled by a 2-DOF system is evaluated for five far field earthquake ground acceleration records. For simplicity, a typical interior bridge pier is considered in the seismic analysis of the bridge. Seismic responses of the system are evaluated by conducting nonlinear dynamic analysis based on the direct time integration approach using the 4th order Runge-Kutta method. An eigen-value analysis has been carried out to grasp the fundamental dynamic properties of the system. The natural periods of the system isolated by LRB and SRB are found to be, respectively, 2.05 and 1.6 sec. From the acceleration response spectra (Fig.2b) it is found that the spectrum values corresponding to both the natural periods of the system are very close to each other indicating that the bridge responses, while subjected to the seismic ground accelerations considered in the study, should not be very far from each other.

In comparative assessment of seismic responses of the system, a few standard response parameters obtained for each earthquake ground motion are addressed in the subsequent subsections: pier displacement, bearing displacement, deck acceleration, deck displacement, residual displacement of the bridge deck after earthquake and bearing force. Each response parameter of the system equipped with LRB is compared with SRB. Figs. 3 and 4 present typical responses of the bridge pier for EQ-1 and EQ-4. The similar trends of the results were also obtained for the remaining earthquakes (EQ-2, EQ- 3 and EQ-5). The simulation results are summarized in Tables 2 and 3 for LRBs and SRBs, respectively.

4.1 *Pier Displacement*

The two factors affecting the pier displacement are energy dissipation by the bearings and the forces developed in the bearings. The pier displacement decreases with increase in energy dissipation but increases with

increase in the bearing forces. Therefore, the SRBs usually produce larger pier displacement than LRBs. As seen from Tables 2 and 3, the bridge with SRB has larger pier displacement for EQ-1, EQ-3 and EQ-5 than the LRBs; however, for EQ-2 and EQ-4, the bridge with SRB shows lesser pier displacement. Figs. 3(a) and 4(a) present the time histories of the pier displacement with LRB and SRB showing the similar pattern with different magnitudes. From each of the Figs. 3(a) to 4(a) it is interesting to note that the residual displacement of the pier is larger in case of LRB compared to SRB. This interesting result would be helpful at the design phase of a seismically isolated bridge system.

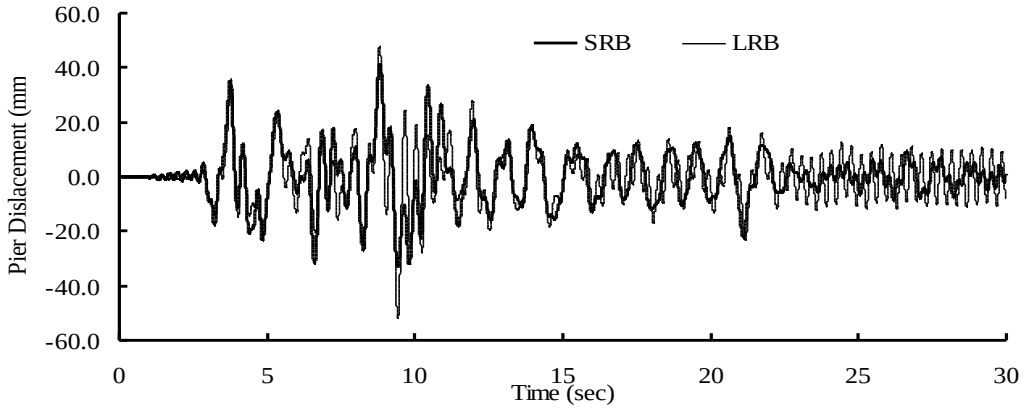

(a)

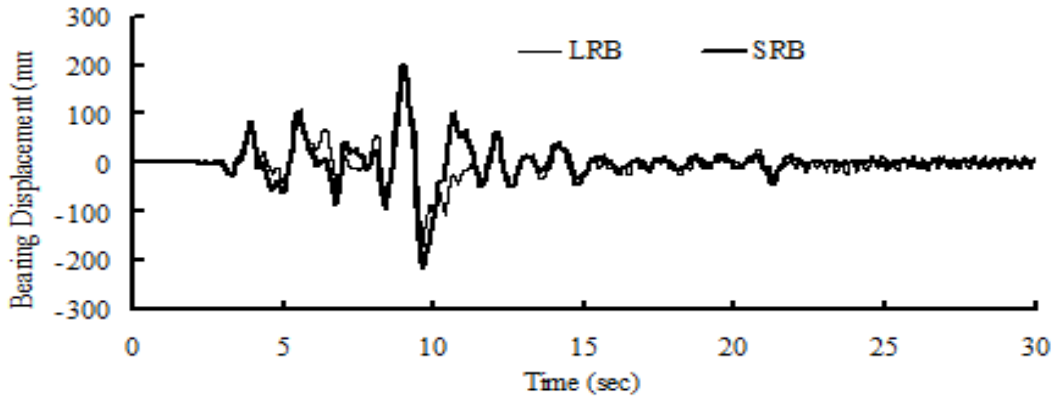

(b)

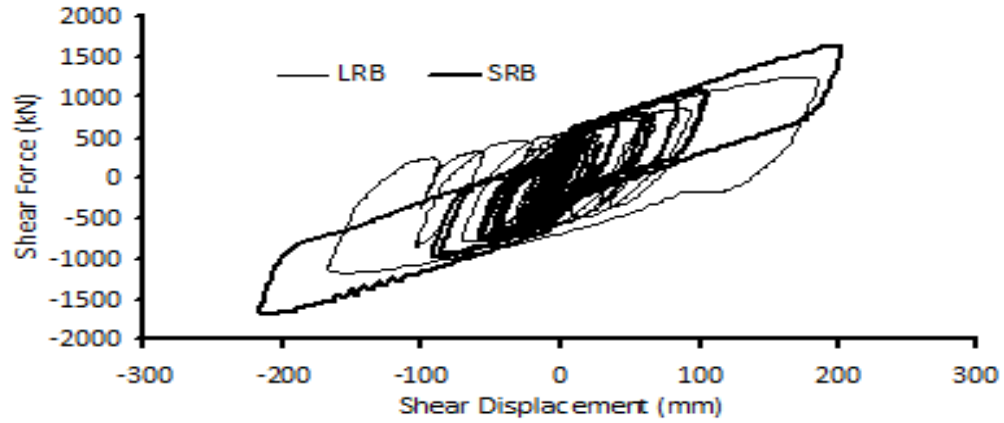

(c)

Figure 3. Seismic responses of the bridge pier due to EQ-1 ground motion (a) pier displacement (b) bearing displacement, and (c) bearing force and displacement behavior.

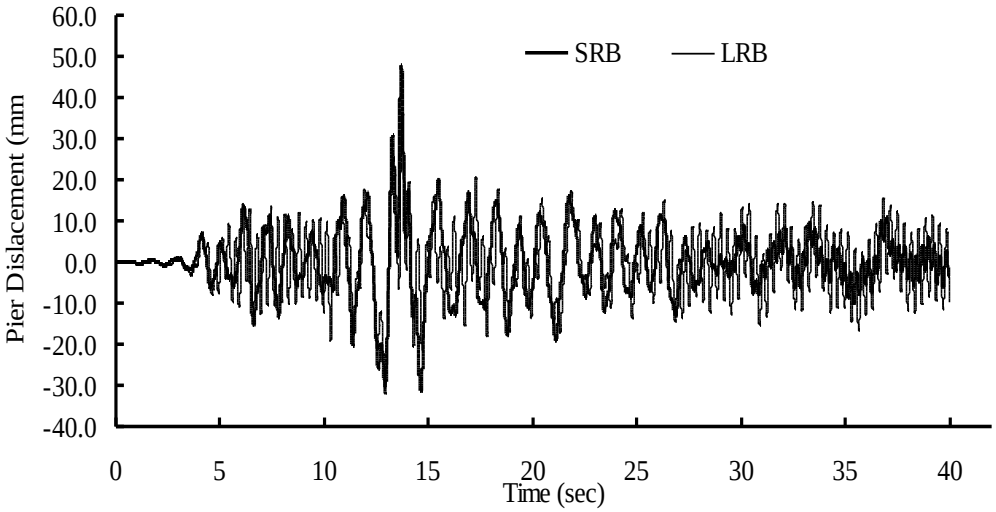

(a)

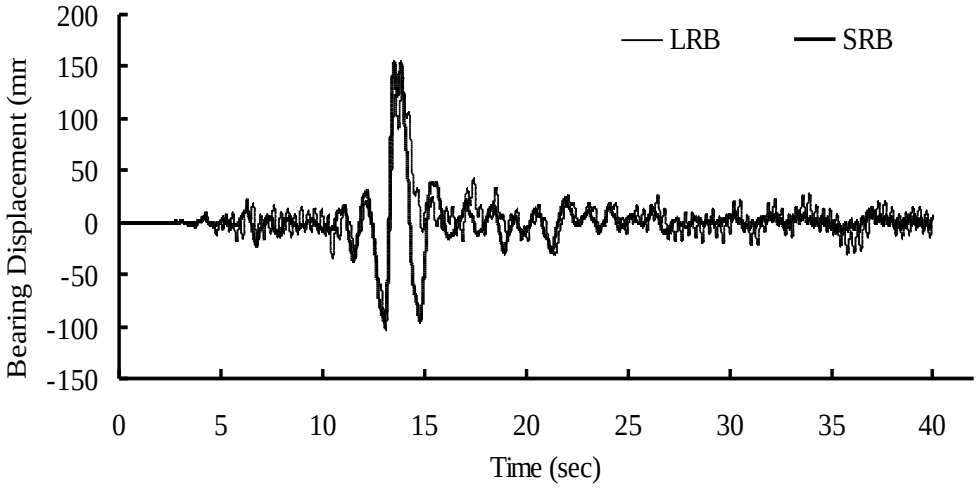

(b)

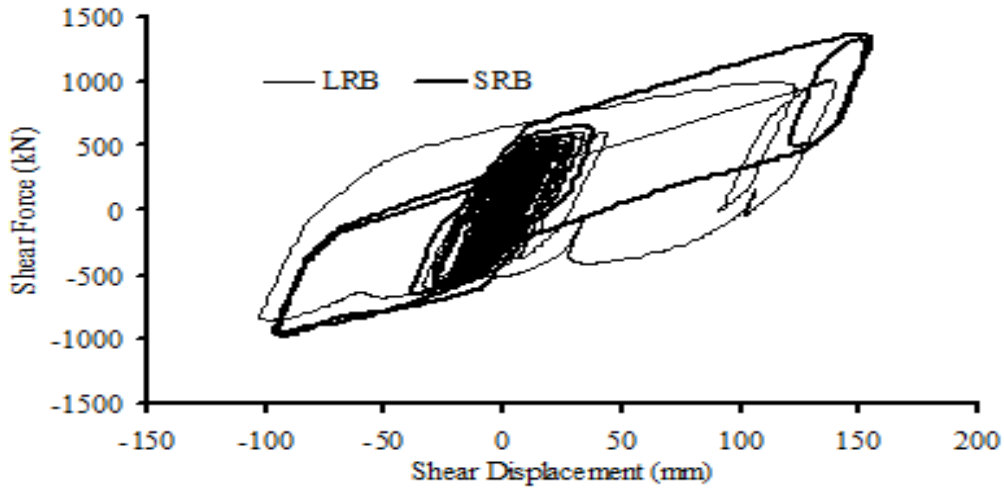

(c)

Figure 4. Seismic responses of the bridge pier due to EQ-4 ground motion (a) pier displacement (b) bearing displacement, and (c) bearing force and displacement behavior.

4.2 *Bearing Displacement*

The bearing displacements were obtained from relative displacements between deck and pier. The second columns of Tables 2 and 3 present the maximum bearing displacements for the seismic ground motion records considered in the current study. Figs. 3(b) and 4(b) present the time histories of the bearing displacements with LRBs and SRBs giving the similar pattern with different magnitudes as tabulated in Tables 2 and 3. Bearing displacements directly related to its energy dissipation capacity when subjected to seismic excitations. Bearing displacement increases with the decrease in energy dissipation of the bearings as revealed from Figs. 3(c) and 4(c). It appears from the Figs. 3(b) and 4(b) that the residual displacements of LRBs are bigger in magnitude than SRBs, which corresponds to the observations of the pier displacements (Figs. 3(a) and 4(a)). The residual displacements of the bearings play a significant rule in selecting the approaches for proper repair and maintenance works of a highway bridge after a seismic excitation.

As per the damage states of the bearings defined in Table 4, the peak displacements of the isolation bearings (LRB and SRB), shown in Tables 2 and 3, indicate that the isolation bearings generally experience some degrees of damage for most of the earthquakes except for the earthquake EQ-1; however, an extensive damage takes place in SRB due to EQ-1. As per the damage states of the bearings (Table IV) it can be entitled as DS3 indicating that degradation of the bearing without collapse will take place due to EQ-1.

For deck displacement, the bridge with SRBs has larger deck displacements for EQ-1 and EQ-4; however, for EQ-2, EQ-3 and EQ-5, the bridge with SRBs has smaller deck displacements if compared to LRBs. By comparing between the 2nd and 4th columns of Tables 2 and 3 it has been noted that almost a similar pattern of the response is obtained, which confirms the consistency with structural idealization considered in the analysis. Almost a similar trend in the deck acceleration for the two isolation bearings has also been observed, presented in Tables 2 and 3.

4.3 *Residual Displacement*

The residual displacement of the bearing is computed by taking the arithmetic average of the stable absolute values of the last 10 to 15 sec of the time history of bearing displacements as obtained from the dynamic analysis of the system for each earthquake. The residual displacements of SRBs are smaller than LRBs for all earthquakes as presented in Tables II and II. The characteristics of the earthquakes, energy dissipation and hardening feature of the bearings have the effect on the results of residual displacements.

Table 2. Absolute maximum responses of the bridge pier isolated by LRB.

Earthquake	Bearing Displace.	Deck Acc.	Pier Displace.	Deck Displace.	Residual Displace.
	Mm	m/s^2	mm	mm	mm
EQ-1	185.77	4.34	48.14	172.32	29.98
EQ-2	193.97	6.17	57.87	218.87	56.00
EQ-3	71.97	5.52	32.69	65.43	12.40
EQ-4	140.61	3.59	36.15	138.98	11.4
EQ-5	130.47	2.84	37.77	126.37	10.60

Table 3. Absolute maximum responses of the bridge pier isoalted by SRB.

Earthquake	Bearing Displace.	Deck Acc.	Pier Displace.	Deck Displace.	Residual Displace.
	Mm	m/s^2	mm	mm	mm
EQ-1	202.70	5.14	41.30	211.94	14.45
EQ-2	195.93	5.73	81.33	201.99	23.00
EQ-3	62.10	5.49	26.20	63.28	5.70
EQ-4	155.26	3.63	47.94	171.95	5.40
EQ-5	119.89	2.89	37.72	122.75	4.50

Table 4. Damage/Limit States of Bridge Components.

Physical Phenomenon	Damage State (FEMA (2003))	Displacement Ductility μ_d (Hwang et al., (2001))	Shear Strain γ (%) (Zhang and Huo, (2009))
Cracking	Slight (DS=1)	μ_d >1.0	γ >100
Moderate cracking and spalling	Moderate (DS=2)	μ_d >1.2	γ >150
Degradation without collapse	Extensive (DS=3)	μ_d >1.76	γ >200
Failure leading to collapse	Collapse (DS=4)	μ_d >4.76	γ >250

5 CONCLUDING REMARKS

This study presents the seismic performance assessment of a bridge system isolated by lead rubber bearing (LRB) and NiTi shape memory alloy based natural rubber bearing (SRB). The bridge was analyzed for a suit of far field earthquake ground motions. The nonlinearity of the bridge pier is considered by employing a bilinear force-displacement relationship. A fixed restraint condition at bottom of the pier was considered. A complicated strain-rate dependent constitutive model for the LRB was used whereas a viscoelasticity based analytical model was used for SRB.

The numerical results have revealed that the SRB satisfactorily restrains the residual displacement of the bridge deck and the displacement of the bridge pier for the suite of earthquakes considered in the study. However, for bridge deck and bearing displacements, the bridge with LRBs has usually resulted in smaller responses in compared to SRBs. Almost a similar trend of the results is also observed in the case of deck accelerations. The early activation of hardening effect of SRBs in comparison with LRBs might have significant effect on the seismic responses of the system. The LRBs designed in this study shows a larger dissipation of energy than that of SRBs. However, the capacity of dissipation energy of SRBs can be increased by increasing the size SMA wires. From the numerical analysis conducted in the current study it appears that not only the magnitude but the other characteristics of earthquake ground motions also have significant effect on the seismic responses of the bridge which should be carefully considered in the design phase of bridge system.

6 REFERENCES

Abe, M., Yoshida, J., and Fujino, Y., (2004). "Multiaxial behaviors of laminated rubber bearings and their modeling. I: Experimental study", J. Struct. Eng., 130, 1119-1132.

ANSYS Inc. (2010)"ANSYS version 12.0", ANSYS, Inc., 2010.

Bhuiyan, A. R., Okui, Y., Mitamura, H., and Imai, T., (2009). "A Rheology model of high damping rubber bearings for seismic analysis: identification of nonlinear viscosity", Intl. J. Solids Struct., 46, 1778-1792.

Bhuiyan, A. R., (2009). "Rheology modeling of laminated rubber bearings". PhD dissertation, Graduate School of Science and Engineering, Saitama University, Japan.

California Department of Transportation (2004) , "Seismic Design Criteria (CALTANS)", Sacramento, CA., 2004.

Chaudhary, M. T. A., Abe, M., and Fujino, Y., (2001). "Performance evaluation of base- isolated Yama-agé bridge with high damping rubber bearings using recorded seismic data", Engineering Structures, 23, 902-910.

Chaudhary, M.T.A., Abe, M., Fujino, Y., and Yoshida, J., (2000). "System identification of two base-isolated bridges using seismic records", J. Struct. Eng., 126, 1187-1195.

Choi, E., Nam, T., and Cho, B., (2005). "A new concept of isolation bearings for highway steel bridges using shape memory alloys", Canadian Journal of Civil Engineers 32, 957–967.

Dall'Asta, A., and Ragni, L., (2006). "Experimental tests and analytical model of high damping rubber dissipating devices", Engineering Structures, 28, 1874-1884.

DesRoches, R., and Delemont, M., (2002). "Seismic retrofit of simply supported bridges using shape memory alloys". Engineering Structures, 24, 325–332.

Dicleli, M., and Baddaram S., (2006) "Effect of isolator and ground motion characteristics on the performance of seismic-isolated bridges". Earthquake Eng Struct Dyn, 35, 233-250.

Federal Emergency Management Agency (FEMA) (2003). "HAZUS-MH software," Washington DC.

Ghobarah, A., (1988). "Seismic behavior of highway bridges with base isolation", Canadian Journal of Civil Engineering, 15, 72-78.

Ghobarah, A., and Ali, H. M., (1988). "Seismic performance of highway bridges", Engineering Structures, 10, 157-166.

Hwang, J. S., Wu, J. D., Pan, T, C., and Yang, G., (2002). "A mathematical hysteretic model for elastomeric isolation bearings", Earthq. Eng.Struct. Dyn., 31, 771-789.

Hwang, H., Liu, J. B. , and Chiu, Y. H., (2001). "Seismic fragility analysis of highway bridges" MAEC report: project MAEC RR-4. Urbana: Mid-America Earthquake Center.

Karim, R., and Yamazaki, F., (2007). "Effect of isolation on fragility curves of highway bridges based on simplified approach". Soil Dyn Earthquake Eng, 27, 414-26.

Kelly, J. M., (1997). "Earthquake resistant design with rubber", 2nd ed., Springer-Verlag Berlin Heidelberg, New York.

Kikuchi, M., and Aiken, I. D., (1997). "An analytical hysteresis model for elastomeric seismic isolation bearings", Earthquake. Eng Struct. Dyn. 26, 215-231.

Ozbulut, O. E, and Hurlebaus, S., (2010). "Evaluation of the performance of a sliding-type base isolation system with a NiTi shape memory alloy device considering temperature effects." Engineering Structures, 32, 238–249.

Ozbulut, O. E., and Hurlebaus, S., (2011a). "Optimal design of superelastic-friction base isolators for seismic protection of highway bridges against near-field earthquakes." Earthquake Eng Struct Dyn , 40, 273–291.

Ozbulut, O. E., and Hurlebaus, S., (2011b). "Seismic assessment of bridge structures isolated by a shape memory alloy/rubber-based isolation system", Smart Materials and Structures, 20.

Resp-T (2006). "User's Manual for Windows, Version 5", 2006.

Robinson, W. H., (1982). Lead rubber hysteresis bearings suitable for protecting structures during earthquakes, Earthquake Engineering and Structural Dynamics, 10, 593-604.

SeismoStruct (2011). SeismoStruct help file. Available from www.seismsoft.com, 2011.

Skinner, R. I., Robinson, W. H., and McVerry, G. H., (1993). "An introduction to seismic isolation, DSIR Physical Science", Wellington, New Zealand.

Wilde, K., Gardoni, P., and Fujino, Y., (2000). “Base isolation system with shape memory aalloy device for elevated highway bridges.” Engineering structures, 22, 222–229.
Zhang, Y., Hu, X., and Zhu, S., (2009). “Seismic performance of benchmark base-isolated bridges with superelastic Cu-Al-Be re-straining damping device.” Structural Control and Health Monitoring, 16, 668–685.
Zhang, J., and Huo, Y., (2009). “Evaluating effectiveness and optimum design of isolation devices for highway bridges using the fragility function method.” Engineering Structures, 31, 1648-1660.

NCEED 2015 -National Conference on Earthquake and Environmental Disaster; December 17, 2015; CUET, Chittagong, Bangladesh
Bhuiyan M. A. R., Pal S. K., Mazumder M. H., Mazumder R. K., Omi F. R. (eds.)

Investigation of Soil-Structure Interaction Effect on Seismic Response of a Base-Isolated Nuclear Power Plant Structure Using Wavelet Analysis

Shafayat Bin Ali
Institute of Earthquake Engineering Research, Chittagong University of Engineering & Technology, Chittagong, Bangladesh

Dookie Kim
Department of Civil and Environmental Engineering, Kunsan National University, South Korea

ABSTRACT: The inelastic behavior of soil beneath a structure during seismic loading may play a significant role in altering the seismic responses of the superstructure. The present study investigates the effect of soil-structure interaction (SSI) on the seismic response of base-isolated nuclear power plant (NPP) using a time frequency tool based on wavelet analysis. A comparison has drawn between seismic performance of the base-isolated NPP and rigidly fixed NPP to the ground with considering SSI effect. In the study, a nuclear power plant structure with total height of 65.8m is modelled as a lumped mass stick model and lead rubber bearing (LRB) base isolators are used to adopt the base isolation system. To incorporate SSI effect the infinite underlying soil medium is assumed as a homogenous half-space and modelled by the concept of visco-elastic cone model. Two different shear wave velocities of soil are considered to reflect the real rock site conditions of NPP structures. The wavelet analysis is used to deduce accumulative total energy of the non-stationary acceleration response of structure. The study shows that the wavelet analysis proves to be an efficient tool to investigate the effect of SSI on the response of the structure. Finally the results conclude that the seismic performance of the base-isolated NPP is not sensitive to SSI effect than the rigidly fixed NPP rested on rock sites.

1 INTRODUCTION

During seismic ground excitation the dynamic behaviour of inelastic structure is a complex non-stationary process. The conventional Fourier analysis has been considered as a primary tool to obtain the frequency content of the signal, which gives no information about the location of these frequencies in the time domain. To overcome this problem scientists have developed a method called wavelet analysis which can provide both time and frequency localization information simultaneously. Recently, wavelets have been implemented in geotechnical earthquake engineering to analyse the non-stationary seismic response of dynamic system (Iyama and Kuwamura, 1999, Chatterjee and Basu, 2004).

Seismic base isolation is a well-known flexible approach to reduce the potential damage caused by seismic ground motions. In recent time, seismic base isolation has become a widely used structural design technique for conventional structures, bridges, and infrastructures. Nowadays, only six nuclear reactors in two nuclear power plants have been isolated in France and South Africa (Huang et al. 2010). In addition, many studies have been conducted to investigate the seismic responses of NPP using base isolation system (Micheli et al. 2004, Zhao and Chen, 2013). Forni et al. (2012) provided the state-of-the-art of the application of seismic base isolation to NPPs. Up to date, no specific standards are available for the application of base isolation to NPPs.

The Soil-structure interaction may play a significant role to change the seismic responses of superstructure. The common practice usually neglects the SSI effects on seismic response of base isolated structure. In recent years several studies have shown the effectiveness of considering SSI effect in the design of base-isolated structure. Novak and Henderson (1989) investigated the effect of SSI on the modal properties of base-isolated structures. Tongaonkar and Jangid (2003) assessed the effect of SSI phenomena on a three-span bridge with

LRBs and concluded that SSI causes an increase in the seismic displacements. Spyrakos et al. (2009) presented the importance of SSI on the seismic response of base-isolated buildings and shown that the SSI effects are more pronounced on the modal properties of the system.

The primary objective of this study is to evaluate the effect of SSI on base-isolated NPP rested on the different rock site conditions. In that regard, a wavelet-based technique is applied to identify the time frequency characteristics of acceleration response of base-isolated NPP structure. Finally, the wavelet analysis is used to evaluate the degree of correlation between the input ground motions and the seismic responses of the structures.

2 NUCLEAR POWER PLANT (NPP) STRUCTURE

2.1 *NPP Stick Model*

In the present study, a simplified model of Advanced Power Reactor (APR1000) is used for numerical analysis. The structural model of base-isolated NPP established with a lumped mass stick model, base mat and base isolation devices. The total height of NPP stick model is 65.8m with fourteen nodes and thirteen three dimensional beam elements. The total dimensions of base mat are 100 x 80 x 4 m. Moreover, the base mat dimensions under the stick model are 20 x 16 x 12 m. Total 121 LRB isolators are used for adopting base isolation system. The BI-NPP model is constructed by OpenSees Navigator (Schellenberg et al. 2013). The structural model of BI-NPP model is shown in Figure 1.

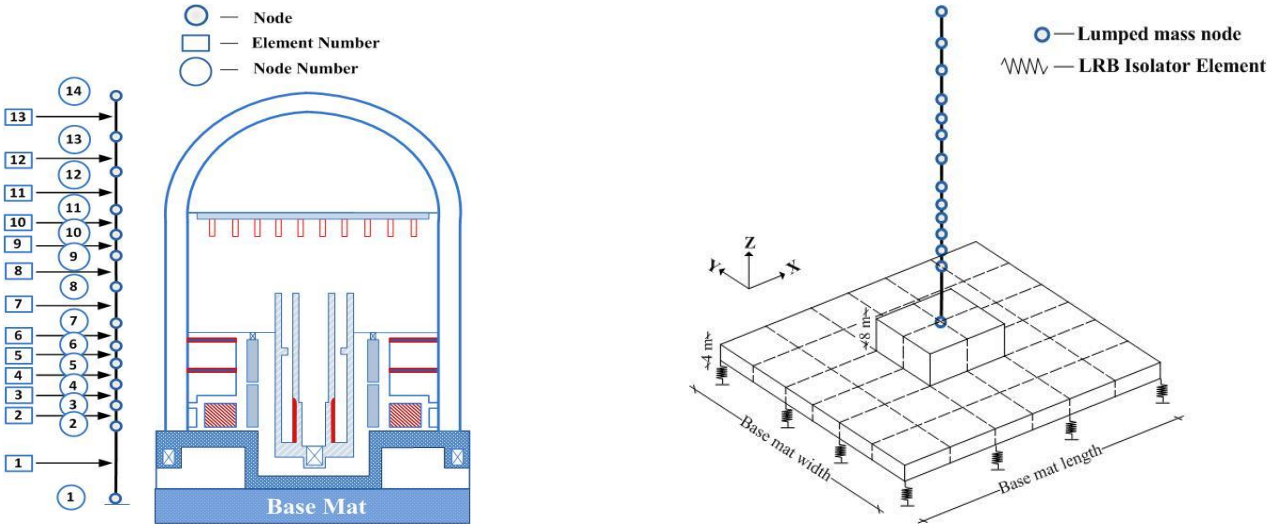

Figure 1. NPP containment building sectional elevation and stick model (left), Nuclear island base mat dimensions (right).

2.2 *Design of LRB Isolators*

In the study, Lead rubber bearing (LRB) isolator is used which consists of low damping natural rubber, steel plates and a lead plug damper. The rubber is an elastic material and the lead plug damper acts as a plastic material at low levels of stresses, therefore, as a whole, the LRB device shows nonlinear dynamic properties. In this study, the international Organization for Standardization (ISO) specification (2010) is followed to design the LRB isolator. The equivalent linear properties are also used for isolation device analysis which is shown in Figure 2. In Figure 2 K_u is the linear horizontal tangential stiffness and K_d is the post-yield horizontal stiffness. K_H represents the effective horizontal stiffness of the isolator. Q_d and F_y denote the characteristic strength and yield strength respectively. δ_{max} is the maximum horizontal displacement and δ_{min} is the minimum horizontal displacement of the isolator. Furthermore, F_{max} and F_{min} are the maximum and minimum horizontal forces corresponding to the maximum and minimum horizontal displacements of the isolator, respectively. Table 1 illustrates the dynamic properties of LRB isolator.

Table 1. Properties of LRB isolator.

Horizontal Stiffness	Post-yielding Stiffness	Yield Strength	Characteristic Strength	Yield Displacement	Hardening Ratio
K_H (KN/m)	K_d (KN/m)	F_y (KN)	Q_d (KN)	δ_y (mm)	A
8436.10	7089.55	303.73	269.31	4.85	0.113

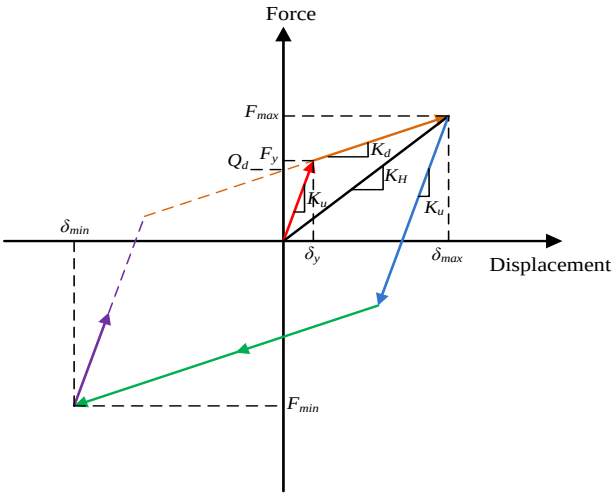

Figure 2. Linearization of the force-displacement relationship of LRB isolator (ISO, 2010).

3 WAVELET ANALYSIS

The wavelet transform are of two types; the continuous wavelet transform and the discrete wavelet transform. Iyama and Kuwamura (1999) illustrated that discrete wavelet transform is more useful because it represents a signal characteristics as well. Therefore, the discrete wavelet transform is used in this paper and simply referred as wavelet transform.

3.1 *Wavelet decomposition*

The wavelet decomposition process starts with splitting the acceleration signal into two parts, the approximation and the detail, by passing through two complementary filters. The approximations are the high scale and contain the low frequency component of the signal. However, the details are the low scale and contain the high frequency component. The decomposition process is presented by the Equation 1.

$$A_j(t) = a_{j+1}(t) + d_{j+1}(t) \tag{1}$$

where *A(t)* is the original acceleration signal, *a(t)* is the approximations component, *d(t)* is the details component, and *j* is the level number representing the particular range of frequency content of the signal.

The frequency range of each decomposition level is expressed by Equation 2.

$$\omega_j = \left[\frac{1}{2^{j+1}\Delta t}, \frac{1}{2^j \Delta t}\right] \tag{2}$$

where Δt is the time step of discretized signal. Sarica and Rahman (2003) illustrated that the original signal can be reconstructed from details without losing any information and can be written by Equation 3.

$$A_o(t) = \sum_{j=1}^{n} d_j(t) \tag{3}$$

where *n* represents the total number of decomposition levels. Using linear combination of wavelet basis function the details components of the original signal can be represented by Equation 4.

$$d_j(t) = \sum_{-\infty}^{\infty} c_{j,k}\psi_{j,k} \tag{4}$$

where *k* is an index of time scale, $\psi_{j,k}$ are the basis wavelet function and $c_{j,k}$ are corresponding wavelet coefficients. The basis wavelet function can be written by following Equation.

$$\psi_{j,k} = 2^{\frac{j}{k}}\psi(2^j t - k) \tag{5}$$

In the study, 4th-order Daubechies mother wavelet is used as a basis wavelet function.

3.2 *Energy Calculation*

Walker (1999) illustrated that the total energy of a discrete signal can be expressed by the sum of the squares of its values.

$$E = \Delta t \sum_{t=0}^{t} A_o^{\,2}(t) \tag{6}$$

Moreover, the total energy can be represented in the form of details only at each decomposition level. In this study, this concept is used to determine the cumulative energy of signals which is expressed by the Equation 7.

$$E = \sum_{j=1}^{n} \sum_{k=0}^{t} d_j^{\,2}(t) \tag{7}$$

4 SOIL-STRUCTURE SYSTEM IDEALISATION

In the study, the sub-structure methodology is used to adopt the SSI model. The infinite soil medium beneath structure is assumed as a homogeneous half-space and modelled by the concept of Voigt visco-elastic Cone Models. Five degree of freedoms are considered for sway and rocking motions about x and y axis and rotation about z axis. In addition, a set of frequency-independent springs and dashpots are used to consider the inertial interaction between structure and soil (Ghaffar-Zade and Cahpel, 1983). The soil model is represented in Figure 3.

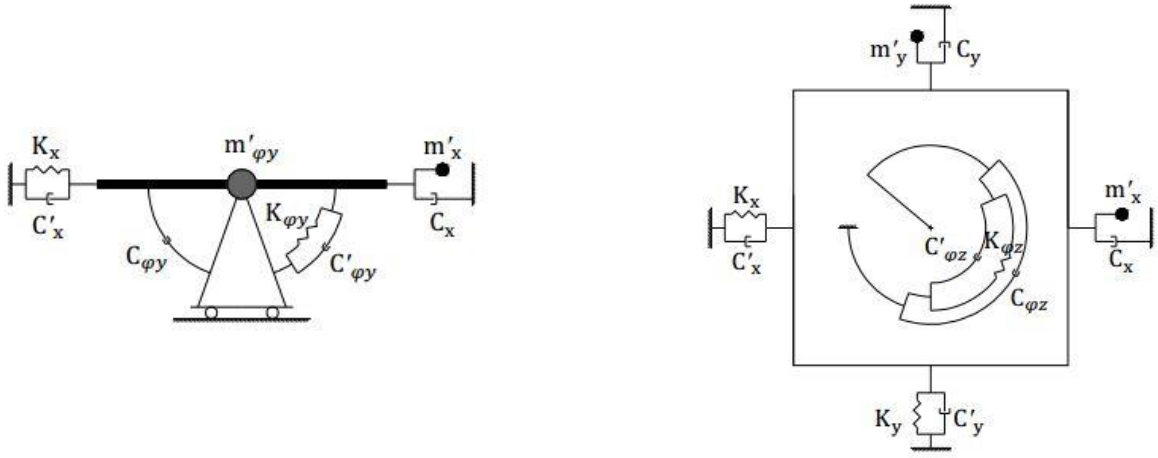

Figure 3. Soil model (Kenarangi and Rofooei, 2010).

The soil related parameters are presented by Equation 8 and 9.

$$K = \frac{\rho V^2 A}{z}, \quad C = \rho V A, \quad C' = 2\frac{\zeta}{\omega}K, \quad m' = \frac{\zeta}{\omega}C \tag{8}$$

$$K_\varphi = \frac{3\rho V^2 I}{z}, \quad C_\varphi = \rho V I, \quad C'_\varphi = 2\frac{\zeta}{\omega}K_\varphi, \quad m'_\varphi = \frac{\zeta}{\omega}C_\varphi \tag{9}$$

where V is the shear wave velocity for sway and torsional motions and the dilatational wave velocity for rocking motions, ρ is the specific mass of soil and z is the apex height of the cone model. A and I denote the area of foundation and the area moment of inertia about the axes of rotation respectively. Furthermore, ζ and ω represent the damping ratio of soil and fundamental frequency of the soil-structure system respectively.

5 RESULTS AND DISCUSSIONS

5.1 *Total Energy of acceleration response*

Figure 4 demonstrates the accumulative total energy profile of applied ground excitations and acceleration responses of the top node of NPP and BI-NPP models. Figure 4 (a) and (c) illustrate that, for NPP structure the total energy of response increased greatly then the applied El-Centro and Kobe ground motions. However,

when the SSI effect is considered the energy related to response of structure decreased dramatically. Under El-Centro excitation the amount is 92% and 83%, whereas, for Kobe earthquake it is 88% and 75% for soft and rock sites respectively. Moreover, the rate of decrement is greater, which is more than 50% for soft rock site under two ground motions. Furthermore, Figure 4 (b) and (d) show that, after implementing the base isolation device to NPP structure the increase of total energy is relatively low than the applied ground motions, whereas, the consideration of SSI effect is negligible which is less than 1% to alter the energy. It can be concluded that, SSI has great effect to decrease the accumulative total energy of response of NPP structure, whereas, the effect is negligible for BI-NPP structure. Moreover, the rate of change of the total energy is prominent for NPP rested on soft rock site.

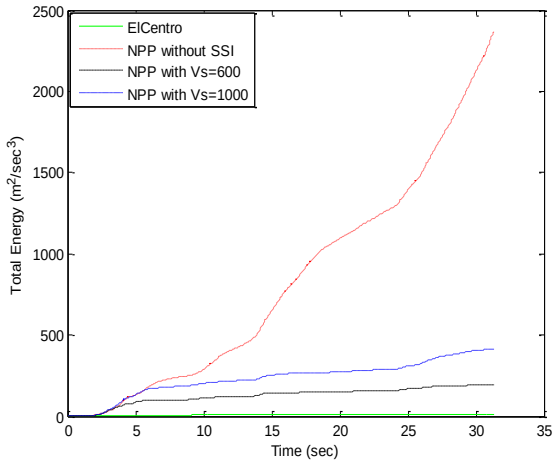

(a) NPP under El-Centro ground motion

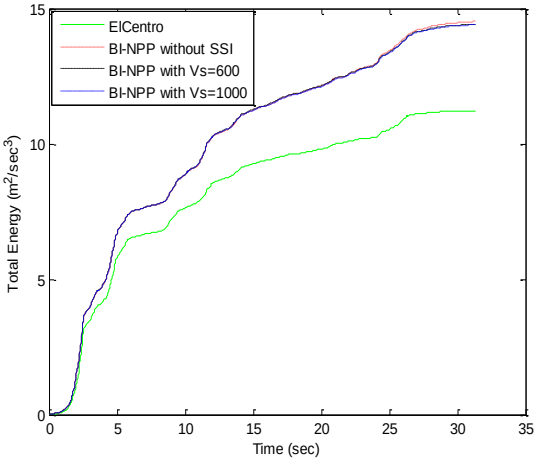

(b) BI-NPP under El-Centro ground motion

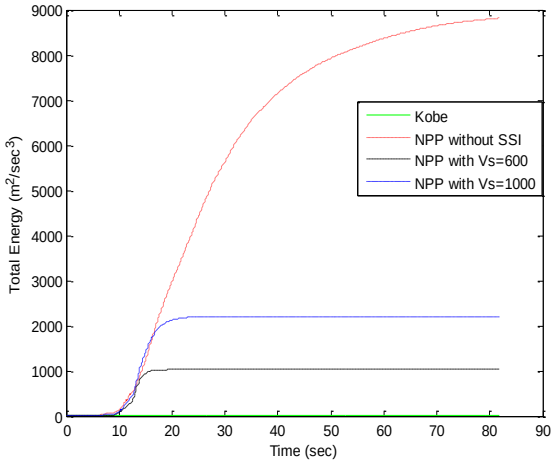

(c) NPP under Kobe ground motion

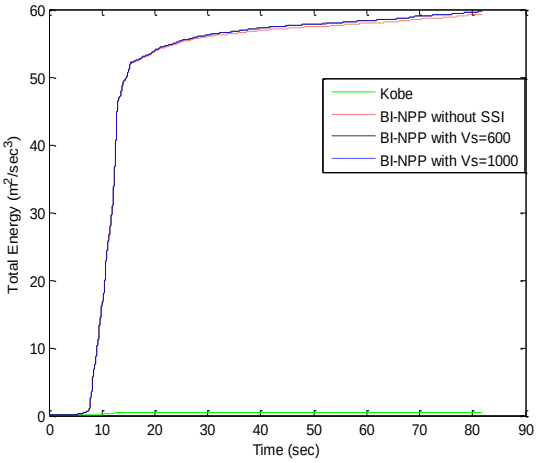

(d) BI-NPP under Kobe ground motion

Figure 4. Total energy of acceleration responses of nuclear power plant models.

5.2 *Comparison of input motion and structural response*

Wavelet analysis can be applied to identify short-term changes in the frequency content of a signal which can be used to detect the change of dynamic characteristics of structure, such as the initiation sign of stiffness degradation or the sudden occurrence of non-ductile events (Goggins et al. 2006). The change of wavelet coefficients can be identified by determining the degree of correlation between two signals, which is expressed by Equation 10,

$$\rho_{xyj} = \frac{\sum_i w_{xj} w_{yj}}{\sqrt{\sum_i w_{xj}^2} \sqrt{\sum_i w_{yj}^2}} \qquad (10)$$

where ρ_{xyj} is the correlation coefficient. w_{xj} and w_{yj} are the details of input ground motion and the acceleration response of structure at level j.

The variation of degree of correlation for input ground motions and acceleration responses of NPP and BI-NPP models in conjunction with SSI are shown in Figure 5. It is observed from Figure 5 (a) and (c) that, for

NPP structure poor correlation exists for all levels under two different ground records. For El-Centro record, level 3 contains the fundamental frequency of NPP model with highest energy portion, shows lowest correlation. Similar observation can be made at level 4 for Kobe earthquake. However, after adding SSI effect correlation coefficients increase almost all levels under two earthquakes. Relatively better correlation exists when soft rock site is considered for NPP structure. On the other hand, it can be noticed from Figure 5 (b) and (d), good agreement exist between BI-NPP responses and input ground motions. As shown in Figure 5 (b), nearly perfect relation is observed between response and El-Centro record at levels 3-5 where most of the energy of the response lies. Moreover, better relationship displays at level 6 which contains the fundamental frequency of BI-NPP structure. Figure 5 (d) shows similar scenario for Kobe excitation. Furthermore, correlation coefficients do not suffer much change when SSI effect is adopted. It can be concluded that, frequency content of NPP response is not related with input ground excitation, whereas, soft rock site relatively increases the relation. However, BI-NPP response directly correlates with ground motions and the relation does not change much when SSI effect is considered.

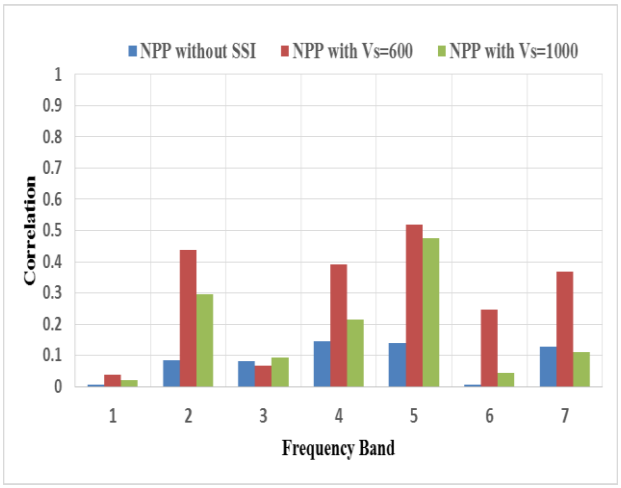

(a) NPP under El-Centro ground motion

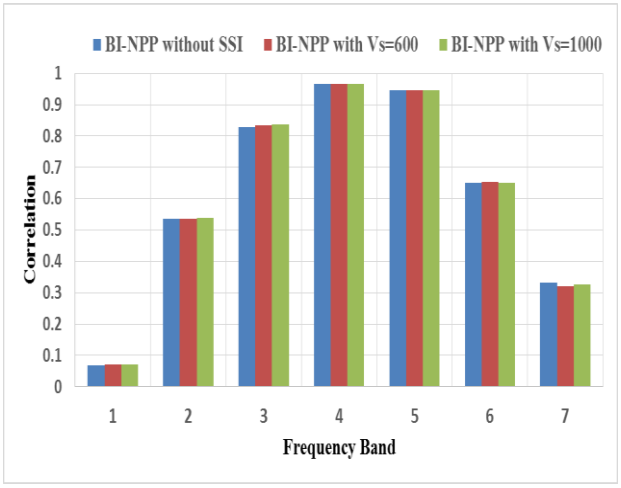

(b) BI-NPP under El-Centro ground motion

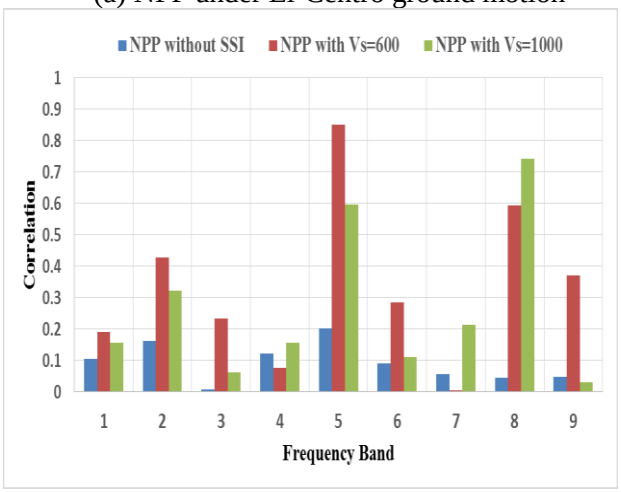

(c) NPP under Kobe ground motion

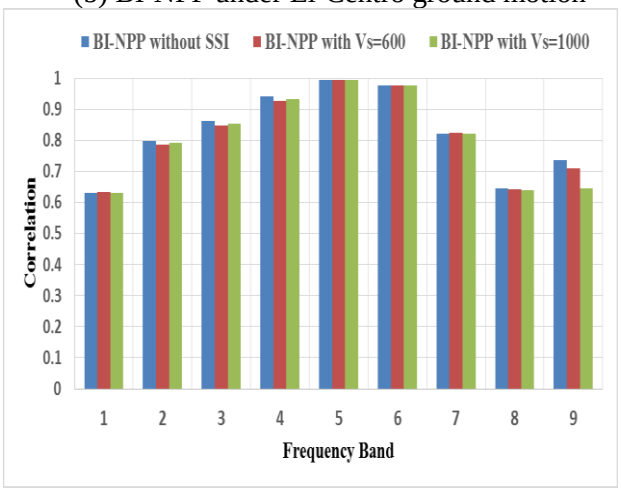

(d) BI-NPP under Kobe ground motion

Figure 5. Degree of correlation between ground motions and acceleration responses of nuclear power plant models.

6 CONCLUSIONS

The current study investigates the effect of SSI on seismic responses of NPP structure with and without considering base isolation system using wavelet analysis. The findings are as follows:

- The energy calculation process based on wavelet transform is an efficient tool to investigate the effect of SSI on frequency content of the acceleration responses of nuclear power plant structures.
- The consideration of SSI effect causes significant decrease of accumulative total energy of the acceleration response of NPP structure, especially for soft rock site. This indicates that, NPP structure suffers

less acceleration when SSI effect is adopted whereas the effect is negligible on energy content of response for BI-NPP structure.

- Poor correlation exists between acceleration response of NPP structure and input ground excitation, whereas, for soft rock site the relation increases significantly. Conversely, the frequency content of the response of BI-NPP is directly related to the input motions at the levels where most of the energy lie, however, SSI has negligible contribution to change the relation.

Finally it can be concluded that the seismic performance of the base-isolated NPP is not sensitive to SSI effect than the rigidly fixed NPP rested on rock sites.

7 ACKNOWLEDGEMENT

This work was supported by the Nuclear power Core Technology Development Program of the Korea Institute of Energy Technology Evaluation and Planning (KETEP) grant financial resource from the Ministry of Trade, Industry & Energy, Republic of Korean (No. 2014151010170A).

8 REFERENCES

Iyama, J. and Kuwamura, H. (1999). Application of wavelets to analysis and simulation of earthquake motions. Earthquake engineering and Structural Dynamics, 28 255-272.

Chatterjee, P. and Basu, B. (2004). Wavelet-based non-stationary seismic rocking response of flexibility supported tanks. Earthquake Engineering Structural Dynamics, 33 157-181.

Huang, Y.-N., Whittaker, A.S. and Luco, N. (2010). Seismic performance assessment of base-isolated safety-related nuclear structures. Earthquake Engineering & Structural Dynamics, 39 1421-1442.

Micheli, I., Cardini, S., Colaiuda, A. and Turroni, P. (2004). Investigation upon the dynamic structural response of a nuclear plant on a seismic isolating devices. Nuclear Engineering and Design, 228 319-343.

Zhao, C. and Chen, J. (2013). Numerical simulation and investigation of the base isolated NPPC building under three-directional seismic loading. Nuclear Engineering and Design, 265 484-496.

Forni, M., Poggianti, A. and Dusi, A. (2012). Seismic isolation of nuclear power plants. Proc., 15th World Conference of Earthquake Engineering, paper no. 1485, Lisbon, Portugal, September.

Novak, M. and Henderson, P. (1989). Base-isolated buildings with soil-structure interaction. Earthquake Engineering Structural Dynamic, 18 751-765.

Tongaonkar, NP. and Jangid, RS. (2003). Seismic response of isolated bridges with soil–structure interaction. Soil Dynamics and Earthquake Engineering, 23(4) 287-302.

Spyrakos, C.C., Koutromanos, I.A. and Maniatakis, Ch.A. (2009). Seismic response of base-isolated buildings including soil-structure interaction. Soil Dynamics and Earthquake Engineering, 29 658-668.

Schellenberg, A., Yang, T.Y. and Kohama, E. (2013). OpenSees Navigator 2.5.2, https://nees.org/resources/osnavigator.

International Standard Organization (ISO), (2010). Elastomeric seismic-protection isolators-part 3: Applications for buildings-specifications. ISO 22762-3:2010.

Sarica, R.Z. and Rahman, M.S. (2003). A wavelet analysis of ground motion characteristics. Proc., U.S.-Taiwan workshop on soil liquefaction, Taiwan.

Walker, J.S. (1999). A primer on wavelets and their scientific applications. Chapman and Hall/CRC, New York.

Ghaffar-Zade, M. and Cahpel, F. (1983). Frequency-independent impedance of soil-structure system in horizontal and rocking modes. Earthquake Engineering & Structural Dynamics, 11 523-540.

Kenarangi, H. and Rofooei, F. R. (2010). Application of tuned mass dampers in controlling the nonlinear behaviour of 3-D structural models, considering the soil-structure interaction. Proc., 5th National Congress on Civil Engineering, Mashhad, Iran.

Goggins, J., Broderick, B.M., Basu, B. and Elghazouli, A.Y. (2006). Investigation of the seismic response of braced frames using wavelet analysis. Structural Control and Health Monitoring, 14 627-648.

NCEED-CUET National Conference on Earthquake and Environmental Disasters, December 17, 2015, Chittagong, Bangladesh
Bhuiyan M. A. R., Pal S. K., Mazumder M. H., Mazumder R. K., Omi F. R. (eds.)

Seismic Behavior of Short Column Originated from the Level Difference on Sloping Ground

S.R. Chowdhury, M. Nurunnabi, M.T.Hasan & S. Monira
Ahsanullah University of Science and Technology, Dhaka, Bangladesh

ABSTRACT: Columns those are short-heighted or have shorter effective height to that of the other regular (taller) columns within the same stories are called short columns. Short column occurs in presence of unreinforced masonry infill of partial height of adjoining RC column, conditions arising from sloping ground, presence of a mezzanine slab, presence of a staircase beam/slab. In this paper only short column arising from sloping ground is being considered. Seismic analysis of reinforced concrete (RC) building with different height and cross section of critical column at ground floor (height and cross section of others column are same) are performed with the finite element software ETABS 9.6. The model generated in this study is verified with the numerical results as described in Ramin & Mehrabpour (2014) paper. Although the agreements are not exactly same but it has fallen within acceptable limit. The effect of changing cross section and height of critical short column on moment, shear and deflection of other ground storey columns are also observed. Only earthquake load is considered as lateral load. Analysis has been performed only up to linear stage.

1 INTRODUCTION

Columns those are short-heighted or have shorter effective heights to that of the other regular (taller) columns within the same storied are called short columns. Short column occurs in presence of unreinforced masonry infill of partial height of adjoining RC column, conditions arising from sloping ground, presence of a mezzanine slab, presence of a staircase beam/slab or K-braces on building columns, presence of a plinth beam. In this study only short column arising from sloping ground is being considered. The short column shows an enormous potential for serious damage by earthquake in the case of an inappropriate design. To facilitate a way of designing short column, originated from sloping ground as well as reducing the adverse effect of short column building during earthquake, an attempt has been made in this study with the help of structural software ETABS 9.6.0.

The chief role of column is to transfer the inertia force originated from earthquake to columns. The main part of these forces is exerted on the short column since the stiffness varies from column to column. Thus, the short column shows an enormous potential for serious damage by earthquake in the case of an inappropriate design. The column stiffness is reversely proportional to the third power of height. Therefore, the stiffness and energy absorption capacity of column gets 8 times greater as its length falls by half (Murty, 2004). Since lateral stiffness of columns is inversely proportional to the cube of its height, this short column effect is more severe when heights over which the columns are prevented from moving are large (or the unrestricted height of columns is small). However in present time we have new regulations in place for construction that greatly contributes to earthquake disaster mitigation and are being applied in accordance with world practice (Ashimbayev et al, 2004).

Fiber Reinforced Polymer (FRP) completely changes the rupture modulus in columns so that it changes from brittle to flexible in a completely reinforced column. When columns are reinforced with the bands placed at constant distances, rupture occurs at flexural-shear modulus (Colomb et al, 2008). Liang and Fragomeni (2009) have suggested a general model for non-linear non-elastic analysis and design of the concrete-filled steel short columns under axial loads as well as an accurate structural model for the high-resistance and medi-

um-resistance concrete enclosed inside cylindrical short columns. They have also employed numerical methods to model the non-linear behavior of cylindrical columns.

Columns are key structural elements for the seismic performance of buildings. Therefore, special attention should be given to their structural response under load reversals. Moreover, earthquake effects generally require the inclusion of two horizontal component loads that are considered to be more damaging than single direction actions. Many situations with short column effect arise in buildings. When a building is rested on sloped ground, during earthquake shaking all columns move horizontally by the same amount along with the floor slab at a particular level (this is called rigid floor diaphragm action). If short and tall columns exist within the same storied level, then the short columns attract several times larger earthquake force and suffer more damage as compared to taller ones (Alqatamin, 2009).

In this study, seismic analysis of reinforced concrete (RC) building with different height and cross section of critical column at ground floor (height and cross section of others column are same) are performed with the finite element software ETABS 9.6. The model generated in this study was verified with the numerical results as described in Ramin & Mehrabpour (2014) paper. Although the agreements are not exactly same but it has fallen within acceptable limit. The effect of changing cross section and height of critical short column on moment, shear and deflection of ground storied column were also observed. In new buildings, short column effect should be avoided to the extent as possible during architectural design stage itself.

2 MODELING OF BUILDING AND VERIFICATION

2.1 *Modeling*

In this study, modeling of 4 storied RC buildings (Fig. 1) was performed for verification with the work of Rahim & Mehrabpour (2014) paper comparing bending moment, shear force and displacement and for modeling of 4 storied RC buildings, the following material properties and geometrical properties have been used for beams, columns and slabs. Dimensions of the columns were 40cm × 40cm for first and second floors and 35cm × 35cm for third and fourth floors, while the dimensions of beams were 40cm × 35cm for first two floors and 35cm × 30cm for second two floors. Slab thickness is used as 1.52cm.

RC beam column frame structure is selected for this study. 6 kN/m udl load is imposed in all beams of the frame. Zone-III (Z = 0.16), special revisiting moment frame (RF = 5) and medium soil type is selected. ultimate tensile strength of steel-415 N/sq.mm and Concrete strength of 30 N/sq.mm were chosen. Each beams length are equal to 5 m for Y direction and 3.8 m for X direction. Height of each storied are given below:
1) For the case where the structure is on the level ground, all the supporting columns at ground floor are of 4 m height (3.2 m for other stories).
2) For the case where the structure is on sloping ground, all the column heights were same as that of level ground structure with the exception of ground columns on a sloping ground of 20 percent.

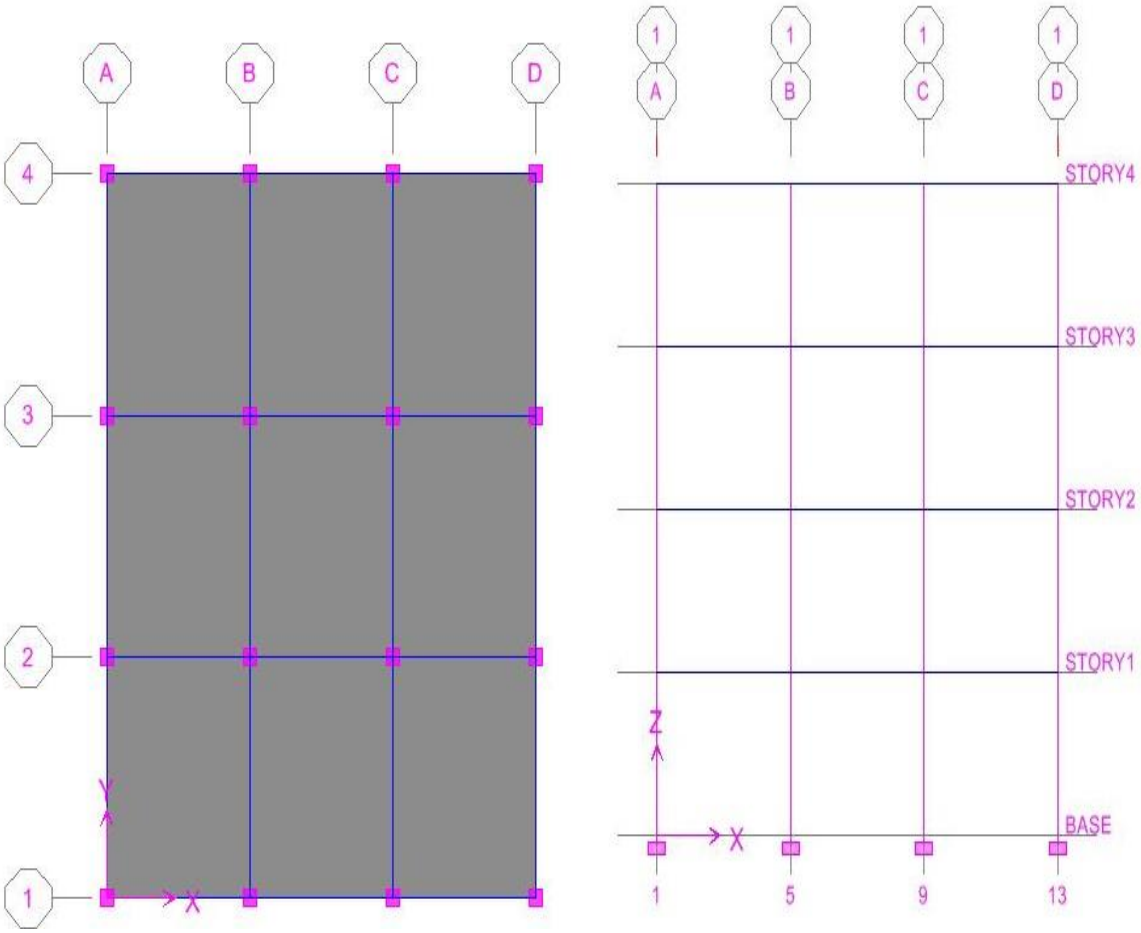

(a) (b)

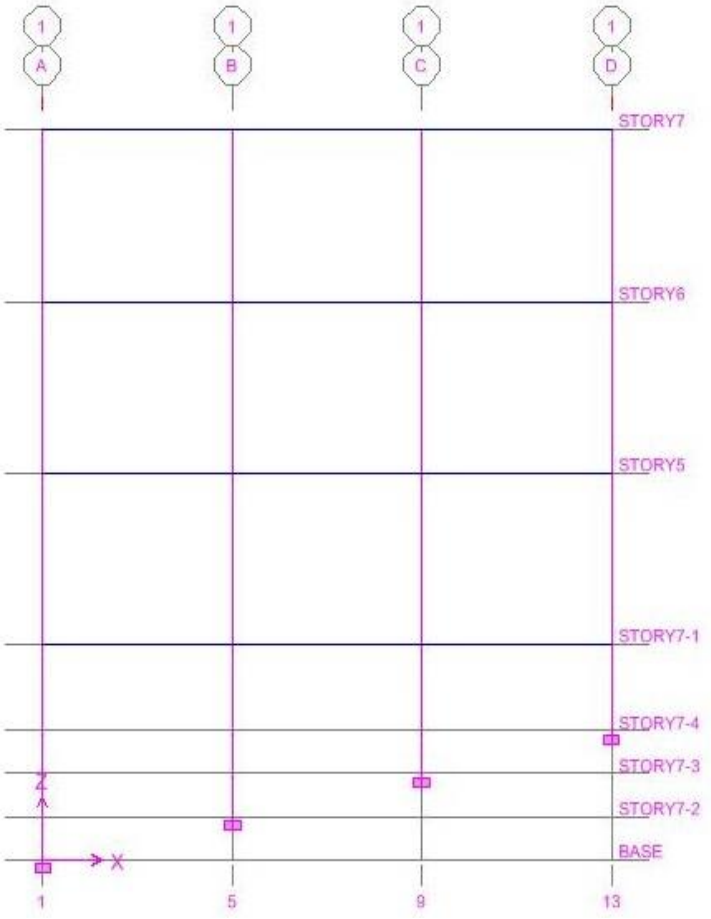

(c)

Figure 1. Plans and frames (along X-coordinate) of the studied structure (a) The consider plan of both structure (b) The flexural frame for the structure on flat ground and (c) The flexural frame on sloping ground; C1, C5, C9 & C13 denote columns.

2.2 *Verification*

Figures 2 and 3 respectively shows the variation of shear force of flat and sloping ground columns of base floor of present and previous work. Present work represents the results obtained from this study and previous work denotes the results of Rahim & Mehrabpour (2014) paper. Although the agreements are not exactly same but it has fallen within acceptable limit. This model is now ready to do some parametric study especially for the 4 storied RC building exists on sloping ground.

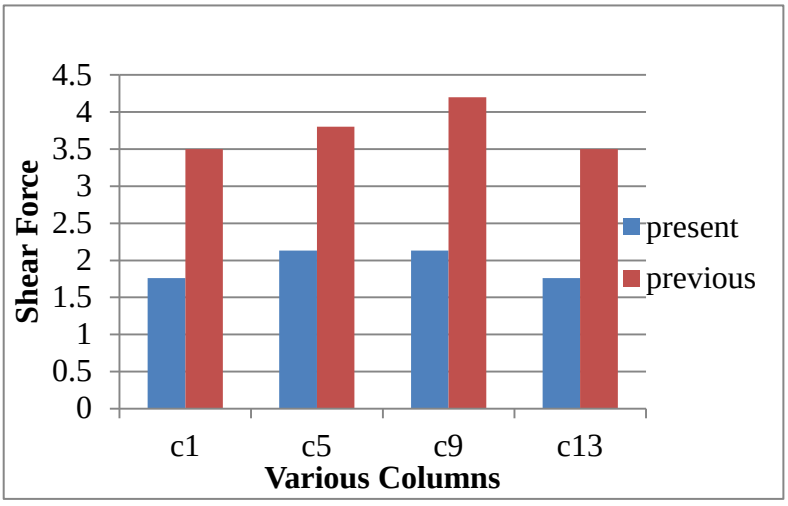

Figure 2. Comparison between present and previous work value of shear force (Ton), of various columns for flat ground in X axis

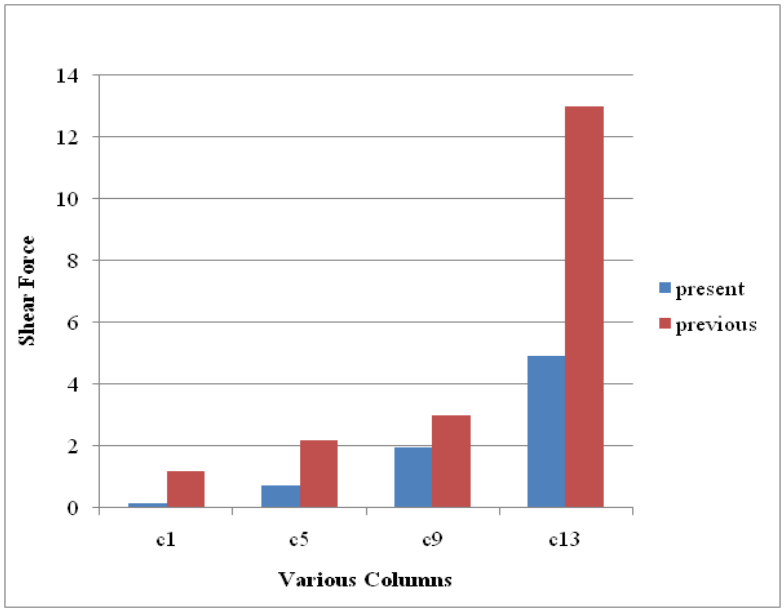

Figure 3. Comparison between present and previous work value of shear force (ton) of various columns for sloping ground in X axis

3 PARAMETRIC STUDY

The verified model in now used to do the parametric study. The parameters are height and cross section of the critical short column at ground floor level. The effect of changing cross section and height of critical short columns on moment, shear and deflection of other ground storey columns will be observed.

Cases:

- Case1:To compare the behavior of four-storied RC building in sloping ground for different length of critical column (height of others columns are constant)
- Case2:To compare the behavior of four-storied RC building in sloping ground for different cross sectional areas of critical column (cross section of others column are constant)

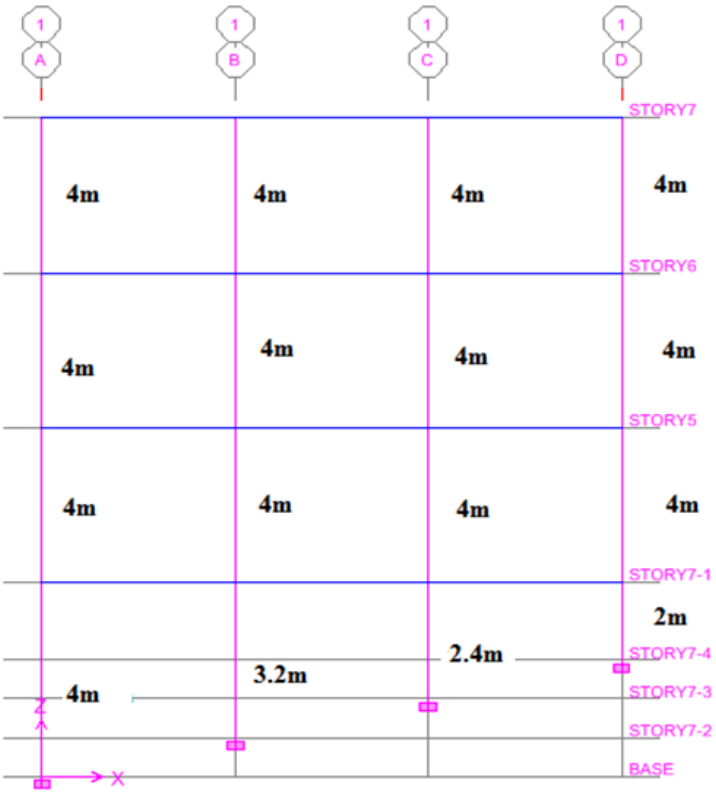

Figure 4. Four-storey RC building in sloping ground of critical column height 2m (dimensions shown in the figure represent height of the column).

3.1 *Case 1*

In Table 1, column A, B, C represents the analysis results for the critical column height of 1.33m, 1.6m, and 2m respectively as shown in Figures 5, 6 and 7. As an example, Figure 4 shows the elevation of a four-storey RC building with critical column height of 2m where others floor's column height are constant of 4m. Table 1 shows different values of bottom storey height of critical column (C13) with height other columns at ground level.

Table 1. Different values of critical column (C13) height.

A		B		C	
Column at ground level	Height	Column at ground level	Height	Column at ground level	Height
c1	4m	c1	4m	c1	4m
c5	3.2m	c5	3.2m	c5	3.2m
c9	2.4m	c9	2.4m	c9	2.4m
c13	1.33m	c13	1.6m	c13	2m

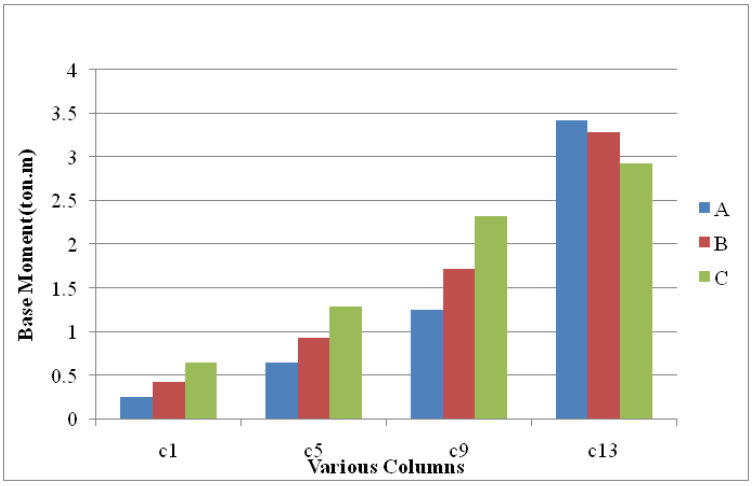

Figure 5. Bending moment with variation of column height in X axis.

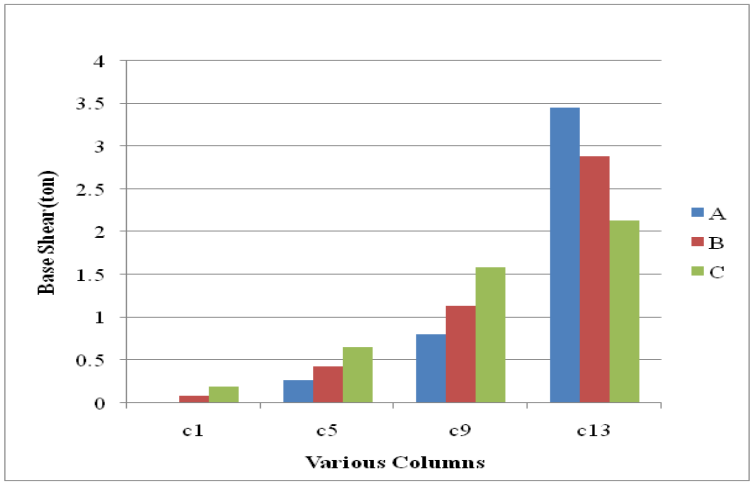

Figure 6. Shear with variation of column height in X axis.

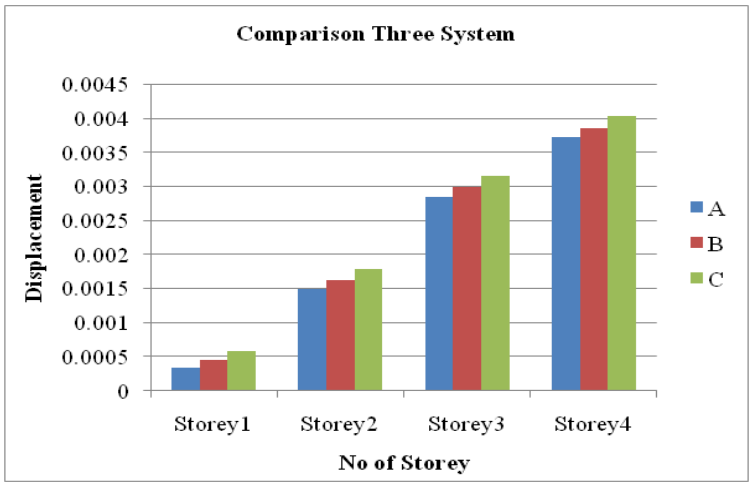

Figure 7. Displacement (m) with variation of storey along X direction

Figures 5 and 6 respectively shows the variation of base column bending moment and base column shear force with different value of critical column height of ground storey. Figure 7 shows the variation of base critical column displacement (C13) in X axis with number of storied. Bending moment and shear force decrease with the increase of critical column height where the other base column moments are increasing. Displacements of critical column as well as other columns increase with increasing critical column height.

3.2 *Case 2*

A, B, C in table 1 represent the analysis results for the critical column cross-section of 35x35 cm^2, 40x40cm^2 and 46x46 cm^2 respectively as shown in Figures 8, 9 and 10. As an example, Figure 8 shows the elevation of a four-storey RC building with critical column (c13) cross section of 35x35 cm^2 where others floor's column cross section are constant of 35x35 cm^2. Table 2 shows different values of cross section of critical column (C13).

Figure 8. Four-storey RC building of cross sectional area of critical column 35cm*35cm (dimensions shown in the figure represent height of the column).

Table 2 Different cross sectional areas of critical column (C13)

	A	B	C
Column	C13	C13	C13
Area(cm^2)	35*35	40*40	46*46

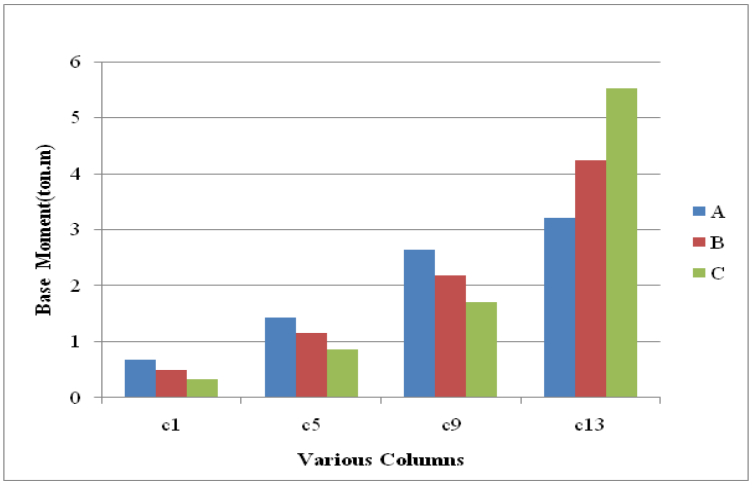

Figure 9. Bending moment with variation of columns in X axis.

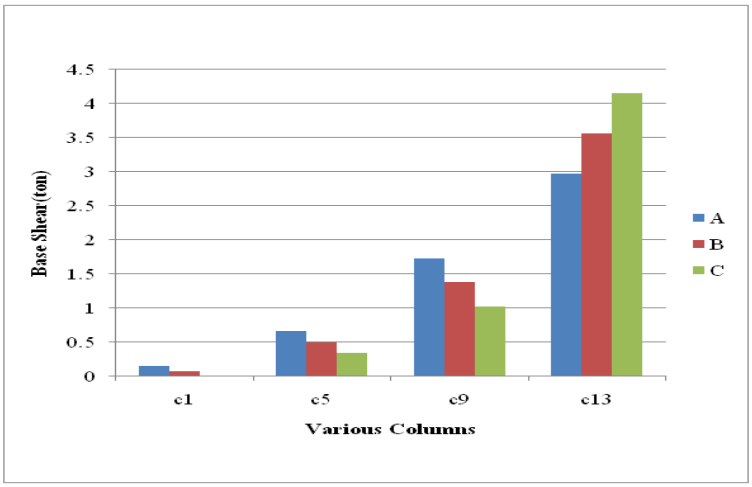

Figure 10. Shear force with variation of columns in X axis.

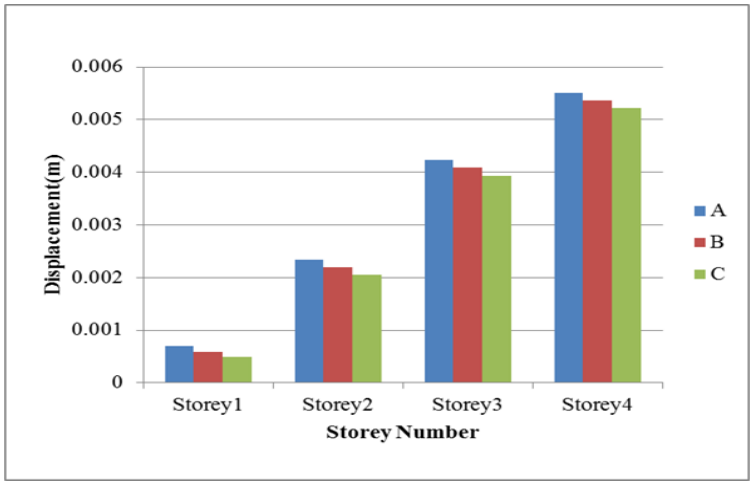

Figure 11. Displacement with variation of storey number in X axis.

Figures 9 and 10 respectively shows the variation of base column bending moment and shear force with different cross sectional area of critical columns. Figure 11 shows the variation of displacement of critical column (C13) in X axis with number of stories. Bending moment and shear force of critical column decreases with the decreasing the cross section of critical column whereas the other ground floor column moment and shear increases. Displacement in X axis increases with the decrease in the cross section of critical column where the other ground floor column displacements in X axis also increases.

4 CONCLUSIONS AND RECOMMENDATIONS

Main findings of the study are given below:

• When critical column height increases, moment and shear of critical column decreases but displacement increases whereas the other ground floor column moment, displacement and shear increases.

• When critical column cross section increases moment, shear of critical column increases but displacement decreases whereas the other ground floor column moment, shear and displacement decreases.

As this study is only for symmetrical building, there are also many scopes for further study covering other possible cases. In this case following may take concern:

- The study is performed without any kind of retrofitted material to increase shear capacity, further can be performed with retrofitted material.
- The study is performed without increasing or decreasing steel bar further can be performed with increasing or decreasing steel bar.
- In this study only finite element software ETABS 9.6.0 is used. There are also some other finite element software such as STAAD-Pro, ANSYS etc to analyze this kind of study.

- Only linear elastic analysis is made in this study. To make comprehensive and complete comment non-linear dynamic analysis is highly recommended. The study can be performed by multi-model analysis.
- For the present study the analysis were performed for the symmetrical buildings to avoid torsional response under pure lateral forces. Further studies can be performed for the non-symmetrical building.
- The study is performed without any shear wall, partition wall, floor finish and any kind of external dead and live load, for further investigation it can be performed with any shear wall, partition wall, floor finish and any kind of external dead and live load.

5 REFERENCES

Ashimbayev, M.U., Itskov, I.E. and Lobodryga, T.D. 2004. Living with Natural and Technological Hazards, Topica.2: Reducing Vulnerabilities in Existing Building and Lifelines. *Seismic Hazard and Earthquake Engineering*, 35: 43-46.

Alqatamin, A. 2009. The Action of Short Columns at Reinforced Concrete Building Constructions.

Colomb, F., Tobbi, H., Ferrier, E. and Hamelin, P. 2008. Seismic Retrofit of Reinforced Concrete Short Columns by CFRP Mate rials. *Composite Structures*, 82: 475-487.

Liang, Q.Q. and Fragomeni, S. 2009. Nonlinear Analysis of Circular Concrete-Filled Steel Tubular Short Columnsunder Axial.

Murty, C.V.R. 2004. Why Are Short Columns More Damaged during Earthquakes, *Indian Institute of Technology Kanpur*.

Ramin, K. and Mehrabpour, F. 2014. Study of Short Column Behavior Originated from the Level Difference on Sloping Grounds during Earthquake (Special Case: Reinforced Concrete Buildings). *Open Journal of Civil Engineering*, 4: 23-34.

NCEED 2015 -National Conference on Earthquake and Environmental Disaster; December 17, 2015; CUET, Chittagong, Bangladesh
Bhuiyan M. A. R., Pal S. K., Mazumder M. H., Mazumder R. K., Omi F. R. (eds.)

Fragility Assessment of an Existing Reinforced Concrete Hospital Building

Md. Abul Hasan
Department of Disaster & Environmental Engineering, Faculty of Civil Engineering, Chittagong University of Engineering & Technology, Chittagong-4349, Bangladesh, hasanrazu0601056@gmail.com

Md. Abdur Rahman Bhuiyan
Department of Civil Engineering, Faculty of Civil Engineering, Chittagong University of Engineering & Technology, Chittagong-4349, Bangladesh

ABSTRACT: This research paper deals with the fragility assessment of an existing hospital building located in the highly seismic zone, Chittagong, Bangladesh. For developing fragility curves for different damage state provided by FEMA-273 elastic spectrum analysis have been done in this research. Eighteen ground motions having peak ground acceleration (PGA) of 0.325g to 0.785g are used and their corresponding response spectrum loads are applied for calculating structural responses. Inter-story-drift ratio (IDR) as an engineering demand parameter (EDP) is evaluated for generating fragility curve of hospital building. Scaling approach has been applied here for generating a large number (1800) of damage data for better curve. The probabilistic vulnerability assessment of an existing hospital building indicates that it is vulnerable for different damage state for revised Bangladesh national building code (BNBC).

1 INTRODUCTION

Hospital is very crucial for human civilization which provides life saving medical care on a daily basis to the community people when they need (Hasan, 2015). Community expects from hospital and its staff to save lives in an emergency and to care for community members, if they are seriously injured or become seriously ill. All hospital facilities should be capable of continued operation during and after natural disaster. This means special design consideration is needed for the protection of hospital building. For this reason, every building code in the world considers higher importance factor for seismic design of hospital building so as to withstand operation during and after an earthquake. The Bangladesh National Building Code (BNBC 1993) suggests for consideration of 25% higher importance than the standard occupancy building. Similarly, in Euro Code 8, Australian Building Code (AS 11704) and New Zealand Building Code (NZS 4203) suggest for providing 75%, 20% and 30% higher importance than normal building respectively.

The world has suffered huge loss of confidence, as well as economic losses on account of damages occurred in hospital buildings from earthquake disasters. Damage of existing hospital building structures was observed in 1971 San Francisco Earthquake, 1994 Northbridge Earthquake and 2001 Bhuj Earthquake etc. The frequent occurrence of earthquakes around the world has heightened the need for studying the seismic performance of existing hospital buildings. Bangladesh is geographically located in high seismic risk zone. Building constructed before 1993 did not consider the load from earthquake because there was not any guideline for designing building structure in Bangladesh. In 1993, Bangladesh National Building Code (BNBC-1993) was developed. But recent research has shown that there might hit greater earthquake than the considered in BNBC-1993. For this reason, BNBC-1993 has been revised to consider the greater effect of earthquake. But the building structure constructed within the time from 1993 to 2006 might be vulnerable as per revised code. For this reason it is essential to check the earthquake resistivity of these buildings for revised BNBC.

An emerging tool in assessing the seismic vulnerability of building structure is the use of fragility curve which describes the probability of a structure being damaged beyond a specific damage state for various lev-

els of ground shaking. It can be either empirical or analytical. Empirical fragility curves are usually based on the reported building damage from past earthquakes. Due to lack of damage data analytical fragility curve can be developed using non-linear time history analysis, elastic spectral analysis or non-linear static analysis.

2 METHODOLOGY OF SEISMIC FRAGILITY FUNCTION

Towashiraporn et al., (2004) proposed a method for formulating the meta-model for fragility curve generation using response surface method, in which, the input variables are composed of two components: random variable and a control variable. Random variables are those that define uncertainties in structural properties, while the control variable is deterministic with its fixed values characterizing different response prediction models (Towashiraporn et al., 2004). The first step in calculating the seismic fragility curves using the meta-model concept is to define the input and output (response) variables. A response like inter story drift ratio that best describes damage from seismic loadings is selected.

Computational seismic analyses were performed on the models which represent different earthquake-structure scenarios. This is repeated for different combinations of input variables. The response resulting from the analysis is recorded for each ground motion, and the mean and standard deviation for each particular combination is calculated. Meta-models for the mean and standard deviation of the responses are formulated by applying the HDMR technique. Once the meta-model for mean and standard deviation are formed, they are combined to form the overall meta-model as given in equation (1).

$$y = y_{\mu} + N\left[0, y_{\sigma}\right] \tag{1}$$

The following steps are followed to develop the fragility curve.

Step 1 (Selection of building type): Firstly the building type is required to select. For our case it is hospital building.

Step 2 (Analytical Model of structure): The analytical model of hospital building is developed in SAP 2000 for structural analysis.

Step 3 (Selection of ground motion): After that the required ground motion is selected for elastic response spectrum analysis. For our case, 18 ground motions have selected.

Step 4 (EDP calculation): From elastic response spectrum analysis maximum IDR values as engineering demand parameter are calculated and scaling approach has been used to generate huge (1800) number of data for better curve.

Step 5 (Distribution of IDR): After that the IDR values are distributed in different damage grades and corresponding spectral acceleration is determined.

Step 6 (Development of PDF): In this stage probability distribution function are developed by using equation (2).

$$\int(x) = \frac{1}{\sqrt{2\pi\sigma}} e^{-\frac{(x-\mu)^2}{2\sigma^2}} \tag{2}$$

Step 7 (Development of CDF from PDF): After developing probability distribution curve then cumulative distribution curve is developed by using following equation (3).

$$F(x) = p(d > D) = \phi\left[\frac{\ln(X) - \mu}{\sigma}\right] \tag{3}$$

3 CHARCTERISTICS OF DAMAGE STATE

Fragility curve represents the probability of exceeding a damage limit state for a given structure type subjected to a seismic excitation (Shinozuka et al., 2000; Ellingwood et al., 1980). Three discrete structural performance levels and two intermediate structural performance ranges are defined here. The structural performance levels are the Immediate Occupancy Level (DS-1), the Life Safety Level (DS-3), and the Collapse Prevention Level (DS-5). The structural performance ranges are the Damage Control Range (DS-2) and the Limited Safety Range (DS-4).

Structural performance level DS-1, Immediate Occupancy, means the post-earthquake damage state in which only very limited structural damage has occurred. The basic vertical and lateral-force-resisting systems

of the building retain nearly all of their pre earthquake strength and stiffness. The risk of life threatening injury as a result of structural damage is very low, and although some minor structural repairs may be appropriate, these would generally not be required prior to preoccupancy. Structural performance level DS-3, Life Safety, means the post-earthquake damage state in which significant damage to the structure has occurred, but some margin against either partial or total structural collapse remains. Some structural elements and components are severely damaged, but this has not resulted in large falling debris hazards, either within or outside the building. Injuries may occur during the earthquake; however, it is expected that the overall risk of life-threatening injury as a result of structural damage is low. It should be possible to repair the structure; however, for economic reasons this may not be practical. While the damaged structure is not an imminent collapse risk, it would be prudent to implement structural repairs or install temporary bracing prior to preoccupancy. Structural performance level DS-5, Collapse Prevention, means the building is on the verge of experiencing partial or total collapse. Substantial damage to the structures has occurred, potentially including significant degradation in the stiffness and strength of the lateral force-resisting system, large permanent lateral deformation of the structure and to more limited extent degradation in vertical-load-carrying capacity.

However, all significant components of the gravity load- resisting system must continue to carry their gravity load demands. Significant risk of injury due to falling hazards from structural debris may exist. The structure may not be technically practical to repair and is not safe for preoccupancy, as after-shock activity could induce collapse. Structural performance range DS-2, Damage Control, means the continuous range of damage states that entail less damage than that defined for the Life Safety level, but more than that defined for the Immediate Occupancy level. Design for Damage Control performance may be desirable to minimize repair time and operation interruption; as a partial means of protecting valuable equipment and contents; or to preserve important historic features when the cost of design for Immediate Occupancy is excessive. Structural performance range DS-4, Limited Safety, means the continuous range of damage states between the Life Safety and Collapse Prevention levels. In this study, the inter story drift ratio of the hospital building is adopted as damage index (DI). For different damage state and performance range the limit value of IDR is enlisted in Table 1.

Table 1. Structural performance levels and damage as per FEMA 273.

		Structural Performance Levels				
Elements	Type	Immediate Occupancy (DS-1)	Damage Control Performance Range (DS-2)	Life Safety (DS-3)	Limited Safety Performance Range (DS-4)	Collapse Prevention (DS-5)
Concrete Frame	Drift (transient)	<1%	<1.5%	<2%	<3%	<4%

4 PHYSICAL DESCRIPTION AND MODELLING OF HOSPITAL BUILDING

Chittagong Medical College Hospital was established in the year 1957 and started functioning in the present location in 1960 with only 120 beds and few outpatient services. It has built an ancillary building which has foundation of ten stories. Seven stories of ten stories have constructed and the construction is going on. The total area of 1st floor is 12661.11 sq. ft.

Fig.1 represents the Ancillary Building of Chittagong Medical College Hospital (CMCH). Two types of column (rectangular and circular) have been used in this building. The rectangular columns having six different physical dimensions are used here with maximum size of 750 mm X 625 mm. Three types of circular column were used with maximum diameter of 625 mm.

Figure1. 3-D of Ancillary Building.

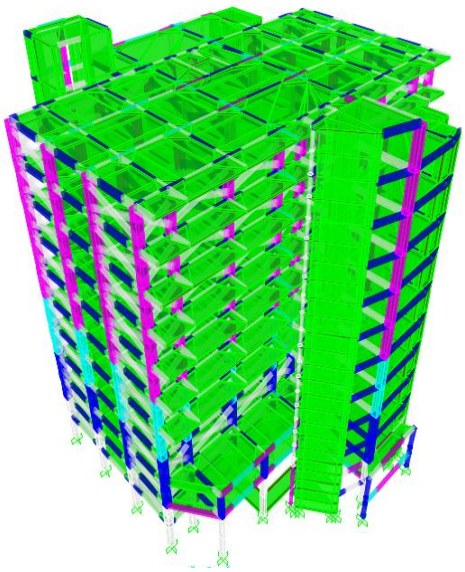

Figure2. Analytical Model of BMHB.

From structural drawings it is found that the compressive strength, modulus of elasticity and poisson's ratio of concrete is 25 Mpa, 23670 MPa and 0.2 respectively. The tensile strength of steel is considered as 415 MPa with Modulus of elasticity 200000 MPa. For modeling purposes the compressive strength, modulus of elasticity and poisson's ratio of clay brick is considered as 13.7 MPa, 12930 MPa and 0.19 respectively. For detailed analysis of the hospital building, an analytical model which represents the actual condition of the building is developed using structural analysis software SAP 2000. Beam and column elements are modeled as frame element; floor, roof, mat foundation and shear wall are modeled as shell element. The existence of masonary infill is modeled as equivalent strut model by Stafford-Smith and Carter (1969). Fig.2 represents the analytical model of considered benchmark hospital building of CMCH.

5 ELASTIC RESPONSE SPECTRUM ANALYSIS HOSPITAL BUILDING

Response spectrum analysis is used for analyzing the performance of structures under earthquake motions. The method assumes a single degree of freedom system to be excited by a ground motion in order to obtain the response spectrum curves for peak displacement, peak velocity or peak acceleration. Numbers of requested modes is selected such that their combined participating mass is at least of 90% of the total effective mass in the structure. Once the number of significant modes is established, several methods are used for the purpose of estimating the peak response values. The Square Root Some of Squares (SRSS) of the maximum modal values is one of the popular methods. The benchmark

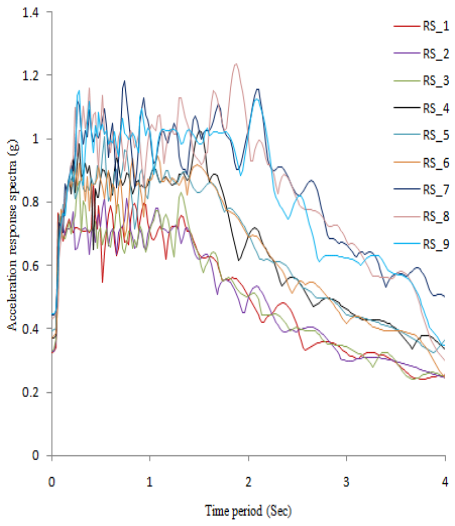

Figure 3. Response spectrum (RS_1 to RS_9)

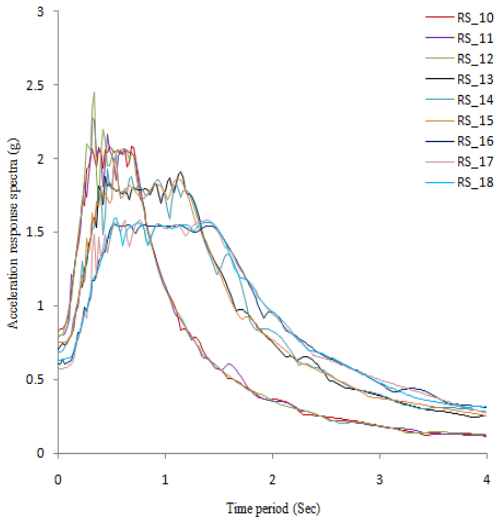

Figure 4. Response spectrum (RS_10 to RS_18)

hospital building (BMHB) is analyzed for eighteen response spectrum loading. Fig.3 and Fig.4 represents selected response spectrum loading.

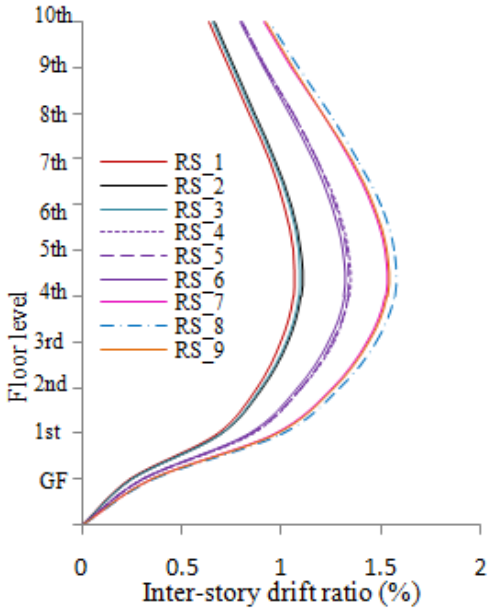

Figure 5. IDR (%) of BMHB for RS_1 to RS_9

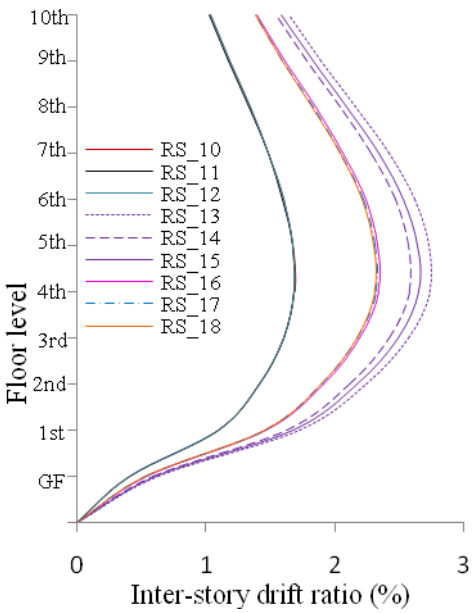

Figure 6. IDR (%) of BMHB for RS_10 to RS_18

The results of response spectrum analysis are graphically presented in Fig.5 and Fig.6. From the Fig.5 and Fig.6 it is seen that the inter-story drift value is initially increases up to maximum IDR values for 4th floor after that it decreases with floor levels.

6 FRAGILITY ASSESSMENT OF HOSPITAL BUILDING

By using the IDR values as Engineering Demand Parameter fragility curve is developed for three damage state (DS-1, DS-3 and DS-5) and two performance range (DS-2 and DS-4). The probability of exceedance of each damage state and damage range for BNBC-1993 and revised BNBC has also been checked here. From the Fig.7 which represents the fragility curve for immediate occupancy level; the probability of exceedance of DS-1 is 14% for seismic zoning coefficient, Z=0.15g suggested by BNBC-1993 for this zone and the value increases to 79%. From Fig.9 which represents fragility curve of considered hospital for life safety (DS-3) performance level. Fig.9 states that there is no probability of exceedance

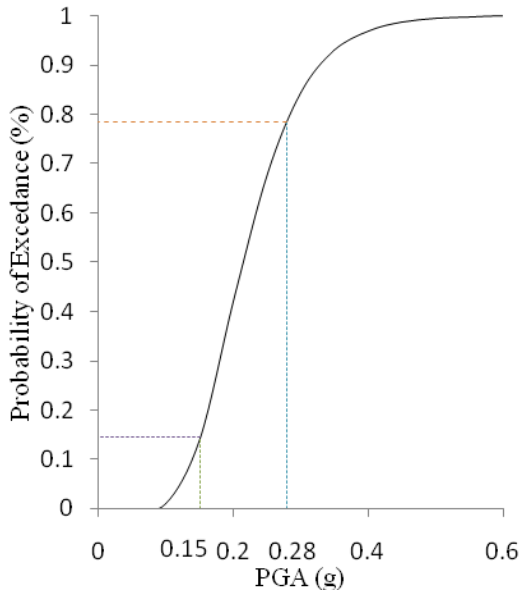

Figure 7. Fragility Curve of BMHB for DS-1

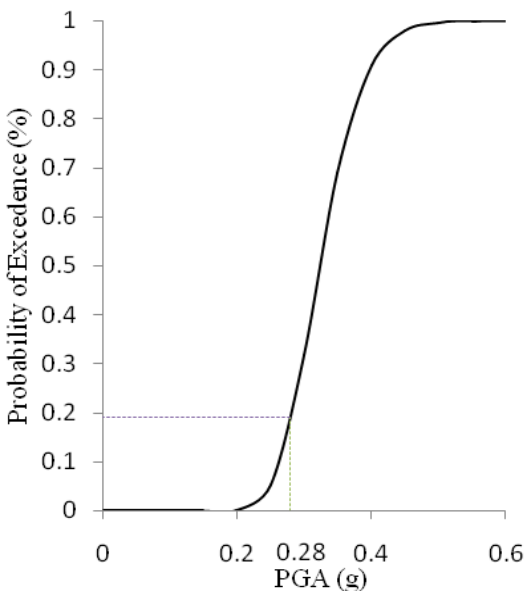

Figure 8. Fragility Curve of BMHB for DS-2

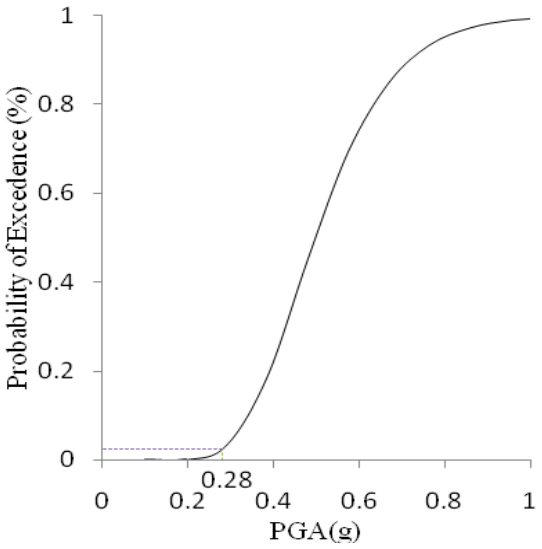

Figure 9. Fragility Curve of BMHB for DS-3.

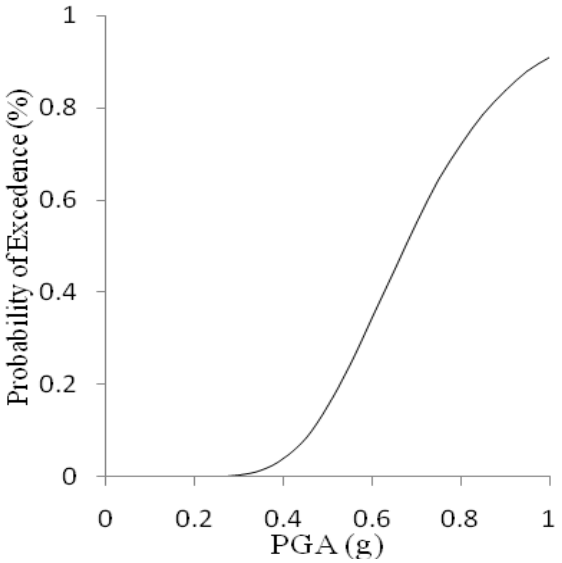

Figure 10. Fragility Curve of BMHB for DS-4.

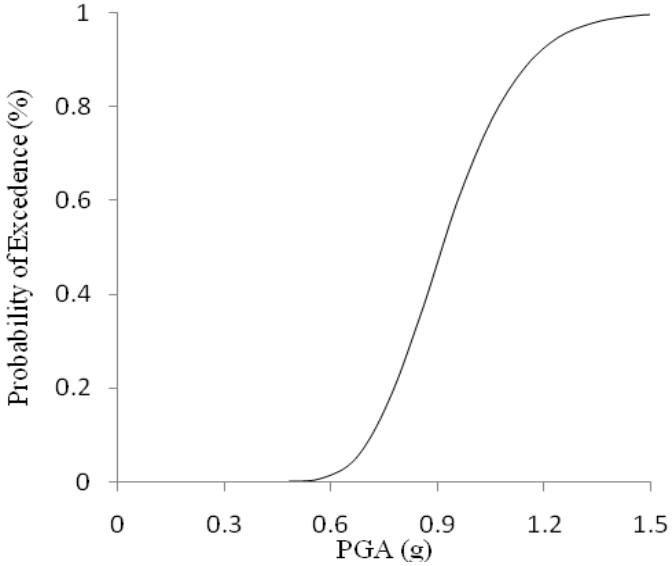

Figure 11. Fragility Curve of BMHB for DS-5.

for Z=0.28g which is suggested by revised BNBC. Fig.8 which resembles the fragility curve for DS-2 shows that there is no probability of exceedance of DS-2 for Z=0.15g. In case of Z=0.28g, there is probability of exceedance of damage control performance range which is 19% of DS-3 level for Z=0.15g but for Z=0.28g the probability of exceedance of this damage state is 3%. For DS-4 and DS-5 there is no probability of exceedance for considered seismic zoning coefficient which is plotted in Fig.10 and Fig.11.

7 CONCLUSIONS

The fragility assessment of the hospital building is done. From the fragility curve of DS-1 it is found that, the probability of exceedance of DS-1 for considered hospital building is 14% for PGA 0.15G (as per BNBC-1993). Similarly in case of PGA 0.28g (as per revised BNBC) the probability of exceedance of immediate occupancy level is 78%. From the fragility curve for DS-2, it is seen that for PGA 0.15g the probability of exceedance for DS-2 is zero whereas for PGA of 0.28g the probability of exceedance of DS-2 for hospital building is 19%. The probability of exceedance of hospital building for DS-3 is zero for PGA 0.15g. But for PGA 0.28g the probability of exceedance for DS-3 is 3% for BMHB. From fragility curve for DS-4 and DS-5 it is observed that there is no probability of exceedance of DS-4 for earthquake having PGA of 0.15g and 0.28g. So it can conclude from this research that the considered existing hospital building is vulnerable as per re-

vised BNBC. The probability of exceedance of different damage state is high. To reduce vulnerability and to keep hospital building functional during and after earthquake proper retrofitting strategy should be adopted.

8 REFERENCES

AS11704, 1993. Australian Building Code.

BNBC, 1993. Bangladesh National Building Code, Housing and Building Research Institute.

BNBC, 2006. Bangladesh National Building Code, Housing and Building Research Institute

Euro Code, 8.

Federal Emergency Management Agency 273.

NZS 4203, 1992. New Zealand Building Code

Stafford- Smith, B., 1966. Behavior of square In-Filled Frames. *Journal of the structural Division, ASCE*, vol.92.

Park, Y.J., Wen, Y.K., and Ang, A.H.S., 1986. Random vibration of hysteretic systems under bi-directional ground motions, Earthquake Engineering and Structural Dynamics, Vol. 14, pp. 543-557.

Towashiraporn, P., Goodno, B., and Craig, J., (2004). Building Seismic Fragilities Using Response Surface Metamodels. Ph.D. dissertation .Georgia Institute of Technology.

Nagarajaiah, S., Reinhorn, A.M., and Constantinou, M.C., 1991. Nonlinear dynamic analysis of 3–D base isolated structures, Journal of Structural Engineering, ASCE, Vol. 117, pp. 2035– 2054.

Japan Road Association, 2002. Specification for highway bridges - part V: Seismic design, Tokyo, Japan.

Ellingwood B., Galambos T., 1980. Probability Based Load Criteria for American National Standard, Washington, National Bureau of Standards.

Hasan, M.A., 2015. Assessment of Seismic Fragility and Retrofit of Hospital Building Using Base isolation Devices, M.Sc thesis.

NCEED 2015 -National Conference on Earthquake and Environmental Disaster; December 17, 2015; CUET, Chittagong, Bangladesh
Bhuiyan M. A. R., Pal S. K., Mazumder M. H., Mazumder R. K., Omi F. R. (eds.)

Generation of Analytical Fragility Curves from Capacity Spectrum: A Case Study of Reinforced Concrete Frame Building with URM Infill Walls

Rajen Dey, Ram Krishna Mazumder* and Md. Abdur Rahman Bhuiyan
Institute of Earthquake Engineering Research, Chittagong University of Engineering and Technology, Chittagong, 4349, Bangladesh

ABSTRACT: This paper represents generation of fragility curves for the Reinforced Concrete (RC) frame structure with Unreinforced Masonry (URM) infill walls from Capacity Spectrum. Over last decade, RC building with URM infill walls became most preferable and suitable choice of construction practice in Bangladesh especially in urban city areas. However, due to lack of incorporation in the earthquake resistance features and proper modeling prior design became vital issues in case of vulnerability assessment of existing building. Most of the cases building design have been done without considering interaction of URM infill wall and RC frame. Current study aims to incorporate interaction between masonry walls and RC frame in the structural modeling and analysis. Capacity spectrum based method, considering four damage states, was used to derive fragility curves of a typical six story RC building with URM infill walls.

1 INTRODUCTION

Since Bangladesh is one of the rapid developing countries in the world, urbanization is on the peak of its progression where RC structure with URM infill walls became most popular construction practice. The purpose of URM infill walls is to protect inside of the structure from environmental and separate internal spaces. In past structural design practices, infill walls in a RC frame building are typically considered as nonstructural elements. Therefore, interaction between infill walls and RC frames are overlooked, which may result inaccurate prediction of the lateral stiffness, strength, and ductility of the structure. This case study was performed to derive fragility curves from capacity spectrum. During modeling stage, it was given as prime responsibility to select proper model of URM infill walls based on state-of-art literature review. The structural model generation and structural analyses were performed in software package SeismoStruct v7.0. Fragility curves were obtained for four damage stages.

2 STRUCTURAL MODELING

2.1 *Modeling of URM Infill Walls*

In past, significant amount of research has been performed to characterize seismic behavior of masonry infill wall inside a RC panel. Experimental and analytical results for the interaction between RC frame and URM infill walls were compared by several researchers (Decanni et al. 2004), (Baron and Sevil 2010). Performance of URM infill walls inside RC frame varied during lateral loads application on the structure. URM infill remains in contact with RC frame under very low lateral loads and hence there is composite action between RC frame and URM infill walls. Most of the cases it has been observed that lateral stiffness increased initially for the URM infill model in comparison with bare frame model. In past research works, equivalent diagonal strut model was preferred due to its simplification in modeling of URM behaviors (Mazumder et al., 2015).

Masonry infill generally contains high stiffness and strength values which play an important role during lateral loading on main Reinforced Concrete (RC) frame structure. Material properties of masonry infill vary mostly from place to place depending on local raw material sources (Mazumder, 2015). In Bangladesh, the in-

fill walls are commonly made of masonry bricks of various strength and brittleness. With a view to improve the simulation of actual performance of the infill frame, various infill panel models have been suggested in the literature. There have been several research conducted in past studies to develop micro model for the numerical simulation of infill panels using two dimensional finite element (Ellul et al 2012) however, the diagonal strut model (see Figure 1) is the most widely accepted by the researchers because of its simplified approach for bulk analysis, and has been advocated in many documents and guidelines (CSA 2004), (NZSEE 2006). For the purpose of current analysis, simplified diagonal strut model was used.

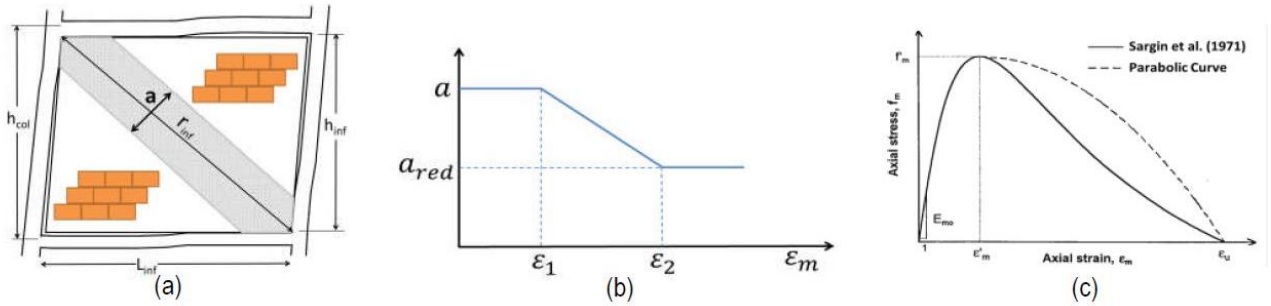

Fig.1. Diagonal strut for masonry infill panel (a) equivalent diagonal strut representation of an infill panel; (b) variation of the equivalent strut width as function of the axial strain; (c) envelope curve in compression (Source: SeismoStruct v7.0, 2014)

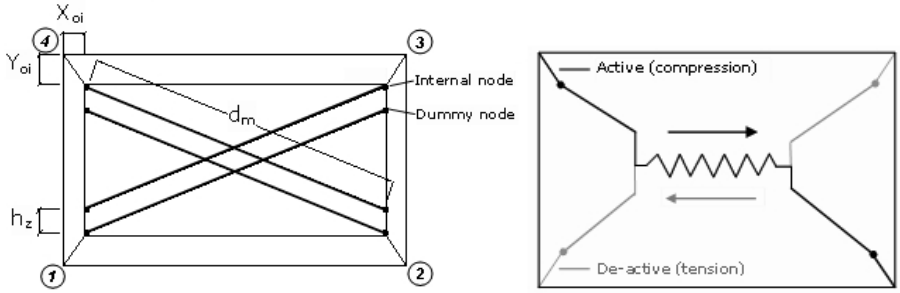

Fig.2. Infill panel element: compression struts (left) and shear strut (Crisafulli, 1997)

A four-node masonry panel element was generated and initially programmed by Crisafulli in 1997 and implemented in SeismoStruct by Blandon in 2005, for the modeling of the nonlinear response of infill panels in framed structures. Each panel is represented by six strut members; each diagonal direction features two parallel struts to carry axial loads across two opposite diagonal corners and a third one to carry the shear from the top to the bottom of the panel. This latter strut only acts across the diagonal that is on compression; hence its activation depends on the deformation of the panel. The axial load struts use the masonry strut hysteresis model, while the shear strut uses a dedicated bilinear hysteresis rule (Crisafulli 1997; Blandon 2005).

Strut area (a) is defined as the product of the panel thickness and the equivalent width of the strut, which normally varies between 10% and 40% of the diagonal of the infill panel, as concluded by many researchers based on experimental data and analytical results (D'Ayala, D. and Meslem 2013) A. Introduced as percentage of a, and which aims at accounting for the fact that due to cracking of the infill panel, the contact length between the frame and the infill decreases as the lateral and consequently the axial displacement increases, affecting thus the area of equivalent strut. It is assumed that the area varies linearly as function of the axial strain (as shown in 1a), with the two strains between which this variation takes place being defined as input parameters of the masonry strut hysteresis model. For the equivalent contact length, dimensionless relative stiffness parameter (λ) was computed (Mazumder 2015). Stiffness and strength of an infill panel is calculated from width of equivalent strut using formula proposed by Mainstone and Weeks (Mainstone et al 1970; Maistone 1971).

$$a = 0.175(\lambda_i h_{col})^{-0.4} r_{inf} \quad \text{..... (1)}$$

where, $$\lambda_i = \left[\frac{E_m t_{inf} \sin 2\theta}{4 E_c I_{col} h_{inf}}\right]^{\frac{1}{4}} \quad \text{.....(2)}$$

Where λ is the coefficient used to determine equivalent width of infill strut; h_{col} is column height between centerlines of beam; h_{inf} is height of infill panel; E_c is expected modulus of elasticity of frame material; E_m is expected modulus of elasticity of frame material; I_{col} is moment of inertia of column; r_{inf} is diagonal length of

infill panel; t_{inf} is thickness of infill panel and equivalent strut; and θ is angle whose tangent is the infill height-to-length aspect ratio.

2.2 *Modeling of RC Frame*

In this current study, structural model for the index building was developed in the structural package Seismo-Struct v7.0. Material properties were chosen for Bangladeshi context, uniaxial concrete constitute law was used following proposed model of Mader et al. (Mander et al 1988) whereas cyclic rules included in the model for the confined and unconfined concrete proposed by Martinez-Rueda (Martinez-Rueda 1997) and Elnashai (Elnashai 1993). Reinforced Concrete members are modeled consisting three types of materials. These are unconfined concrete (corresponding to the cover), confined concrete (corresponding to the core concrete) and reinforcing steel. These reinforced concrete components are detailed with reinforcement rebar for both main and transverse direction. Transverse reinforcements provide both shear and confinement strength for the concrete core. In SeismoStruct, so-called fiber approach is developed to represent the cross-section behavior, where each fiber is associated with a uniaxial stress-strain relationship; the sectional stress-strain state of beam-column elements is then obtained through the integration of the nonlinear uniaxial stress-strain response in which the section has been subdivided (Mazumder 2015). The discretization of a typical reinforced concrete cross-section is shown in the Figure 3.

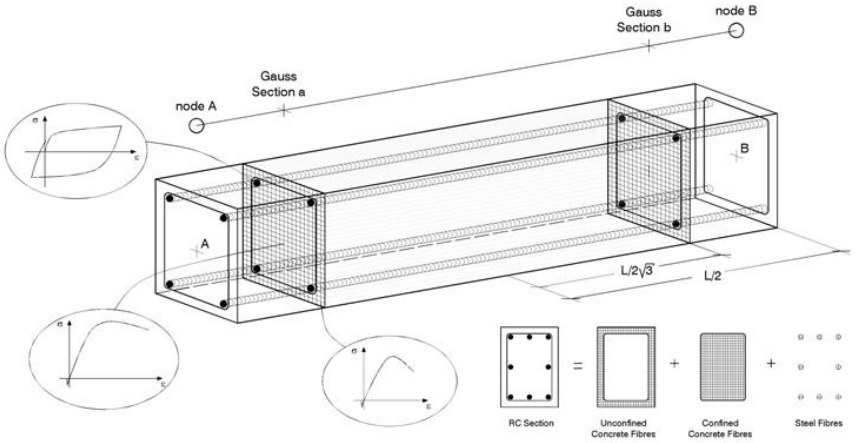

Fig. 3. Reinforced Concrete Section (Source: SeismoSoft v7.0, 2014)

3 BUILDING DESCRIPTION

The selected building prototype is a six storey masonry building located in Chittagong city corporation area. This building was considered as typical representative structure of RC frame with URM infill wall type in this region. The building has a trapezoidal identical plan having 10 ft storey height in each floor. The plan sketch and dimensions are given in Figure 4b. Material properties are taken as typical values used in past decade in Bangladesh (see table 1 and table 2).

Table 1. Material properties

Parameter	Value
Compressive strength of concrete (fc)	2900 psi
Tensile strength of steel (fy)	40000 psi
Unit weight of brick masonry	120 lb/ft3
Compressive strength of infill (fw)	145 psi

Table 2. Structural Details

Parameter	Value
Shorter length (L1)	44 ft
Larger length (L2)	57.67 ft
Width (W)	30 ft
Floor to Floor Height (H)	10 ft
Thickness of infill walls (tw)	6.3 in
Column 1 Column 2 Beam 1 Beam 2 Beam 3	12″x12″ 15″x12″ 14″x10″ 16.5″x10″ 16.5″x10″

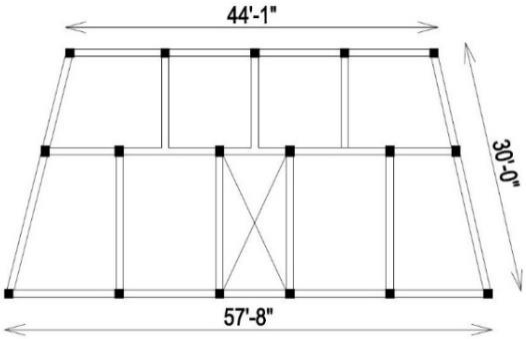

Fig. 4. (a) 3D view of the selected building, (b) typical floor plan

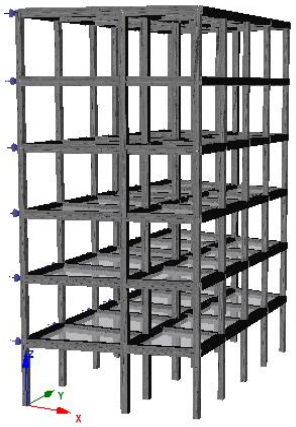

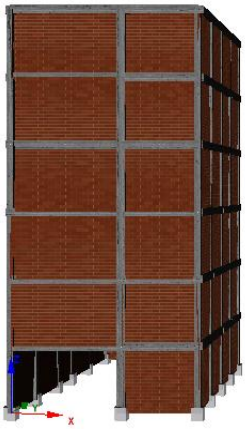

Fig. 5. (a) Bare frame model; (b) URM Infill frame model

4 CAPACITY SPECTRUM AND FRAGILITY CURVES

Capacity curves obtained from pushover analysis were used to identify expected damage level of the structure. Inverse triangular displacement pattern (similar to dynamic first mode shape of a structure) was used for the pushover analyses. Simplified method was used in this study to obtain damage state thresholds as shown in table 3. Seismic fragility function of structure defines the probability of physical damage as a function of ground motion intensity parameter. For a given type of building and damage state, these curves define the probability of equaling or exceeding a considered damage state for a given seismic action. The damage is quantified by the fragility curves which can be obtained from the following equation:

$$P[\mathrm{ds}|S_\mathrm{d}] = \Phi\left[\frac{1}{\beta_\mathrm{ds}}\ln\left(\frac{S_\mathrm{d}}{\overline{S}_\mathrm{d,ds}}\right)\right] \quad \ldots\ldots\ldots\ldots\ldots\ldots\ldots\ldots (3)$$

Where ϕ is the cumulative lognormal distribution, d is the expected damage, S_d is the spectral displacement and $S_{d,dsi}$ and β_{dsi} are the median values and standard deviations of the corresponding normal distributions. For simplicity we call $S_{d,dsi}$ as μ_i and β_{dsi} as β_i.μ_i is also called damage state threshold, and the probability of exceedance of the damage state d_{si} for $S_d = \mu_i$ is equal to 0.5. The following simplified assumptions allow obtaining fragility curves from the bilinear form of the capacity spectrum. Two assumptions were used as per Risk-UE project (Risk-UE 2004; Milutinovic and Trendafiloski 2003; Lagomarsino and Giovinazzi 2006) and used to estimate fragility curves in many studies. These are i) μ_i are related to the yielding and ultimate capacity points as in *t*able 3 and ii) the expected seismic damage follows a binomial probability distribution. The first assumption is based on expert opinion and relates the expected damage to the stiffness degradation of the structure; the second one is based on the damage observed in past earthquakes (Grünthal, 1998). Once capacity curve of the structure is calculated, it is useful to transform it into capacity spectrum by means of the pro*cedure proposed in the ATC-40*. The capacity spectrum is represented in spectral acceleration-spectral dis-

placement coordinates (s_a-s_d) and is often used in its simplified bilinear form, defined by the yielding point (D_y, A_y) and the ultimate capacity point (D_u, A_u), as it can be seen in Figure 6.

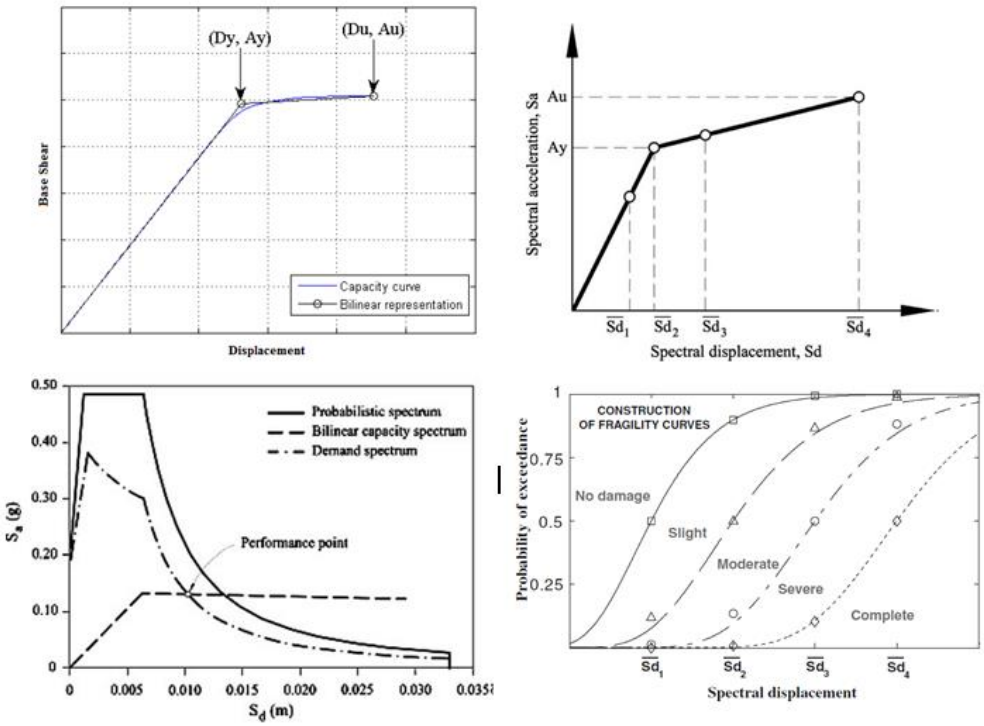

Fig. 6. a) & b) an example of capacity curve and its simplified bilinear form c) capacity spectrum performance and d) fragility curves for damage states

Table 3: Damage state thresholds according to the capacity spectrum

Damage State	Damage state thresholds
Slight (S_{d1})	$\mu_1 = 0.7D_y$
Moderate (S_{d2})	$\mu_2 = Dy$
Severe (S_{d3})	$\mu_3 = D_y + 0.25\,(D_u - D_y)$
Collapse (S_{d4})	$\mu_4 = D_u$

5 RESULTS AND ANALYSES

In order to compare the non linear static analysis results, same analysis performed for both RC building with URM infill and bare frame models. Equivalent static seismic loads were calculated following Bangladesh National Building Code guideline. Figure 7 and figure 8 represents comparison of seismic base shear and floor share distributions for both model, respectively. It was estimated that base shear for bare frame structure was 50.14 kips whereas that of structure incorporated with URM infill walls was 76.49 kips. Pushover analysis was performed by applying a controlled displacement (Response control) at the top of a particular frame.

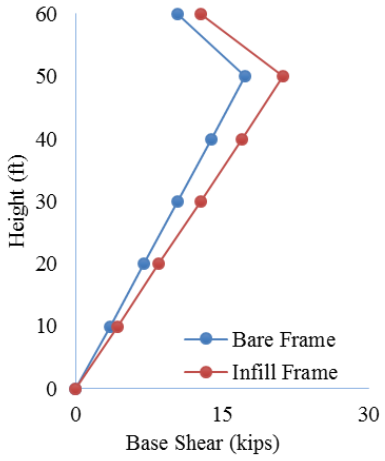

Fig. 7. Base shear distribution

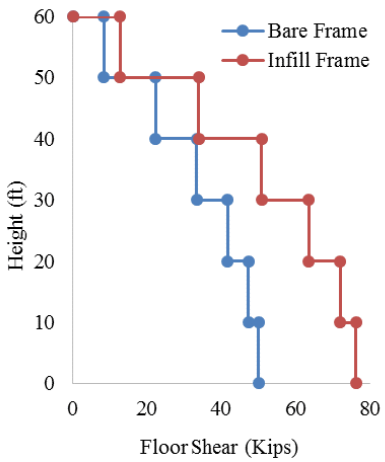

Fig. 8. Story shear distribution

Comparative results from pushover analysis for the case study building are shown in Figure 9. It was observed that initial stiffness in the infill frame is significantly higher than bare frame model. It revealed that lateral stiffness was increased due to the contribution of masonry infill walls. However, after first yield occurred capacity of infill frame dropped and first crush in confined concrete observed earlier in infill model in compare to bare frame model. Both yielding and ultimate capacity point were identified considering first yield and first crush in confined concrete member, respectively. Bilinear capacity curve was derived for the bare frame to obtain yielding point. Using definition of damage grades in table 3, fragility curves are obtained for both models in figure 12. To obtain standard deviation values for each limit state, compressive strength values range was considered from 2500 psi to 4500 psi with a variable of 500 psi and yield strength of steel was considered from 40 ksi to 60 ksi with a variable of 5 ksi.

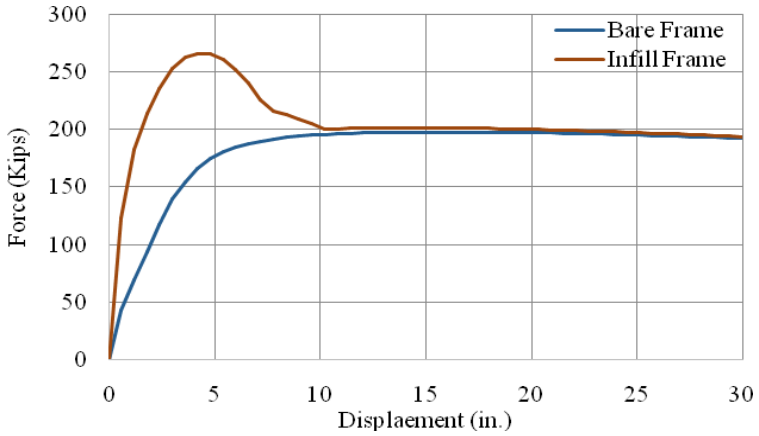

Figure 9: Comparison in pushover curves

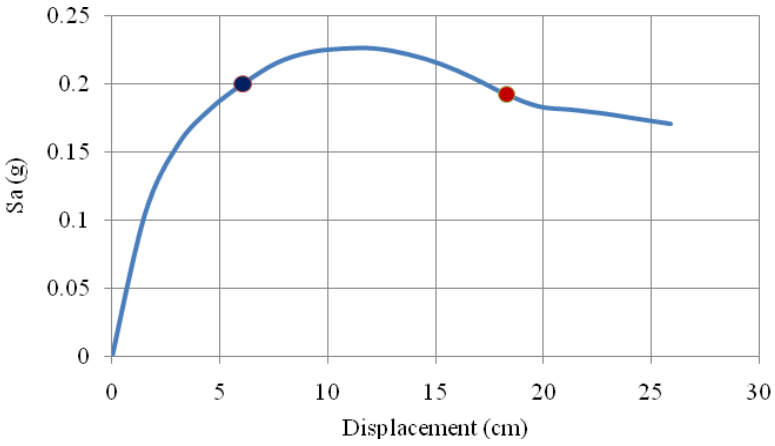

Figure 10: Capacity curve for Infill model

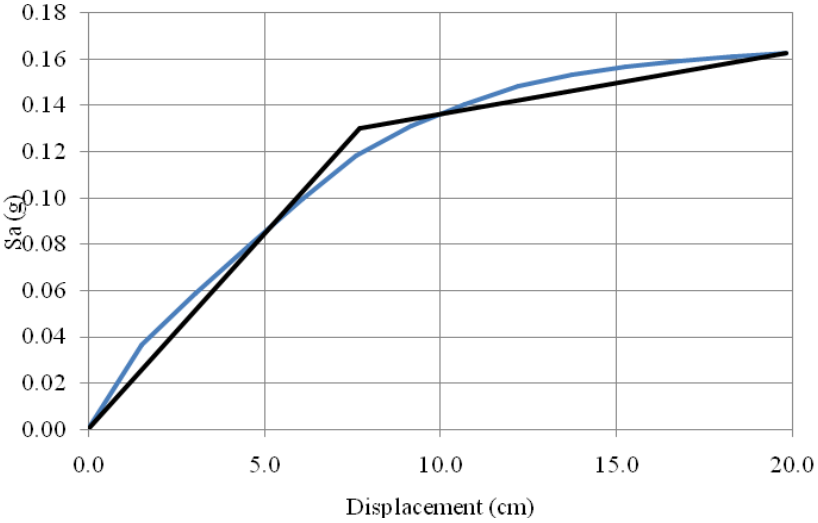

Figure 11: Capacity curve for bare frame model

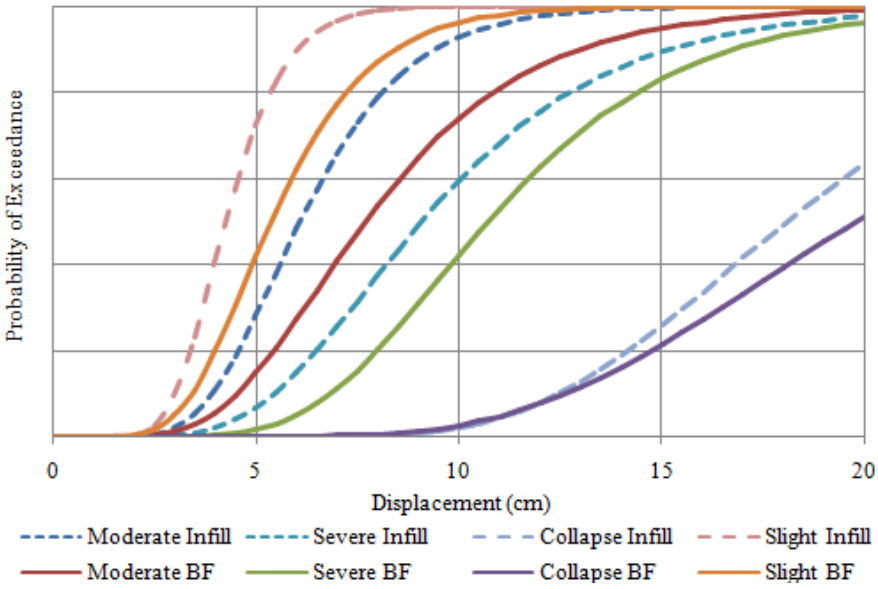

Figure 12: Fragility curves for both masonry infill model and bare frame model

6 CONCLUSIONS

The index building was a six story ordinary moment resisting RC frame with URM infill walls in Chittagong. Overall objective of this study was to derive fragility curves based on non linear static pushover analyses in terms of capacity spectrum. The results from the analysis have revealed the effect of masonry infill integration. Infill walls increases lateral strength of the building. Initial stiffness increased significantly whereas ductile behavior reduces if compared to bare frame model. Only a limited number of analyses were performed to obtain standard deviation parameter for each limit states, which is a limitation to calculate fragility curves.

7 ACKNOWLEDGEMENT

The authors would like to acknowledge Seismosoft for providing SeismoStructv7 academic license which was used in this study.

8 REFERENCES

Decanini L.,Mollaloli F., Mura A. and SaragoniR (2004) Seismic performance of masonryInfilledR/C Frames, *Proceeding of 13th World conference on Earthquake Engineering*. Vancouver, B.C., Canada.

Baran M., and Sevil T. (1981-1998,2010) Ana1ytical and experimental studies on infilled RC frames. *int. J. of the Physical Sciences*, 5(13).

Ellul, F.L. and D'Ayala, D. (2012). Realistic FE models to enable push-over nonlinear analysis of masonry infilled frames, *The Open Construction and building Technology Journal*, 6: 213-235, 2012.

Canadian Standards Association (CSA) (2004).Design of masonry structures (S304.1), Ontario, Canada.

New Zealand Society for Earthquake Engineering (NZSEE). (2006) Assessment and Improvement of the Structural Performance of Buildings in Earthquakes.

Crisafulli F.J. (1997) Seismic Behaviour of Reinforced Concrete Structures with Masonry Infills, *PhD Thesis*, University of Canterbury, New Zealand.

Blandon, C.A. (2005) Implementation of an Infill Masonry Model for Seismic Assessment of Existing Buildings, Individual Study, *European School for Advanced Studies in Reduction of Seismic Risk (ROSE School)*, Pavia, Italy, 2005.

Mainstone, R. J. and Weeks, G. A. (1970) The influence of bounding frame on the racking stiffness and strength of brick walls.*2nd International Brick Masonry Conference*, Stoke-on-Trent, UK.

Mainstone, R. J. (1971) On the stiffness and strengths of infilled frame. Proceedings, *Institution of Civil Engineers*, Supplement IV, 57–90.

Mander J.B., Priestley MJN, Park R. (1988) Theoretical stress-strain model for confined concrete. *Journal of Structural Engineering*, Vol. 114, No. 8, 1804-1826.

Martinez-Rueda JE. (1997) Energy Dissipation Devices for Seismic Upgrading of RC Structures. *PhD Thesis,* Imperial College, University of London, London, UK.

Elnashai A.S, Elghazouli AY. (1993) Performance of composite steel/concrete members under earthquake loading, Part I: Analytical model. *Earthquake Engineering and Structural Dynamics,* Vol. 22, pp. 315-345.

Mazumder R. K. (2015) Development of Seismic Fragility Curvesof Reinforced Concrete Building with URM Infill Walls in Bangladesh, *CERG-C 2014 Memoire Dissertation, Specialisation certificate in geological and climate related risk*, University of Geneva, Switzerland, February.

Mazumder R. K., Dey R. and Bhuiyan A. R. (2015) Structural Response Analysis of Reinforced Concrete Frame with Unreinforced Masonry Infill Walls, *International Conference on Recent Innovation in Civil Engineering for Sustainable Development (IICSD-2015)*.

D'Ayala, D. and Meslem. (2013) A. Draft Guide for selection of existing analytical fragility curves and Compilation of the Database, *GEM Technical Report,* GEM Foundation, Pavia, Italy.

Lantada N., Pujades L. G., Barbat L. H., (2008) Vulnerability index and capacity spectrum based methods for urban seismic risk evaluation. A comparison, *Springer Science+Business Media B.V.*, Nat Hazards (2009) 51:501–524, DOI 10.1007/s11069-007-9212-4 .

NCEED-CUET National Conference on Earthquake and Environmental Disasters, December 17, 2015, Chittagong, Bangladesh
Bhuiyan M. A. R., Pal S. K., Mazumder M. H., Mazumder R. K., Omi F. R. (eds.)

Use of Friction Damper in Seismic Performance Evaluation of Infill RC Building Frame

S. Das, M. J. Alam, M. A. R. Bhuiyan
Department of Civil Engineering, Chittagong University of Engineering & Technology, Chittagong, Bangladesh

M. H. Haque
Bangladesh Water Development Board (BWDB), Nilfamari

ABSTRACT: Damping systems are designed for physically limiting the forces in the structure and concentrating deformations in dissipative devices. A lot of energy is released during an earthquake. For a building with certain input energy, the demand on energy dissipation through inelastic deformation can be eliminated by using highly dissipative structural protective systems. The main objective of this study was to investigate the effectiveness of using friction dampers to control the structural responses of a multistoried RC building frame. A 10 storied building with a simple floor plan is taken into consideration. The lateral stiffness of the ground floor with columns only (without infill brick wall) was less than 70% of the adjacent first floor with columns and infill brick wall, ensuring the presence of a soft storey in the ground floor. Two separate cases were considered, the first being a conventional frame structure with in-filled brick wall and the second was a damping system with a friction damper in the ground floor. This improved model was then analyzed. Results indicate that the drifts of soft storey are reduced to an allowable limit and all the soft storey columns are safe under earthquake loads.

1 INTRODUCTION

In many residential buildings a soft storey exists in the ground floor due to parking or commercial space. Such a soft storey is an ideal place for providing damping system. Damping system is a kind of structural control system that introduces a stiff-ductile mechanism into the structure. By doing so, the structure becomes an assembly of rigid bodies moving in a defined pattern with internal forces limited by the yield level of the yielding shear panel device that are placed in the joints between the rigid bodies. Such an assembly dissipates almost all the input energy due to an earthquake in these devices through plastic yielding or friction.

Damping systems are designed such that they physically limit the forces in the structure and concentrate deformations in dissipative devices (YSPD). A lot of energy is released during an earthquake. For a building with certain input energy, the demand on energy dissipation through inelastic deformation can be eliminated by using structural protective systems. As a result of this approach, the building consists of several rigid parts connected by highly dissipative structural fuses. In this study, a 10 storey building with a simple floor plan is taken into consideration. The building is assumed to have a soft story in the ground floor. It is considered in two versions: First as conventional rigid frame structure with infill brick wall, second as a damping system with YSPD in between cross bracing in ground floor. This study presents relations between force, local stresses, and energy dissipation as limiting the storey drift. The results demonstrate again the superior performance and economy of a Damping system and its capacity to protect conventional rigid frame structure against earthquakes. Recent devastating earthquakes around the world have underscored the lack of understanding the way in which civil engineering structures respond to such loading. Earthquakes have demonstrated the vulnerability of many residential buildings. This is mainly due to poor construction practice and the application of insufficient design standards. Many of these buildings are wall bearing masonry buildings or

reinforced concrete frames and steel structures with masonry infill that have poor detailing and therefore this results in a collapse in a brittle fashion.

1.1 *Soft Storey*

Infill walls are built for architectural needs and aesthetical reasons in framed structures. In the ground floor, such walls are missing in some cases such as necessitates of parking or commercial space, resulting in occurrence of soft storey and a rigid body above. Often, walls and openings are placed in an unsymmetrical fashion which causes torsion in the building. Recent earthquakes have shown that a lot of buildings fail in the ground floor suffering from maximum base shear.

1.2 *Seismic Retrofitting of Structures*

Retrofitting of existing structures with insufficient seismic resistance are accounts for a major portion of the total cost of hazard mitigation. Thus, it is of critical importance that the structures that need seismic retrofitting are identified correctly, and an optimal retrofitting is conducted in a cost effective fashion. Once the decision is made, seismic retrofitting can be performed through several methods with various objectives such as increasing the load, deformation, and/or energy dissipation capacity of the structure (FEMA, 2000).

1.3 *Supplemental Energy Dissipation and Structural Control*

An alternative and often more cost efficient retrofitting strategy compared to base isolation is installation of supplemental energy dissipation devices in structures as a means for passive or active structural control (Housner et al., 1997; EERI, 1993; Constantinou and Symans, 1993; Symans and Constantinou, 1999; Soong, 1990; Soong and Dargush, 1997, FEMA, 2000). The objective of structural control is to reduce structural vibrations for improved safety and/or serviceability under wind and earthquake loadings.

Passive control systems reduce structural vibration and associated forces through energy dissipation devices that do not require external power. These devices utilize the motion of the structure to develop counteracting control forces and absorb a portion of the input seismic energy.

The severity of seismic demand on a structure is proportional to its stiffness and inversely proportional to its damping or energy dissipation capacity. Thus, installing supplemental energy dissipating devices in the structure reduces the seismic demand and results in increased safety of the structure and its contents from the damaging effects of earthquakes. In recent years, considerable attention has been paid to research and development of structural control devices, with particular emphasis on improving wind and seismic response of buildings and bridges. In both areas, efforts have been made to develop the structural control concept into a workable technology, and as a result, such devices have been installed in a variety of structures around the world. The most challenging aspect of vibration control research in civil engineering is the fact that this is a field that requires integration of a number of diverse disciplines, some of which are not within the domain of traditional civil engineering.

2 EXPERIMENTAL PROGRAMME

Modeling of a 10-storied soft storey RC building Using SAP-2000 was done here. At first the Stiffness of brick wall (including columns of 1st floor) & ground floor (only columns) was determined. Due to lower lateral stiffness (70%) of 1st floor than ground floor, it may be ensured as soft storey. Analysis of the building without damper was done. A Yielding Shear Panel Device (YSPD) as a requirement for damper system was designed. Then again analysis of the building with friction damper in the ground floor which is confirmed as soft storey. Comparison between building without damping system & building with damping system was also performed here.

2.1 *Design Approach*

To find the required damping system parameters, especially the relative stiffness of the YSPD & damping coefficient are selected.

2.1.1 *Yielding Shear Panel Device (YSPD):*

Schmidt and Dorka have proposed a simple yielding shear panel device, consisting of a short length of square hollow section (SHS) with a diaphragm plate welded inside it. The device is positioned between the braces and the main members of a braced frame, with the diaphragm lying in the plane of the frame, so that it is loaded in pure shear as the frame undergoes lateral deformation. Energy is dissipated through shear yielding of the diaphragm, which is restrained from buckling by the surrounding SHS. Tests have been performed on

devices based on a 120 × 120 × 4 mm thick square hollow section, with diaphragm plates between 1 and 4 mm thick.

Diagonal tension field that develops in the post-buckling regime of a thin steel plate under shear offers significant strength and ductility and hence can be utilized to dissipate energy. This concept led to the development of a new metallic passive energy dissipating device 'Yielding Shear Panel Device' (YSPD). YSPD was introduced by Williams and Albermani based on the design proposed by U.E Dorka at the University of Kassel, Germany to exploit the energy dissipative capability of steel plates through in-plane shear deformation and the concept was further explored by Schmidt et.al. and Williams and Albermani. YSPD relies on the in-plane shear deformation of a thin diaphragm steel plate welded inside a square hollow section (SHS). This device can be placed beneath a structural beam using a X-braceso that it automatically comes into play in the event of any horizontal excitation.

3 MODELING OF BUILDING

Concrete strength , f_c'	3000 psi
Steel strength ,f_y	60000 psi
Unit wt. of concrete	150lb/ft^3
Unit wt. of brick	120 lb/ft^3
Type of soil	S_3=1.5
Storey no.	10
Storey ht.	10 ft
Live load (roof slab)	42 psf
Live load (floor slab)	42 psf
Live load (stair)	100 psf
Floor finish	5 psf
Lime tracing(3") at roof	30 psf
Earthquake load	As per BNBC-93 code
Wind load	As per BNBC-93 code
Zone co-efficient	Z=.15g
Beam dimension	12"X18"
Column dimension at ground floor	14"X14" (exterior column) 16"X16" (interior column)
Column dimension from (1^{st} -9^{th}) floor	18"X18" (exterior column) 20"X20" (interior column)
Slab thickness	6 inch.
Stiffness of YSPD	K_{YSPD} = 242193 N/mm = 16600 k/ft = 1383 k/in.
Fundamental Time Period, T	0.94 sec.
Damping Coefficient	25%

3.1 *Lateral Stiffness at Ground Storey*

Total lateral stiffness along X-direction=673597 lb/in
Total lateral stiffness along Y-direction=673597 lb/in

3.2 *Lateral Stiffness at Upper Storey*

Total lateral stiffness along X-direction=27164620 lb/in
Total lateral stiffness along Y-direction=51568340 lb/in
Lateral stiffness of ground storey is 2.5% (<70%) of the adjacent upper storey in x- direction i.e. soft storey.
Lateral stiffness of ground storey is 1.3% (<70%) of the adjacent upper storey in y- direction i.e. soft storey.

3.3 *Critical Load Combinations:*

COMB.-3:.9DL+1.43 EQP/EQN
COMB.-4: .9DL+1.3WP/WN
COMB.-6: 1.4DL+1.4LL+1.4EQP/EQN
COMB.-7: 1.05DL+1.275LL+1.275WP/WN
COMB.-9: 1.05DL+1.275LL+1.4025EQP/EQN

3.4 *Storey Drift Limitation (as per BNBC-93):*

Storey drift is the displacement of one level relative to the level above or below due to the design lateral forces. Calculated storey drift shall include both translational and torsional deflections and conform to the following requirements:
Storey drift, Δ, shall be limited as follows:
$\Delta \leq 0.03h/R \leq 0.004h$ for $T \geq 0.7$ second
Where, h = height of the building
The allowable storey drift in storey -1=.03h/R=.03x30.5/8=.114m=114 mm

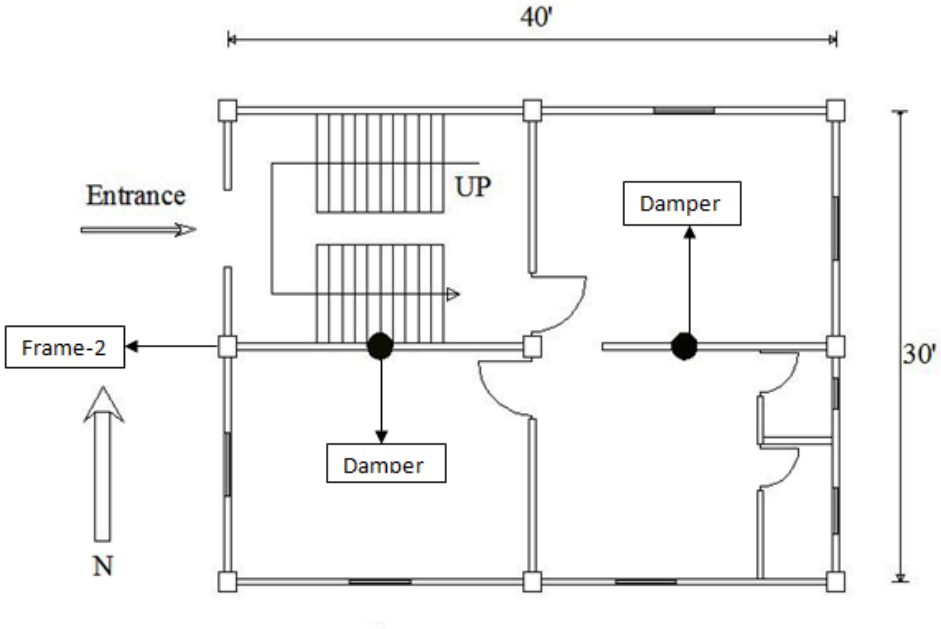

Figure 1. Plan of the building with Friction Damper Location

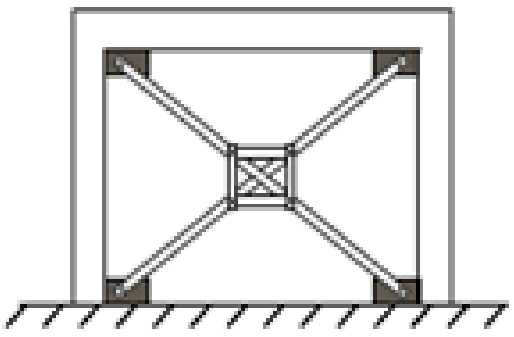

Figure 2. Friction Damper

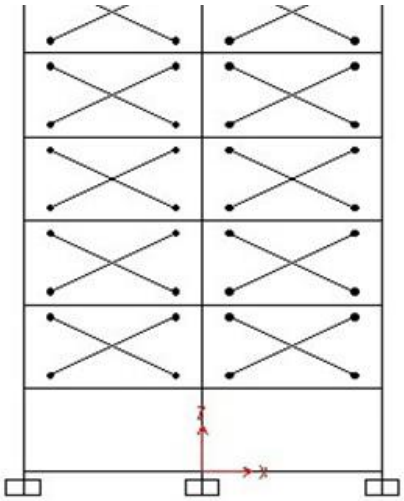

Figure 3. Elevation of Frame-2 with Equivalent Strut

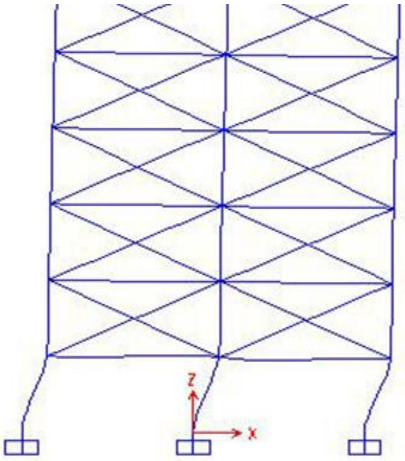

Figure 4. Deformed shape of frame-2 of after analysis due to EQ Load

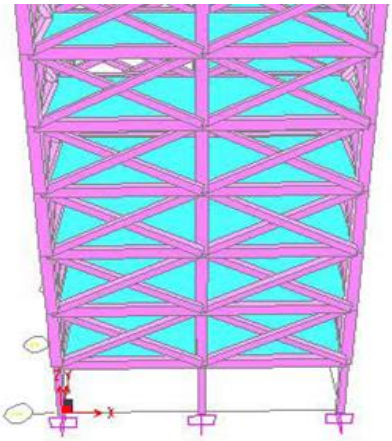

Figure 5. 3-D frame of the building
With Equivalent Strut

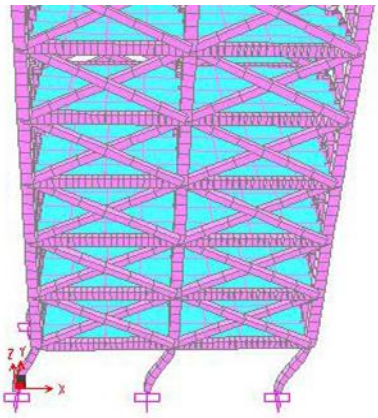

Figure 6. Deformed shape of 3-D frame of the building
after analysis due to EQ Load

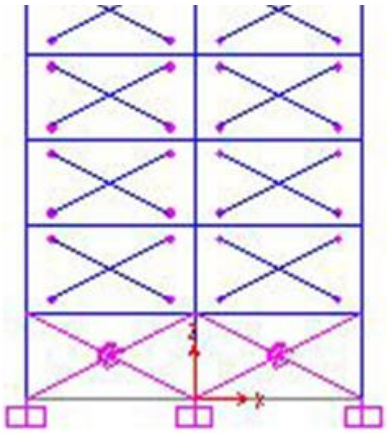

Figure 7. Elevation of Frame-2 with Friction Damper
placed at ground floor (soft storey)

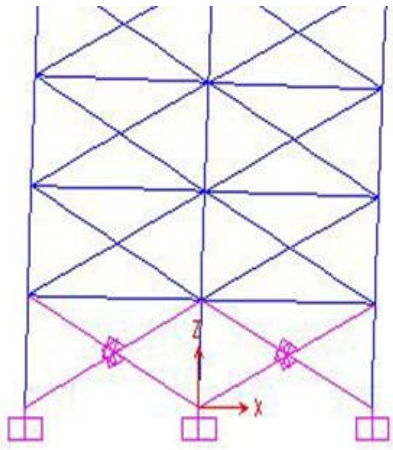

Figure 8. Deformed Shape of Frame-2 after Analysis with
Damper due to EQ Load

4 RESULTS AND DISCUSSIONS

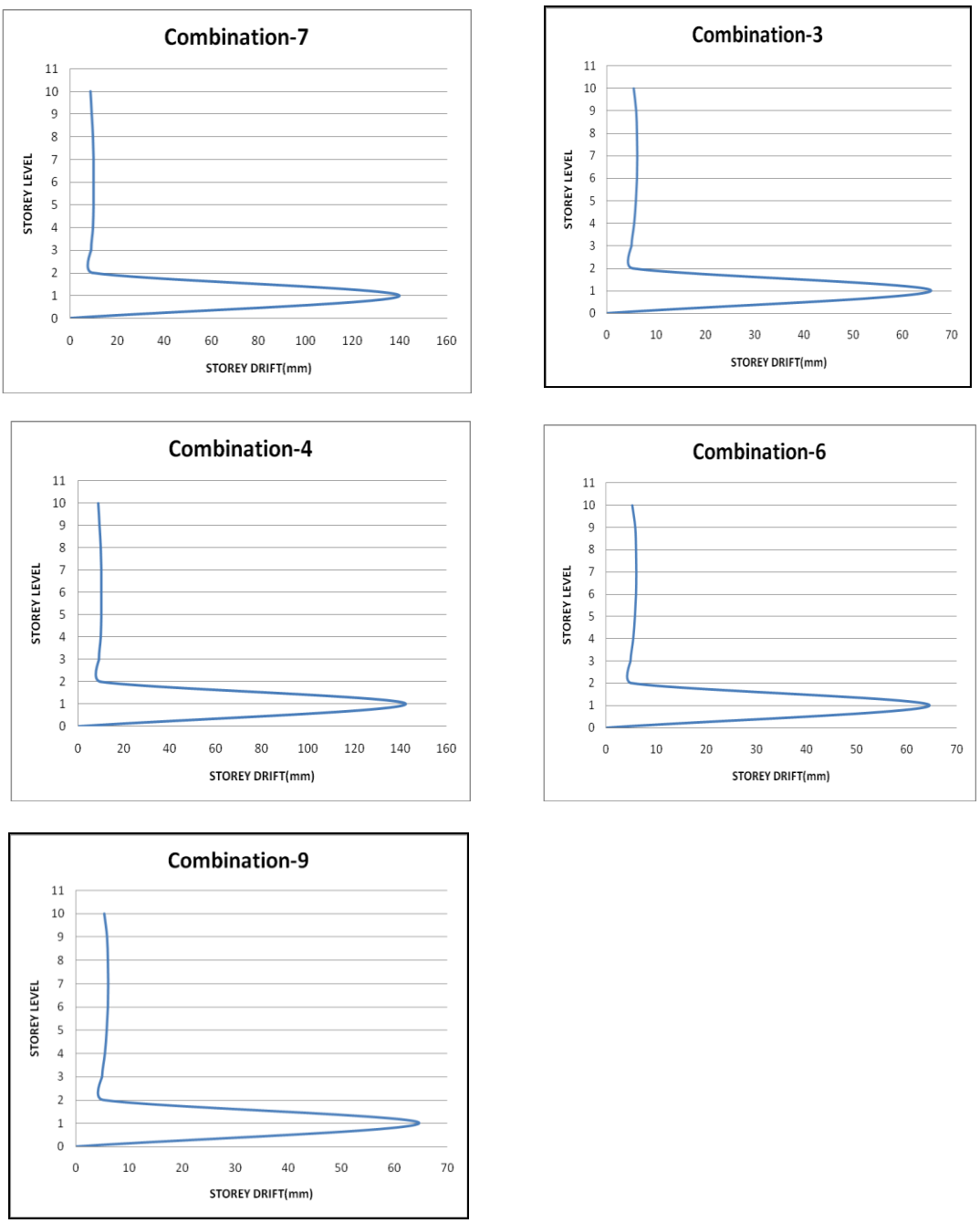

Figure 9. Storey Drift VS. Storey Level for various combinations without Friction Damper.

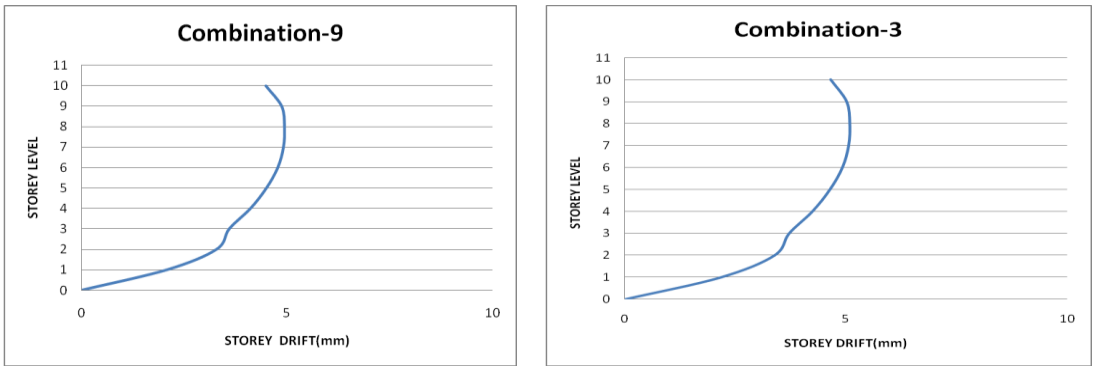

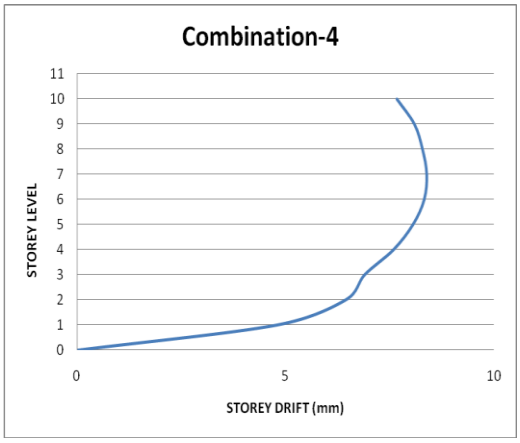

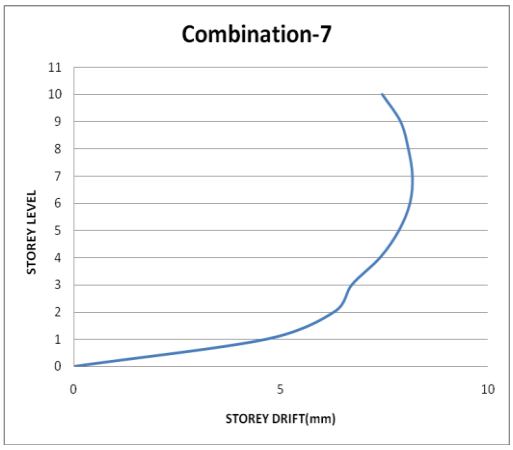

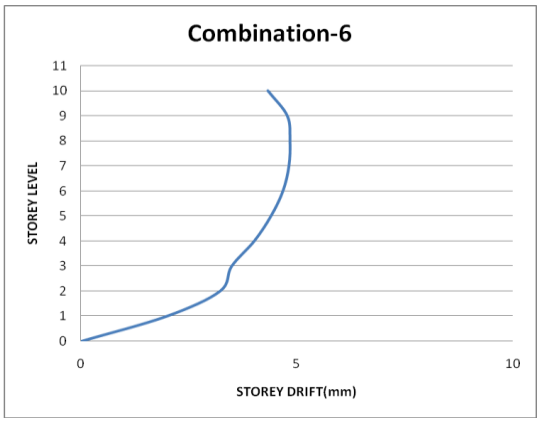

Figure 10. Storey Drift VS. Storey Level for various combinations with Friction Damper at GL.

5 CONCLUSIONS

- Conventional structures cannot be produced with the quality required for earthquake safety of large numbers of buildings due to a multitude of critical details: too much can and will go wrong.
- Structural control systems are superior in performance, reliability and price; and have become a viable alternative.
- Damping systems use passive control and may be used in new structures as well as in structural rehab.
- The damping system is of particular advantage providing a better performance and price for low to medium high residential or mixed residential-commercial buildings.
- The damping system is the most economical concept to retrofit soft storey buildings.
- After an extensive and systematic study following conclusions could be derived.
- A seismic design manual for reinforced concrete building with damping system is presented.
- After applying damping system the storey drift is reduced to an allowable limit provided by BNBC code.
- After applying damping system all the soft storey columns are safe under earthquake loads.
- An economic & efficient yielding shear panel device (YSPD) is used in this design.
- Overall performance of the structure is improved by the Damping system.
- Shears and deformations are also reduced by using this device.
- This leads to substantial savings when compared to conventional retrofitting (60% and higher).
- A model of damping system was simulated here by using friction damper, within which the Damping properties were included.

6 REFERENCES

ACI 318-02, “American Concrete Institute, Building Code Requirements for Structural Concrete and Commentary”. U.S.A

Agarwal.P.and Manish, S.K.,“Earthquake Resistant Design of Structures”,4th Edition, 2007, Prentice-Hall of India

BNBC, (1993), “Bangladesh National Building code”, Housing and Building Research Institute, Mirpur, Dhaka, Bangladesh

Corfu, Greece, 25–28 May 2011

IITK-GSDMA-EQ26, “Design Example of a Six Storey Building”, Dr. H. J. Shah and Dr. Sudhir K Jain .Kanpur

Md. Raquibul Hossain, Mahmud Ashraf, Faris Albermani School of Civil Engineering, The University of Queensland COMPDYN 2011 III ECCOMAS “Thematic Conference on Computational Methods in Structural Dynamics and Earthquake Engineering”, M. Papadrakakis, M. Fragiadakis, V. Plevris (eds.)

Nilson, H, and Winter George, “Design of Concrete structures”, 13th edition, 2003, Tata Mc Graw-Hill Company

Pall, A. S., and Marsh, C., "Friction Damped Concrete Shear Walls," Journal of American Concrete Institute, May~June, 1981

Smith, B.S. and Coull, A. (1991), “Tall Building Structures”, John Wiley & Sons, Inc

NCEED-CUET National Conference on Earthquake and Environmental Disasters, December 17, 2015, Chittagong, Bangladesh
Bhuiyan M. A. R., Pal S. K., Mazumder M. H., Mazumder R. K., Omi F. R. (eds.)

Numerical Modeling of Masonry Infilled RCC Structure Under Seismic Loading

S.R. Chowdhury, S. Zubair, R. Karim & R. Sarker
Ahsanullah University of Science and Technology, Dhaka, Bangladesh

ABSTRACT: Non-ductile RCC frames with masonry infill walls are a popular form of construction in seismic regions worldwide. The interaction of masonry units and the adjoining frame members may be insignificant during static load analysis procedure. However, when the same reinforced concrete frame undergoes lateral drifts due to dynamic forces, the behavior of the infill walls becomes noteworthy. But the design practices of RCC frames generally ignore the effects of infill walls as it is considered as a non structural element, due to the fact that, these structures exhibit a highly nonlinear inelastic behavior resulting from the interaction of the masonry infill panel and the surrounding frame, which makes the modeling of this structure complicated. In this study, comparing methods of modeling in-filled frame structure on the basis of displacements, width ratios, amount of deflections etc have been discussed but recommend the use of Pauley & Priestley relation.

1 INTRODUCTION

In-filled frame structures are commonly used in buildings, even in those located in seismically active regions. Present codes unfortunately, do not have adequate guidance for treating the modeling, analysis and design of in-filled frame structures. As a result, treating infill as a non-structural component is a common practice in the seismic analysis and design of low rise buildings in developing countries. The contribution of the infill to the lateral strength and stiffness of a structure is disregarded in the current seismic codes used in these countries. These codes do not have adequate guidance due to insufficient research information on the complex seismic response of infill frame structures and due to the wide variation of opening sizes and material properties of the infill. Despite large amount of research performed in this field both experimentally and numerically in the last few decades, present seismic codes provide limited guidance which may not be adequate for the varying properties of infill.

Several methods have been developed on modeling infills, and they are grouped in two main categories: macro-models, based on the equivalent strut method, and micro-models, based on the finite element method. The main advantages of macro-modeling are computational simplicity and the use of structural mechanical properties obtained from masonry tests, since the masonry is a very heterogeneous material and the distribution of material properties of its constituent elements is difficult to predict. Holmes (1961) was the first in replacing the infill by an equivalent pin-jointed diagonal strut. Smith and Carter (1969) proposed a theoretical relation for the width of the diagonal strut based on the relative stiffness of infill and frame. Alternative proposals were Liaw and Kwan (1984), and more recently by Paulay and Priestley (1992), Cavaleri and Papia (2003). On the other hand, micro-modeling is a more complex method based on dividing the masonry panel and the concrete frame into several elements. This modeling can provide an accurate computational representation of both material and geometrical aspects, but is too time-consuming to be used in large and practical-oriented analysis.

Conducted study compares the results of these experimentally and numerically performed researches with respect to width ratio of the strut, inter storey drift ratio, deflections etc. and indicates the most reasonable approach in modeling and analysis of the infill. The result of the conducted study may be helpful in further study of the topic, which may pave the way towards the improvement of the prevailing codes regarding the modeling, analysis & design of in-filled frames.

2 MODELING OF BUILDING

In this study, a 3D reinforced concrete moment resisting building has been analyzed. The plan view of the model we have analyzed is shown in the Figure 1.The frame was kept fixed at the bottom. The columns were taken to be square to simplify the analysis. The columns and beams of the frame were modeled using two-noded frame or beam elements. Masonry infill walls were modeled as:

- Equivalent diagonal struts using two nodded beam elements.
- Finite elements using shell elements.

The effect of unreinforced masonry infill is modeled with equivalent strut model as mentioned earlier in the literature review. Two other models, an RCC bare framed structure and framed structure in filled with brick work, is also analyzed to compare the displacement results found from the equivalent strut model. An eleven storied building modeled with equivalent strut (Figure 2) as well as a bare frame model and a brick in-filled model is generated in this study. Here in the model, no doors and windows have been used to simplify the result and to avoid any unwanted results.

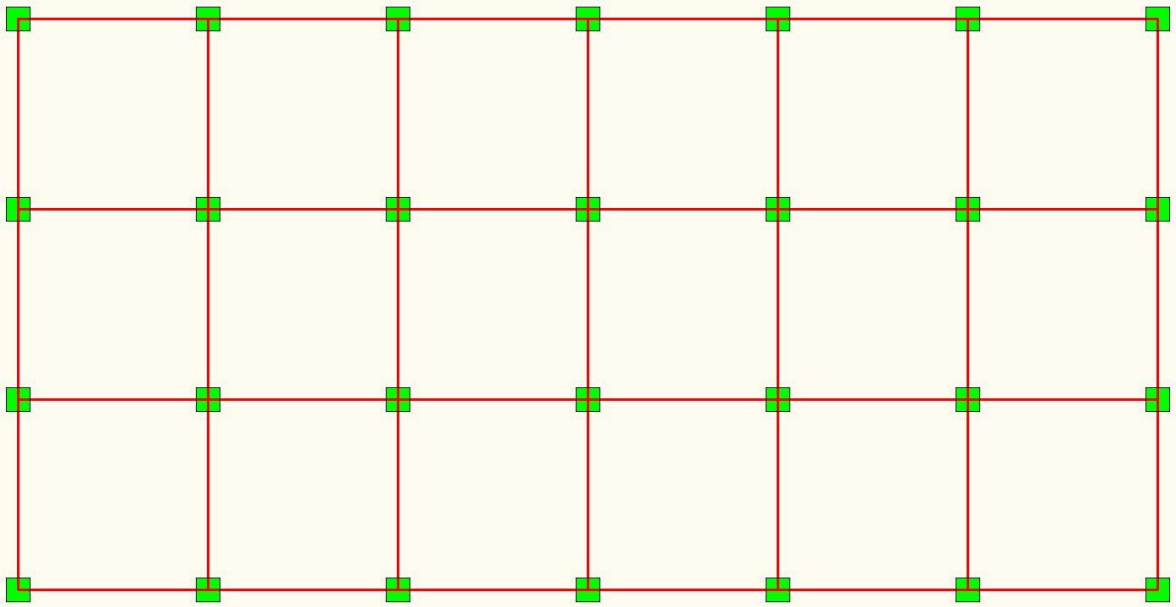

Figure 1. Plan at a typical storey of the example building considered in the study.

For modeling frame in the study, the following material properties and geometrical properties have been used for beams, columns, masonry infill. Values of elastic moduli of concrete and masonry are taken as 30×10^6 psi and 4.5×10^6 psi respectively. Poison's ratios for concrete and masonry are taken as 0.2 and 0.19 respectively. The unit weights of concrete and masonry are taken as 23.56 kN/m^3 and 18.88 kN/m^3. The live load, floor finish and partition wall load was taken as 60 psf, 40 psf and 70 psf respectively. The cross sectional area of column and beam was taken 18"×18" and 18"×16" respectively. Infill walls and slabs are modeled as 10" and 6" thick respectively for all models. Wind speed has taken 210 km/hr.

2.1 *Case Study*

Case 1: An eleven storied building has been analyzed using different widths of equivalent strut.
Methods used to find the strut's width are:

1. Holmes's method
2. Smith & Carter's method
3. FEMA 273 method
4. Liaw & Kwan's method
5. Pauley & Priestly's method.

Case 2: An eleven storied building frame has been analyzed which was in-filled by brick work.
Case 3: An eleven storied building has been analyzed as a bare frame.

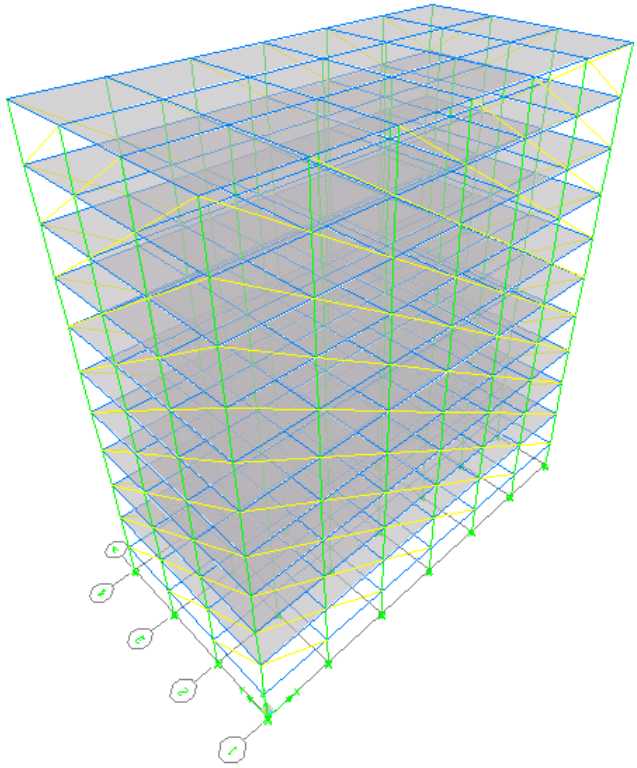

Figure 2. An eleven storied building frame modeled with equivalent strut 3D view from ETABS.

2.2 *Variation of width of equivalent diagonal strut*

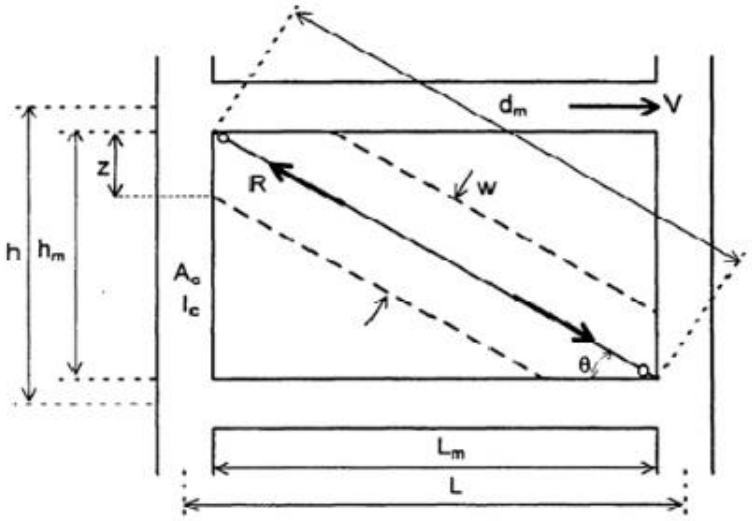

Figure 3. Effective width of diagonal strut.

The first approximation to calculate the width of the equivalent sturt was proposed by Holmes, in the lack of experimental data, assuming that:

$$w=d_m/3 \quad (1)$$

where d_m, is the diagonal length of the masonry panel. Later, Stafford Smith conducted a large series of tests using infilled steel frames and proposed different charts to calculate the equivalent width "w". And he defined it by:

$$\lambda_h=\sqrt[4]{((E_m\ t\ \sin 2\theta)/(4E_c\ I_c\ h))} \quad (2)$$

In the equation, t and h_m are the thickness and the height of the masonry panel, respectively, Θ is the inclination of the diagonal of the panel. E_m and E_c are the modulus of elasticity of the masonry and the concrete, respectively, and I_c is the moment of inertia of the columns.

Pauley and Priestley pointed out that a high value of w will result in a stiffer structure, and, therefore potentially higher seismic response. They suggested a conservative value useful for design proposal, given by:

$$w=0.25d_m \quad (3)$$

Mainstone and Liaw& Kwan proposed the following equations based on experimental and analytical data, respectively. FEMA 273 adopted Mainstone (1974) suggested model to calculate the strut width. The expressions from Mainstone (1974) & Liaw & Kwan (1984) are:

$$w=0.16\lambda_h^{(-0.3)}\, d_m \quad (4)$$
$$w=(0.95h_w \cos\theta)/\sqrt{(\lambda_h)} \quad (5)$$

Different widths for equivalent strut have been found, from different methods for calculating widths. These different values of widths are shown in the table 1.

Table 1. Different values of width

Serial no.	Methods	Width (m)
1	Smith & Cartar	5.21
2	Pauley & Priestley	1.27
3	FEMA 273	0.575
4	Holmes	1.702
5	Liaw & Kwan	1.22

3 RESULTS AND DISCUSSIONS

3.1 *Variation of displacements at different story levels for different cases*

The graphs comparing the displacements at different storey levels from the analysis for different cases are given in Figures 4 and 5. In these figures BW stands for Building frame in-filled by Brick Work, BF stands for building of bare frame.

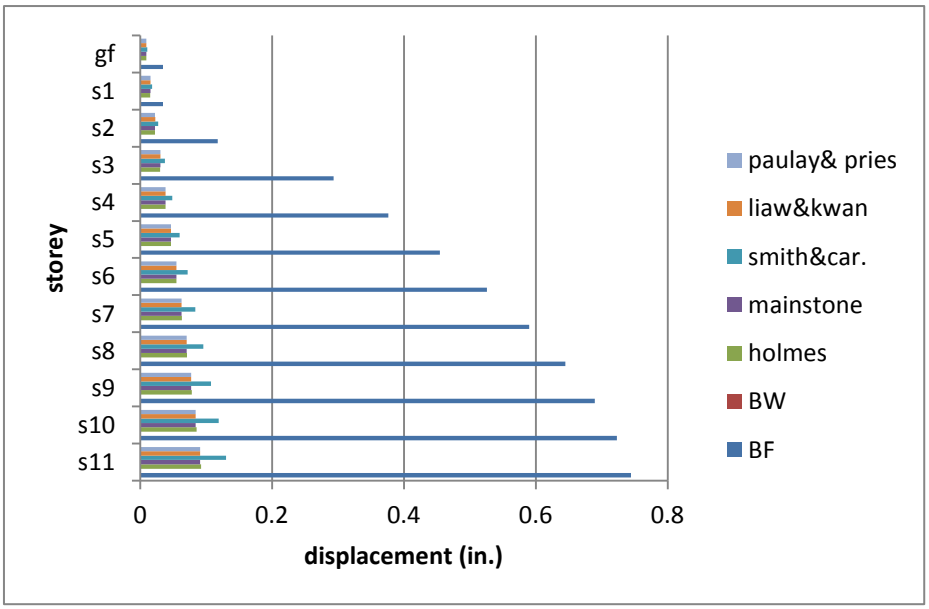

Figure 4. Total lateral displacement profile for different building models along X direction.

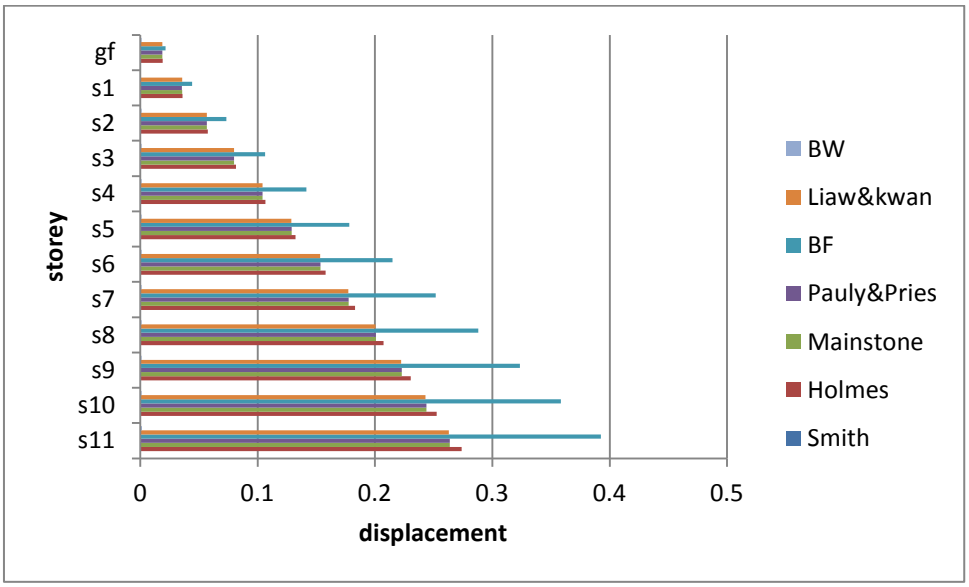

Figure 5. Total lateral displacement profile for different building models along Y direction.

The graphs comparing the storey drifts at different storey levels from the analysis for the different cases are given in the Figures 6 and 7.

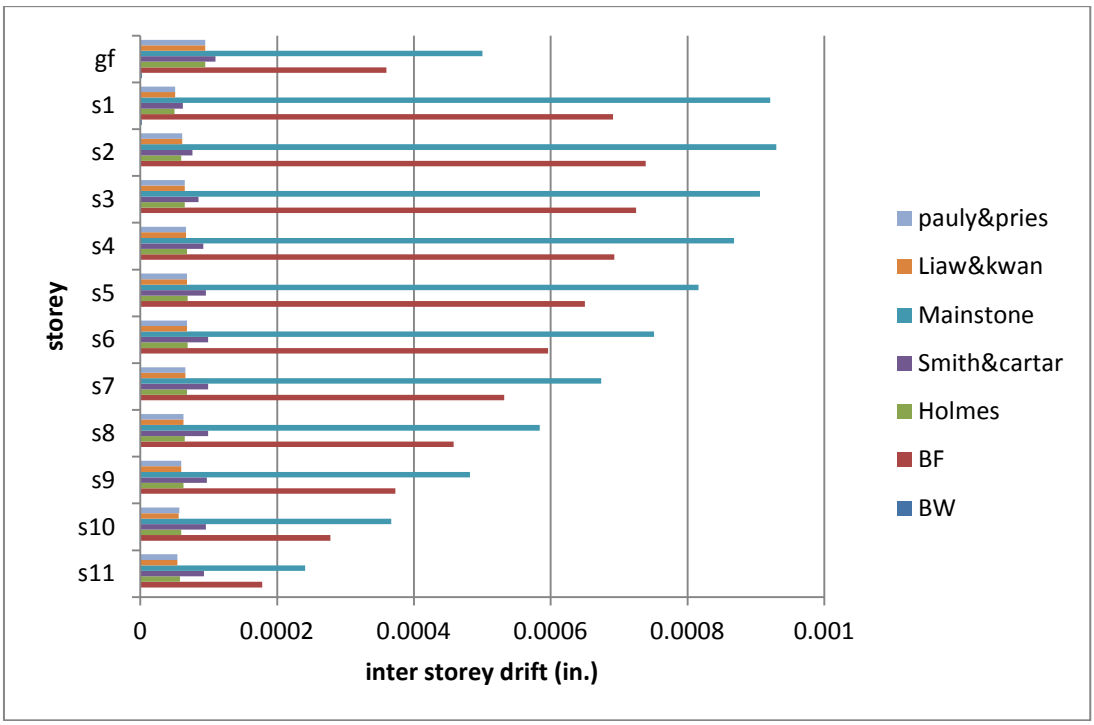

Figure 6. Total storey drift profile for different building models along X direction.

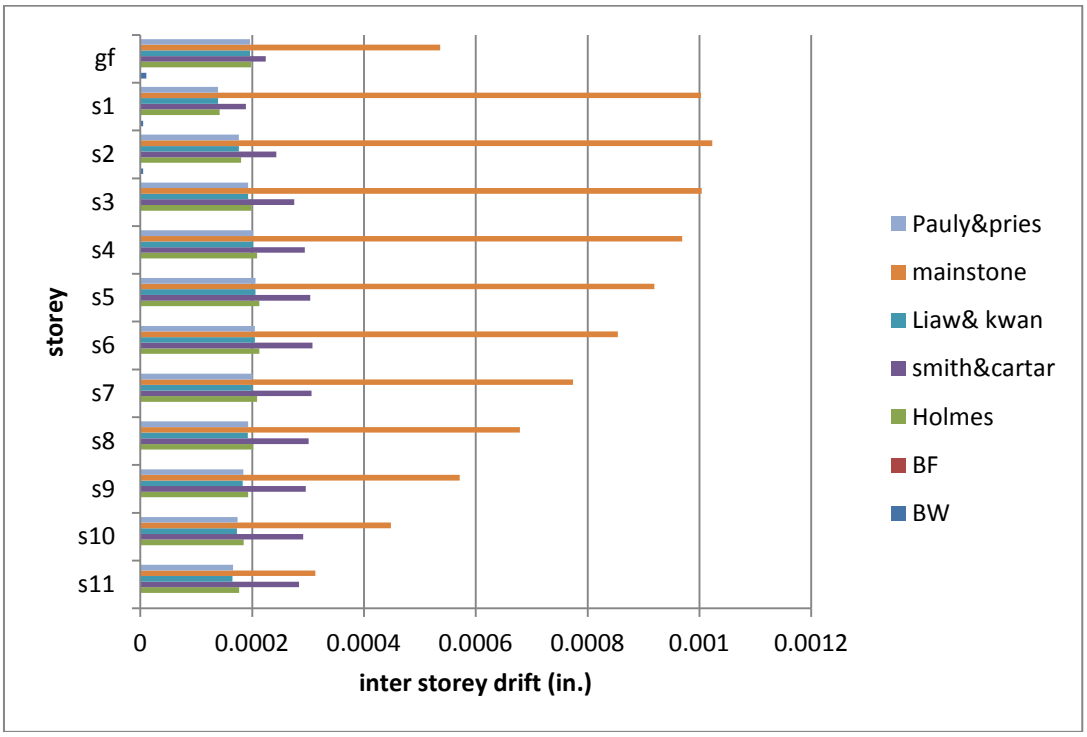

Figure 7. Total storey drift profile for different building models along y direction.

Table 1 shows the variation of values among different approaches of determination of width of equivalent strut. From these values it is seen that, Smith & Cartar relation yields the maximum value of width where Mainstone's relation yields the lowest width for equivalent strut. Values from Holmes's relation and Pauley & Priestley's relation are close, due to the fact that, both of the expressions are pretty similar.

Figures 4 & 5 show that, the bare frame model has the maximum displacement at all storey levels in both directions and the brick wall model has the minimum displacement at all storey levels in both directions. The bare frame model and the brick in-filled model are included in the figures to show the comparison of each method with respect to these two models. From these figures it is seen that, the other methods yield somewhat closer values of displacement.

4 CONCLUSIONS AND RECOMMENDATIONS

It can be concluded from the study that, the masonry infills, although do not interfere in the vertical load resisting system for the RC frame structure, they significantly affect the lateral load-resisting system of the same structure. And among all the modeling approaches of masonry infills available in literature, Smith and Carter's method gives the high value and FEMA gives the least value for the width of the equivalent diagonal strut. Whereas the methods proposed by Paulay |& Priestleyand Liaw & Kwan give intermediate values for the width. Among all the methods available in literature, Paulay and Priestley's method is the simplest of all the methods as its formulation is only 0.25 times the diagonal length of the masonry infill and do not give due considerations to the characteristics of the masonry infill. And due to that simplicity and as it gives an approximate average value (among those studied), this study reveals that Pauley and Priestley's equation is the most suitable choice for calculating the diagonal strut width among all other different expressions.

As only symmetrical building is analyzed, there are also many scopes for further study covering other possible cases. In this case the followings may be concerned:

- In this study finite element software ETABS 9.7.0 is used. There are also some other finite element softwares such as STAAD-PRO, ANSYS etc to analyze this kind of study.
- Brick walls and equivalent struts at every storey of the building to simplify the study have been considered. But a more realistic modeling is always possible with the inclusion of doors & windows in the model.
- For the present study, the analysis was performed for the symmetrical building to avoid torsional response under pure lateral forces. Further studies can be performed for the non-symmetrical buildings.
- Only linear analysis is made in this study. To make comprehensive and complete comment non-linear dynamic analysis is highly recommended.

5 REFERENCES

Holmes M. 1961. Steel frames with brickwork and concrete infilling. *Proceedings of the Institution of Civil Engineers*.

Liaw, T.C & Kwan K.H. 1984. Nonlinear behaviour of nonintegral infilled frames. *Comput Struct*, 18: 551-560.

Mainstone, R. J. 1974. Supplementary notes on the stiffness and strength of Infilled frames. *Proc .of Institution of Civil Engineers supplement IV*, 57-90.

Pauley, T. & Priestley, M. J. N. 1992. Seismic design of reinforced and masonry buildings. *USA:Wiley Interscience Inc*.

Papia, M., Cavaleri, L. & Fossetti, M. 2003. Infilled frames: developments in the evaluation of the stiffening effect of infills. *Structural Engineering and Mechanics*, 16:6, 675-693.

Smith, S. B. & Carter, C. 1969. A method of analysis for infilled frames. *Proc. of Institution of Civil Engineers Part 2*, 44, 1969:31-48.

NCEED 2015 -National Conference on Earthquake and Environmental Disaster; December 17, 2015; CUET, Chittagong, Bangladesh
Bhuiyan M. A. R., Pal S. K., Mazumder M. H., Mazumder R. K., Omi F. R. (eds.)

Comparative Study on Tensile Strength of Concrete Obtained from Different Test Methods

Sanjoy Roy, Md. Arafat Ul Islam & Md. Maksimul Islam
Department of Civil Engineering, Bangladesh University of Engineering & Technology, Dhaka, Bangladesh

ABSTRACT: This study attempts to investigate the relationship between the tensile strengths obtained from two different test methods (Flexure test and Split cylinder test). This study has adopted three test methods commonly used in practice along with compression test on the cylinder to correlate the obtained tensile strength with compressive strength. In this experimental study, two different types of coarse aggregates (Brick and Stone) were used to observe the variation of their effect on tensile strength of concrete. Sylhet sand was used as fine aggregate in all cases. Three different mix ratios (1:2:4, 1:1.5:3 and1:1.25:2) were considered in this experimental study. Experiments have also been conducted on six concrete beams to determine the tensile strength of concrete in bending (modulus of rupture). In all cases, Portland Composite Cement (PCC) has been used and w/c ratio was kept constant at a value of 0.5. The results obtained from the experiments produced correlation among different parameters. The Modulus of Rupture was found to be 1.25 times higher than the corresponding split cylinder strength for concrete with brick aggregates and 1.50 times higher than the corresponding split cylinder strength for concrete with stone aggregates.

1 INTRODUCTION

The tensile strength of concrete is one of the most important property yet most neglected feature during the design stage of any structure. As there is no standard method of obtaining the true tensile strength of concrete, we have to depend on the Flexure test and Split cylinder test for the value. In the practical case, the situation may not directly reflect the flexural tensile and split tensile strength, in that case, the tensile strength value should be lowered than usual value. Tensile strength is needed in designing water retaining structures, runway slabs, pre-stressed concrete members, bond and shear failure of reinforced concrete members and cracking of mass concrete works. Moreover, cracking plays an important role in the durability of RC structures. When concrete cracks, its permeability increases and the processes of concrete deterioration and rebar corrosion get accelerated [1, 2].

For flexural element, the tensile strength is the reason for cracking rather than compressive strength. But this tensile strength varies with the aggregate type and mix ratios. Moreover, researchers have argued that, because of the significance of shrinkage on the serviceability of RC structures, other cracking criteria, such as the direct or indirect tensile strength of concrete, should be used as evidence of concrete cracking [3]. Three methods are commonly used to measure concrete cracking strength: flexural, splitting, and direct tension test. While the flexural strength test and splitting tensile strength test can be conducted in accordance with the American standard test method (ASTM), ASTM C 78 [4] and ASTM C 496/C 496M [5], respectively, ASTM has no recommendations for direct tension test of concrete, as it is challenging to ensure that uniaxial stress along the specimen is evenly applied [6]. Here, brick and stone aggregate has been used as coarse aggregate. Both values of flexural strength and splitting tensile strength for different mix ratios are lower for brick aggregate and higher for stone aggregate. The tensile strength trend to have an increasing order with leaner to richer mix.

The Modulus of Rupture is 1.25 times higher than the corresponding split cylinder strength for concrete with brick aggregates. The Modulus of Rupture is 1.505 times higher than the corresponding split cylinder strength for concrete with stone aggregates.

2 MATERIALS AND METHODOLOGY

2.1 Cement and aggregates

Portland Concrete Cement (PCC) was used and in this study both stone and brick chips were used as coarse aggregate with range of size between ¾'' to 0.187''. Sylhet sand was used as fine aggregate with sieve size between mesh no 4 to mesh no 100.The coarse aggregates were properly washed and removed salinity as possible. Unit weight of sand, stone, brick and cement was 37.83 kg/cft, 39 kg/cft, 27.08 kg/cft, 33.41 kg/cft.

2.2 Mold preparation

Experiment was conducted over 18 (4" x 8") concrete cylinders, 18 (6" x 12") concrete cylinders and 6 (3' x 10" x 6").

2.3 Mix proportion

Mix ratio maintained was 1:2:4, 1:1.5:3 and1:1.25:2 as cement: fine aggregate: coarse aggregate. In this study, water to cement (w/c) ratio was kept at a constant value of 0.5.

2.4 Curing

Curing was done in open space though ASTM standard suggests to cure the concrete in lime mixed water with temperature of 27 degree Celsius. But in this project, curing was done by covering the sample with rugged wet sack and applied normal water for 30 days. In case of direct tensile strength test, epoxy coating was applied in the specimen and kept for hardening for 30 days.

2.5 Test Methods

Compressive Strength: The load was applied continuously and without shock at a rate of 20 to 50 psi/second and the ultimate load was recorded. Compressive strength is calculated by dividing maximum load (P) by cross-sectional area of cylinder (A).

Compressive Strength = P/A

Flexural strength: The flexural strength is expressed as Modulus of Rupture (MR) in psi/MPa and is determined by standard test methods ASTM C 78 [13] (third-point loading) or ASTM C 293 (center-point loading). In this experiment third-point loading method has been carried out.
Modulus of rupture was calculated from following formula;

$R= PL/bd^2$

whereR = Modulus of rupture, psi
P = maximum applied load indicated by the testing machine, lb.
L = span length, in
b = average width of the specimen at the fracture, in
d = average depth of the specimen at the fracture, in
Splitting Tensile Strength: The split cylinder test is also a measure of testing tensile strength of concrete. This test was done in compliance with ASTM standard C 496/C for testing splitting tensile strength of concrete. The split tension test is conducted by loading a cylindrical concrete specimen along its length.

Split tensile strength = $2P/ (\pi LD)$

HereP = load applied
L = length of the specimen
D = Diameter of the concrete cylinder
Π = Pi

3 RESULT AND DISCUSSION

Compressive strength shows increased order following mix ratio 1:2:4, 1:1.5:3 and 1:1.25:2. It is due to concrete mix is richer with mix ratio. It was different for the variation of aggregate types such as brick and stone aggregate (Figure 1). Fracture type was mainly shear failure. Concrete containing smooth gravels began to crack at a lower compressive stresses than concretes containing rough textured aggregate.

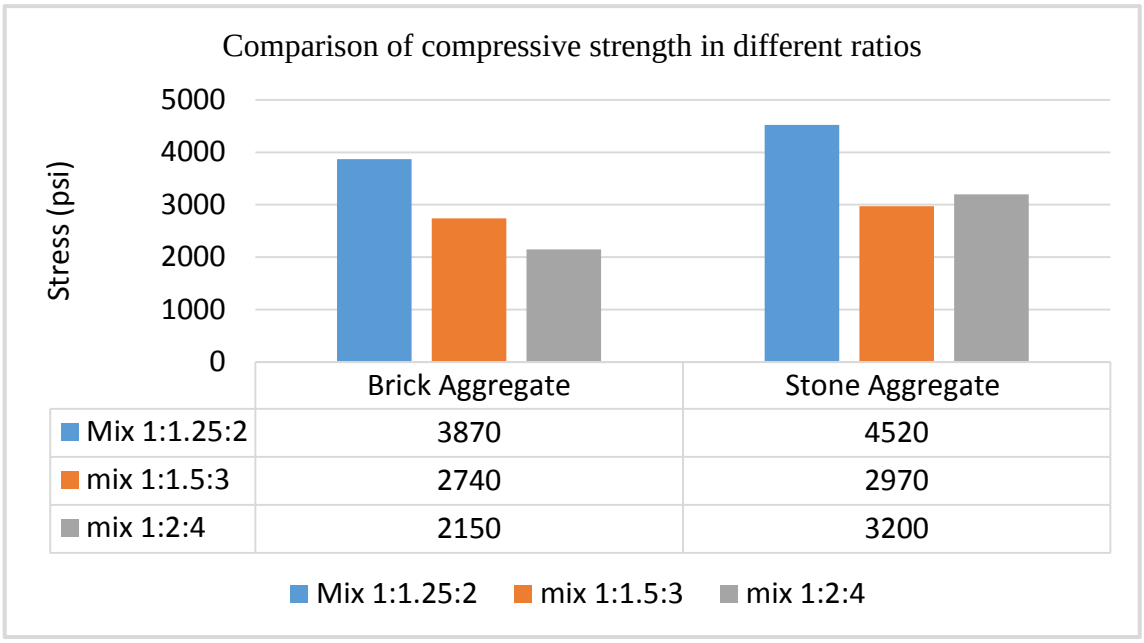

Figure 1. Compressive strength comparison between brick and stone aggregate.

Splitting tensile strength is a measurement of tensile strength of concrete. Experimental investigation shows that it increases with richer concrete mix. The tensile strength also differs with aggregate type, brick and stone chips. The tensile strength of concrete specimen found from brick aggregate was lower than that of stone aggregate. In brick specimen concrete failure was mainly combined with crack of specimen while on the other hand, mortar failure occurred in cylinder having stone aggregate. As mortar failure occurred in the periphery of the stone aggregate more strength is needed to fail the specimen. Thus stone aggregate has higher splitting value than brick aggregate.

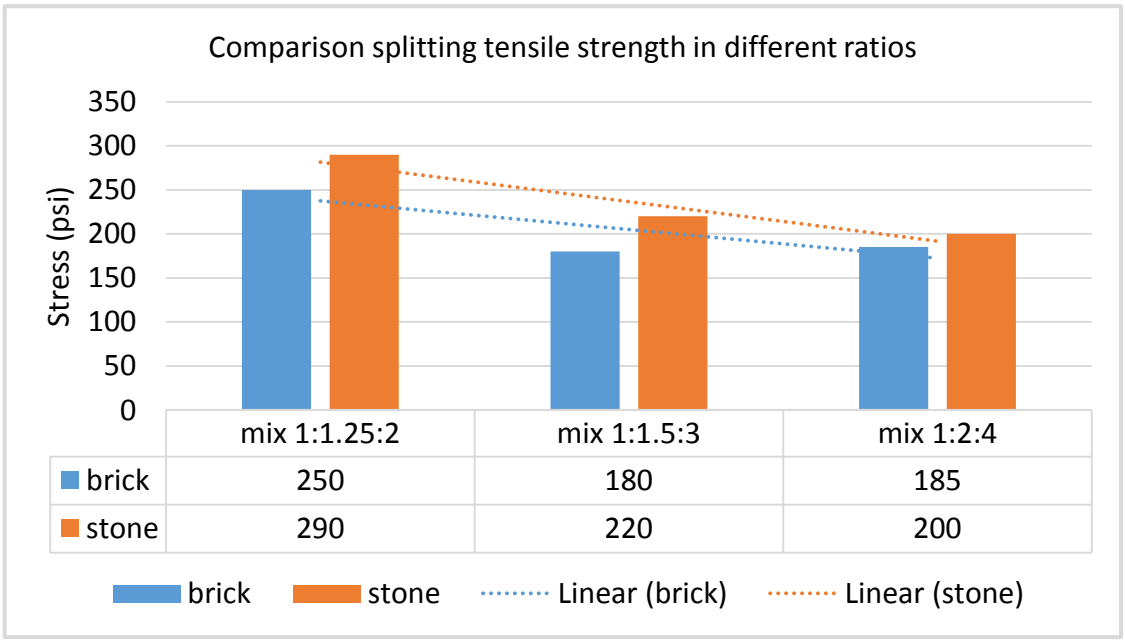

Figure 2. Comparison splitting tensile strength.

The ideal method for determination of tensile strength of concrete is the flexural test, since it matches the real life situation in concrete flexural members. A simply supported beam specimen of concrete is loaded on two equidistant points from the ends. The crack should occur at mid-point of the section. Like splitting tensile strength, the value of modulus of rupture of concrete using stone specimen is larger than that of brick specimen. The mix ratio of 1:1.25:2 has the highest value of modulus of rupture regardless of the type of aggregates used.

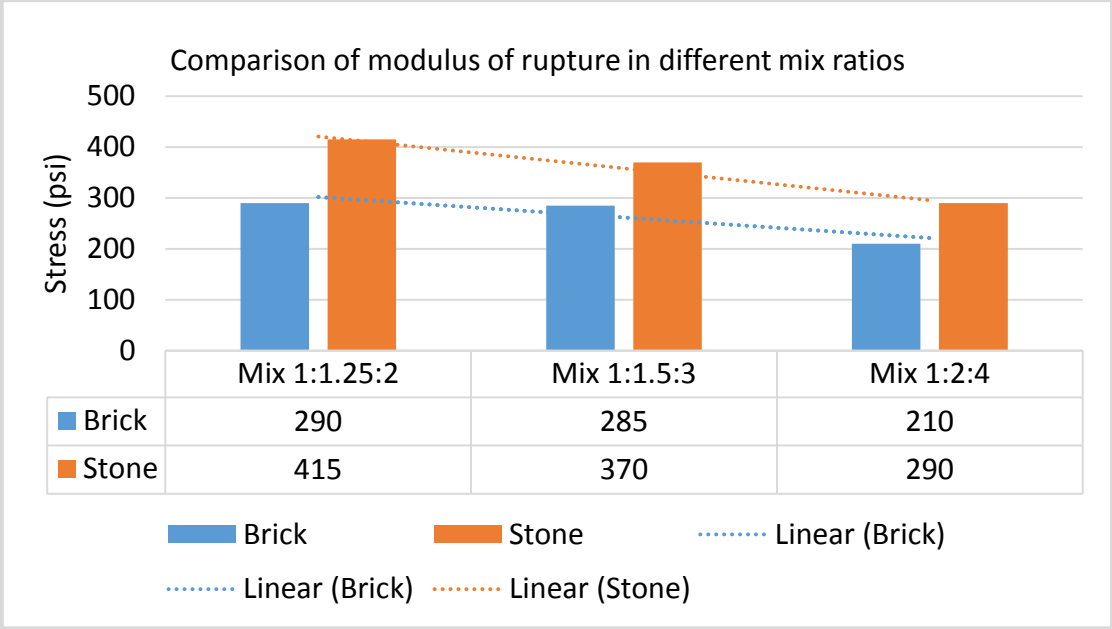

Figure 3: Comparison of modulus of rupture in different mix ratios.

In conclusion, a comparison is made among different strength of brick specimen and stone specimen as is shown in Tables 1 and 2.

Table 1. Comparison of strength in different method using brick aggregate.

Method	Compressive strength (Mpa)	Modulus of rupture (Mpa)	Splitting tensile strength (Mpa)
Aggregate type	Brick	Brick	Brick
mix 1:1.25:2	26.7	2.00	1.70
mix 1:1.5:3	18.9	1.95	1.55
mix 1:2:4	14.8	1.60	1.20

Table 2. Comparison of strength in different method using stone aggregate.

Method	Compressive strength (Mpa)	Modulus of rupture (Mpa)	Splitting tensile strength (Mpa)
Aggregate type	Stone	Stone	Stone
mix 1:1.25:2	31.2	2.95	2.00
mix 1:1.5:3	20.5	2.35	1.50
mix 1:2:4	21.9	2.00	1.40

The interrelation between the strengths should be as follows [7]:

$f_r = 1.75 f_{sp} = 2.50$(Mpa)

wheref_r=Modulus of rupture, (Mpa)
f_{sp}=Splitting tensile strength, (Mpa)
f_t =Direct tensile strength, (Mpa)

As the direct tensile strength has not been performed in this experiment, correlation among flexural and split cylinder tensile strength was developed only.

The relation above represents the correlation of flexural tensile strength and splitting tensile strength using stone aggregate and the correlating factor is 1.75. Here in this experiment the correlation factor was 1.505 for

stone aggregate and 1.25 for brick aggregate. The correlation factor deviates as in this experiment Portland Concrete Cement was used instead of Ordinary Portland Cement which exhibit less strength than PCC. The strength from brick specimen has been found less than stone specimen and it was expected as a crushing strength of brick chips is lower than stone chips.

Findings from this experiment:

f_r=1.505f_{sp} (Mpa) for stone specimen

f_r=1.25f_{sp} (Mpa) for brick specimen

And the results of splitting tensile strength and flexural strength also satisfies the range of values [8]:

f_{sp}=6~8 $\sqrt{f_c}$ (psi) for normal weight concrete (stone specimen)

f_{sp} = 4~6 $\sqrt{f}$ (psi) for light weight concrete (brick specimen)

f_r = 8~12 $\sqrt{f_c}$ (psi) for normal weight concrete (stone specimen)

f_r = 6~8 $\sqrt{f_c}$ (psi) for normal weight concrete (stone specimen)

4 CONCLUSION AND RECOMMENDATION

The following conclusion may be drawn from this experimental study:

- The tensile strength of concrete with stone aggregate was found to be higher than the concrete with brick aggregate for all cases.
- The modulus of rupture is 1.25 times higher than the corresponding split cylinder strength for concrete with brick aggregates.
- The modulus of rupture is 1.505 times higher than the corresponding split cylinder strength for concrete with stone aggregates.
- The study shows the obvious result of the compressive strength of concrete being much higher than the tensile strength of concrete. But tensile strength of concrete provides the nature of cracking of the structure.
- During the design of water retaining structure or structure under hoop stress action, flexural or splitting tensile value will not be applicable. In that case, it is recommended to use lower value of tensile strength or using more reinforcement to avoid cracking in the concrete structure. As concrete made with stone aggregate has more tensile strength value than brick made concrete, it is recommended to use stone made concrete in the tensile strength prone area of structures.

5 LIMITATIONS

- Formworks were not stiff enough to withhold the expansion swelling of wood as curing was done in open space. As a result, the shapes of concrete beams were not uniform in all section which affected the strength.
- As a saturated surface-dry (SSD) condition for aggregates cannot be done perfectly in field condition, the w/c ratio might be varied in the casting of concrete. Due to this reason obtained compressive strength had been lower than average value.
- The test was performed by analyzing results of 36 concrete cylinder and 6 concrete beams. If more specimen is tested, the result will be more reliable.

6 RECOMMENDATION FOR FUTURE STUDY

In this study, it has been tried to cover a lot of aspects for the accomplishment of the objectives of the study. Even after that, some portion of the study needs further investigationas some limitation had occurred during the experiment. This study recommends following suggestions for future study in this arena:

- Direct tensile strength of concrete could be determined and compared with other tensile strengths.
- Concrete with machine broken aggregate and manually broken aggregate could be considered for the comparative study.

- Future study may be recommended for determining tensile strength for different w/c ratios.
- A comparative study can also be undertaken for determining the difference in tensile strength of concrete made by sharp-edged and round shaped aggregates.

7 REFERENCES

Mehta,P. K. and Monteiro, P. J. M. 2006. Concrete, Microstructure, Properties, and Materials, *McGraw Hill*, New York,N Y, USA, 3rd edition, 2006.

MacGregor, J. G. and Wight, J. K. 2005. Reinforced Concrete, Mechanics and Design, *Prentice Hall*, Upper Saddle Rive, NJ, USA, 4th edition, 2005.

RedaTaha, M. M. and Hassanain, M. A. 2003. Estimating the error in calculated deflections of HPC slabs: a parametric study using the theory of error propagation, in Controlling Deflection for the Future, vol. 210, pp. 65–92, ACI Specia l Publication.

ASTM C 78-02. 2002. Standard Test Method for Flexural Strength of Concrete (Using Simple Beam with Third-Point Lo ading), American Standard Test Method, West Conshohocken, Penn, USA.

ASTM C 496/C 496M-04. 2004. Standard Test Method for Splitting Tensile Strength of Cylindrical Concrete Specimens, American Standard Test Method, West Conshohocken, Penn, USA.

Kim J. J. andRedaTaha, M. 2014. Experimental and Numerical Evaluation of Direct Tension Test for Cylindrical Concre te Specimens, Hindawi Publishing Corporation Advances in Civil Engineering, Volume 2014, Article ID 156926.

Relation between Compressive and Tensile Strength of Concrete. Retrieved from http://civil-engg-world.blogspot.com/2009/ 04/relation-between-compressive-and.html

NCEED 2015 -National Conference on Earthquake and Environmental Disaster; December 17, 2015; CUET, Chittagong, Bangladesh
Bhuiyan M. A. R., Pal S. K., Mazumder M. H., Mazumder R. K., Omi F. R. (eds.)

Experimental Study on the Strength Behavior of Concrete Using Stone Dust as Fine Aggregate

M. Nuruzzaman, M. Salauddin and M. Saiful Islam
Department of Civil Engineering, Chittagong University of Engineering and Technology, Chittagong-4349, Bangladesh

ABSTRACT: Concrete is a composite material which is predominantly used throughout the world. The demand of natural sand for infrastructural facilities has increased a lot which results an increase in price and the reduction of sources as well. Thus it becomes inevitable to find a suitable substitute which should be at the same time inexpensive and eco-friendly. Stone dust, a by-product from the crushing process during quarrying activities is one of such materials. In this paper an attempt has been made to find out the strength behavior of concrete by using stone dust as a partial replacement of sand. The test specimens were made from three different grades of concrete i.e. mix ratios 1: 1.5: 3, 1: 2: 4, 1: 2.5: 5. Only the compressive strength tests were conducted in this research. The basic strength properties of concrete were investigated by replacing natural sand with stone dust at replacement levels of 0%, 10%, 20%, 30%, 40%, 50% & 60%. For the different grades of concrete studied, the value of the compressive strength are observed to be maximum at 30% replacement level of sand. Moreover, the result shows that the maximum increase in compressive strength is 15% in comparison to normal concrete (0% sand replacement level) for the concrete mix-ratio 1: 1.5: 3.

1 INTRODUCTION

Conventionally concrete is a mixture of cement, sand and aggregate which is the mostly used man-made materials (Lomborg, 2001). Every year around 7.5 km^3 of concrete is being made (Hendrik and van Oss, 2007). To prepare this huge amount of concrete it needs a lot of sand, which is one of the prime constituent of concrete. As a result, the natural sources of sand are getting depleted (Palaniraj, 2003). Therefore, an alternative material of sand is needed to be explored. Stone dust is such a material which can be used to substitute sand as a fine aggregate in concrete (Nagabhushana and Sharadabai, 2011; Mahzuz *et al.* 2011; Balamurugan and Perumal, 2013; Muhit*et al.* 2014). Moreover, stone dust from stone quarries or stone crusher treated as wastage creates a great problem for disposal (Reddy *et al.* 2015). Different researchers took different initiatives at different time to find out a proper way to dispose waste (Kameswari*et al.*, 2001; Sanchez *et al.* 2002; Shih and Lin, 2003). Hence, the use of stone dust in concrete will not only serve as an alternative of natural sand but also reduce the environmental burden.

In different parts of the world, researchers have conducted different study to find out the effect of stone dust in concrete. Shukla *et al.* (1998) and Nagabhushana and Sharadabai (2011) have concluded their report by saying that up to 40% replacement of sand by crushed rock powder, the strength of concrete is not affected. Reddy and Reddy (2007) reported an increasing compressive strength by the use of crushed stone dust. Mogaveera*et al.* (2011) have pursued a study on sand replacement in concrete for different mix proportions by quarry dust and they have drawn a result by saying that up to 20% - 25%, sand can be replaced by quarry dust effectively. Some other researchers have also drawn an outline in their reports that replacing sand by stone dust improved the compressive strength of concrete (Nagpal *et al.* 2013; Sukesh *et al.* 2013).

The present study is aimed at utilizing stone dust as fine aggregate in concrete by replacing natural sand at relatively smaller percentages. The current study is intended to determine the compressive strength of concrete on different replacement level of natural sand by stone dust with different concrete mix-ratios.

2 LABORATORY SET-UP

The experimental program was planned to study the effect of replacement of fine aggregate with supplementary material stone dust on the strength of hardened cement concrete. Fine aggregate i.e. natural sand replacement at various percentage levels were used in investigation to observe the effects of different stone dust levels on concrete in developing strength at different curing ages.

2.1 *Materials*

Concrete test specimens were cast using ASTM type-I Ordinary Portland Cement (OPC), crushed stone chips as coarse aggregate, natural river sand and stone dust as fine aggregate. Table 1 provides the physical properties and the chemical compositions of the ordinary Portland cement (Aziz, 1995; Hossain and Seraj, 1985).

The coarse aggregate used was crushed stone with a maximum nominal size of 12.5 mm; the fine aggregate was river sand and stone dust. The grading of aggregates is shown in Table 2. Further, the physical properties of aggregates are shown in Table 3.

Table 1. Physical properties and the chemical compositions of ordinary Portland cement.

Sl. No	Characteristics	Value obtained	Value specified as
1	Fineness (#200 sieve)%	95%	>90%
2	Blain specific surface (cm^2/gm)	3300	>2800
3	Normal consistency (%)	24.5%	22%-30%
4	Setting times-Vicat test (minutes)		
	Initial	135	>45
	Final	190	<375
5	Specific gravity	3.15	
6	Compressive strength (MPa)		
	3 days	15.4	>12.4
	7 days	19.8	>19.3
	28 days	30.2	>27.6

Table 2: Grading of aggregates.

Coarse aggregate		Fine aggregate (Stone Dust)	
Sieve size (mm)	Cumulative percentage retained	Sieve size (mm)	Cumulative percentage retained
25	0	4.75	0
12.5	0	2.36	5.24
9.5	55	1.18	28.62
4.75	100	0.6	75.20
-	-	0.3	85.90
-	-	0.15	92.84
-	-	Pan	100

Table 3: Physical properties of Aggregates.

Properties	Coarse aggregate	Fine aggregate	
		River sand	Stone dust
Specific Gravity	2.7	----	2.51
Unit Weight (kg/m3)	1603.3	1709.2	1606.8
Fineness Modulus	6.45	----	2.88
Absorption Capacity (%)	1	----	0.31

2.2 *Variables Studied*

(a) Mix Proportions: Three different mix proportions of concrete are used in the program which are 1:1.5:3, 1:2:4 and 1:2.5:5 those gives concrete of three grades namely M35, M28 and M23 respectively.
(b) Exposure Period: Test specimens are tested periodically after the specified curing periods of 7 days, 14 days, 28 days and 90 days in plain water.
(c) Size of specimens: Cube specimens are used in this program in which each side of the cube is 101.6 mm long.
(d) Percent level of sand replacement by stone dust: In this program the percent levels of sand replacement by stone dust were 0%, 10%, 20%, 30%, 40% and 50% which are denoted in different figures as SD0, SD10, SD20, SD30, SD40 and SD50 respectively.
(e) Test: Compressive strength test is conducted in this program.

2.3 *Test Procedures*

The concrete specimens are tested for compressive strength at the ages of 7, 14, 28, 90 days in accordance with the BS EN 12390-3:2009. At each case, the reported strength is taken as the average of three tests results.

3 RESULTS AND DISCUSSIONS

The compressive strength of normal and stone dust concrete of three different grades M35, M28 and M23 has been graphically presented in Fig.1, Fig.2 and Fig.3. Also for the ease of comparison, the relative compressive strengths are plotted in Fig.4, Fig.5 and Fig.6. From the early age of curing, stone dust concretes achieve relatively higher compressive strength as compared to normal concrete.

Test result shows that 7 days compressive strength of M35SD10, M35SD20, M35SD30, M35SD40 and M35SD50 concrete is 17%, 20%, 28%, 15% and 20% higher than normal concrete i.e. M35SD0. From the initial age of curing, compressive strength is seen to increase with the increase of stone dust content as a partial replacement of fine aggregate i.e. natural sand.

14 days compressive strength of normal concrete of M28 grade is lower by around 21%, 4%, 22%, 7% and 5% respectively for M28SD10, M28SD20, M28SD30, M28SD40 and M28SD50 concrete. Similarly, 28 days compressive strength of normal concrete of M23 grade is lower by around 4% and 9% respectively for M23SD10 and M23SD30 concrete, whereas the same value is reported to be higher by around 3%, 13% and 5% for M23SD20, M23SD40 and M23SD50 concrete respectively.

From the test consequence it is found that the 90 days compressive strength of M35SD10, M35SD20 and M35SD30 concrete is 4%, 4% and 13% higher than normal concrete but at the same curing duration the compressive strength of M35SD40 and M35SD50 concrete is 4% and 2% lesser than normal concrete.

Concrete normally gains its maximum percentage of strength within 28 days. Now with respect to 28 days M35SD0 concrete the compressive strength of 7 days and 14 days M35SD30 concrete is lower by 25% and 22% respectively, whereas for 28 days and 90 days M35SD30 concrete is higher by 18% and 23% respectively.

Rate of strength attainment for different types of concrete is observed to vary with the grade of concrete. Gain in strength is higher for the higher grade of concrete. Among all the concrete studied, 28 days compressive strength is increased by about 6%, 5% and 18% for concrete M35SD10, M35SD20 and M35SD30 respectively as compared to 28 days M35 grade normal concrete, whereas the same value is increased by about 8%, 3% and 16% for concrete M28SD10, M28SD20 and M28SD30 respectively than M28 grade normal concrete, similarly the assessment is conducted for M23 grade concrete also and the same value is found to be increased by 4%, -3% (i.e. decreased by 3%) and 9% than the normal concrete. So it can be concluded that strength gaining is relatively faster for higher grade concrete as compared to lower grade concrete.

The value of compressive strength of concrete is observed to be optimum for 30% sand replacement level. The compressive strength of concrete is around 15% higher than normal concrete for 30% sand replacement by stone dust. The compressive strength of concrete is observed to be maximum for M35 grade concrete. For different sand replacement level, the minimum compressive strength of concrete is found at 40% sand replacement level.

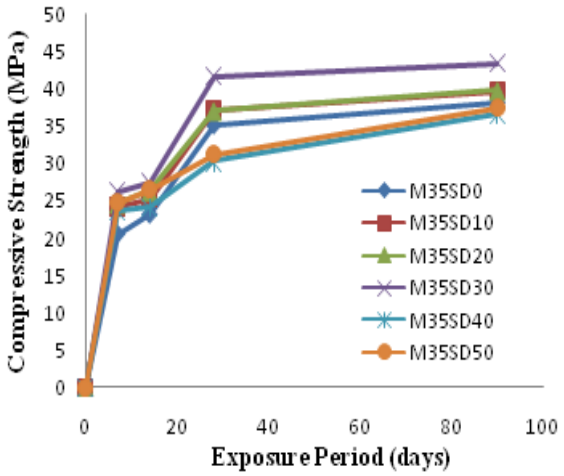

Figure 1. Compressive strength of M35 concrete.

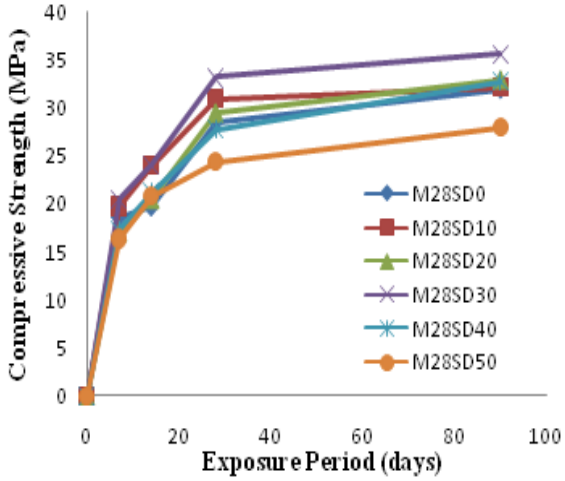

Figure 2. Compressive strength of M28 concrete.

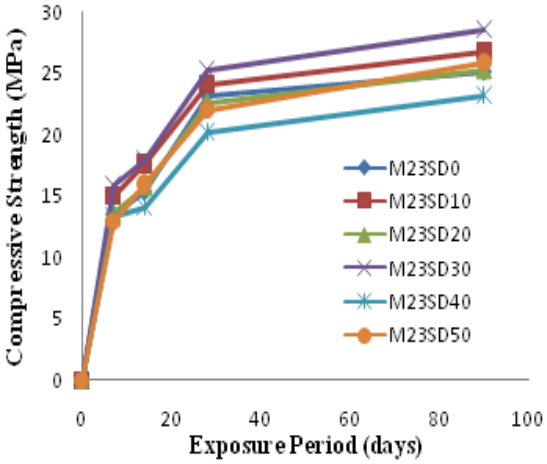

Figure 3. Compressive strength of M23 concrete.

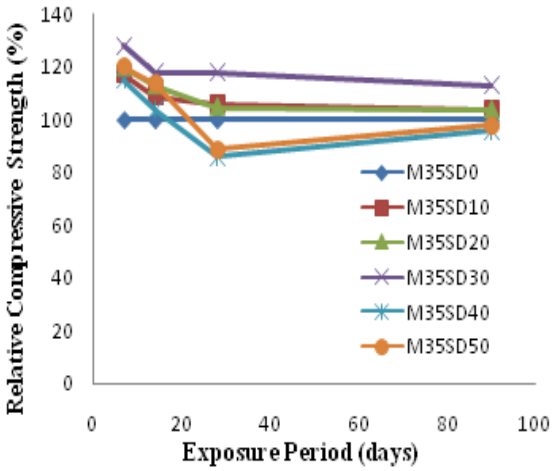

Figure 4. Relative Compressive strength of M35 concrete.

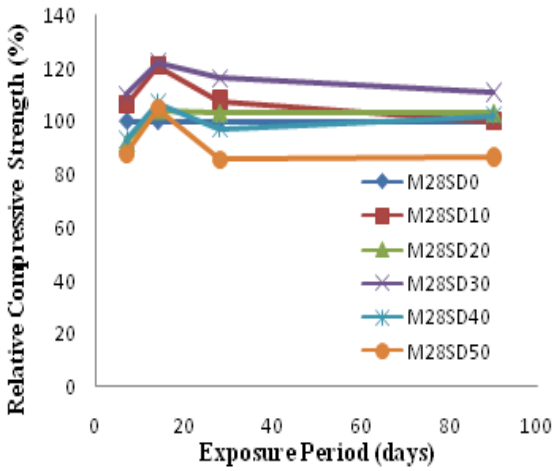

Figure 5. Relative Compressive strength of M28 concrete.

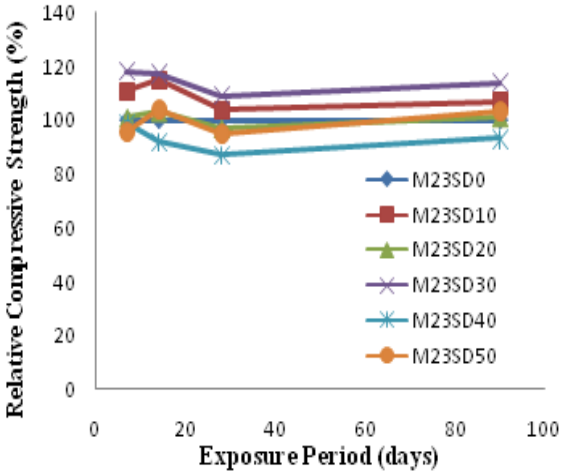

Figure 6. Relative Compressive strength of M23 concrete.

4 CONCLUSIONS

The test results of this study have great significance for providing high strength as well as durable concrete by using stone dust. This paper presents the compressive strength of concrete for 7 days, 14 days, 28 days & 90 days curing periods. For the different grades of concrete studied, the values of the compressive strength are observed to be maximum at 30% replacement level of sand replacement. Furthermore, the result shows that the maximum increase in compressive strength is 15% in comparison to normal concrete (0% sand replacement level) for the concrete mix-ratio 1: 1.5: 3.

5 ACKNOWLEDGEMENTS

Technical Supports from Strength of Materials Lab and Engineering Materials Lab of Department of Civil Engineering of Chittagong University of Engineering & Technology (CUET) is gratefully acknowledged.

6 REFERENCES

Aziz, M.A., (1995), Engineering Materials, Z and Z Computer and Printers, Dhaka, Bangladesh.

Hendrik, G. and van Oss (2007), Mineral Commodity Summaries- Cement. US Geological Survey, 40-41.

Hossain, T. and Seraj, S.M. (1985), Laboratory Mannual on CE-202 Material Sessional. Department of Civil Engineering, Bangladesh University of Engineering and technology, Dhaka, Bangladesh.

Kameswari, K.S.B., Bhole, A.G. and Paramasivam, R. (2001), Evaluation of Solidification (S/S) Process for the Disposal of Arsenic Bearing Sludge in Landfill sites. Environ. Eng. Sci., 18: 167-176.

Lomborg, B. (2001), The Skeptical Environmentalist: Measuring the Real State of the World. Cambridge University Press, UK.

Mogaveera, G., Sarangapani, G., and Anand, V. R. (2011), Experimental investigation on the effect of partial replacement of sand by quarry dust in plain cement concrete for different mix proportions, ProcEmerging Trends in Engineering, NMAMIT, Nitte, pp. 812-817.

Muhit, I.B., Raihan, M.T., Nuruzzaman, M. (2014), Determination of Mortar Strength using Stone Dust as a Partially replaced material for Cement and Sand, Advances in Concrete Construction, Vol. 2, No. 4, pp. 249-259.

Nagabhushana and Sharadabai, H. (2011), Use of Crushed Rock Powder as replacement of Fine aggregate in Mortar and Concrete, Indian Journal of Science and Technology, Vol. 4, No. 8.

Nagpal, L., Dewangan, A., Dhiman, S. and Kumar, S. (2013), Evaluation of Strength Characteristics of Concrete using Crushed Stone Dust as Fine Aggregate, International Journal of Innovative Technology and Exploring Engineering (IJITEE), Vol.2, Issue. 6.

Palaniraj, S. (2003), Manufactured sand. Intl. Conf. on Recent trends in Concrete Technology and Structures, (INCONTEST), Coimbatore.

Reddy, M.V. and Reddy, C.N.V.S., (2007), An experimental study of rock flour and insulator ceramic scrap in concrete, Journal of Institute of Engineer (India), Vol-88, pp. 47-50.

Reddy, M.V.S., Mrudula, D., Seshalalitha, M. and Hariprasad, P. (2015), The effect of Crushed Rock Powder and Super plasticizer on the fresh and hardened properties of M30 grade Concrete, International Journal of Civil, Structural, Environmental & Infrastructure (IJCSEIERD), Vol. 5, pp. 25-30.

Sanchez, F., Garrabrants, A.C., Vandecasteele, C., Moszkowicz, P. and Kosson D.S. (2002), Environmental Assessment of Waste Matrices Contaminated with Arsenic. J. Hazard. Mater., 96: 229-257.

Shih, C.J., Lin, C.F. (2003), Arsenic Contaminated Site at an Abandoned Copper Smelter Plant: Waste Characterization and Solidification/ Stabilization Treatment. Chemosphere, 53: 691-703.

NCEED-CUET National Conference on Earthquake and Environmental Disasters, December 17, 2015, Chittagong, Bangladesh
Bhuiyan M. A. R., Pal S. K., Mazumder M. H., Mazumder R. K., Omi F. R. (eds.)

Potential Use of Phosphogypsum for Sustainable Concrete Construction

G. M. Sadiqul Islam, S. K. S. Amit and M. R. Islam
Department of Civil Engineering, Chittagong University of Engineering and Technology, Chittagong 4349, Bangladesh

M.T. Raihan
Development Design Consultants Limited, 47 Mohakhali C/A, Dhaka-1212, Bangladesh

ABSTRACT: Industrial activities generally produces considerable amount of waste. Proper management of these materials without affecting the environment is always a key concern. Construction industry has the extensive opportunity to utilize these wastes/byproducts which can lead to sustainable development. Phosphogypsum, a by-product of Phosphoric acid manufacturing process, produced in bulk quantity especially from the fertilizer industry. It has use as a supplementary fertilizer for soil treatment. However, environmental hazard concern from this activity has been raised by researches. Moreover, disposal of this materials in the form of landfill also need huge area. The material has therefore tried to incorporate in concrete construction for its sustainable use. In manufacturing process of Portland cement, phosphogypsum has been used as a substitute of natural gypsum (helps to control the hydration rate of cement). It can also be used as supplementary material of cement in concrete. Limited studies have found relating to phosphogypsum as partial replacement of different aggregates in concrete and in the production of artificial aggregates for soil stabilization and road construction. Bricks and blocks made with phosphogypsum show better outcomes as potential building materials. The main objective of this paper is to investigate the potential use of phosphogypsum as construction material along with its different environmental implications.

1 INTRODUCTION

Phosphogypsum is a by-product from the wet manufacturing process of phosphoric acid (ammonium phosphate fertilizer) by the action of sulphuric acid on the rock phosphate. Approximately 4.5 to 5.5 tons of phosphogypsum is generated per ton of phosphoric acid production using wet process. World phosphogypsum production is estimated to be around 100–280 Mt per year (Becker, 1989). Phosphoric acid is produced by reacting phosphate ore (apatite) with sulphuric acid according to the following reaction where X may include OH, F, Cl, or Br. (Banu & Haq, 2015):

$$Ca_5(PO_4)3X + 5H_2SO_4 + 2H_2O \rightarrow 3H_3PO_4 + 5CaSO_4.\,2H_2O + HX \quad (1)$$

Dumping of phosphogypsum into open air has environmental and health concerns. The stockpiled material which is dominated mainly by calcium sulphate dehydrate (around 94-98% by wt.), contains approximately up to 5-6% of impurities including heavy metals, fluoride and radionuclides (Szynkowska *et al.*, 2011). These toxic substances can be transported by wind over long distances. In consequence it could contaminate soil and or groundwater. This continuous process leads to increase in the content of substances in various components in the environment and thereby affects the food chain. Another prime concerns often expressed about phosphogypsum storage is the potential for contamination of fresh water aquifers underlying the stacks (Nigong, 1998). Detailed studies are necessary in order to fully understand the transfer process of toxic substances into the adjacent environment and to assess their impact (Al-Masri *et al.*, 2004; Arocena *et al.*, 1995; Rutherford *et al.*, 1995). One of the main concerns of phosphgypsum is it sometimes enriched with radionuclide, Radium^{226} – the parent isotope of Radium^{222}, which further decays to produce Radon gas (Rn^{222}). Radon gas has a short half-life of 3.8 days and intense radiation capacity. Upon decay of the radon gas, alpha particles are emitted, which is known to cause significant damage to internal organs (USEPA, 2002). The USEPA, there-

fore, currently classified phosphogypsum as a "Technologically Enhanced Naturally Occurring Radioactive Material" (TENORM) (USEPA, 2002).

The environmental management of the industrial phosphogypsum is a challenge and concern for several countries (Rutherford *et al.*, 1994). Its potential use leads to environmental protection along with sustainable development. Several researchers had studied the use of phosphogypsum in various fields. Phosphogypsum has considerable use in agricultural sector also (Mullins, 1990). Its effectiveness was found similar to the crushed natural gypsum. However, the dosage limit should be restrictive considering the health concern. Treated phosphogypsum can be used in the manufacturing process of plaster. It has been found that the phosphogypsum is suitable for making good quality plaster which shows similar characteristics to natural gypsum plaster (Singh, 2002; Singh, 2003; Singh, 2005). Countries deficient with natural quarries can take the advantage in this regard. The phosphogypsum was also used in soil stabilization (Degirmenci *et al.* 2007). Phosphogypsum has been studied to be used in hollow blocks (Kumar, 2003) and light brick (Abali*et al.*, 2007).But the most important and motivating use of phosphogypsum could be in the construction industry. In the manufacturing process of cement, phosphogypsum used as a replacement of natural gypsum which plays the role of a set retarder (Potgieter*et al.*, 2003; Atlun & Sert, 2004), or to reduce the clinkerization temperature (Kacimi *et al.*, 2006).

In this study the properties of phosphogypsum and its potential use shave been reviewed to suggest sustainable development.

2 PROPERTIES OF PHOSPHOGYPSUM

2.1 *Physical Properties*

Calcium sulfate can be either in di-hydrate ($CaSO_4.2H_2O$) or hemihydrate ($CaSO_4.0.5H_2O$) form depending on the reaction temperature used to produce phosphoric acid. Usually free moisture content between 25 and 30 percent exists in the gypsum cake after filtration. The generated hemihydrate form of phosphogypsum, in the presence of free water can rapidly convert to dehydrate form (Bhawan & Nagar, 2012). Moreover, if the process is left undisturbed it will set up into a relatively hard cemented mass. Di-hydrate form consists principally silt-size (<0.075mm) and relatively soft aggregates of crystals (Wissa, 2015). It depends on the source of the phosphate rock and the reactor conditions.

Typical engineering properties (e.g. density, strength, compressibility, permeability) of phosphogypsum cannot be defined within fixed limits. They are not controlled only by the rock source and reaction process during preparation. The method of deposition, age of the gypsum stack, location where it is disposing etc. influence the properties of the produced phosphogypsum. The deeper the phosphogypsum is within a stack and the higher age of phosphogypsum, the higher its density and lower its compressibility and permeability. It is important that properties should be considered without modification from water or other man made and environmental effects.

2.2 *Chemical Properties*

Phosphogypsum consists mainly calcium sulphate dehydrate with small amount of silica. The mineralogical composition of phosphate ore, as described by various researchers (Carbonell- Barrachina*et al.*, 2002; Oliveira &Imbernon, 1998) is dominated by fluorapatite, goethite and quartz, with minor amounts of Al-phosphates, anatase, magnetite, monazite and barite. Heavy metals and trace elements such as cadmium (Cd) and nickel (Ni) are also detected sometimes. With regard to radioactivity, phosphogypsum could contain U-series radionuclides naturally present in the phosphate rock and depending on the quality of the rock source; phosphogypsum can contain as much as 60 times the levels normally found prior to processing (Taiyibi*et al., 2009*) The most important source of phosphogypsum radioactivity is reported to be ^{226}Ra (Rutherford *et al.*, 1994).

Environmental concerns have developed in the last ten years due to the presence of the trace toxic metals and radionuclides in phosphogypsum and its pore water. For this reason, Florida Department of Environmental Protection (FDEP) and U.S. Environmental Protection Agency (USEPA) regulated phosphogypsum's usage, transportation and storage (Banu & Haq, 2015).

3 MANUFACTURING OF PHOSPHOGYPSUM

Phosphoric acid can be produced by several different methods viz. thermal, hydrochloric and nitric acidulation and the sulfuric acidulation (FIPR, 1987). Different processes along with different raw materials are used

in the manufacture of phosphoric acid. When the raw material is elemental phosphorus, the process is known as thermal manufacturing process. However, this process is not practiced currently because of the required energy level. Wet process is an economic and alternative way to produce phosphoric acid by using phosphate minerals which are decomposed by acid (EFMA, 2000). There are three possible subgroups of wet processes depending on the type of acid used. This variation is required because of difference in rocks and gypsum disposal systems. The storage and transfer of phosphoric acid is the same for all the acids and does not depend on the method of production. Approximately5 tons of gypsum is generated per ton of P_2O_5 produced as phosphoric acid (Jenkins *et al.*, 2002). This represents a serious disposal problem with the individual phosphoric acid production units of over 1,000 tons per day capacity. Commonly this gypsum is disposed either to land or in water. Fig. 1 shows the process diagram of a common wet method using sulphuric acid.

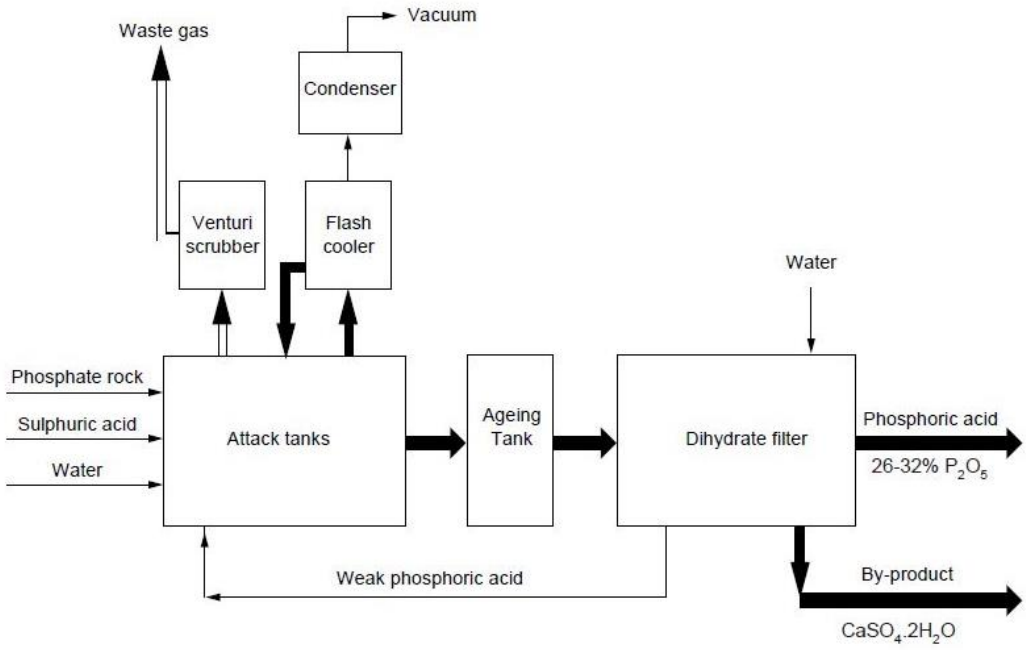

Figure 1. Dihydrateprocess of phosphoric acid production and by-product $CaSO_4.2H_2O$ (adapted from EFMA, 2000)

4 POTENTIAL USE OF PHOSPHOGYPSUM

4.1 *Agricultural Application*

The use of phosphogypsum as an agriculture fertilizer has been practiced in many parts of the world for decades (Mullins & Mitchell, 1990; USEPA, 1992). An important aspect regarding phosphogypsum is its potential to solve sulphur deficiency in soils (IFA, 2015). While elemental sulphur and organic sulphur must undergo microbial conversion before sulphur is made available to plant, the sulphur in phosphogypsum becomes readily available for being present in sulphate form. It has been applying in agricultural soils as calcium, phosphorus and sulfate supplement to enhance crop production and also used sometimes to recover acidic soils reducing aluminum toxicity (Toma & Saigusa, 1997; Alva & Sumner, 1990; Garrido *et al.*, 2003). Moreover, when agricultural soils are exposed to heavy rainstorms, phosphogypsum can be used alone or in addition with different synthetic organic polymers to prevent runoffs and erosion (Tang *et al.*, 2006). The Impact of phosphogypsum on bacteria, plants, invertebrates etc. present in soil is also an important issue. Different organisms in soil are responsible for the arrangement of individual soil functions with the related ecosystem (Lavelle *et al.*, 2006). The recommended amount of phosphogypsum for improving the agricultural soil varies between 500 to 1000 kg per hector (Al-Hwaiti, 2010).Recently, Nayak *et al.* (2011) reported that, 10% addition of posphogypsum in soil have a positive effect on microbial growth along with on cellulose and amylase activities. Research showed that phosphogypsum has favorable use in several regions e.g. Brazil, India, Spain, USA etc. (USEPA, 1992, Nayak *et al.*, 2013, Enamorado *et al.*, 2014).

4.2 *Transportation Facilities*

Different authors have proposed to use phosphogypsum as a road construction material. Thimmegowda (1994) studied with various mixtures of cement stabilized phosphogypsum composites in order to determine their usefulness as a secondary material for different construction purposes such as road construction and pro-

tection in embankment. Nanni and Chang (1989) investigated phosphogypsum as an aggregate in construction of different Roller Compacted Concrete (RCC) slabs. In three individual mixing procedures, several phosphogypsum-based mixtures were prepared. Then those materials were compacted using vibrator. The study also suggested a thickness design procedure of concrete pavement and indicated that phosphogypsum based RCC suitable for pavement construction applications.

Shen *et al*. (2007) studied the effect of incorporating phosphogypsum in lime–phosphogypsum (PG)–fly ash binder for a road base material application to replace a lime–fly ash binder characterized by low early strength. The results showed that phosphogypsum has a more pronounced binder action than lime and promotes a rapid reaction between lime and fly ash. Therefore, lime–PG–fly ash binders reached higher strengths than those manufactured with lime–fly ash only. Compared to the mechanical behavior of some other road base materials such as cement soil, cement–lime soil, lime–fly ash soil, the lime–PG–fly ash binder showed the highest improve in mechanical properties for all ages. These results were corroborated by the microscopic study. The lime–PG–fly ash mixture confirmed the presence of large amounts of needle like crystals (possibly ettrigite, a hydration products) surrounding the fly ash particles and therefore, enhancing the joints between the different particles in the binder. No significant hydration products were observed in the case of the lime–fly ash binder.

Phosphogypsum-ash mixes with no binder can be used in the construction of lower layers of road embankments, because they meet the requirements set for materials for the construction of road embankments below the frost penetration zone. Folek*et al*. (2011) attempted to use phosphogypsum in road construction. They performed strength tests after half a year and after one and a half year of parking lot operation confirmed the feasibility, established earlier in laboratory tests, of utilizing phosphogypsum mixes with fly ash and steadying binder. The study found that the strength and frost resistance results obtained in field tests were much better than the laboratory test results. The compressive strength measured in laboratory tests after 180 and 360 days of sample curing under conditions protecting against moisture loss and after 14 days of complete immersion in water (1.26 and 1.36 MPa respectively) was comparable to the strength of a sample cut from the experimental parking lot base (1.7 MPa) after 200 days of its use. Higher differences in strengths were determined in frost resistance tests. Despite large temperature differences that occurred during the experiment duration (autumn-winter-spring season), frequent crossing of the freezing point and atmospheric precipitation, the strength measured was much higher than that determined in laboratory tests of frost resistance (0.38 MPa). The subsequent winter-spring season has not caused strength reduction. After 490 days the strength increased to 5.1 MPa and was 3 times more than the strength measured after 200 days. These mixes (composites) can be used in the construction of upper layers of road embankments and sub-bases of pavements loaded with light traffic.

Extensive studies of using phosphogypsum in road engineering were also steered in Finland between 1998 and 2002. Mixtures containing 90% phosphogypsum and 10% fly ash (dry matter basis) were prepared, followed by adding 6% of binder material. The alternative binders were cement, admixtures of pulverized blast-furnace slag with cement (proportions 1:1 and 7:3), or lime and blast-furnace slag alone. In total, 7,600 m of gravel road was built using these mixtures in various multilayer pavement structures. Traffic loading of the road during a period of two years did not change its purposeful properties, and the highest bearing capacity was attained by that section of the road, where phosphogypsum mixed with blast-furnace slag and cement was used.

4.3 *Construction Industry*

Phosphogypsum is exerting in preparation of concrete since last four decades. Initially, Gutt (1978) proposed some practical approaches about the potential use of phosphogypsum in concrete. Erdogan *et al.* (1994) studied the possessions on the setting and mechanical properties of partly-refined boric acid and phosphogypsum mixed with Portland and Trass cements and it was paralleled with a Portland cement containing high grade natural gypsum. The study found that the partly refined boric acid and phosphogypsum mixture can be used in place of natural gypsum for Portland and Trass cements.

Chandara *et al.* (2009) experimented to use waste gypsum in exchanging natural gypsum with ordinary portland cement. It was found that the presence of hemihydrate in waste gypsum was found to play an important role in decreasing the setting time of cement modified waste gypsum. The setting time of cement modified waste gypsum was decreased by 15.29% and 13.67% for initial and final setting times respectively. El Nouhy *et al.* (2015) investigated the effects of phosphogypsum on the properties of both cement pastes and mortars and found that it is possible to partially replace cements by phosphogypsum up to 8% and 15% with regard to cement/sand ratio of (1:3) and (1:2) respectively.

Singh & Garg (1995) mixed fly ash with calcinedphosphogypsum, fluorogypsum, lime sludge, and chemical activators of different fineness to formulate cementitious binders. The binders are suitable for partial spare

(up to 25%) of the cement in concrete without sacrificing the strength. Rao & Kumar (2014) studied about a low cost and environment friendly material naming FaL-G is the product name derived from a cementitious mixture composed of Fly ash (Fa), Lime (L) and gypsum (G) mainly phosphogypsum used for preparation of hollow masonry blocks for construction.

Smadi *et al.* (1999) studied the utilization of phosphogypsum as cement (both OPC and PPC) replacement agents in mortars and found decreased compressive strength but increased flexural strength comparing with conventional mix. Phosphogypsum's presence in the cement has increased its initial strength rapidly. This strength development was due to the formation of anhydrate at higher temperatures. Taher (2004) reported that substitution of Portland cement with 5% calclainedphosphogypsum at 800 ^{o}C in presenceof 5% silica fume improves the hydraulic properties of cement due to the presence of calcinedphosphogypsum. It augments the formation of ettringite.

Altun & Sert (2004) investigated the usability of weathered phosphogypsum from remainder areas as a set retarder in Portland cement. Different ratios of phosphogypsum used with Portland cement to check the setting and mechanical properties. It was compared with a Portland cement containing natural gypsum. The phosphogypsum added in ratios 1, 3, 5, 7, 10, and 12.5 percent by wt. of Portland cements. It was found that phosphogypsum can be used in place of natural gypsum for Portland cement. The maximum compressive strength in 28-days was found with 3 % phosphogypsum sample.

Taher (2007) attempted to treat phosphogypsum thermally at different temperatures 200, 400, 600 and 800^{o}C to cleanse phosphogypsum and increase its quality to make it suitable for the production of Portland slag cement (PSC) and concluded that the hydraulic properties of Portland slag cement could be improve when phosphogypsum is thermally treated at 400, 600 and 800^{o}C instead of raw gypsum. It was also found that the highest hydraulic properties of Portland slag cement transpires by using thermally treated phosphogypsum at 800^{o}C.

Huang *et al.* (2009) investigated a cementitious material by utilizing two industrial by product, phosphogypsum and steel slag, combined with another industrial waste ground granulated blast-furnace slag (GGBFS) and limestone. The 28 days compressive strength of 45% phosphgypsum, 10% steel slag, 35% GGBFS and 10% limestone mixture exceeded 40 MPa. Phosphogypsum residuals are connected by the hydration products and framework structure was built at early ages. With continuous hydration reaction, pores were filled by secondary C–S–H gel and ettringite. It was concluded that steel slag in the cement acted as an alkalinity activator. However, over dosage of steel slag may cause unsoundness.

Reddy *et al.* (2010) experimentally investigated compressive, tensile and flexural strength characteristics of partially cement replaced phosphogypsum concrete using 0, 10, 20, 30 and 40% replacement with different water-binder ratios of 0.40, 0.45, 0.50, 0.55, 0.60 and 0.65. Curing periods of cubes, cylinders and beams elements were 7, 28 and 90 days. They found that replacement of a certain amount of cement with phosphogypsum helps to develop a comparatively good and hardened concrete which is also economical. However, above 10% replacement of phosphogypsum in concrete leads to drastic reduction not only in the compressive strength but also in the split-tensile strength. In addition the flexural strength decreases as width and number of cracks increases significantly at replacement above 10% of cement with phosphogypsum at different water binder ratios. Banu & Haq (2015) studied an experimental work for designing a self-compacting concrete mixes using different percentages of phosphogypsum varying from 0, 10, 20 and 30 percent. At 10% replacement of cement with phosphogypsum gave maximum flexural strength than the other replacement of cement with phosphogypsum, the width and number of cracks increased with the 20% and 30% replacement of phosphogypsum. Fig. 2 shows a comparison between percentages of phospogypsum used in different studies found in literature.

Therefore, from the abovementioned studies it is seen that phosphogypsum has several aspects of use in construction purposes. Certain percentage of phosphogypsum as a substitute or supplementary material with other associated construction materials can give positive outcomes. However, the associated environmental issues need to address carefully to ensure safe use to the by-product.

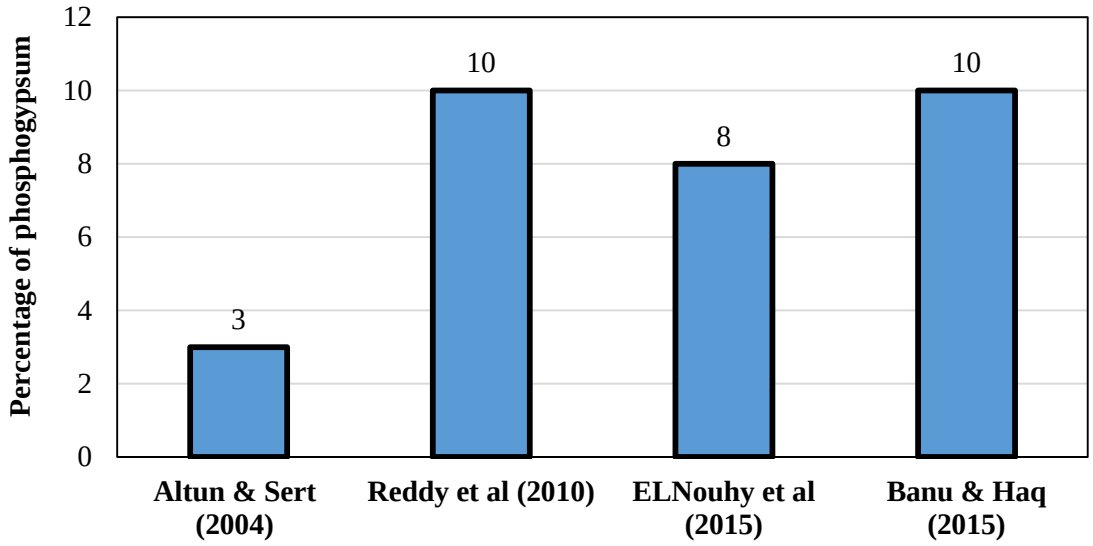

Figure 2. Phosphogypsum in Cement & Concrete.

5 ENVIRONMENTAL ISSUES

Several researches studied the environmental issues associated with the use of phospogypsum. Fan (1997) studied stabilized phosphogypsum and cement composite blocks immersed in both fresh and saltwater for leaching characteristics and structural integrity. High release rates of Ra^{226} were observed during the initial stages of leaching, with a gradual decline thereafter. The blocks fabricated at 3629 kg (8000 lb) compaction level met the unconfined compressive strength requirements. Guo (1998) conducted the research to measure the calcium effective diffusion coefficients of phosphogypsum-fly ash-cement composites subjected to salt-water conditions. It was found that higher diffusion coefficients of phosphogypsum: fly-ash:cement composites results in separation and failure of the composites. Deshpande (2003) conducted a research work focusing on stabilizing phosphogypsum with Portland Type II cement and Class C fly ash for use in marine environments. The stabilized phosphogypsum composites were submerged in an aquatic environment that can provide double protection against the escape of radon gas. That application showed minimization of the radon exposure as the heavy metals and the radionuclide contaminants get immobilized in the waste matrix by regulating its migration into the environment.

6 CONCLUSION

TSP complex is the main source of phosphogypsum production in Bangladesh. The industry sometimes sale this product in a very low price but mainly dump them after production process. A more detailed research and development work might help to ensure better use of this material in various sectors. Considering the quality and properties of phosphogypsum, industry based research work for the potential use of the material would establish mutual improvement of productivity and research. Cement industry might then reduce the dependency on natural gypsum for their production. Environmental concern is an important issue in this regard. Therefore, ensuring proper use of this material commands to sustainable development of the society.

7 REFERENCES

Abal, Y., Yurdusev, M. A., Zeybek, M. S., &Kumanlıoğlu, A. A. 2007. Using phosphogypsume and boron concentrator wastes in light brick production. *Construction and Building Materials*, 21(1), 52-56.

Al-Hwaiti, M. S., Ranville, J. F., & Ross, P. E. 2010. Bioavailability and mobility of trace metals in phosphogypsum from Aqaba and Eshidiya, Jordan. *Chemie der Erde-Geochemistry*, 70(3), 283-291.

Al-Masri, M. S., Amin, Y., Ibrahim, S., & Al-Bich, F. 2004. Distribution of some trace metals in Syrian phosphogypsum. *Applied Geochemistry*, 19(5), 747-753.

Altun, İ. A., &Sert, Y. 2004. Utilization of weathered phosphogypsum as set retarder in Portland cement. *Cement and Concrete Research*, 34(4), 677-680.

Alva, A. K., & Sumner, M. E. 1990. Amelioration of acid soil infertility by phosphogypsum. *Plant and soil*, 128(2), 127-134.

Arocena, J. M., Rutherford, P. M., &Dudas, M. J. 1995. Heterogeneous distribution of trace elements and fluorine in phosphogypsum by-product. Science of the total environment, 162(2), 149-160.

Banu, S. S., &Haq, M. N. 2015. A Study on the Mechanical Properties Such as Compressive Strength, Split Tensile Strength and Flexural Strength for Various Percentages of Phosphogypsum. *International Journal of Emerging Trends in Engineering and Development*, Issue 5, Vol. 4

Becker, P. 1989. Phosphates and phosphoric acid: raw materials, technology, and economics of the wet process. Revised and expanded (Vol. 6). Marcel Dekker, Inc.

Bhawan, P., & Nagar, E. A. 2012. Guidelines for Management and Handling of Phosphogypsum Generated from Phosphoric Acid Plants (Final Draft).

Carbonell-Barrachina, A., DeLaune, R.D., Jugsujinda, A., 2002. Phosphogypsum chemistry under highly anoxic conditions. *Waste Management* 22 (6), 657-665.

Chandara, C., Azizli, K. A. M., Ahmad, Z. A., & Sakai, E. 2009. Use of waste gypsum to replace natural gypsum as set retarders in portland cement. *Waste management*, 29(5), 1675-1679.

Degirmenci, N., Okucu, A., &Turabi, A. 2007. Application of phosphogypsum in soil stabilization. *Building and environment*, 42(9), 3393-3398.

Deshpande, P. S. 2003. The Determination of AppropiatePhosphogypsum:Class C Fly ash:Portlant Type II Cement Compositions for use in Marine Applications, A Master's Thesis, Louisiana State University.

EFMA. 2000. Production of Phosphoric Acid. Best Available Techniques for Pollution Prevention and Control in the European Fertilizer Industry. Brussels, Belgium.

El Nouhy, H., Khattab, E., &Zeedan, S. 2015. Behavior of Cement Pastes and Mortar Containing Phosphogypsum. *Key Engineering Materials Trans Tech Publications*, 668, 181-188.

Enamorado, S., Abril, J. M., Delgado, A., Más, J. L., Polvillo, O., & Quintero, J. M. 2014. Implications for food safety of the uptake by tomato of 25 trace-elements from a phosphogypsum amended soil from SW Spain. *Journal of hazardous materials*, 266, 122-131.

Erdogan, Y., Demirbas, A., &Genc, H. 1994. Partly-refined chemical by-product gypsums as cement additives. *Cement and concrete research*, 24(4), 601-604.

Fan, Y. 1997. Leaching Characteristics and Structural Integrity of Cement-stabilized Phosphogypsum, A Master's Thesis, Louisiana State University.

FIPR. 1987. Phosphogypsum: A Review of the Florida Institute of Phosphate Research Programs to Develop Uses for Phosphogypsum. *Florida Institute of Phosphate Research*, Publication No. 0l-000-035.

Folek, S., Walawska, B., Wilczek, B., &Miskiewicz, J. 2011. Use of phosphogypsum in road construction. *Polish Journal of Chemical Technology*. 13(2), 18.

Garrido, F., Illera, V., Vizcayno, C., &García-González, M. T. 2003. Evaluation of industrial by-products as soil acidity amendments: chemical and mineralogical implications. *European Journal of Soil Science*, 54(2), 411-422.

Guo, T. 1998. Determination of Optimal Composition of Stabilized Phosphogypsum Composites for Saltwater Application, A PhD Dissertation, Louisiana State University.

Gutt, W. 1978. The use of by-product in concrete (CP 53/74), BRE research series, Concrete: Practical studies from BRE. *The construction press*, 1, 47-66.

Huang, Y., & Lin, Z. 2010. Investigation on phosphogypsum–steel slag–granulated blast-furnace slag–limestone cement. *Construction and Building Materials*, 24(7), 1296-1301.

IFA. 2015. www.fertilizer.org/Phosphogypsum (last accessed on October, 2015)

Jenkins, R., Barton, J., Bartzokas A., Hesselberg J., Knusten, H. M. 2002. Environmental Regulation in the New Global Economy - The Impact on Industry and Competitiveness.

Kacimi, L., Simon-Masseron, A., Ghomari, A., &Derriche, Z. 2006. Reduction of clinkerization temperature by using phosphogypsum. *Journal of hazardous materials*, 137(1), 129-137.

Kumar, S. 2003. Fly ash–lime–phosphogypsum hollow blocks for walls and partitions. *Building and Environment*, 38(2), 291-295.

Lavelle, P., Decaëns, T., Aubert, M., Barot, S., Blouin, M., Bureau, F. & Rossi, J. P. 2006. Soil invertebrates and ecosystem services. European Journal of Soil Biology, 42, S3-S15.

Mullins, G. L., & Mitchell, C. C. 1990. Wheat forage response to tillage and sulfur applied as PG. *Proceedings of the third international symposium on PG*, Orlando, USA, 1, 362-75).

Nanni, A., & Chang, W. F. 1989. Phosphogypsum-based roller compacted concrete. *Concrete International*, 11(11), 48-64.

Nayak, S., Mishra, C. S. K., Guru, B. C., &Rath, M. 2011. Effect of phosphogypsum amendment on soil physico-chemical properties, microbial load and enzyme activities. *Journal of Environmental Biology*, 32(5), 613.

Nayak, A. K., Mishra, V. K., Sharma, D. K., Jha, S. K., Singh, C. S., Shahabuddin, M., &Shahid, M. 2013. Efficiency of Phosphogypsum and Mined Gypsum in Reclamation and Productivity of Rice–Wheat Cropping System in Sodic Soil. *Communications in soil science and plant analysis*, 44(5), 909-921.

Nigong, G. D. 1998. How does Phosphogypsum Storage Affect groundwaters. FIPR Project #94-05-042. Final Report, Environmental Radioactivity Measurement Facility, Department of Oceanography, Florida State University, Tallahassee, Florida 32306-4320.

Oliveira, S.M.B., Imbernon, R.A., 1998. Weathering alteration and related REE concentration in the Catalão I carbonatite complex, central Brazil. *Journal of South American Earth Sciences*, 11 (4), 379–388.

Potgieter, J. H., Potgieter, S. S., McCrindle, R. I., &Strydom, C. A. 2003. An investigation into the effect of various chemical and physical treatments of a South African phosphogypsum to render it suitable as a set retarder for cement. *Cement and concrete research*, 33(8), 1223-1227.

Rao, S. V. & Kumar, P. 2014. Application of FAL-G Hollow Masonry Blocks in Building Construction. International Journal of Engineering Technology, *Management and Applied Sciences*, 2(6), ISSN 2349-4476

Reddya, T. S. S., Kumarb, D. R., &Raoc, H. S. 2010. A Study on Strength Characteristics of phosphogypsum Concrete. *Asian Journal of Civil Engineering (Building ad Housing)*, 11(4), 411-420.

Rutherford, P. M., Dudas, M. J., &Samek, R. A. 1994. Environmental impacts of phosphogypsum. Science of the total environment, 149(1), 1-38.

Rutherford, P. M., Dudas, M. J., &Arocena, J. M. 1995. Radioactivity and elemental composition of phosphogypsum produced from three phosphate rock sources. *Waste Management & Research*, 13(5), 407-423.

Shen, W., Zhou, M., & Zhao, Q. 2007. Study on lime–fly ash–phosphogypsum binder. *Construction and Building Materials*, 21(7), 1480-1485.

Singh, M., & Garg, M. 1995. Phosphogypsum—Fly ash cementitious binder—its hydration and strength development. *Cement and concrete research*, 25(4), 752-758.

Singh, M. 2002. Treating waste phosphogypsum for cement and plaster manufacture. *Cement and Concrete Research*, 32(7), 1033-1038.

Singh, M. 2003. Effect of phosphatic and fluoride impurities of phosphogypsum on the properties of selenite plaster. *Cement and Concrete Research*, 33(9), 1363-1369.

Singh, M. 2005. Role of phosphogypsum impurities on strength and microstructure of selenite plaster. *Construction and building materials*, 19(6), 480-486.

Smadi, M. M., Haddad, R. H., &Akour, A. M. 1999. Potential use of phosphogypsum in concrete. *Cement and Concrete Research*, 29(9), 1419-1425.

Szynkowska, M.I., Pawlaczyk, A., Rogowski, J. 2011. Characterization of Particles Transmitted by Wind from Waste Dump of Phosphatic Fertilizers Plant Deposited on Biological Sample Surfaces. *Air Quality Monitoring, Assessment and Management. InTech*.

Taher, M. A. 2004. Influence of thermally treated phosphogypsum on the properties of Portland cement in presence of silica fume. *Silicates industrials*, (9-10), 68-72.

Taher, M. A. 2007. Influence of thermally treated phosphogypsum on the properties of Portland slag cement. Resources, Conservation and Recycling, 52(1), 28-38.

Tang, Z., Lei, T., Yu, J., Shainberg, I., Mamedov, A. I., Ben-Hur, M., & Levy, G. J. 2006. Runoff and interrill erosion in sodic soils treated with dry PAM and phosphogypsum. *Soil Science Society of America Journal*, 70(2), 679-690.

Tayibi, H., Choura, M., Lopez, F. A., Alguacil, F. J. and Lopez-Delgado,A. 2009 Environmental impact and management of phosphogypsum (Review).

Thimmegowda, H. 1994. Generation and Evaluation of Raw and Cement Stabilized Phosphogypsum Leachates, A Master's Thesis, Louisiana State University.

Toma, M., &Saigusa, M. 1997. Effects of phosphogypsum on amelioration of strongly acid nonallophanicandosols. Plant and soil, 192(1), 49-55.

United States Environmental Protection Agency (USEPA) 2002. National Emission Standards for Hazardous Air Pollutants: Subpart R: Radon from Phosphogypsum Stacks.

USEPA. 1992. Potential uses of phosphogypsum and associated risks. Background information Document for 40 CFR 61 Subpart R. National Emission Standards for Radon Emissions from Phosphogypsum Stacks, Technical Report 402-R-92-002. Washington DC.

Wissa, A. E. Z., M.A., Phosphogypsum Disposal and the Environment. Available online at:www.ardaman.com/phosphogypsum_disposal.htm (last accessed on October, 2015)

NCEED 2015 -National Conference on Earthquake and Environmental Disaster; December 17, 2015; CUET, Chittagong, Bangladesh
Bhuiyan M. A. R., Pal S. K., Mazumder M. H., Mazumder R. K., Omi F. R. (eds.)

A Comparative Study on Hydrological Modelling of Urban Water Logging

Ahad Hasan Tanim
Center for River, Harbor & Landslide Research, Chittagong University of Engineering & Technology, Chittagong, Bangladesh

Syed Abdullah Mohit
Z. H. Sikdar University of Science & Technology, Bangladesh

Aysha Akter
Department of Civil Engineering, Chittagong University of Engineering & Technology, Chittagong, Bangladesh

ABSTRACT: Recently increased rainfall experiences due to climate change and thus posing increasing threat to the rain induced stagnant runoff in city areas. Chittagong, like many other urban areas is facing this problem often in monsoon. Increasing trend in temperature and precipitation along with the land use changes and improper drainage facilities exaggerate this water logging problem. To overcome this issue as well as to reduce the subsequent losses, detail hydrological model is urgent which can simulate all the controlling parameters of urban hydrology like land use, climate, topography etc. In this study, rainfall-runoff modeling has been carried out using two numerical models, i.e., Hydrologic Engineering Center Hydrological Modeling System (HEC-HMS) v3.5 and Storm Water Management Model (SWMM) v5. The geometrical and physical characteristics of watershed are efficiently determined by using Arc-GIS v9.3. Then, those hydrological models are interrelated with identical watershed properties, meteorological data to compare their practical feasibility. The peak discharge obtained from SWMM hydrographs are 5-8% lower than the hydrograph obtained from HEC-HMS. The runoff hydrograph comparison of identical sub-catchment shows both model can be efficiently applicable for hydrologic modeling of urban storm water logging in Chittagong City area. Finally, the obtained comparative hydrographs from these hydrological models showed a reasonable relationship and thus they can provide valuable guidance for urban water logging prediction.

1 INTRODUCTION

Due to rapid urbanization along with climate changes, increased paved areas in Chittagong city like other city of Bangladesh, usually experiences more frequent and devastating stagnant runoff during monsoon. Considering climate change issues, for last few decades urban hydrology and its subsequent problems are clearly gaining importance around the world (Elga et al, 2015). In this regard researchers tried to apply different modelling approach for urban flooding prediction using different models i.e., HEC-GeoHMS and HEC-RAS (Suriya and Mudgal, 2011), BASINS (Brun and Band, 2000), SWMM, SWMM and inundation model (Krebs et al. 2014), MOUSE and FORM (Thorndahl and Willems, 2008), InfoWORKS (Hurford et al. 2010). Among those models, HEC-HMS and SWMM were selected for this paper to identify the potentialities of hydrological modeling in Chittagong city. This comparative study showed simulation procedures of urban hydrologic features and their relative advantages on each other.

2 METHODOLOGY

2.1 Study Area

Since 2013 field survey showed 13 most vulnerable water logged areas in Chittagong city (Mohit et al., 2014) and this study area covers 4 most water logging prone areas among them. The four sub-catchments in this study cover 558.26 hectares with varieties of land uses (Table 1).The soil is mainly sandy type but there are silty and clayey types also.

Table 1. Sub-catchments properties

Sub-catchment ID	Area(hectares)	Width(m)	% imperviousness	% slope
Badurtala	210.17	1340	39.64	3.17
Muradpur	207.07	2637	27.44	2.44
Kapasgola	41.27	605	57.13	2.92
Chaktai	99.75	950	26.25	3.26

(a)

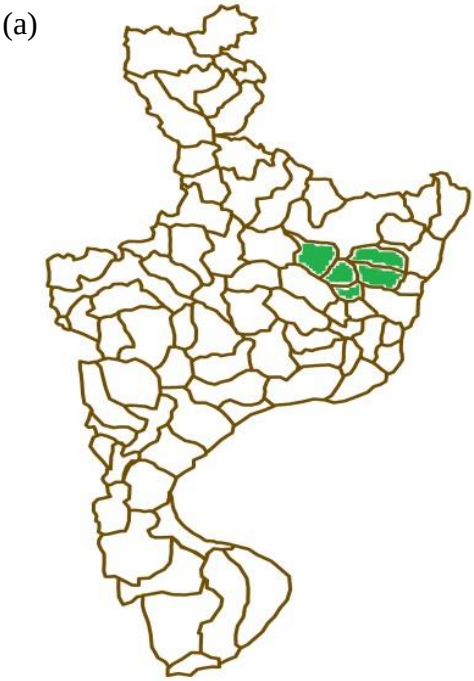

(b)

Figure 1(a). HEC-GeoHMS sub-catchments boundaries for Chittagong City Corporation area
Figure 1(b). Study area

2.2 Model set up

The modelling approach broadly involved with two models (HEC-HMS and SWMM). The stepwise modelling approach with the development of numerical modeling using SWMM and HEC-HMS, GIS, and Digital Elevation Model (DEM), automated techniques of sub-catchments delineation (Figure 1a) using HEC-GeoHMS has described in Figure 2. SRTM 30m DEM was used for spatial analysis. In HEC-HMS the total city was featured as basin, the natural catchments as sub-basin and the natural streams were considered as reach. With the basin model components of HEC-HMS the positions of sub-basins and reaches were located and connections were made between them providing upstream and downstream data. The final outlet of our basin, the Bay of Bangle was considered as a sink (Figure 3). Drainage or stream geo metry was created by CDA vector data. SCS-CN (Soil Conservation Service Curve Number) method w as used for infiltration calculation. Evapo-transpiration was computed by Penman-Monteith Method. Meteorological data such as precipitation, evapo-transpiration, wind speed, radiation, and temperature was obtained from Bangladesh Meteorological Department (BMD) Potenga Weather Station. Both models were analyzed for a simulation period of May 2013 with a time interval of 4 hour to compare runoff hydrograph of identical sub-catchments Muradpur, Kapasgola, Badurtala, Chaktai.

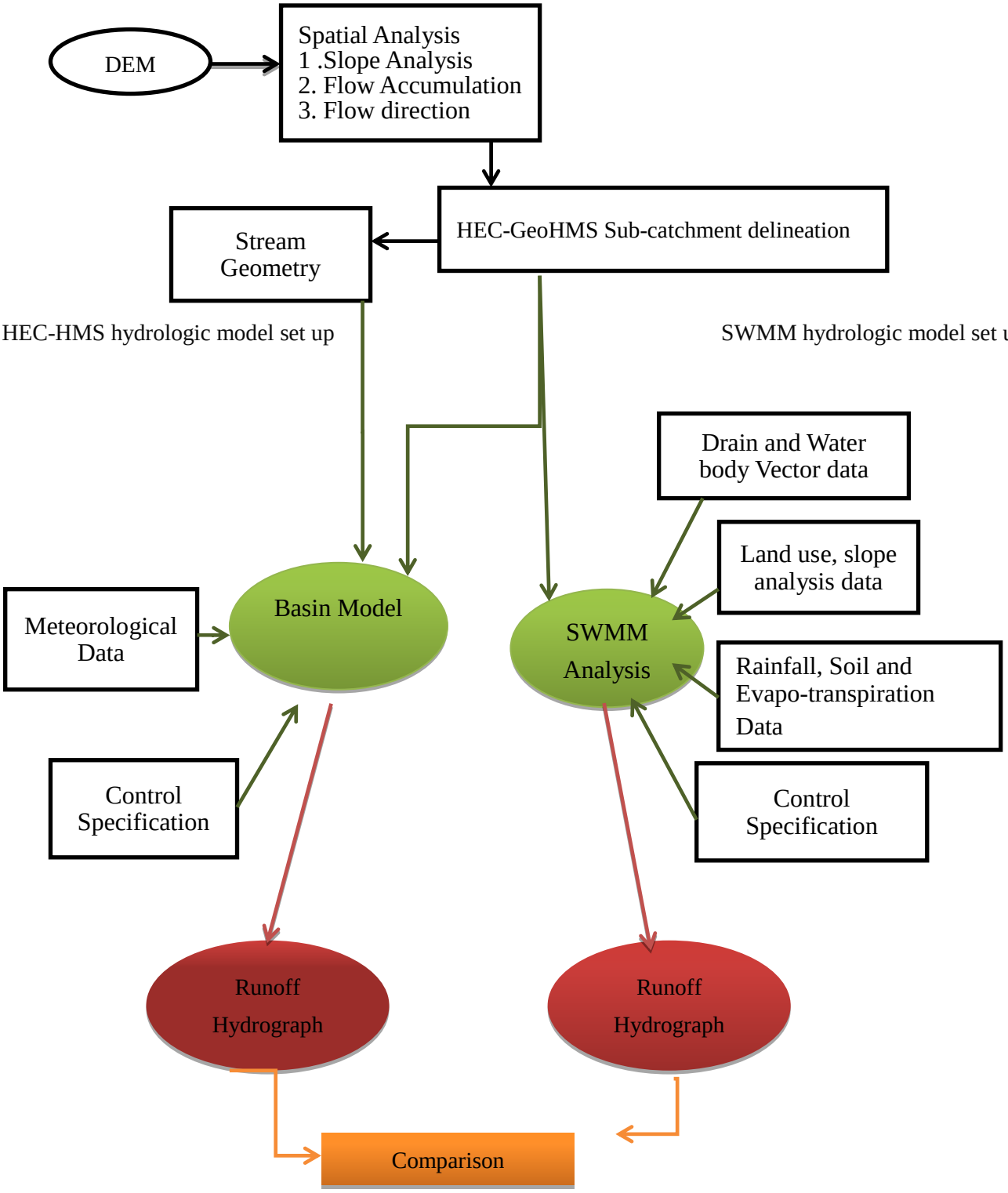

Figure 2. Stepwise model setup for this study.

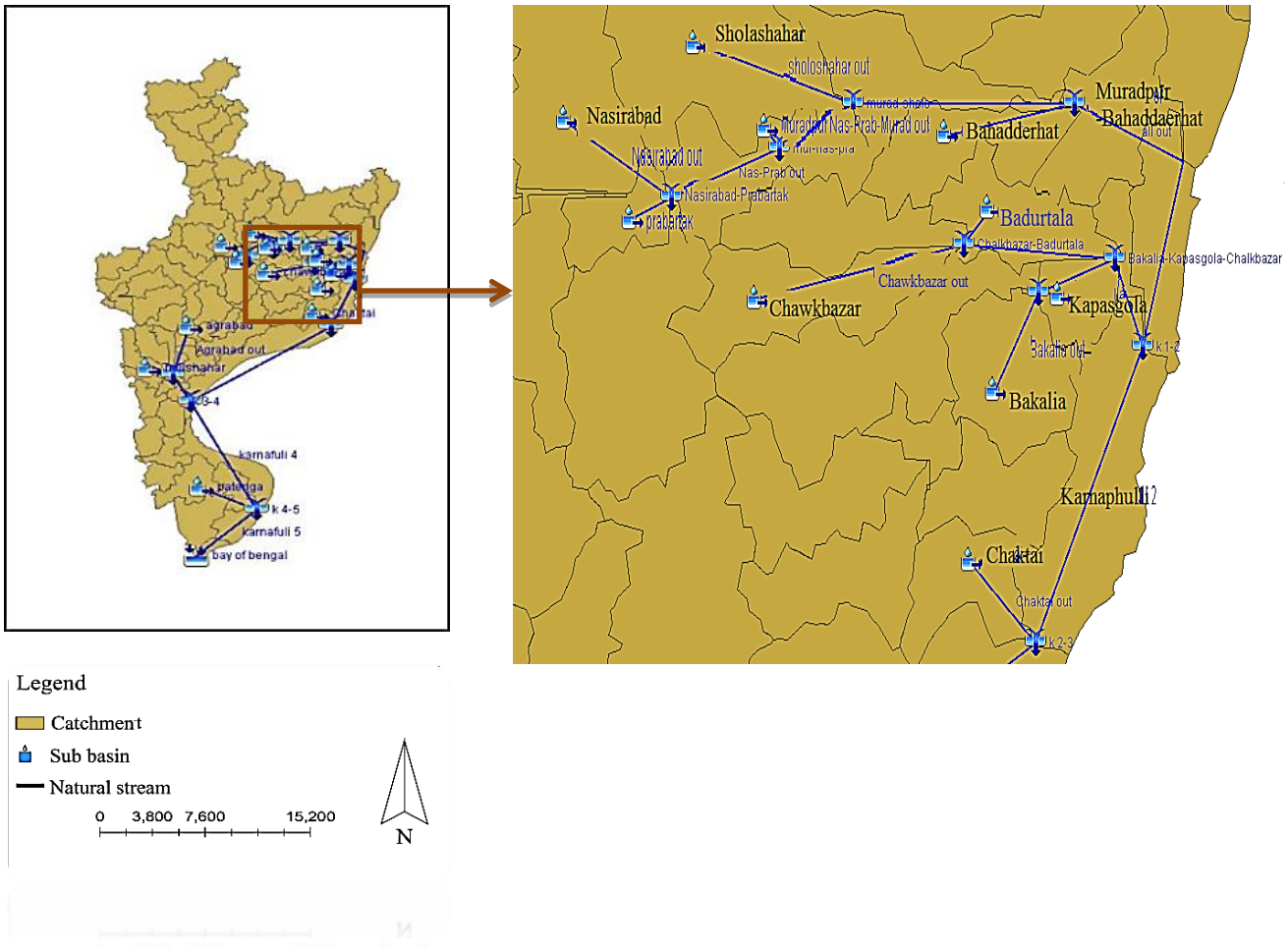

Figure 3. Model set up in HEC-HMS.

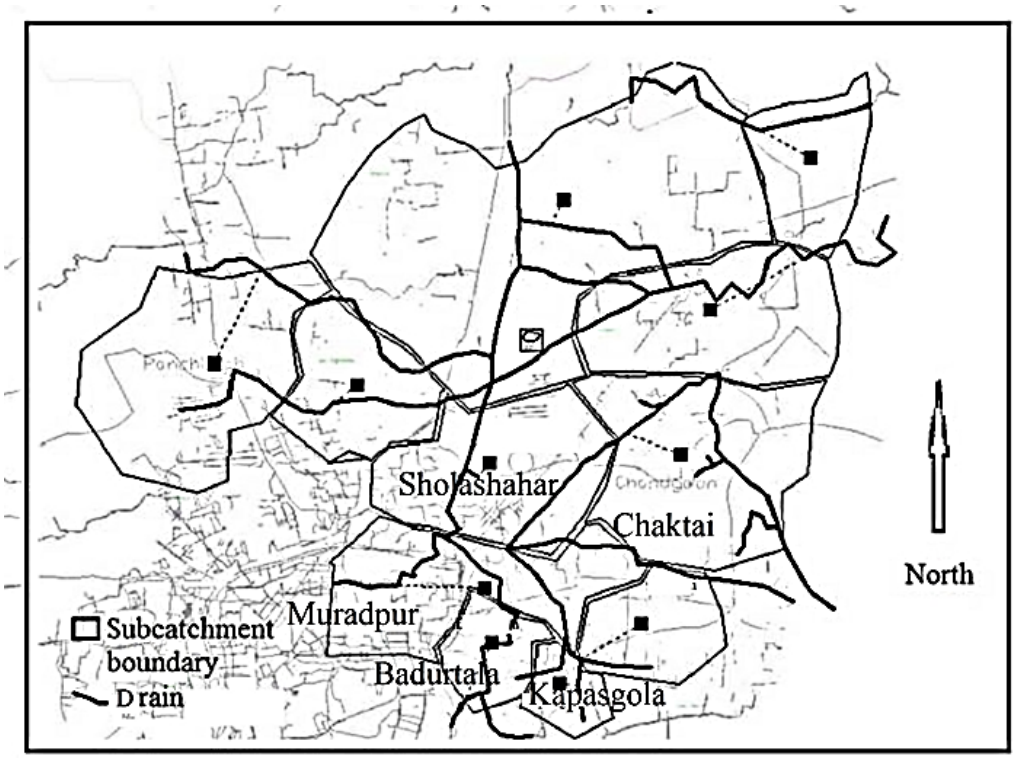

Figure 4. Model set up in SWMM.

3 MODELS OUTCOME

The hydrographs obtained from both models for a continuous simulation of 4 hour interval time series (May 2013) are represented in Figure 5.

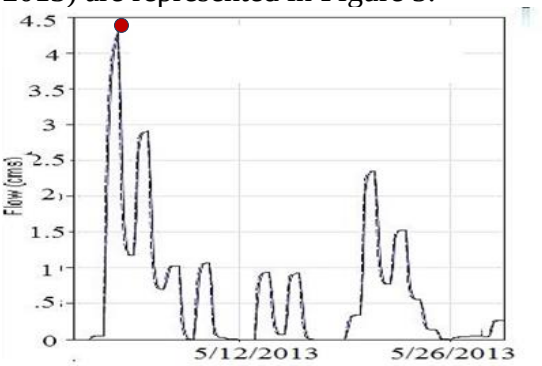

Figure5(a). Runoff Hydrograph of Sub-basin Badurtala(HEC-HMS)

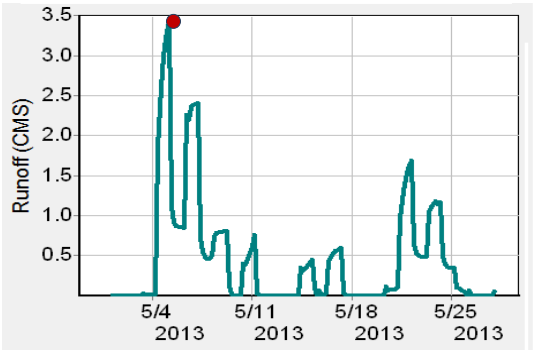

Figure 5(b). Runoff Hydrograph of Sub-catchment Badurtala(SWMM)

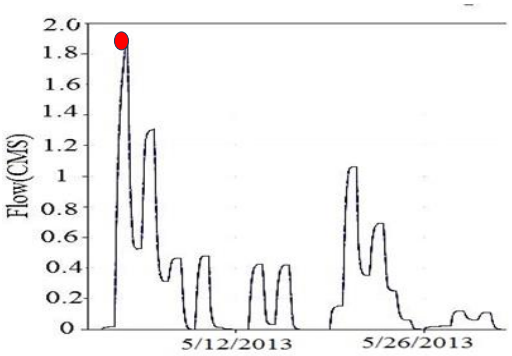

Figure 5(c). Runoff Hydrograph of Sub-basin Chaktai(HEC-HMS)

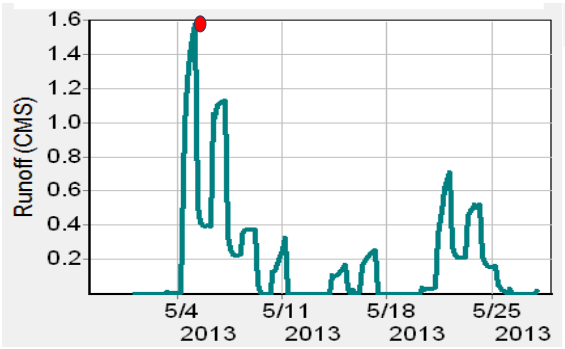

Figure 5(d). Runoff Hydrograph of Sub-catchment Chaktai(SWMM)

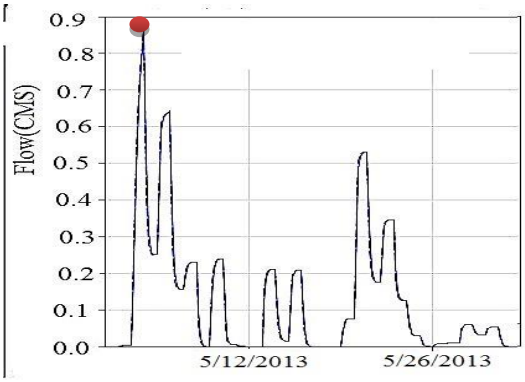

Figure 5(e). Runoff Hydrograph of Sub-basin Kapasgola(HEC-HMS)

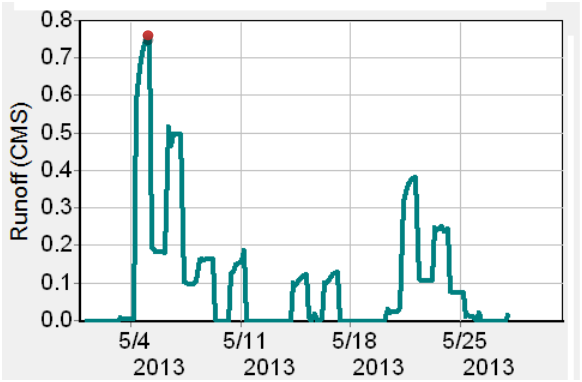

Figure 5(f). Runoff Hydrograph of Sub-catchment Kapasgola(SWMM)

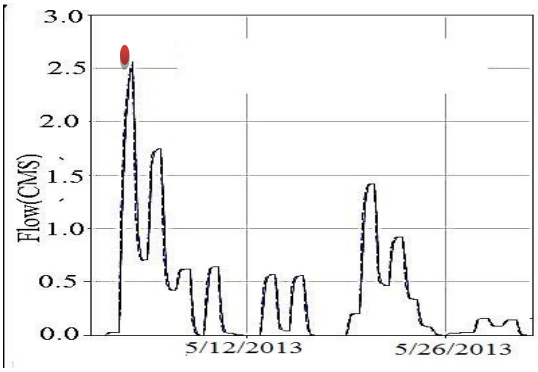

Figure 5(g). Runoff Hydrograph of Sub-basin Muradpur(HEC-HMS)

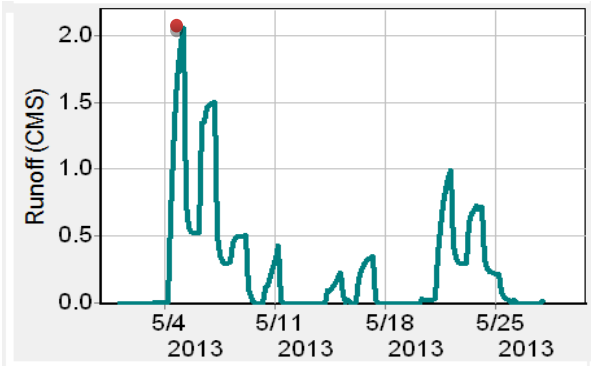

Figure 5(h). Runoff Hydrograph of Sub-catchment Muradpur(SWMM)

Although using Arc-GIS and Arc-hydro tool produces identical watershed boundaries, the peak discharges of SWMM hydrograph varies 5-8% from the hydrograph obtained from HEC-HMS .The fundamental reasons are:

- The base flow and depression storage was considered in SWMM;
- The evaporation time series that was used in SWMM reduces effective runoff; and
- The routing method in SWMM is dynamic wave routing whereas in HEC-HMS is kinematic wave routing.

On the other hand, SWMM was developed for evaluating storm water runoff hydrology and storm water drainage and collection systems in an urban setting for single event and continuous simulation (Lewis A. Rossman, 2008).In SWMM for a watershed, the selections of manning's N for pervious and impervious areas are always challenging because the movement of sheet flow is highly sensitive to surface. The sub catchment width is determined by taking the area of the sub catchment and dividing it by the average overland flow path length. The average overland flow path is determined by measuring the length from the sub catchment outlet to the sub catchment perimeter and averaging these values. The watershed is essentially modeled as an equivalent rectangle, and SWMM computes the overland flow path from the area and width of the sub catchment which have to supply as input. The length of the overland flow path supposes to govern how quickly water shows up at the bottom of the watershed. On the contrary, HEC-HMS is a model for major event predictions from a large tributary area. A unit graph method is a lumped approach that does not produce different peak flows due to overland flow length.

Again, SWMM is able to simulate both kinematic and dynamic wave routing options whereas for HEC-HMS is able to simulate kinematic wave routing. However, the computational procedure used in HEC-HMS for kinematic routing is different than that used for kinematic routing in SWMM. The kinematic routing in SWMM uses a Newton-Raphson function and only breaks the overland plane into one segment and in a numerical sense is a little more crude (Wayne C. Huberand, Robert E. Dickinson,1988).

4 CONCLUSIONS

This paper outlined urban hydrological modeling approach using HEC-HMS and SWMM. Hydrological processes in urban environment differ from those in natural catchment because urbanization modifies the physical environment and hence the water quantity, quality and its dynamics. Natural hydrological processes, such as infiltration, overland flow etc. are altered and new processes are introduced, like the artificial storm water drainage flow. These processes strongly interact with each other and are characterized by specific spatial and temporal scales. HEC-HMS and SWMM were tested in this study to feature those parameters in urban hydrology. But several urban modeling features of SWMM make it convenient to simulate those parameters than HEC-HMS. However, to improve the urban water logging following issues should be taken into consideration:

- Required numbers of gauges should be placed at necessary places to spread study on water logging;
- For major rainfall event of a large tributary it is convenient to use HEC-HMS rather than SWMM due to its computational steps regarding overland flow length and sub-catchments areas;
- To simulate dry weather flow for urban hydrology with special land use features, backwater effect and sewer design, it is recommended to use SWMM; and
- For single event storm with a close interval of few hours or less than an hour SWMM dynamic wave routing technique is expected to perform better.

5 REFERENCES

Brun, S. E. & Band, L. E. 2000. Simulating runoff behavior in an urbanizing watershed. *1043 Comput. Environ. Urban Syst.*, 24(1): 5-22.

Elga, S., Jan, B. & Okke, B. 2015. Hydrological modelling of urbanized catchments: a review and future directions. *Journal of Hydrology*, doi: http://dx.doi.org/10.1016/j.jhydrol.2015.06.028

Hurford, A. P., Maksimovic, C. & Leitao, J. P. 2010. Urban pluvial flooding in Jakarta: applying state-of-the art technology in a data scarce environment. *Water Sci. Technol.*, 62(10): 2246-2255.

Lewis A. Rossman. 2008. *SWMM5 Manual Storm Water Management Model Quality Assurance*, 159-193.

Mohit, S.A., Huq, M.A. & Akter, A. 2014. Prediction of water logging in Chittagong city using hydrological model. *In proceedings of the 2nd International Conference on Advances in Civil Engineering 2014 (ICACE 2014), WRE061*, 26 – 28 December 2014, CUET, Chittagong, Bangladesh, pp. 1151-1156.

Suriya, S. & Mudgal, B. V. 2011. Impact of urbanization on flooding: The Thirusoolam sub watershed – A case study. *J. Hydrol*., 412-413: 210-219.

Thorndahl, S. & Willems, P. 2008. Probabilistic modelling of overflow, surcharge and flooding in urban drainage using the first-order reliability method and parameterization of local rain series. *Water Res*., 42(1-2): 455-466.

WayneC., Huberand Robert E.& Dickinson,1988. *User's Manual,Extran Addendum*, pp. 216-256.

NCEED 2015 -National Conference on Earthquake and Environmental Disaster; December 17, 2015; CUET, Chittagong, Bangladesh
Bhuiyan M. A. R., Pal S. K., Mazumder M. H., Mazumder R. K., Omi F. R. (eds.)

Effect of Climate Change on Boro Rice Production in Bangladesh and its Assessment by Using DSSAT Model

Md. Manir Mia & Md. Alauddin
Rajshahi University of Engineering and Technology, Rajshahi, Bangladesh

ABSTRACT: Bangladesh is the largest deltas in the world which is vulnerable to uncertain climate change every year. Rice is the staple food in our country and our economy depends on rice. Rice production should be increased with the increasing populations of our country. If the rice production decreases, our economy will go down. Boro rice is one of the most produced rice in our country. Boro rice is a potential area for increasing rice yield, which currently accounts for about 50% of total rice production in the country (BRRI, 2006). Effect of climate change on yield of two varieties of boro rice has been assessed using the DSSAT (Decision Support System for Agro technology Transfer, version 4) modeling system. The DSSAT modeling system is an advanced physiologically-based rice crop growth simulation model which has been widely applied to understanding the relationship between rice and its environment. The model estimates yield of irrigated and non-irrigated rice, determine duration of growth stages, dry matter production and effect of soil water and soil nitrogen contents on photosynthesis, carbon balance and water balance. The yield of BR3 and BR14 boro varieties for the years 2008, 2030, 2050 and 2070 have been simulated in this model for 12 locations (districts) of Bangladesh. Available data on soil and hydrologic characteristics of these locations, and typical crop management practices for boro rice are used in the simulations. Therefore, DSSAT modeling system can be a useful tool for assessing possible impacts of climate change on boro rice production.

1 INTRODUCTION

Bangladesh is one of the worst affected among countries that are facing the impacts of climate change mostly in agricultural sector. The climate in Bangladesh is changing and it is becoming more unpredictable every year. The impacts of higher temperature, more variable precipitation, more extreme weather events, and sea level rise are already felt in Bangladesh and will continue to intensify. Climate change poses now-a-days severe threat mostly in agricultural sector and food security among all other affected sectors [1]. Despite technological advances such as improved crop varieties and irrigation systems, weather and climate are still key factors in agriculture productivity. Often the linkage between these key factors and production losses are obvious, but sometimes the linkages are less direct. The impacts of climate change on food production are global concerns, and they are very important for Bangladesh. Agriculture is the largest sector of Bangladesh's economy, which accounts for about 35% of the GDP and about 70% of the labor force. Agriculture in Bangladesh is already under pressure both from huge and increasing demands for food, and from problems of agricultural land and water resources depletion [2]. Bangladesh needs to increase the rice yield in order to meet the growing demand for food emanating from population growth. Irrigated rice or Boro rice is a potential area for increasing rice yield, which currently accounts for about 50% of total rice production in the country [3]. However, climate change is a potential threat towards attaining this objective. It is therefore very important to understand the effect of climate change on rice production, especially boro production.

Various studies have been carried out to assess impacts of climate change and variability on rice productivity in Bangladesh using the CERES-Rice model [5, 6 and 7]. These studies mainly focused on the effects of higher air temperature and atmospheric CO_2 concentration on rice yield. It may be noted that weather data requirement for DSSAT (Decision Support System for Agro technology Transfer, version 4) model include daily maximum and minimum air temperatures, daily precipitation and daily solar radiation, all of which could affect rice yield significantly. In this study, future climate scenarios, including daily maximum and minimum

temperatures, precipitation and solar radiation, for selected locations of Bangladesh have been generated and used for predicting yield of boro rice. The yield of two boro varieties (BR3 and BR14) have been predicted in the present study for the years of 2008, 2030, 2050 and 2070, using the DSSAT modeling system. The future climate scenarios have been generated using the climate model named Providing REgional Climates for Impact Studies (PRECIS).

2 METHODOLOGY

2.1 *Selection of locations*

The yield of two boro varieties BR3 and BR14 for the years of 2008, 2030, 2050 and 2070 have been simulated for 12 districts of Bangladesh. The districts were selected from among the major rice growing areas in different regions of Bangladesh. Among them, Rajshahi, Bogra and Dinajpur were selected from northwestern region; Mymensingh and Tangail were selected from central region; Jessore and Satkhira from southwestern region; Barisal and Madaripur from southern region; Chandpur and Comilla from southeastern region; and Sylhet district from eastern region.

2.2 *Selection of rice variet*

The DSSAT model is able to predict rice yield and rice plant response to various environmental conditions. In order to predict crop growth and yield, the model takes into effect of weather, crop management, genetics, soil water, C and N. The model also uses a detailed set of crop specific genetic co-efficients. These co-efficients allow the model to respond to diverse weather and management conditions. Therefore, in order to get reliable results from model simulations, it is necessary to have the appropriate genetic co-efficient. The DSSAT model is variety-specific (e.g., BR3 boro) and is able to predict rice yield and rice plant response to various environmental conditions. In predicting crop growth and yield, the model takes into account the effect of weather, crop management, genetics, soil, water, C and N. The model also uses a detailed set of crop specific genetic coefficients. These co-efficients allow the model to respond to diverse weather and management conditions. Therefore, in order to get reliable results from model simulations, it is necessary to have the appropriate genetic co-efficients for the selected cultivars [7]. The two boro rice varieties BR3 and BR14 have been selected in the present study because genetic co-efficients for these varieties are available in the DSSAT modeling system. Although these varieties are not widely used at present time, the effects of climate change and variability on these varieties provide insights into possible impact of climate change on boro rice yield in the future for the selected cultivars.

2.3 *Soil and crop management input*

In this model a quite detailed set of input data on soil and hydrologic characteristics and crop management are required. These input data's are related to soil characteristics including soil texture, number of layers in soil profile, soil layer depth, pH of soil for each depth, clay, silt and sand contents, organic matter, cation exchange capacity etc. Required data on soil and hydrologic characteristics for the 12 selected locations (districts) were collected from Bangladesh Rice Research Institute (BRRI) [5, 8] and Soil Resources Development Institute (SRDI, Dhaka). The soil profile data used in the model for the North Eastern Barind Tract (i.e., Agro-Ecological Zone, AEZ-27) covering Dinajpur, Rangpur, Bogra, Gaibandha, and Joypurhat districts is presented in Table 1.

Table 1. Soil profile data for North Eastern Barind Tract (AEZ-27).

Depth bottom (cm)	Clay (%)	Silt (%)	Stones (%)	Organic carbon (%)	PH in water	Cation exchange capacity meq/100gm	Total Nitrogen (%)
5	19	17.5	0	0.79	5.2	5.25	0.14
15	19	17.5	0	0.79	5.2	5.25	0.14
30	19	17.5	0	0.75	5.2	5.25	0.13
45	19	17.5	0	0.63	5.2	5.25	0.11

Soil Texture: Loamy.

The crop management data required by the model include planting date, planting density, row spacing, planting depth, irrigation amount and frequency, fertilizer application dates and amounts. The input data used in this model simulation are shown in Table 2. Using these inputs, the average (of 12 locations) yields of BR3 and BR14 for the year 2008, estimated by the model, were about 5500 $kgha^{-1}$ and 4050 kg ha^{-1} respectively; these values are close to the reported yields of these varieties (BRRI, 2006). These crop management inputs

were used in all model simulations under the predicted weather scenarios for the years 2008, 2030, 2050 and 2070.

Table 2. Crop management data used in the model simulations.

Parameter	Input Data
Planting method	Transplant
Transplanting date	1, 5, 15 and 25 January
Planting distribution	Hill
Plant population at seedling	35 plants per m^2
Plant population at emergence	33 plants per m^2
Row spacing	20 cm
Planting depth	3 cm
Transplant age	35 days
Plant per Hill	2
Fertilizer (N) application	
18 days after transplanting	30 $kgha^{-1}$
38 days after transplanting	70 $kgha^{-1}$
56 days after transplanting	30 $kgha^{-1}$
Application of irrigation	855 mm in 14 applications

2.4 *Weather data*

In this study, a regional climate model named Providing REgional Climate for Impacts Studies (PRECIS) was used to generate daily weather data needed for running the DSSAT model. The special report on emission scenarios (SRES) A2 ECHAM4 has been used as PRECIS input. In this study PRECIS runs with 50-km horizontal resolution for the present climate (2008) using baseline lateral boundary conditions (LBCs) runs with 50-km horizontal resolution for the present climate (2008) using baseline lateral boundary conditions (LBCs). In the next step PRECIS run was completed for the year 2030, 2050 and 2070 using ECHAM 4 SRES A2 as the model input. The PRECIS outputs that were used in the DSSAT model include daily maximum temperature (T_{max}), daily minimum temperature (T_{min}), and daily incoming solar radiation (Srad), daily precipitation.

3 MODEL APPLICATIONS AND RESULTS

3.1 *Impact of climate change on rice yield*

Tables 3 and 4 show predicted yields of BR3 and BR14 boro rice varieties, respectively at 12 locations of Bangladesh in the years 2008, 2030, 2050 and 2070. These predictions have been made using a fixed concentration of atmospheric CO_2 of 379 ppm (the value reported for the year 2005 in the fourth assessment report of IPCC) and for planting date of 15 January. The Tables show significant reduction in rice yield in the future due to predicted changes in climatic condition. Compared to 2008, predicted average reductions of BR3 variety for the 12 selected locations are about 11% for the year 2030, 21% for 2050 and 54% for 2070. The corresponding reductions for BR14 variety are about 14%, 25% and 58% for the years 2030, 2050 and 2070, respectively.

Table 3. Predicted yield of BR3 variety of boro rice (kg ha-1) at 12 selected locations for the years 2008, 2030, 2050 and 2070.

Station Name	Cultivar	2008	2030	2050	2070	% change in yield for 2030	% change in yield for 2050	% change in yield for 2070
Rajshahi	BR3	3063	4083	3265	1785	33.3	6.59	-41.7
Bogra	BR3	5741	5119	4070	2036	-10.8	-29.1	-64.5
Dinajpur	BR3	6848	4824	4364	2692	-29.6	-36.3	-60.7
Mymensingh	BR3	5995	5275	4455	2739	-12.0	-25.7	-54.3
Tangail	BR3	5487	5160	3874	1938	-5.95	-29.4	-64.7
Jessore	BR3	5571	4432	4583	1997	-20.4	-17.7	-64.2
Satkhira	BR3	4700	4364	3603	2066	-7.14	-23.3	-56.0
Barisal	BR3	6043	4006	3972	2091	-33.7	-34.3	-65.4
Madaripur	BR3	4582	4017	3647	2186	-12.3	-20.4	-52.3
Chandpur	BR3	5975	5455	4039	2772	-8.70	-32.4	-53.6
Comilla	BR3	6115	5987	4456	3075	-2.09	-27.1	-49.7
Sylhet	BR3	5960	5117	5750	3595	-14.1	-3.52	-39.7

Table 4. Predicted yield of BR14 variety of boro rice (kg ha-1) at 12 selected locations for the years 2008, 2030, 2050 and 2070.

Station Name	Cultivar	2008	2030	2050	2070	% change in yield for 2030	% change in yield for 2050	% change in yield for 2070
Rajshahi	BR14	2334	2771	2392	1148	18.7	2.48	-50.8
Bogra	BR14	4306	3668	2637	1398	-14.8	-38.8	-67.5
Dinajpur	BR14	5047	3374	3023	1656	-33.1	-40.1	-67.2
Mymensingh	BR14	4353	3790	3186	1873	-12.9	-26.8	-57.0
Tangail	BR14	4104	3883	2565	1297	-5.38	-37.5	-68.4
Jessore	BR14	4032	3160	3153	1305	-21.6	-21.8	-67.6
Satkhira	BR14	3153	3171	2434	1377	0.57	-22.8	-56.3
Barisal	BR14	4397	2889	2705	1457	-34.3	-38.5	-66.9
Madaripur	BR14	3229	2606	2578	1491	-19.3	-20.2	-53.8
Chandpur	BR14	4389	3981	2801	1842	-9.29	-36.2	-58.0
Comilla	BR14	4678	4368	3063	1978	-6.62	-34.5	-57.7
Sylhet	BR14	4596	3764	4240	2378	-18.1	-7.74	-48.3

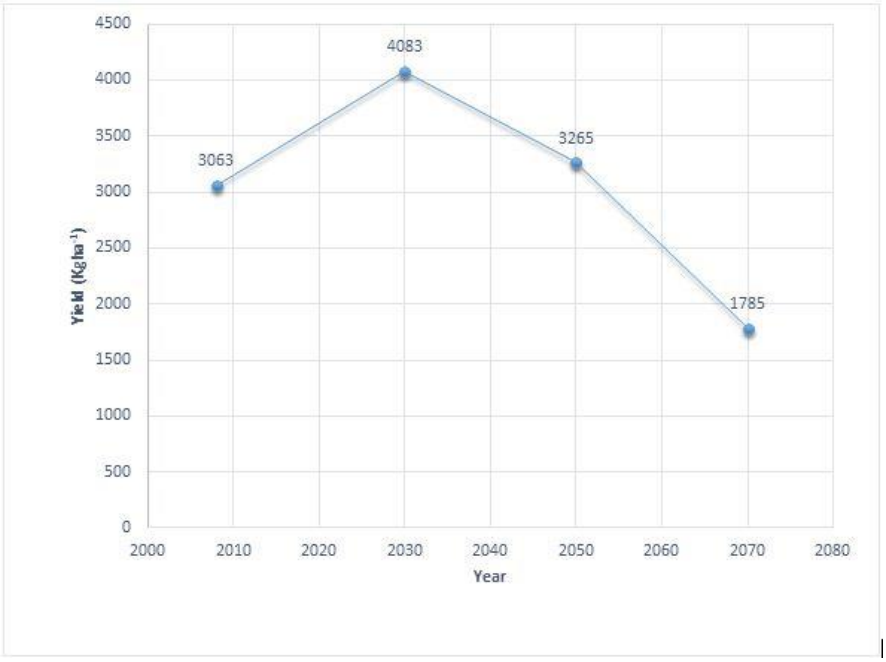

Figure 1. Predicted yield of BR3 varieties of rice for Rajshahi.

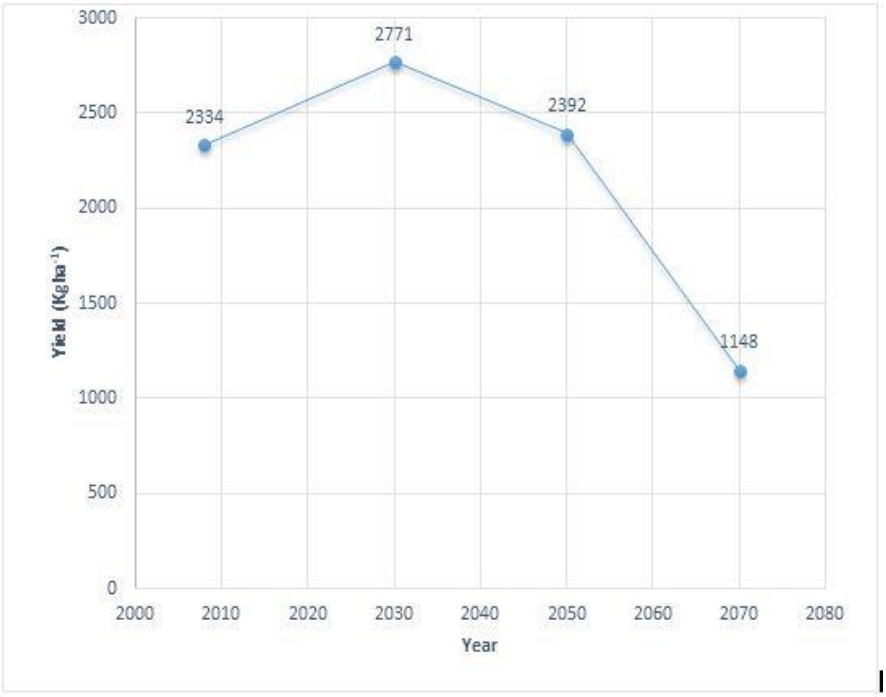

Figure 2. Predicted yield of BR14 varieties of rice for Rajshahi.

3.2 *Effect of climate change on physiological maturity*

This model results also showed significant effect of climate change on physiological maturity of rice. The duration of physiological maturity has been predicted to decrease significantly due to changes in climatic scenario. For example, predicted physiological maturity (in days) of BR3 rice varieties varied from 93 (in Satkhira) to 114 (in Sylhet) in 2008; while the corresponding values are 77 and 90 in 2070. For BR14, it varied from 92 (in Rajshahi) to 121 (in Sylhet) in 2008; while the corresponding values are 86 and 95 in 2070. Some regional variation could be observed in the predictions [4].

Table 7. Predicted physiological maturity (days) of BR3 for different locations.

Location	2008	2030	2050	2070
Rajshahi	88	95	84	83
Bogra	100	100	89	83
Dinajpur	105	99	89	82
Mymensingh	106	105	96	86
Tangail	99	98	87	84
Jessore	96	91	84	80
Satkhira	93	89	82	77
Barisal	99	94	87	80
Madaripur	96	94	86	80
Chandrapur	99	97	87	81
Comilla	102	100	92	82
Sylhet	114	114	104	90

Table 8. Predicted physiological maturity (days) of BR14 for different locations.

Location	2008	2030	2050	2070
Rajshahi	92	99	88	86
Bogra	105	105	90	87
Dinajpur	110	104	93	85
Mymensingh	112	111	101	90
Tangail	104	104	90	87
Jessore	101	96	87	83
Satkhira	97	94	86	81
Barisal	105	99	91	84
Madaripur	101	98	91	85
Chandrapur	105	102	92	84
Comilla	109	105	96	85
Sylhet	121	121	110	95

Figure 3 shows predicted physiological maturity in days for BR3 for different regions of Bangladesh.

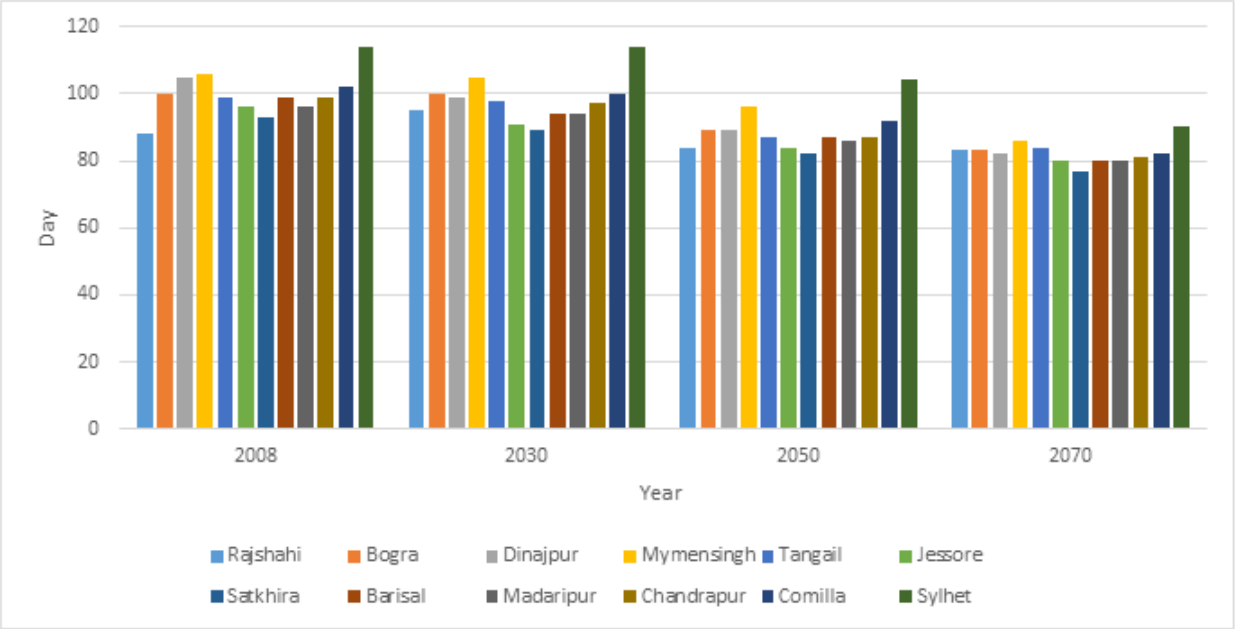

Figure 3. Region-wise prediction of physiological maturity (in days) of BR3 rice.

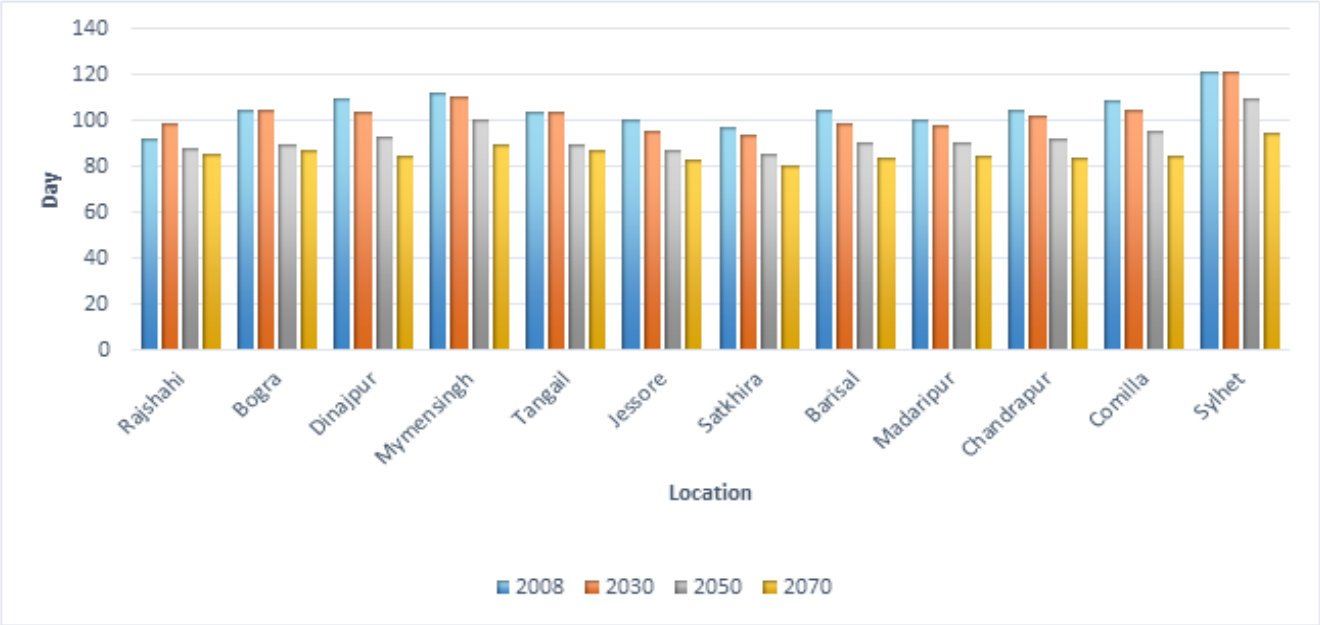

Figure 4. Region-wise prediction of physiological maturity (in days) of BR14 rice.

3.3 *Effect of locations for water requirement*

Table 9. Predicted water requirement (mm) of BR3 for different locations.

Location	2008	2030	2050	2070
Rajshahi	795.4	852.8	795.4	783.4
Bogra	862.4	800.6	841.6	792.8
Dinajpur	787.6	752	831.6	797
Mymensingh	651.8	549.2	703.2	687.8
Tangail	844	761.6	771.6	770.8
Jessore	841.8	755.6	840.4	778.2
Satkhira	779	742.6	760.2	733.2
Barisal	729.6	611.4	689.4	673
Madaripur	742.2	667.8	721.8	673.4
Chandrapur	712.4	650.2	702.8	703
Comilla	700.4	656.4	723.8	726.2
Sylhet	535.2	439.4	558.4	592.8

Table 10. Predicted water requirement (mm) of BR14 for different locations.

Location	2008	2030	2050	2070
Rajshahi	834.8	879.8	837.8	748.4
Bogra	935.8	855	845	770.2
Dinajpur	842.2	807	892.2	784.8
Mymensingh	683.4	589.6	771.2	677.2
Tangail	903	845	807.6	752.4
Jessore	888.8	814.4	868.6	775.2
Satkhira	840.8	806.8	790.6	735
Barisal	788.8	640.6	714.4	696.2
Madaripur	770.8	681.6	755.6	702.2
Chandrapur	772.8	694	742	702.8
Comilla	774.8	691.8	740.2	724.6
Sylhet	569.6	460	580.2	613.2

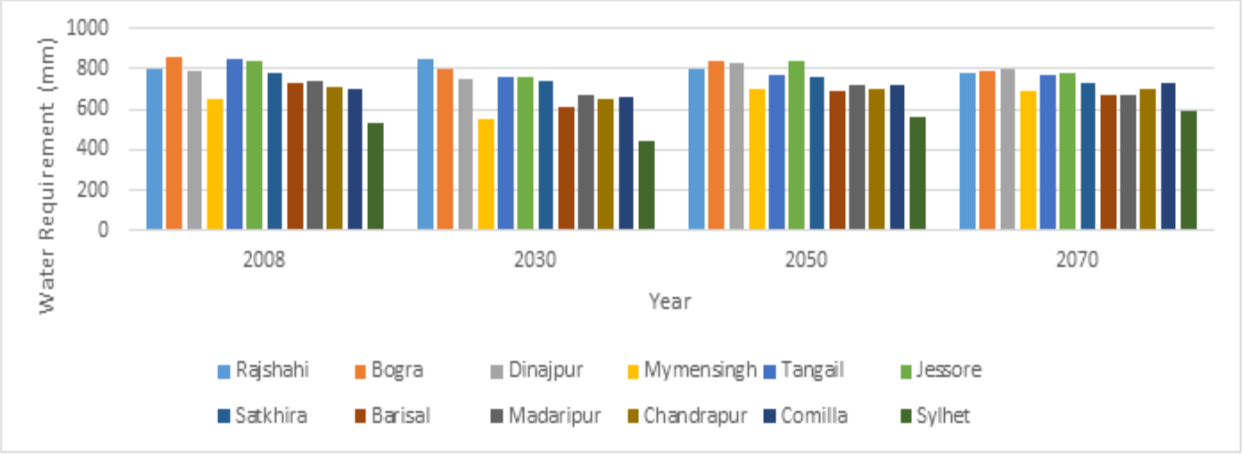

Figure 5. Region-wise prediction of water requirement (mm) of BR3 rice.

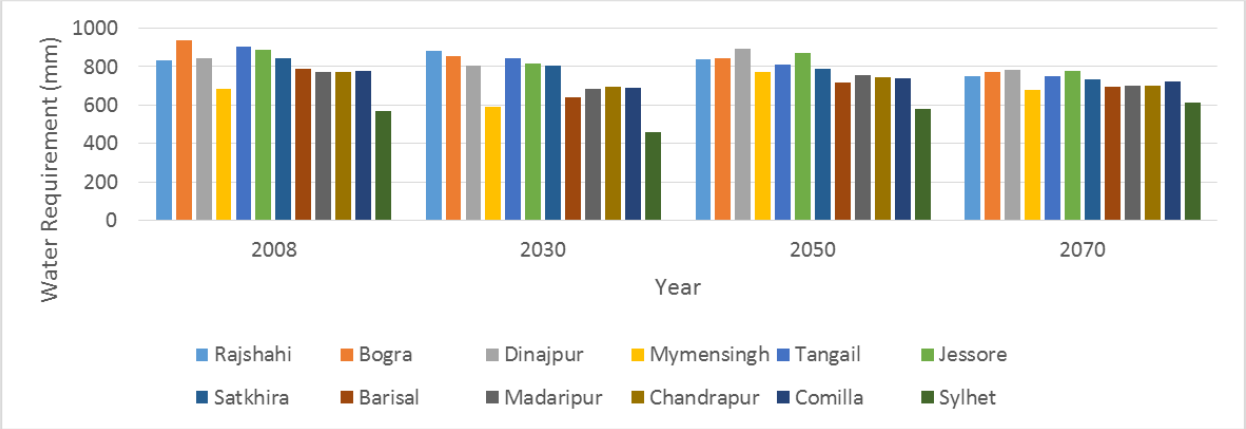

Figure 6. Region-wise prediction of water requirement (mm) of BR14 rice.

3.4 *Effect of climate change on irrigation water requirement*

Tables 9 and 10 show predicted irrigation water requirement for BR3 and BR14 rice varieties for the selected locations. Figure 4 shows variation of average water requirement for BR3 rice variety for different regions. The DSSAT model does not count the water required for preparation of land before transplanting (which usually varies from 200 to 300 mm, depending on soil and weather condition). In general, the model predicted slightly decreasing water requirement in the future, especially for the central, southwestern and southern regions (compared to 2008). Higher water requirements are predicted in northwestern region which is a drought prone region, relatively lower water requirements are predicted in eastern region where more rainfall occurs. Planting date also affects water requirement significantly according to model results. Model results show that water requirement is comparatively higher if boro rice is planted earlier, i.e., 1 or 5 January, compared to plantation on 15 or 25 January) [4]. The amount of water available for plant growth is affected by a combination of climatic and non-climatic variables such as precipitation, temperature, sunshine, wind speed as well as soil porosity, slope, etc. Climatic factors and duration of physiological maturity have significant roles on water requirement for plant. While higher evapotranspiration increases water requirement, shorter physiological maturity decreases water requirement. Higher temperature and higher solar radiation lead to higher evapotranspiration but shorten the period of physiological maturity. Predicted shorter physiological maturity in is one of the main reasons for lower water requirement in some of the future years, especially in 2070.

4 CONCLUSIONS

At present, BR3 and BR14 rice varieties are not widely used in our country. But the model simulations carried out in this study provides useful insight into the possible effects of climate change on boro rice yield. The growth and yield of crops are directly related to the rate of photosynthesis and phenology and their response to temperature, solar radiation and rainfall. In our country, optimum temperatures for maximum photosynthesis range from 25 to 30 ºC for rice under the climatic conditions. Increased temperatures during the growing season cause grain sterility. The very high temperature in this model has been predicted above 35℃ for the years 2050 and 2070 due to climate change. The crop model simulation results suggest that if climate change

causes significant increase in temperatures, this may in turn cause significant reduction in rice yield. The model simulations also suggest that changes in rainfall patter may also adversely affect rice yield. In order to assess the effect of climate change on the rice varieties currently being grown in Bangladesh, it is necessary to determine their genetic coefficients through carefully controlled experiments. It is also necessary to develop high temperature-resistant rice varieties and modify management practices to offset the adverse effects of climate change. Finally, it can be noted that DSSAT modeling system can be very useful in assessing possible impacts of climate change and management practices on rice yield. This model shows the system of reducing impacts of climate change on boro rice varieties.

5 REFERENCES

[1] Sikder, M. T. 2010. The Impacts of Climate Change on the Coastal Belt of Bangladesh: An Investigation of Risks & Adaptations on Agricultural Sector. *Hokkaido University, Sapporo*, Japan.

[2] Ahmed, A. & Ryosuke, S. 2000. Climate change and agricultural food production of Bangladesh: an impact assessment using GIS-based biophysical crop simulation model. *Center for Spatial Information Science, University of Tokyo*, 4-6-1 Komaba, Japan.

[3] BRRI. 2006. Improvement of standard Boro rice. *BRRI (Bangladesh Rice Research Institute) Annual Report for July 2005-June 2006*. Plant Breeding Division, BRRI, Gazipur, Bangladesh.

[4] Basak, J. K. 2009. Effects of climate change on boro cultivation in Bangladesh. *Masters of Science in Environmental Engineering*, 2 May, 2009, Department of Civil Engineering, Bangladesh University of Engineering and Technology (BUET), Dhaka, Bangladesh.

[5] Karim, Z., Hussain, S.G. & Ahmed, M. 1996. Assessing Impact of Climate Variations on Food grain Production in Bangladesh, *Water Air and Soil Pollution*, 92, 53-62.

[6] Mahmood, R., Meo, M., Legates, D. R. & Morrissey, M. L. 2003. *The Professional Geographer*, 55(2), 259-273.

[7] Basak, J. K., Ali, M. A., Islam, M. N. and Rashid, M. A. 2010. Assessment of the effect of climate change on boro rice production in Bangladesh using DSSAT model.

[8] BARC 2005. Fertilizer Recommendation Guide-2005, *Bangladesh Agricultural Research Council (BARC)*, Dhaka, Bangladesh. Soils publication no. 45, ISBN: 984-32-3166-X.

NCEED 2015 -National Conference on Earthquake and Environmental Disaster; December 17, 2015; CUET, Chittagong, Bangladesh
Bhuiyan M. A. R., Pal S. K., Mazumder M. H., Mazumder R. K., Omi F. R. (eds.)

A Case Study on the Sustainable Coastal Zone Management

M. Salauddin
Dept. of Civil Engineering, Chittagong University of Engineering and Technology, Chittagong 4349, Bangladesh

M. Nuruzzaman
Dept. of Civil Engineering, Chittagong University of Engineering and Technology, Chittagong 4349, Bangladesh

ABSTRACT: Due to the geographical condition, coastal area of Bangladesh is more diverse and dynamic than many other parts of the world. In the southeast part of the Bay of Bengal, severe erosion problems has been observed in many studies mainly due to sea level rise, variability in the sediment supply, storm waves, longshore sediment transport etc. This research is aimed to describe a process for the sustainable coastal zone management. A case study of sustainable coastal zone management along the coast of Rhône delta, France has been selected in this research. The Rhône delta is situated in the PACA region, south east of France bordered by the Mediterranean Sea with a coastline extending 90 km in length. Over the years, significant changes have occurred along the coastline zone. The issues focused for the implementation of sustainable coastal management in Rhône Delta were coastal erosion, sedimentation in the approach channel of the port, tourism development and salinity intrusion. The objectives of the pursuance of sustainable coastal area management were to reduce erosion along coastline, to fix the shoreline position, to reduce the sedimentation in the approach channel and to stabilize the Gracieuses spit. For the sustainable coastal development, after identifying each problem all the possible solutions were evaluated based on social equity and environmental sustainability. The study area was divided into several zones for simplifying the morphological modelling. The morphological modelling was done using 1D Matlab model and Delft 3D. To investigate the impact of different alternate measures, the coastlines were also modelled without any measure (base case) and compared with the results of the different alternative measures. To solve the erosion problems along the coastline, sand nourishment has been found as an effective solution. For the sustainable development of port and Gracieuses spit, multiple groynes were found more effective in comparison to a single groyne or breakwater. For the sustainable coastal development along the shoreline of Bangladesh this knowledge can be applied considering the geometry and nature of the coast.

1 INTRODUCTION

Due to the geographical condition coastal area of Bangladesh is more diverse and dynamic than many other parts of the world. In the southeast part of the Bay of Bengal, severe erosion problems has been observed in many studies mainly due to sea level rise, variability in the sediment supply, storm waves, longshore sediment transport etc. This research is aimed to describe a process for the sustainable coastal zone management. A case study of sustainable coastal zone management along the coast of Rhône delta, France has been selected in this research.

The Rhône delta is situated in the PACA region, south east of France bordered by the Mediterranean Sea with a coastline extending 90 km in length. The delta coastline is built up of fine sands from shores, dunes, and spit bars. The development of shore is highly dictated by economic, industrials, ports, and tourist activities. For the protection of wetlands during high tide and during storms coastline position along with coastal

defenses play a vital role in this area. Besides, the coastline zone is also very important for economic activities such as tourism and port activity (Port of Marseille-Fos).

However, over the years, significant changes have occurred along the coastline zone which can be seen in Figure 1. The coastline shows erosion and accretion in different places with different trends as a function of time over the last 60 years. In the PACA area, there are two rivers, Grand Rhône (eastern part) and Petit Rhône (western part), that contribute the sediments to the shoreline. In the east of the Grand Rhône, there is Port of Fos-sur-Mer. The coastline position of this zone has been changed over the past centuries as a result of the changed flow regime in the Rhône catchment. The decreasing sediment load in the Rhône as a result of the construction of structures (dams) and the resulting retreat of the coastline threatens activities in this area. At the same time, sedimentation also has been observed in the approach channel from the Glacieuse spit.

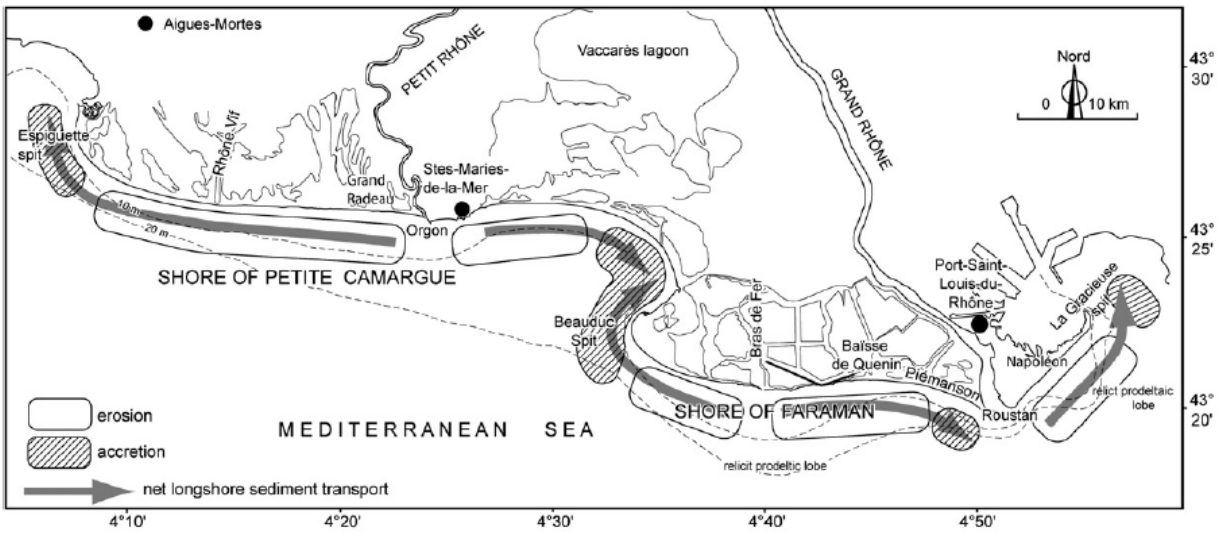

Figure 1: Observed erosion/accretion pattern along the coast of Rhône delta (Sabatier et. al, 2006)

The issues focused for the implementation of sustainable coastal management in Rhône Delta were coastal erosion, sedimentation in the approach channel of the port, tourism development and salinity intrusion. The main objectives of the pursuance of sustainable coastal area management were to reduce erosion along coastline, to fix the shoreline position, to reduce the sedimentation in the approach channel and to stabilize the Gracieuses spit.

2 PRESENT SITUATION OF STUDY AREA

Due to various reasons, erosion and accretion took place along the coast of Camargue over past years. Retreat of shore-line and reduction of beach width in the petite Camargue can be observed in Figure 2. To reduce erosion in this area both hard and soft solutions have been implemented throughout the years. Hundreds of groins along the Camargue coastline have been constructed along the coastline over recent years but till now erosion is a big problem in that area. In addition, the highway next to the shoreline linking the town with inland is in threat of erosion. Due to erosion in the beach, groins have been separated from the beach (Eurosion, 2009). Breakwater that has been built in between two groins did not prevent the swell from crossing over during storms.

However, without groins and breakwater half of the town of Saintes-Maries-de-la-Mer would have completely disappeared in 2000 (Sabatier et. al, 2009). But, these measures produce a negative impact on coastal landscapes, tourism and nature. Dikes locally reduced the retreat of coastline but led erosion to the near-shore zone along the direction of long-shore drift currents. Besides hard solutions, soft solution like coastal spit bar named "Gracieuse spit" also constructed in this coastal area. Although it acts as a natural breakwater and protects wetlands behind but its sustainability is now under threat due to continuous retreat and occurrence of breaches. All together, in the harbour of Fos severe sedimentation is occurring from spit which creates difficulty to enter the approach channel for big vessels with deeper draught.

Lowering of sediment inflow from the rivers could be a significant reason for the loss of coastal area (1.7 Mm^2/yr between 1944 and 1989). The spatial distribution of wave energy and the long-shore gradient in sediment transport are correlated with erosion in different zones. The long term sea-level rise probably causes 10 % of the shoreline retreat. Lastly, transport by winds from the land (Migstral, Tramontane) also causes a de-

flation of the dunes, which are being eroded on E – W trending sections of the beaches. Apart from this the spit extends further and further north-eastward and is starting to cause serious sedimentation in the navigation channel.

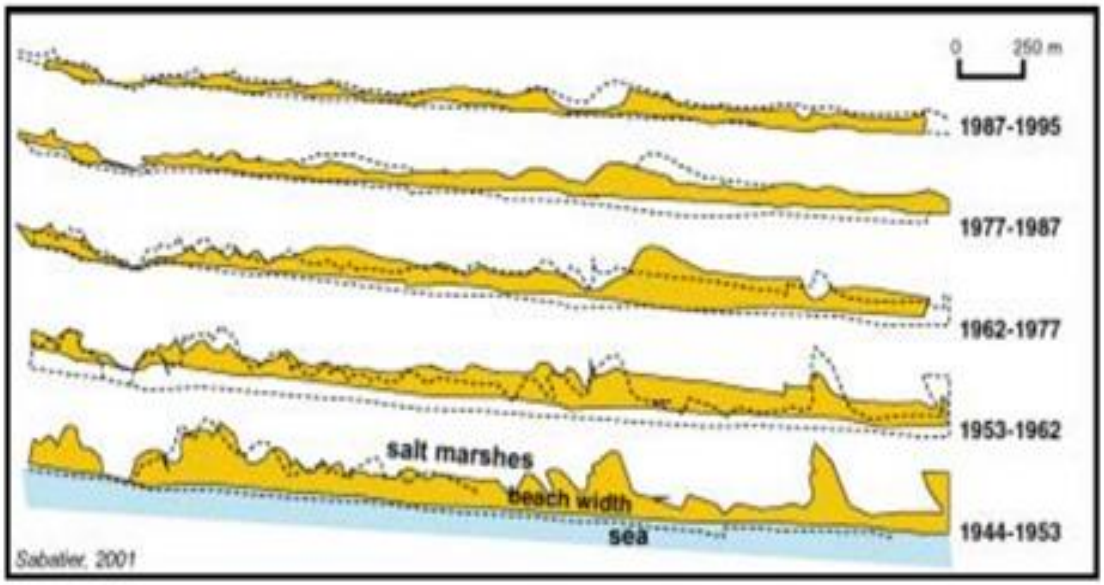

Figure 2: Retreat of shore-line and reduction of beach width in Petite Camargue (Sabatier, 2001)

3 METHODOLOGY

To achieve proper sustainable coastal zone management, after identifying each problem all the possible solutions were evaluated based on social equity and environmental sustainability.

The study area was divided into several zones as follows (see Figure 3):

— Zone-1 : Camargue west- Espiguette spit to Petit Rhône in the shore of Petite Camargue
— Zone-2 : Camargue west- Petit Rhône to Beauduc spit in the shore of Petite Camargue
— Zone-3 : Camargue east- shore of Faraman
— Zone-4 : Gracieuse spit including Gulf of Fos

Figure 3: Google map showing different zones of study area

In the zones 1, 2, 3 along the west and east part of Camargue coastline, Matlab software was used to observe the coastline changes with different alternatives. Then, the coastline changes with time without doing anything (base case) has been compared with the different alternatives. Moreover, to study the near-shore morphological changes (erosion and sedimentation) in zone-4 (Gracie use spit area), Delft 3D tool is used to know the effectiveness of different alternatives to solve the problems in this zone.

4 MORPHOLOGICAL ANALYSIS

The different alternative measures were introduced for solving each problem. Table 1 represents different alternatives which were taken in different zones. As mentioned that lowering input of sediment is one of the main reasons for erosion along the coast line. Beach nourishment is considered as a dynamic and environmentally responsible solution for the coastal protection (Adriaanse and Coosen, 1991). Also, French government approach to sand nourishment at beach is traditionally to couple it with hard structures as supporting measures to reduce sand losses and maintenance (Hanson et. al, 2002). Therefore, considering economy, environment and sustainability of the solution, soft solution like sand nourishment was introduced to solve the erosion problems along the coastline instead of hard solution like groynes.

Table 1: Addressed measures for solving problems

Problems	Addressed Measures
Erosion along coastline in zone-1	Sand nourishment with different possible location and volume of sand
Erosion along coastline in zone-2	Sand nourishment with different possible location and volume of sand
Erosion along coastline in zone-3	Sand nourishment with different possible location and volume of sand
Sedimentation in approach channel and erosion in Graciuses spit (zone-4)	Groynes or Breakwater with different possible length at different locations

It is noted that to solve the erosion along the coastline in zone 1, 2 and 3 simple Matlab tool was used. In all three zones (zone 1, 2 and 3) sand nourishment was introduced as an effective solution considering sustainability of the environment. In this paper, coastline change modeling of only one zone (zone-1) is described.

4.1 *ZONE-1*

In order to predict the coastline changes in zone 1 (Camargue west), beach nourishment at two different locations (see Figure 4) were modelled and compared with base case (doing nothing), see Table 2. The model was setup for 50 years. The depth of sand nourishment was taken in an average of 3.5 m.

Table 2: Different alternative measures applied in zone-1

Cases	Measures	Volume (m^3)
Base	Existing Situation	
Alternative-01	Beach nourishment over 125 m wide and 1600 m length	$1600 \times 125 \times 3.5 = 700{,}000\ m3$
Alternative-02	Beach nourishment in two areas, first one over 125 m wide and 1600 m length and second over 150 m wide and 1600 m length	$(700000) + (1600 \times 150 \times 3.5) = 1{,}540{,}000\ m3$

a) b)

Figure 4: Location of a) alternative 01 and b) alternative 02 in zone 1

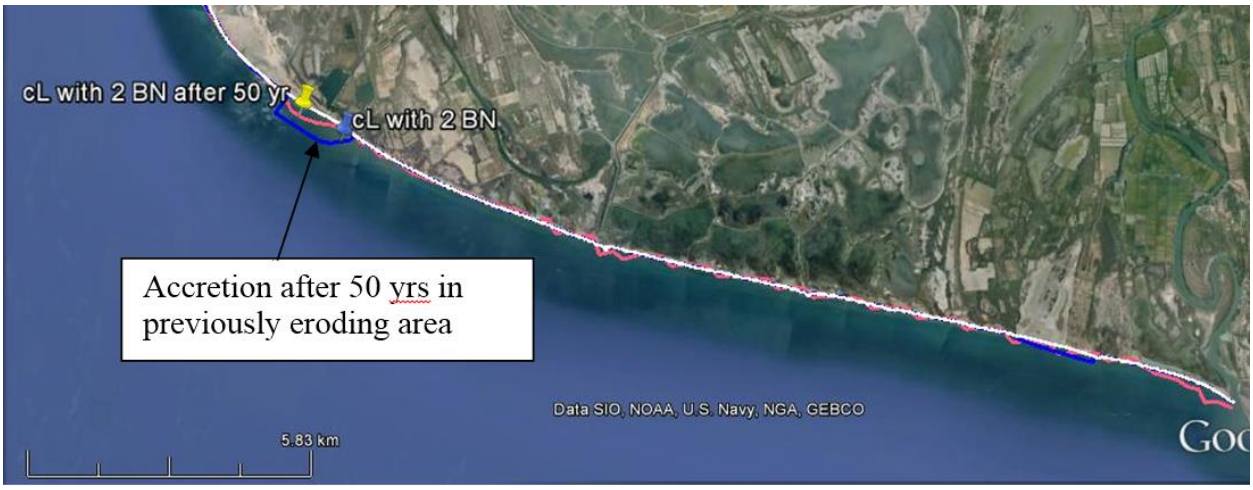

Figure 5: Comparison of coastlines among different alternatives

Based on the observed outputs it was observed that with sand nourishment in beach the coastline will be more protected then the existing situation. Moreover, by providing beach nourishment, beach will be wider compared to the existing one. Furthermore, alternative 02 showed better outputs not only for reducing erosion along coastline but also for widening the beach. Figure 5 shows how the coastline changes after 50 years for different alternative measures.

4.2 *ZONE-4*

In the Gracieuses Spit, mainly two problems were observed which are needed to solve to improve the coastal development in this area. Firstly, the depth of the channel in the port had been reduced due to sedimentation. And, spit which acts as a natural breakwater for Port of Fos was being eroded time by time. To solve those problems, there are four alternatives was taken as shown in Figure 6.
The explanation about alternatives is shown as below :

- Alternative I: single groyne almost at the end of the spit, with 400 m length and around 5 m depth.
- Alternative II: breakwater almost at the end of the spit, with 700 m length and around 14 m depth.
- Alternative III: single groyne almost at the end of the spit, with 150 m length and around 3.5 m depth.
- Alternative IV: multiple groynes along 3,000 m of the spit , with 100 m in length in an interval of 200 m.

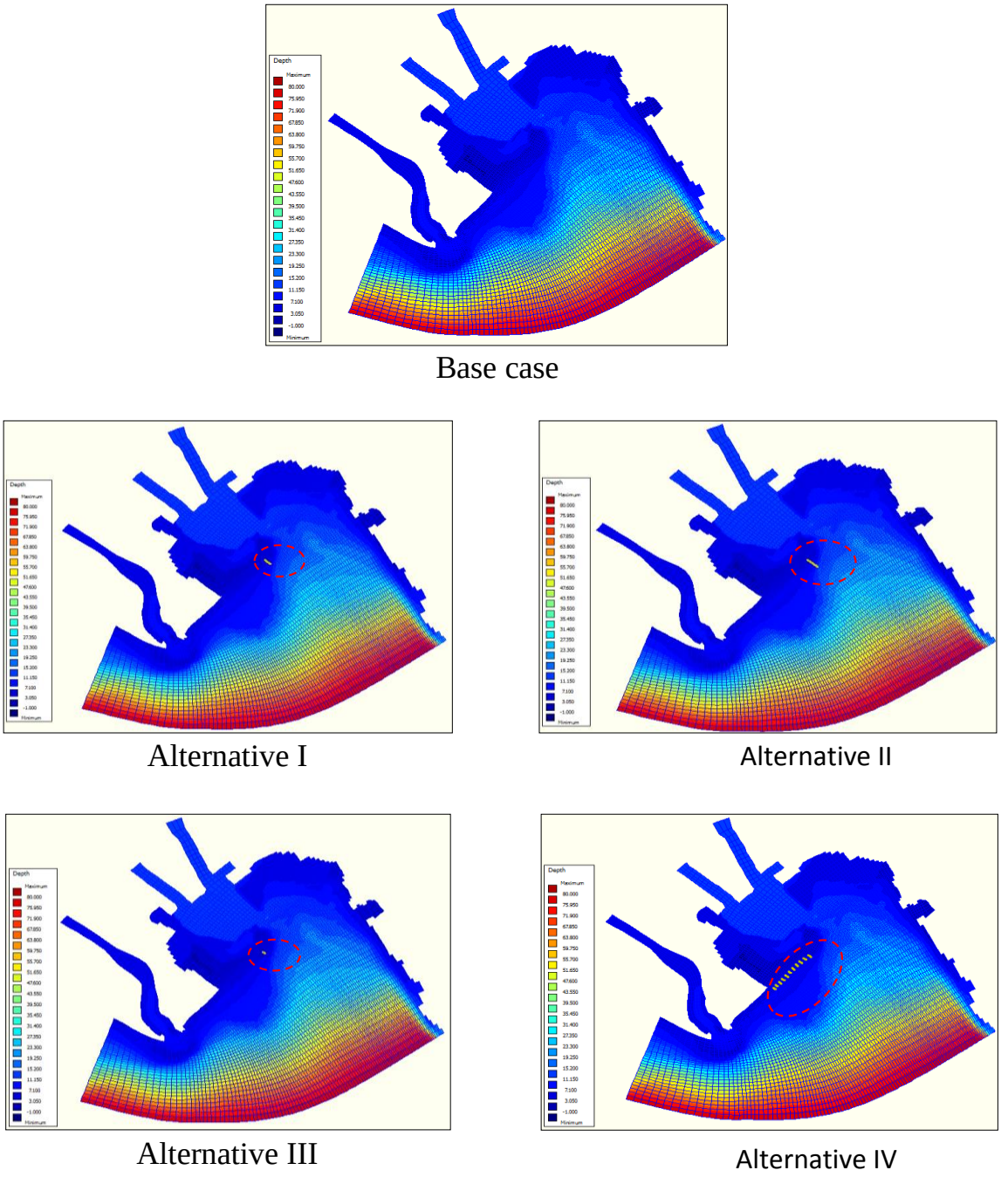

Figure 6: Different alternative measures applied for morphological modelling in Gracieuses spit area

Morphological changes in the model were simulated for 3600 days or around 10 years. The dominant factor to contribute sediment in this area is from Grand Rhone river discharge. From the literature it is observed that there is no significant contribution of the river discharge for the sedimentation in this area. The cumulative sedimentation/erosion in the approach channel for base case (real condition) and propose alternatives is calculated. The observed area for calculating sedimentation and erosion in the approach channel is presented in Figure 7.

Figure 7: Observed area for calculating sedimentation and erosion in the approach channel

In order to evaluate the optimal alternatives to reduce the sedimentation in the port channel, the observed cumulative sedimentation for 10 years is presented in Table 3. From Table 3, it is observed that the alternative I is very effective to reduce volume of sedimentation in the channel port area from $3.37*10^6$ m³ to $1.35*10^6$ m³. Alternative IV also gives the significant result to minimize the sedimentation. On the other hand, Alternative II and III hardly have any influence to reduce the sedimentation in the channel area.

Table 3: Total sedimentation in approach channel (Port area) for 10 Years

Measures	Volume (10^6 x m^3)
Base case	3.37
Alternative I	1.35
Alternative II	2.54
Alternative III	3.14
Alternative IV	1.53

As mentioned before, besides sedimentation in the port channel, stability of the Gracieuses spit is very important as it acts as in natural breakwater for Port of Fos to keep the harbour area from waves attack. Monitoring of morphological changes in the several locations of the spit after some propose measures are presented in Figure 8. From Figure 8, it is seen that the erosion occurs along the Gracieuses spit for existing situation. Some propose measures like constructing a breakwater or a groyne at the end of this spit (Alternative I, II, and III) could not even minimize the erosion in this area. On the other hand, by constructing the multiple groynes along this spit, the erosion will be reduced and accretion will be observed in some areas (see cross-section 6 in Figure 8).

The other thing that taking into account in the design of a structure close to the navigation channel, is to keep the enoough space between the approach channel and the hard structure. It means that constructing groynes as shown in the Alternative IV is more acceptable than constructing a breakwater in this area. Moreover, from the economic point of view, groyne is cheaper than a breakwater.

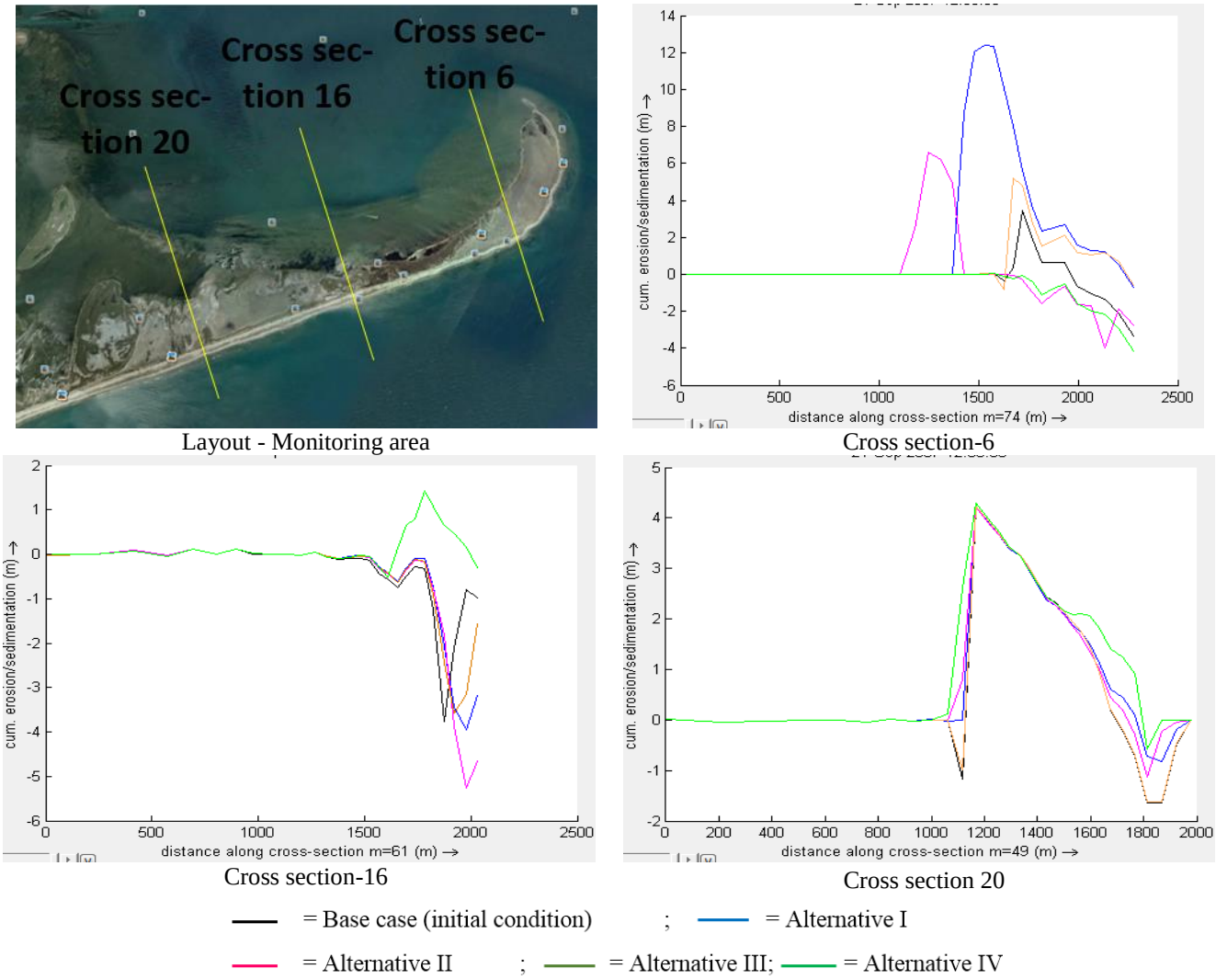

Figure 8: Observation of sedimentation/erosion in the Gracieuses Spit

Finally, based on the model results it was observed that sedimentation in the port channel and also stabilization of the gracieuses spit as a natural breakwater for the port is possible to solve by constructing the groynes along the half of gracieuses spit, 100 m in length at an interval of 200 m. Furthermore, beach nourishment should be done on a regular basis by using sand from sediment load inside the port basin.

5 CONCLUSIONS

- For the sustainable coastal management, beach nourishment is proposed as an effective solution to solve the erosion problems along the coastline. Nevertheless, in order to make sure that existing groynes are working well, maintenance of groynes on a regular basis together with beach nourishment is necessary.

- In the area around Gracieuses spit, multiple groynes give more reliable solution to reduce the sedimentation in the approach channel and sand nourishment along the spit would provide a good solution for the erosion of the spit. But instead of only making groynes as protection, in order to ensure the navigability of channel the maintenance dredging is also proposed. Thus, the combination of groynes with sand nourishment is more effective for these problems.

- For the sustainable coastal development along the shoreline of Bangladesh this knowledge can be applied considering the geometry and nature of the coast.

6 REFERENCES

Adriaanse, L.A., Coosen, J., 1991. *"Beach and dune nourishment and environmental aspects"*, Coastal Engineering 16, pp. 129-146.

Eurosion. (2009). "*Eurosion Case Study*", Centre Européen de Recherche et d'Enseignement des Géosciences de l'Environnent, France.

Hanson H. et. al, 2002, "*Beach Nourishment Projects, Practices, and Objectives-a European Overview"*,Coastal Engineering 47, pp. 81-111.

Sabatier, F. (2001). "*Fonctionnement et dynamiques morpho-sédimentaires du littoral du delta du Rhone*",Ph.D thesis, Aix-Marseille III University, 272p.

Sabatier, F. et. al, 2006. "*Sediment Budget of The Rhone Delta Shoreface since The Middle of The 19th Century",* Marine Geology 234, pp. 143–157.

Sabatier, F. et. al, 2009. "*Connecting large-scale coastal behaviour with coastal management of the Rhône delta",* Geomorphology 107, pp. 79-89

NCEED-CUET National Conference on Earthquake and Environmental Disasters, December 17, 2015, Chittagong, Bangladesh
Bhuiyan M. A. R., Pal S. K., Mazumder M. H., Mazumder R. K., Omi F. R. (eds.)

Predicting Urban Floods Through Tidal Flow Simulation

Aysha Akter
Center for River, Harbor & Landslide Research and Department of Civil Engineering, Chittagong University of Engineering & Technology, Chittagong 4349, Bangladesh

Ahad Hasan Tanim
Center for River, Harbor& Landslide Research, Chittagong 4349, Bangladesh

ABSTRACT: The coastal seaport city Chittagong, which is located in the bank of Karnafuli River as well as in the estuarine of this river and the Bay of Bengal, frequently subjected to the flooding due to a combined effect of heavy rainfall and tidal flow. City dwellers regularly face these floods and experiences with disruption in their daily lives and properties. So, to cope up with this suffering there is a need of a prediction tool to provide information on vulnerable locations subjected to tidal flooding. This paper attempted to outline a coastal flood simulation of Chittagong city area using a numerical model i.e. USEPA Storm Water Management Model (SWMM) v.5 coupling with GIS. The overland flow is simulated using dynamic wave routing method that can account backwater effect and heavy rainfall simultaneously. The flow direction that obtained from the simulation results are expected to effectively used to determine the vulnerable location that more susceptible to tidal effect. Thus, it is expected that SWMM model can be used to determine tidal effect on coastal flooding.

1 INTRODUCTION

Recently, floods occur in Chittagong city due to extreme rainfall and high tides. Thus, subsequent rises of sea level making this issue more severe like usual coastal floods (Shahapure, Eldho and Rao 2011). Tidal fluctuations are the key factor of coastal flooding in the river estuary transition zone as the outfall that located in aforementioned zone always subjected to backwater effect. In most cases the runoff carrying channel having invert elevation less than the maximum elevation of tidal cycle are subjected to tidal effect. According to the hourly tidal records by Chittagong Port Authority (CPA, 2014), the high tide in city adjacent canal has reached even more than 2.8 m above the mean sea level. The situation becomes worse while monsoon heavy rainfall also takes place. While the adjacent coastal region is an urbanized area, the overall flood assessment using numerical face difficulties such as river estuary-ocean model. National Oceanic and Atmospheric Administration's (NOAA's) develop a key mechanism for Coast, Estuary; River Information contributes a river estuary-ocean model linkage with HEC-RAS and SOBEK to achieve this goal (Mashriqui, Halgren and Reed 2014). Historically, NOAA's National Weather Service (NWS) one-dimensional (1D) hydraulic models have proven to be a viable option for generating accurate water-level forecasts in coastal rivers (Fread and Lewis 1985). An unsteady module of the HEC-RAS 1D hydraulic model was used for river forecasting and is accessible to NWS forecasters through the Community Hydrologic Prediction System (CHPS) (Roe et al. 2010). An alternative to using a 1D river hydraulic model to model the transition zone and bridge forecast gaps is extending an estuary ocean model farther upstream. Cho et al. (Cho et al. 2012) have worked towards this capability, showing accurate water-level forecasts for the Washington, DC area from Eulerian - Lagrangian CIRCulation (ELCIRC) simulations of Hurricane Isabel in 2003. The flexible mesh feature of their model allows calculations to be efficiently extended into the riverine environment and coastal estuary. Bai et al (Bai, Morton and Parker 2006) suggests a tidal simulation of Christina River with model XP-SWMM and HSPF.
This paper outlined the tidal effect of Karnafuli River on urban flooding of nearby Chittagong city using GIS coupling with SWMM model.

2 METHODOLOGY

2.1 *Study Area*

The study area comprises of 18 sub-catchments located at the bank of Karnafuli River; having an area of 50.18 km^2 (Figure 1).This area usually faces coastal overland flows due to tidal effect and during monsoon season the magnitude of flood spreads along with heavy rainfall. As per the master plan by Chittagong Development Authority (CDA), there are 3 major primary drains viz. Mohesh Khal, Khal no 18 and a major parts of Chaktai Khal (CDA 1995). There are a numbers of secondary drainage systems; those are connected to this primary drain. Finally, there are 8 outfalls those are disposing in the Karnafuli River. These outfalls are located in the estuary ocean transition zone. Thus, this transition zone is subjected to tidal effect when the invert elevation of these outfalls is below the elevation of tidal water level.

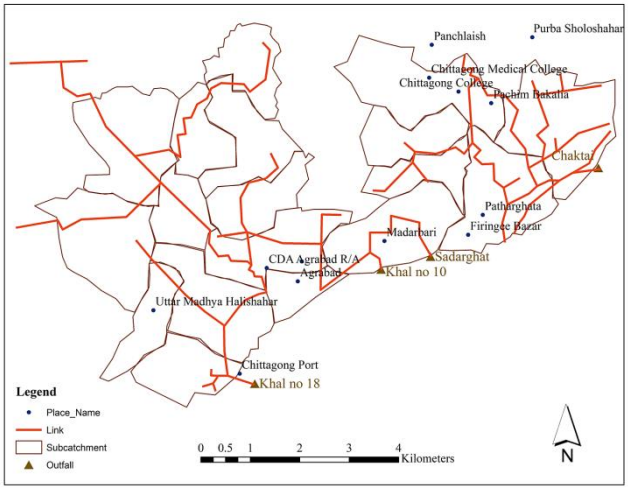

Figure 1 Study area

2.2 *Tidal Harmonics of Karnafuli River*

Observing water level records in coastal waterways, the most obvious clue confirming the presence of the tide is a characteristic, sinusoidal oscillation containing either two main cycles per day (semidiurnal tides), one cycle per day (diurnal tides), or a combination of the two (mixed tides). The underlying principle of tide analysis is that they might appear, tidal oscillations can be broken down into a collection of simple sinusoids (sinusoids usually represented by the cosine function from trigonometry). Each "cosine" wave will have the same period of oscillation as the celestial forcing gives rise to it. Thus, Karnafuli River has two tides a day each tidal cycle lasting about 12 hours (Figure 2). Both of the tidal range and the main water level vary seasonally and place to place along the river (Figure 2 and 3). Figure 2 shows the pattern of tidal fluctuations over month June 2014 in Khal 10. The variation in month shows a neap tide and a spring tide (NOAA, 2006). The tidal fluctuations can be classified as a diurnal fluctuation because tide describes in this case one high and one low water occur in the period of the rise, and also of the fall, of tide is approximately 12 hour (Figure 2).

A tidal analysis is normally a linear regression of a sea level time series in terms of harmonic tidal constituents (sine waves). The analysis results in 'tidal harmonic constants' (amplitudes and phase lags for each tidal harmonic constituent M_2, S_2, K_1 and O_1). There are also tidal analyses based on the response method for a fuller description of tidal analyses). For the purpose of a tidal analysis, the observed sea levels are separated into three components respectively a) Mean sea level, b) Tidal levels ,c) Surge (or residual) levels (NOAA, 2006).

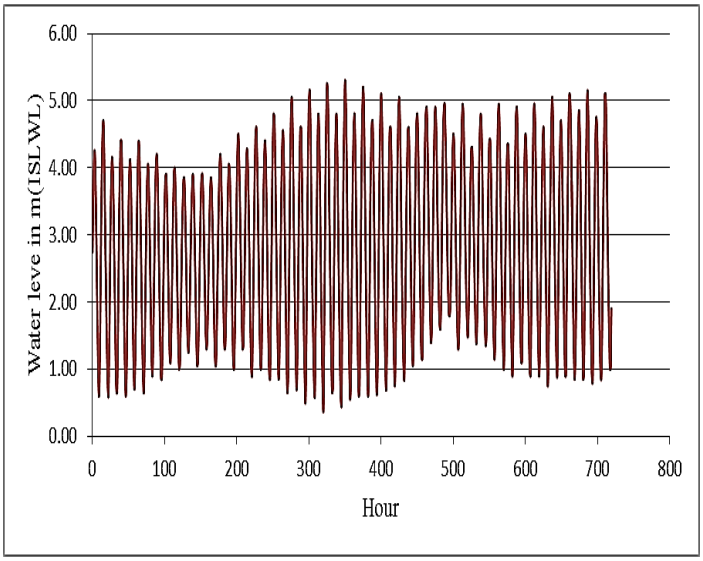

Figure 2 Tidal fluctuations throughout June 2014 in Khal no 10

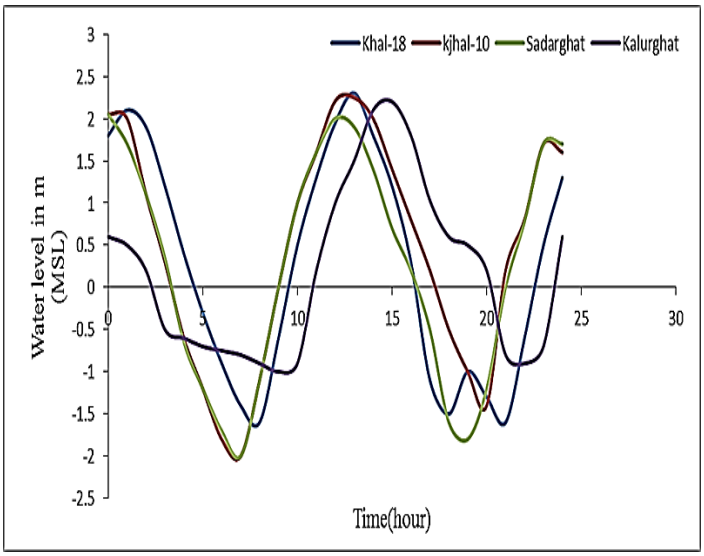

Figure 3 Variation of spring tide curve in different location of Karnafuli River (31 March, 1991)

2.3 *Establishment of datum co-relation*

The datum level of tide is Indian Spring Low Water (ISLW), an arbitrary tidal datum approximating the level of the mean of the lower low water at spring tides also called Indian tidal plane. A tidal datum approximating the lowest water level observed at a place at a level below Mean Sea Level (MSL) being equal to the sum of amplitudes of the harmonic constituents M_2, S_2, K_1 and O_1; usually below that of the lower low water at spring tides. So,

Datum of the ISLW=MSL-(Amplitude of M_2, S_2, K_1, O_1 constituents)

Chittagong Development Authority (CDA) master plan suggests (1995) a relationship (Table 1) between the two datum ISLWL and MSL as former one varies with distance which is used for input tidal curve in model.

Table 1. Relationship between MSL and ISLWL (CDA 1995)

Location	Relationship between MSL and ISLWL
Potenga	MSL-2.27m
Khal no 10	MSL-1.978m
Sadarghat	MSL-1.673m

2.4 *Model set up*

Initially raw data from Shuttle Radar Topography Mission (SRTM) (http://gdex.cr.usgs.gov/gdex/) with 30 m resolution Digital Elevation Model (DEM) was analyzed with Arc-GISv9.3 and HEC-GeoHMSv5.0 terrain processing tool with input stream network. The output 18 sub-catchments were delineated following several steps such as DEM reconditioning, filling sink in DEM, assigning flow direction and flow accumulation. Obtaining stream segmentation finally sub-catchment grid cell was processed which was used with terrain processing of HEC-GeoRAS v4.3 preprocessing with stream network .SCS-CN method was used to compute infiltration. The sub-catchment properties such as % slope and width were obtained using GIS. About 144 channel cross sections were extracted those were further imported in Storm Water Management Model (SWMM v.5) as irregular channel cross section or transects. The invert elevation of transects and maximum depth were followed according to extracted cross sections. Total 8 outfalls were placed to carry runoff to adjacent Karnafuli River. Thus, tidal outfalls were adjusted with tidal curve with curve shown in Figure 4 for the month June, 2014 in SWMM model interface.

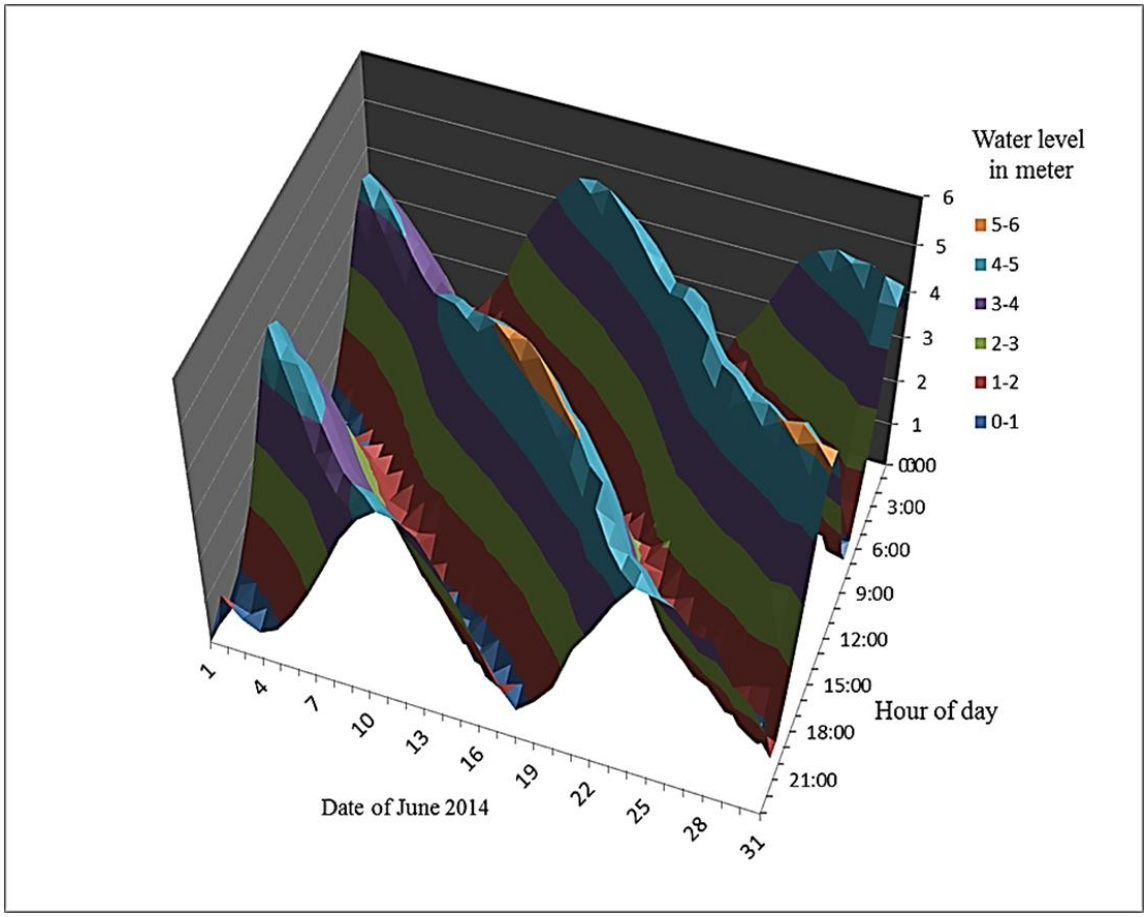

Figure 4 Diurnal tide pattern of Khal no. 10 (datum ISLWL)

2.5 *Routing method and time steps for backwater simulation:*

Dynamic Wave routing method, based on 1D Saint-Venant flow equations, was used for simulation in this study. According to this method flood occurs when the water depth at a node exceeds the maximum available depth, and the excess flow is either lost from the system or can pond on the top of the nodes and re-enter in the drainage system (Rossman 2008). Dynamic wave routing can account for channel storage, backwater effect because it provides combined solutions for both water levels at nodes and flow in conduits. Thus this can be applied to any general network layout; even those are containing multiple downstream diversions and loops. In addition to these, this method expected to perform better for the drainage system in the study area as it subjected to significant backwater effects due to downstream flow regulation with tidal curve. A small time step of less than 1 minute is usually recommended for this method (Rossman 2008). For this reported study, a time steps of 30s was accounted due to establish numerical stability in computational step in model.

3 MODEL OUTCOMES

The gravity flow direction obtained in the link based on slope that assigned by SWMM model (Figure 5). The outfall located in Khal no 10, Khal no 18 and Chaktai Khal can be identified as subjected to backwater effect, thus the adjacent areas are prone to flooding. Thus the affected areas Halishahar, Agrabad and Bakalia showed flood responses due to significant tidal effect when heavy rainfall synchronizes with the backwater (Figure 5). After datum conversion the maximum water level of tidal curve at outfall was observed 2.6m (MSL) during spring tide (Figure 2). The nodes in the drainage network those have invert elevation below 2.6m are found submerged when the tidal curve reaches at this maximum ordinate except sudden variation in the channel topography (Figure 6).

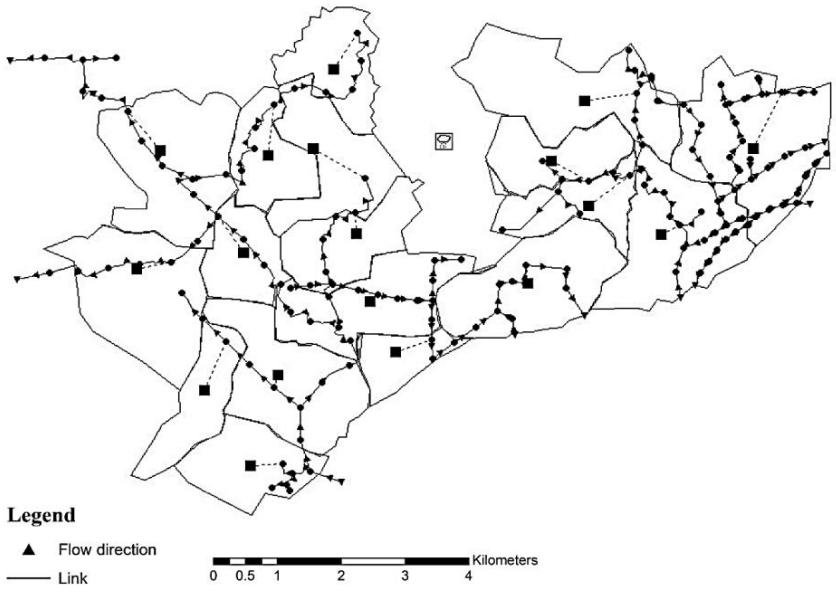

Figure 5 Flow directions in link network

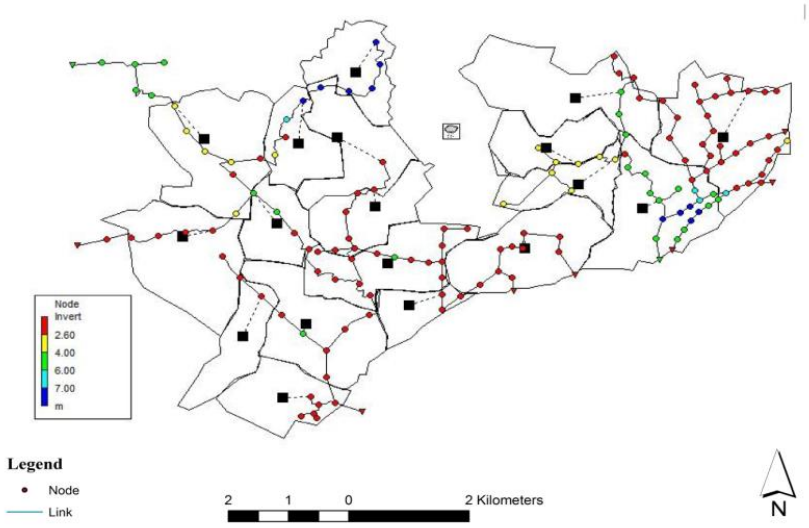

Figure 6: Submerged nodes at the maximum ordinate (2.6m MSL) of spring tidal curve

4 CONCLUDING REMARKS

Based on the model study, the following concluding remarks can be made:

- When rainfall hydrographs superimpose with the peak of tidal curves the water logging problem will be found more severe and backwater effect will be the most prominent. There are two probable peak that may occur in a lunar day in which the superposition of rainfall hydrograph and tidal hydrograph. Due to this superposition recession time will be more. Consequently water logging depth and duration will be more than any period of the day.
- Tidal effect on urban flooding in Chittagong city is more prominent during spring tide rather than neap tide as the water level fluctuations range is more during this period.
- South Bakalia, south Agrabad and Uttar Moddoya Halishahar are the most vulnerable area for coastal flooding. On the Contrary Pahartoli, Andarkilla area has very less tidal effect than any other region of Chittagong.
- Tide level fluctuates during monsoon season (June, July, August, September) more than any month of the year. So tidal effect on urban flooding during this month is more than any month of the year.

5 ACKNOWLEDGEMENTS

The authors gratefully acknowledge the financial supports provided by the Center for River, Harbor & Landslide Research (CRHLSR), Chittagong University of Engineering and Technology (CUET), Bangladesh. Logistic supports from CDA, CWASA and CPA are highly appreciated.

6 REFERENCES

Bai, S., M. Morton & A. Parker. 2006. Modeling Enterococci in the Tidal Christina River. In *Estuarine and Coastal Modeling (2005)*, 305-319. American Society of Civil Engineers.

CDA. 1995. Chittagong Storm Water Drainage and Flood Control Master Plan. In *Main Report. 4th Edition*, 11-53.

Cho, K.-H., H. V. Wang, J. Shen, A. Valle-Levinson & Y.-c. Teng (2012) A modeling study on the response of Chesapeake Bay to hurricane events of Floyd and Isabel. *Ocean Modelling*, 49–50**,** 22-46.

Fread, D. L. & J. M. Lewis. 1985. Real-time hydrodynamic modeling of coastal rivers. In *Applications of real-time oceanographic circulation modeling: Symp. Proc., B. B. Parker, ed., Marine Technology Society, Washington, DC, 269–284.*

Mashriqui, H., J. Halgren & S. Reed (2014) 1D River Hydraulic Model for Operational Flood Forecasting in the Tidal Potomac: Evaluation for Freshwater, Tidal, and Wind-Driven Events. *Journal of Hydraulic Engineering*, 140**,** 04014005.

Roe, J., C. Dietz, P. Restrepo, J. Halquist, R. Hartman & e. a. Ronald Horwood. 2010. NOAA's community hydrologic prediction system. In *Proc., 2nd Joint Federal Interagency Conf. (9th Federal Interagency Sedimentation Conf. and 4th Federal Interagency Hydrologic Modeling Conf.)*. Advisory Committee onWater Information (ACWI), Las Vegas.

Rossman, L. A. 2008. SWMM5 Manual Storm Water Management Model. 80.

Shahapure, S., T. Eldho & E. Rao (2011) Flood Simulation in an Urban Catchment of Navi Mumbai City with Detention Pond and Tidal Effects Using FEM, GIS, and Remote Sensing. *Journal of Waterway, Port, Coastal, and Ocean Engineering*, 137**,** 286-299.

NCEED 2015 -National Conference on Earthquake and Environmental Disaster; December 17, 2015; CUET, Chittagong, Bangladesh
Bhuiyan M. A. R., Pal S. K., Mazumder M. H., Mazumder R. K., Omi F. R. (eds.)

Industrial Pollution and Various Ways to Control Pollution in Aspect of Bangladesh

Md. Abdul Mannan Akanda & A.K.M. Enamul Hoque
Rajshahi University of Engineering & Technology, Rajshahi, Bangladesh

ABSTRACT: At the contemporary, each country of the world are focused on own development and consequently increasing living standards of her inhabitants. With the industrial revolution, humans become able to advance further into the 21st century. Technology developed rapidly, science became advanced and the manufacturing age came into view. With all of these came one more effect, industrial pollution. For the paradigm Bangladesh is a developing country and her industries are growing rapidly as well as industrial pollution. Different industrial pollutants that released from the industries in the form of solid, liquid and gaseous. It contaminates many sources of drinking water, releases unwanted toxins into the air and reduces the fertility of the soil all over the country. Because of solid, liquid and gaseous pollutants associated with noise and radioactive pollution causes environmental imbalance which may give rise to various environmental problems. Some of environmental problems are air, water, soil pollution, hazards on human health, desertification, landslides, extinction of species, vulnerable ecosystem, depletion of natural resources, deforestation, thinning of ozone layer and global warming. Industrial pollution cannot be completely avoided but can be mitigated by finding the reasons and controlling. Lack of policies to control pollution, unplanned industrial growth, use of outdated technologies, presence of large number of small scale industries, inefficient waste disposal, leaching of resources from our natural world are the important factors for the industrial pollution. Pollution is more prone in case of Bangladesh. The present environmental condition of Bangladesh is not at all equilibrium. Severe air, water, soil and noise pollution are threatening human health, ecosystems and economic growth of Bangladesh. This paper analyses solid, liquid and gaseous pollutants from the different industries of the country, their adverse effect, and different ways to improve and control pollution in order to keep environment pollution free and healthy for living.

1 INTRODUCTION

Environmental pollution is as old as the civilization itself. Technological advancement has brought revolutionary changes in life style and national economy with overwhelming power over nature. The protection of environment has become a major issue around the global for the well being of the people and economic development. From the industries solid, liquid and gaseous pollutants are released enormously and contaminate our environments. Industrial solid waste is an important part of the total waste problem. The amount of industrial solid waste is growing in our country; therefore waste management and waste treatment methods are of utmost importance. Water is a source of life and energy, rapid pace of industrialization, population expansion, and unplanned urbanization have largely contributed to the severe water pollution and surrounding soils. The main sources of freshwater pollution can be attributed to discharge of untreated sanitary and toxic industrial wastes, dumping of industrial effluent, and runoff from agricultural fields. It is well known that 70–80% of all illnesses in developing countries are related to water contamination, particularly susceptible for women and children (WHO/UNICEF, 2000). Excessive release of heavy metals into the environment due to industrialization and urbanization has posed a great problem worldwide. Unlike organic pollutants, the majority of which are susceptible to biological degradation, heavy metal ions do not degrade into harmless end products (Gupta et al, 2001). The presence of heavy metal ions is of major concern due to their toxicity to many life forms. Heavy metal contamination exists in aqueous wastes of many industries, such as metal plating, mining operations, tanneries, radiator manufacturing, smelting, alloy industries and storage batteries industries (Kadirvelu et al, 2001). Air pollution can be defined as any atmospheric condition in which substances (natural or man-

made chemical compounds capable of being airborne) are present at concentrations high enough above their normal ambient level to produce a measurable effect on man, animals, vegetation, or materials.

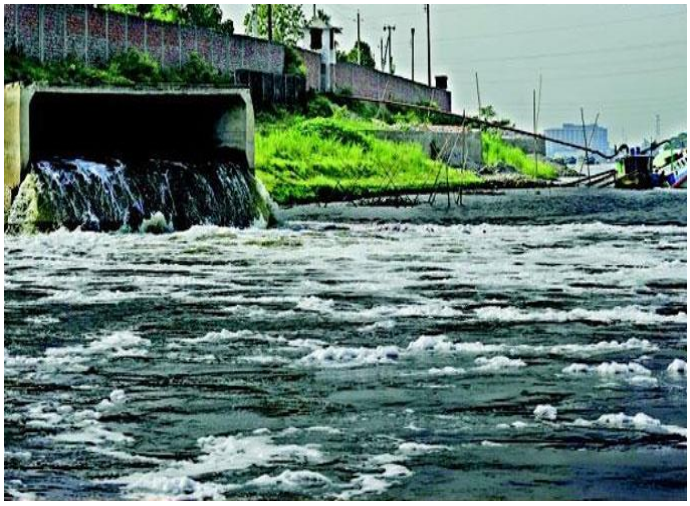

Figure 1. Soil and water pollution by industries.

Figure 2. Air pollution by industries.

The most important pollutants are Carbon monoxide (CO), Sulfur dioxide (SO_2), Nitrogen oxides (NO_x), Ozone (O_3), Hydrocarbons (HC) and Suspended Particulate Matter (SPM). Dhaka is one of the mega cities of the world, witnessed a very fast growth of urban population in recent times. Air pollution in Dhaka city is reported to be serious and damaging to public health. In the winter of 1996-97, air pollution of Dhaka city became the severest when lead in the air was reported higher than in the atmosphere of any other place of the world (Ahmed, 1997). A study of auto-impact of air quality of Dhaka city has been conducted in the year 2000, it is revealed that traffic congestion, fuel quality and brick field emission are the main reasons of air pollution in Dhaka city (Begum, 2004).

2 VARIOUS INDUSTRIAL POLLUTION SCENARIO IN BANGLADESH

2.1 *Iron and steel industry*

Iron and steel industry is rapidly increasing in Bangladesh. The country has somewhere between 250 and 300 rolling mills currently in operation. Bangladesh's domestic steel output is estimated at around 2.2 million tons a year, with sales valued at $1.2 billion. Some 30 percent of this output is contributed by a few big firms. At the present time some 40 ship breaking and recycling yards are in operation in Bangladesh. Many ship breaking yards operate in developing nations with lax or no environmental law, enabling large quantities of highly toxic materials to escape into the general environment and causing serious health problems among ship breakers, the local population, and wildlife. In Bangladesh, for example, 40,000 mangrove trees were illegally chopped down in 2009. The World Bank has found that the country's beaching locations are now at risk from sea level rise (Sarraf & Maria, 2010). Lead, organotins such as tributyltin in anti-fouling paints, polychlorinated organic compounds, by-products of combustion such as polycyclic aromatic hydrocarbons, dioxins and

furans are found in ships and pose a great danger to the environment. A study shows soil contamination found in sites in Bangladesh are Cadmium (0.6 to 2.2 mg/kg), Chromium (2.42 to 22.12 mg/kg), Lead (11.3 to 197.7 mg/kg), Mercury (0.078 to 0.158 mg/kg), Oil (485 to 4,430 mg/kg).

Table 1. Heavy metal concentration in the sediments of ship breaking sites in Bangladesh.

Sampling stations	Trace metal concentration (μg/g)							
	Fe	Cr	Ni	Zn	Pb	Cu	Cr	Hg
Salimpur	12	68	23	84	37	21	0.57	0.02
Bhatiari	35	87	35	102	122	40	0.83	0.02
Sonaichhari	41	78	49	143	148	31	0.94	0.12
Kumira	21	23	25	120	42	28	0.59	0.05
Sandwip	3	19	4	22	9	2	0.19	0.02

The steel industry also produces a number of wastes in large quantities such as blast furnace slag, dust and sludge, etc. There are a large number of outputs that are produced as a result of the manufacturing of iron and steel, the forming of metals into basic shapes and the cleaning and scaling of metal surfaces.

Table 2. Pollution prevention practices in the iron and steel industry.

Process	Recommended pollution prevention practice
Pig iron manufacturing	1. Improve blast furnace efficiency by using coal and other fuels manufacturing (such as oil or gas) for heating. 2. Recover the thermal energy in the gas from the blast furnace before using it as a fuel. 3. Use dry SO_x removal systems. 4. Recycle iron-rich materials such as iron ore fines, pollution control dust, and scale in a sinter plant. 5. Use low NO_x burners to reduce NO_x emissions from burning fuel in ancillary operations.
Steel manufacturing	1. Use dry dust collection and removal systems to avoid the generation of wastewater. 2. Use BOF gas as fuel. 3. Use a continuous process for casting steel to reduce energy consumption.

2.2 *Leather industry*

Leather making is several centuries old technology. However, the wastes generated from this industry make it fall in the "red" category. There are reportedly around 220 tanneries in Bangladesh but, in fact, only 113 tanneries are in effective operation, out of these 20 units are reported to be fairly large. 105 of the tanneries are positioned arbitrarily in the Hazaribagh area in Dhaka where 84 per cent of the total supply of hides and skins are processed in a highly congested area of only 29 hectares of land. The tanneries discharge nearly 22,000 m^3 of untreated and highly toxic (contains chromium) into the water body every day. It produces 100 tons of solid waste every day in the form of trimmings of finished leathers, shaving dust, hairs, trimmed animal flesh skins/hides to contaminate the soil and the water. The daily composite samples are taken from the sewer collecting all wastewaters originating from the industries and named as combined wastewaters.

Table 3. Combined wastewater characterization.

Parameter	Unit	Range	Mean
Flow rate	m^3/d	584-1068	4048
TSS	mg/l	50-9100	2750
COD	mg/l	2250-8200	5300
BOD_5	mg/l	1150-3480	1920
Sulfide	mg/l	20.9-186.3	66
Total Cr	mg/l	22-320	140

Solid and liquid wastes emanating from the tanning industry are known to contain various toxic trace metals. According to our study, Cr is the most toxic element found from the waste of tannery and responsible for cancer. In 2003, the Government of Bangladesh announced that the tanneries located in Hazaribag will be shifted to a purpose-built and modern cluster in Savar. The key highlight of the Savar cluster was to be the Common Effluent Treatment Plant (CETP), conforming to international environmental standards.

2.3 *Textile industry*

Textile is the most important sector of Bangladesh's economy. Bangladesh has emerged, in just one decade, as the twelfth largest garment-manufacturing nation in the world. The garment sector now accounts for about 77% of the country's foreign exchange earnings, and 50% of its industrial work force (European Commission). The textile industry is considered as the most ecologically harmful industry in the world. The eco-problems in textile industry occur during some production processes. Textile industry uses large quantity of water in its production processes and highly polluted and toxic wastewater is discharged into sewers and drains without any kind of treatment. The textile dyeing industries of Gazipur and Narayanganj generate large amount of effluents, sewage sludge and solid waste materials everyday which are being directly discharged into the surrounding channel, agricultural fields, irrigation channels, surface water and these finally enter in to Turag and Shitalakkhya River. It is estimated that factories processing 5 tons of fabric that produces 750-1,800 ton/day of effluent water. The average treatment cost is currently Tk. 20-30 per 1,000 litres. By flow segregation and optimization of chemical dosing, this operating cost can be reduced by up to 30%.Textile and dyeing industrial effluents may cause alteration of the physical, chemical, and biological properties of aquatic environment by continuous change in temperature, odor, noise, turbidity etc. that is harmful to public health, livestock, wildlife, fish, and other biodiversity.

Table 4. Concentration ranges of the physiochemical properties of effluents in the textile industry (Sultana et al, 2009).

Parameter	Concentration	DOE standards (for Inland Surface Water)
Temperature (ºC)	50.22	40
TSS (mg/l)	1123.11	150
TDS (mg/l)	9123.78	2100
Turbidity (FTU)	130.37	10
DO (mg/l)	2.36	4.5-8
pH	9.88	6-9
EC (µs/cm)	14109.56	1200
BOD (mg/l)	573.89	50
COD (mg/l)	1233.33	200

More than 80% industries have no industrial large treatment plant for effluent discharge. Less than 2% are composite units (knitting, dyeing, finishing) which have proper treatment plants. In order to mitigate pollution, treatment plants have to employ. Common Effluent Treatment Plant (CETP) is the concept of treating effluents by means of a collective effort mainly for a cluster of small scale industrial units. The main objective of CETP is to reduce the treatment cost for individual units while protecting the environment.

2.4 *Pharmaceutical industry*

The pharmaceutical industry in Bangladesh is one of the most developed sector. Manufacturers produce insulin, hormones, and cancer drugs. This sector provides 97% of the total medicinal requirement of the local market. The industry also exports medicines to global markets, including Europe. During the past few decades, pharmaceutical industries have registered a quantum jump contributing to high economic growth, but simultaneously it has also given rise to severe environmental pollution in Bangladesh. Recently, in this country the pharmaceutical industries are making headways in responsible for the disposal of hazardous waste. Hazardous wastes can take the form of liquids, solids, contaminated gas or sludge. They can be the by-products of the manufacturing processes or may consist of discarded commercial products, such as cleaning fluids, pesticides. The solid part of this waste is disposed to the open land and dumped in water (Musson & Townsend, 2009). The liquid and gaseous parts are released in water and air respectively with or without any treatment. In general, most of the wastes are toxic to biological and aquatic life and are usually characterized by high Biological Oxygen Demand (BOD), Chemical Oxygen Demand (COD), Total Dissolved Solid (TDS) and suspended solid content. In Bangladesh, pharmaceutical industries are responsible for 15.9% water pollution and 12.6% toxic chemical emission to the environment among the other polluting industries in the country (World Bank, 1997).

Wastes containing toxic elements like cyanide and heavy metals, if discharged without any treatment are harmful to the aquatic life in the stream.

Table 5. Pharmaceutical characteristics of treated effluent generated from the pharmaceutical industries.

Parameters	Units	Measured value	Allowable range
Color	-	Ok	Light Brownish
pH	-	7.5~8.2	6-9
COD	mg/liter	245~378	<400
BOD_5	mg/liter	72~81	<100
TDS	mg/liter	1320~1506	<2100
DO	-	5.3~7.2	4.5-8
Chloride	mg/liter	487~590	<600
Sulfide	mg/liter	0.8~1.6	<2
Conductivity	Microsiemen/cm^2	1090~1120	<1200

Generally three types of waste stream are generated from pharmaceutical industries: process waste water, utility waste water, and domestic waste water. The combine waste streams from different areas of the pharmaceutical industries were subjected to consecutive three stages of treatment- (a) physical treatment, (b) chemical treatment, and (c) biological treatment. Biological treatments again can be subdivided into two types: (i) anaerobic and (ii) aerobic biological treatment.

2.5 *Fertilizer industry*

The fertilizer industries are playing a crucial role in the production of food grain to meet the requirements of increasing population. Country needs currently about 2.6 million tons of fertilizer per year. However, in recent years, fertilizer consumption increased exponentially throughout the country, causes serious environmental problems. Fertilization may affect the accumulation of heavy metals in soil and plant system. The rapid growth of fertilizer industries has caused serious concern to the environmental scientist. Pollution due to fertilizer industry is found in varying degrees in air, water and soil. Virtually every fertilizer industry produces some gaseous effluents. Emissions to the atmosphere from ammonia plants include sulphur dioxide (SO_2), nitrogen oxides (NO_x), carbon monoxide (CO), carbon dioxide (CO_2), hydrogen sulphide (H_2S), volatile organic compounds (VOC_s), particulate matter, methane, hydrogen cyanide, and ammonia. In a urea plant, ammonia and particulate matter are the emissions of concern. Nitric acid plants emit nitric oxide, nitrogen dioxide and trace amounts of nitric acid mist. Depending on the process, emissions in the tail gases can range from 215 to 4,300 mg/m3 for nitrogen oxides.

Table 6. Recommended pollution prevention practices in the fertilizer plants.

Process	Pollution prevention practice
Ammonia plant	1. Where possible, use natural gas as the feedstock for the ammonia plant to minimize air emissions. 2. Use hot process gas from the reformer to heat the primary reformer tubes. 3. Direct hydrogen cyanide gas in a fuel oil gasification plant to a combustion unit to prevent its release. 4. Considering the use of purge gases from the synthesis process to fire the reformer.
Urea plant	1. Using total recycling processes in the synthesis process, as a result microprill formation will be reduced.
Ammonium nitrate plant	1. Microprill formation & carryover of fines through entrainment can be reduced by prill tower. 2. Use of granulators can reduce dust emissions from the disintegration of granules.

2.6 *Brick industry*

Brick industry is one of the largest sources of greenhouse gas emissions in the country, estimated to be on the order of 6 million tonnes of CO_2 annually & is also a major source of land degradation and deforestation. Building structures and major construction works are booming in the urban areas of Bangladesh to keep up the rapid urbanization rate. To meet the need of construction, brickfields are growing sporadically here and there at the fringe zones and within the urban regions. There is a sharp rise of 5.6% per year has been noticed for the construction industry. Eventually, brickfields are producing major environmental pollutants. As very traditional brick making system is followed, so it is destroying the diminishing forest of this country intensifying the emission of carbon in the air polluting environment and endangering the life and livestock of the country. Bangladesh has about 6,000 authorized brickfields and numerous illegal ones. They are located near towns or major construction sites; i.e., Gabtali, Savar, Ashuliya, Keraniganj, Narshingdi, Gazipur and Manikganj. In Dhaka, there are around 4,500 brick kilns in operation, producing about 9.0 billion bricks per year. If Bangladesh maintains its current economic growth rate, continued use of outdated brick-firing technology would raise the level of greenhouse gas emissions to 9 million tons by 2018 by using coal in the pur-

pose. The brick kilns emit toxic fumes containing suspended particulate matters rich in carbon particles and high concentration of CO and SO_x, CO_2, NO_X, NO that are harmful to eye, lungs and throat.

Table 7. Emission rates of different criteria pollutant from different brick klins.

Brick kiln technology	Emission rates (gm/kg of fired brick)				
	SPM	$PM_{2.5}$	SO_2	CO	CO_2
FCK	0.86	0.18	0.66	2.25	115
Zigzag	0.26	0.13	0.32	1.47	103
VSBK	0.11	0.09	0.54	1.84	70

3 ADVERSE EFFECT OF INDUSTRIAL POLLUTION

3.1 *Adverse effect of industrial pollution on human*

Severe environmental pollution is threatening human health and economic growth of Bangladesh. Air pollution mostly affects the urban children. Bangladesh could avoid 10,000 deaths and save between 200 and 500 million dollars a year if indoor air pollution in four major cities can be reduced to acceptable limits. Immediate effect of smoke inhalation causes headache, vertigo, burning sensation of the eyes, sneezing, nausea, tiredness, cough etc. Its long term effect may cause asthma and bronchitis. Carbon monoxide hampers the growth and mental development of an expected baby. If CO enters the bloodstream, it reduces oxygen delivery to the body's organs and tissues. The health threat from CO is most serious for those who suffer from cardiovascular disease. Nitrogen oxides cause bronchitis and pneumonia. Industrial emissions cause different waterborne disease and damage to health. Nitrogen dioxide can irritate the lungs and lower resistance to respiratory infections such as influenza. Major concerns for human health from exposure to particulate matter are effects on breathing and respiratory systems, damage to lung tissue, cancer, and premature death. High concentrations of SO_2 include effects on breathing, respiratory illness, alterations in pulmonary defense and aggravation of existing cardiovascular disease. Heavy metals such as lead, cadmium, chromium, mercury etc. responsible for chronic poisoning, cancer, affect the kidneys, liver, nervous system, and other organs.

3.2 *Adverse effect of industrial pollution on environment*

It leads to the depletion of natural resources air pollution, water pollution and soil pollution the generation of hazardous waste whose safe disposal become a big problem and the degradation of land quality. It also causes global warming, climatic changes, major consequences of industrialization and acid rain. It may also cause metallic contaminant like Cd, Zn, Hg etc., destruction of bacteria and beneficial microorganisms in the soil, undesirable disease caused by radioactive industrial pollutant when food containing radio-nuclides is taken by man, damages of the natural biological purification mechanism of sewage treatment causing several soil and water borne diseases by industrial effluent.

4 TREATMENT OF INDUSTRIAL WASTES

Treatment is any process that changes the physical, chemical, or biological character of a waste to make it less of an environmental threat. Treatment can neutralize the waste, recover energy from a waste, render the waste less hazardous, or make the waste safer to transport, store, or dispose of.

4.1 *Treatment of solid wastes*

Solid waste treatment is most important for industrial pollution control. Solid waste can be treated in various ways. The most significant controlling methods are Incineration, Gasification, Biological treatment, Storage of solid waste, Deactivation, Micro-encapsulation and filling, Dumping and application, Reuse of solid waste.

4.2 *Treatment of liquid wastes*

Treatment of liquid wastes is also most important because it contaminates soil and water. For the treatment of liquid wastes, different treatment methods can be adopted. One of them is anaerobic technology which was used earlier for treating wastewaters of different industries such as paper and pulp, distilleries, tanneries, textile and food processing, ranging from high-strength waste to low-strength waste. Various reactor configurations such as anaerobic contact reactor (ACR), up flow anaerobic sludge blanket reactor (UASB), fluidized

bed reactor (FBR) and anaerobic fixed film reactor (AFFR) have been developed to treat wastewaters from different industries treatment. The anaerobic biological treatment of pharmaceutical wastewater and achieved 60–70 % COD removal efficiency. In aerobic treatment, generally aerobic sequencing batch reactor (ASBR) and activated sludge process have been used for the treatment of industrial waste water. Recently most popular treatment method is membrane bioreactor (MBR). The MBR has been used for the large-scale wastewater treatment of industrial wastewater, domestic wastewater and municipal wastewater. The MBR has several advantages such as complete removal of suspended solids, compact plant size, high rate of degradation, and flexibility in operation, low rate of sludge production, disinfection and odor control, prolonged microorganisms retention time and treatment of recalcitrant and toxic organic and inorganic pollutants. Activated carbon remains an expensive material for waste treatment. In recent years, the need for safe and economical methods for the elimination of heavy metals from contaminated waters has necessitated research of low cost agricultural waste by-products such as sugarcane bagasse, rice husk, sawdust, coconut husk, oil palm shell, neem bark etc., for the elimination of heavy metals from wastewater have been investigated by various researchers.

4.3 *Treatment of gaseous wastes*

Air pollution caused by the gaseous wastes from the industries can be mitigated by techniques without emission control devices and using emission control devices. Without emission control devices practice includes change in fuel, improve dispersion, good operating practices, plant shutdown/relocation etc. SO_2 emission from the industries can be controlled largely by the scrubbing or flue gas desulphurization (FGD) processes. The major FGD processes are: Limestone scrubbing, Lime scrubbing, Dual Alkali processes, Lime-spray drying, Wellman-Lord process. One approach in reducing nitrogen oxide emission is to remove a large part of the nitrogen contained in the fuels. This system promises as high as 90% removal of nitrogen oxides from the flue gases. In a second process, both NO_x and SO_x are removed. The combustion gases are moved across a bed of copper oxide, which reacts, with the sulfur oxide to form copper sulfate. The copper sulfate acts as a catalyst for reducing NO_x to ammonia. Approximately 90% of the NO_x and SO_x can be removed from the flue gases through this process.

5 RECOMMENDATIONS TO CONTROL INDUSTRIAL POLLUTION

- The government should strictly impose rules and regulations according to department of environment to improve pollution scenario.
- Increased awareness among industrialists about the pollution problem and their legal and social responsibility to prevent it.
- It should be mandatory that industries construct and then regularly and efficiently operate their ETPs and monitor their effluents to keep them within the standards set by law.
- Voluntary or public provision of common ETPs may be a solution to serve adjacent small scale industries, operating on a cost sharing basis.
- National and community level bodies should be established and validated to monitor water quality of canals and rivers, and legal actions against offending industries should be taken.
- Environment pollution act should be updated.
- Environment technologies, methods should be introduced and a comprehensive environmental database may be developed.

6 CONCLUSION

The development of Bangladesh accelerated by the rapid establishment of industries. All the development of the country will go in vain if the wastes from the industries are not efficiently managed. With the development of industries, environmental issues have become a major concern due to impact on public health and progress of Bangladesh. So, the solid, liquid and gaseous wastes released from the industries should be treated properly according to government rules. By applying the introduced methods, industrial wastes will be controlled at low cost and will keep the environment healthy for the inhabitants.

7 REFERENCES

WHO/UNICEF. 2000. Global Water Supply and Sanitation Assessment Report 2000. *WHO, Geneva*.

Gupta V.K., Gupta M. & Sharma S. 2001. Process development for theremoval of lead and chromium from aqueous solution using redmud – an aluminum industry waste. *Water Res*. 35 (5) (2001)1125–1134.

Kadirvelu K., Thamaraiselvi K. & Namasivayam C. 2001. Removal of heavy metal from industrial wastewaters by adsorption onto activated carbon prepared from an agricultural solid waste. *Bioresour. Technol*. 76 (2001) 63–65.

Ahmed N. 1997. Air Pollution in Dhaka City. *Key note speech at ChE Division of IEB*, May 1997.

Begum D. A. 2004. Air pollution: A Case Study of Dhaka City. *Presented at the conference BAQ-2004*. Organized by Society of Indian Automobile Manufacturers. December 2004. Agra, India.

Sarraf & Maria. 2010. SHIP BREAKING AND RECYCLING INDUSTRY IN BANGLADESH AND PAKISTAN. siteresources.worldbank.org. *International Bank for Reconstruction and Development/ The World Bank*. Retrieved 3 Aug 2015.

European Commission. Guide book for European investors in Bangladesh: sector profiles, Asia Investment Facility. *The textile sector in Bangladesh*, pp. 6.

Sultana M. S., Islam M. S., Sahaa R. & Al-Mansur M.A. 2009. Impact of the Effluents of Textile Dyeing Industries on the Surface Water Quality inside D.N.D Embankment, Narayanganj, Bangladesh: *Journal of Scientific and Industrial Research*, 44(1), pp.66, 2009. Available online at www.banglajol.info.

Musson SE and Townsend TG. 2009. Pharmaceutical compound content of municipal solid waste: *Journal of Hazardous Materials*, 162(2-3): 730-735.

World Bank. 1997. Industrial Pollution in Bangladesh. A Detailed Analysis: *Workshop Discussion Paper*, The World Bank Dhaka Office 1997.

KEYNOTE SPEECH 1

Title of the Speech: **"**Design, Construction and Maintenance of Bridges in Bangladesh: Past, Present and Future"

by Prof. Dr. A.F.M. Saiful Amin, Department of Civil Engineering, BUET

Abstract of the Talk

Bridges are the life lines of not only a country but a region. Owning a resilient bridge infrastructure for the Asian region considering its location, geomorphological conditions and climatic variations is important for future growth of transportation network. To this end, the paper takes a note of the construction of a few land mark bridges that took place between 1870 to present. The major engineering aspects and the performances are discussed in a broader sense. Finally, the paper presents an outlook identifying the gaps in understanding for achieving an efficient design with the present know-how available elsewhere in the world. The necessity of maintenance aspects are also discussed in short.

Biography of the Speaker: Prof. Dr. A.F.M. Saiful Amin

Professor, Dept. of Civil Engineering, Bangladesh University of Engineering and Technology

Dr. A.F.M. Saiful Amin has been in the field of Civil Engineering since graduating from Bangladesh University of Engineering and Technology (BUET) in 1996. He then earned his Master of Science degree from his Alma Mater in 1998. After being awarded a scholarship in 1998 from the Japanese Government, Dr. Amin completed his PhD in 2001 at Saitama University. He is currently a Professor within the Civil Engineering department at BUET, and has been a Visiting Professor at the University of Federal Armed Forces (Munich, Germany), and the University of Kassel (Germany).

Dr. Amin has been actively contributing to this field in many disciplines over the past two decades including structural engineering with the use of finite element methods and strain theories, cement chemistry, forensic engineering, as well as experimental, structural, and continuum mechanics. His realm of expertise also includes thermodynamics, thermo-physics, and modeling nonlinear material behavior under large deformation.

KEYNOTE SPEECH 2

Title of the Speech: **"**Environmental Disaster from Fecal Sludge: Critical Issues and Way Forward**"**
by Prof. Dr. M. Ashraf Ali, Department of Civil Engineering, BUET

Summary of the Talk

Over the last decades Bangladesh has achieved commendable success in sanitation coverage through usage of onsite sanitation facilities (pit/ pour-flush latrines and septic tanks). Bangladesh has been able to reduce the prevalence of open defecation from 34% in 1990 to 1% in 2015. However, on-site sanitation facilities have been developed in the country without any consideration to the management of "fecal sludge" that accumulates in these facilities (i.e., in pits/septic tanks).

On-site sanitation is prevalent throughout the country, except for a small portion in Dhaka city that is covered by sewerage system. However, in the absence of proper monitoring by competent authorities, onsite sanitation systems have been developed very poorly in all urban areas of Bangladesh. In many urban areas septic tanks are altogether absent, and toilet wastewater is directly discharged into storm drains/sewers. In some cases, there are septic tanks but the soakage pitsare absent. Throughout the country, septic tanks are poorly designed, constructed and maintained, and there is no code/ guideline for design of pit/pour-flush latrines. Due to lack of effective pit emptying services, pit latrines in high density urban slums are being constructed without "pits", and fecal matters from toilets are flushed out into open environment (drains/water bodies). Pit/septic tank emptying is typically carried out manually by traditional pit emptiers (often referred to as "sweepers") without any protective gears, which exposes them to significant health and safety risks. In the absence of treatment/ disposal facilities, the emptied fecal matter is disposed into public sewers/ drains, water bodies and low-lands. For example, 79% of Dhaka city is covered by on-site facilities, and almost the entire fecal sludge from these facilities are discharged into nearby residential environment, drainage system or water bodies. Only 1% of the population could avail "safe emptying" services, but this emptied sludge is again discharged into the open environment. The situation is similar or even worse in most other major cities as well as secondary towns. This is causing severe pollution of the environment on a daily basis, particularly affecting the water bodies within and around cities and town – and should be characterized as a major "environmental disaster".

Globally, on-site sanitation system is no longer considered as a "temporary" system; in fact, with effective fecal sludge management (FSM) service (involving collection, transportation and treatment/disposal of fecal sludge), on-site sanitation systems could serve as long-term and sustainable sanitation solution. In fact, with support from development partners and I/NGOs, limited FSM services are becoming available in some urban centers. However, there is a lack of awareness among City Development Authorities, City Corporations, Paurashavas and real estate developers about the importance of FSM.A root cause for lack of fecal sludge management (FSM) services is that there is no clear assignment of responsibilities with regard to FSM among

the utility service providers (e.g., WASAs), Local Government Institutions (LGIs), and City Development Authorities in large cities. Recently, under the initiative of Local Government Division, MoLGRD&C, an "institutional and regulatory framework for fecal sludge management (FSM) in Bangladesh" has been drafted. It is expected that the framework would pave the way for introduction of effective FSM services throughout the country, and save the country from the environmental disaster from fecal sludge.

Biography of the Speaker: Dr. M. Ashraf Ali

Professor, Dept. of Civil Engineering, Bangladesh University of Engineering and Technology

Dr. Muhammad Ashraf Ali is a Professor in the Department of Civil Engineering at Bangladesh University of Engineering and Technology (BUET).Currently, he is also serving as the Director of the International Training Network Center of BUET (ITN-BUET). He received his Ph.D. degree in Civil and Environmental Engineering from Carnegie Mellon University, Pittsburgh, Pennsylvania, USA in 1994; he received his M.S. degree from the same university in 1991. He received his B.Sc. degree in Civil Engineering from Bangladesh University of Engineering and Technology (BUET) in 1988.

His research interests include arsenic contamination of groundwater, surface water pollution, sanitation, and environmental impact assessment. He has been involved with a number of major research initiatives on arsenic contamination of groundwater with the Massachusetts Institute of Technology (MIT)-USA, EAWAG-Switzerland, and the United Nations University-Tokyo. These research works have resulted in a series of publications in well-renowned journals, including Science and Nature Geoscience. He has been actively pursuing research works, and so far 35 students have completed their post-graduate degrees (Master's and Ph.D.) under his supervision. He is currently working with the Ministry of Local Government, Rural Development and Cooperatives on fecal sludge management. He has also been involved with a number of major development projects in the country, including the Hatirjheel project, Dhaka Elevated Expressway Project, and development of National Action Plan for Reduction of Short Lived Climate Pollutants.

KEYNOTE SPEECH 3

Title of the Speech: **"**Earthquake Related Research and Activities in Bangladesh during the Last Two Decades**"**

by Prof. Dr. Mehedi Ahmed Ansary, Department of Civil Engineering, BUET

Abstract of the Talk

In this keynote speech, a brief summary of the activities and researches undertaken in the field of earthquake engineering in Bangladesh for the last twenty years have been presented. Also description of completed and current BUET researches is briefly discussed. Currently, BUET, CUET, DU, Bangladesh Earthquake Society (BES), CDMP and some government and non-government organizations, and media are playing a major role in earthquake risk mitigation efforts. Still Bangladesh needs to go a long way to achieve a satisfactory level of earthquake disaster mitigation. Some general recommendations are also provided to meet this objective.

Biography of the Speaker: Dr. Mehedi Ahmed Ansary

Professor, Dept. of Civil Engineering, Bangladesh University of Engineering and Technology

Prof. Dr. Mehedi Ahmed Ansary graduated from the Department of Civil Engineering, BUET in 1991 and joined at the same Department as a Lecturer in June 1991. He obtained his PhD in Civil Engineering from the University of Tokyo in 1996. He was promoted as a Professor in the Department of Civil Engineering, BUET in 2006. His research interest is urban disaster mitigation which includes development of microzonation maps for cities of Bangladesh, assessment of building and lifeline vulnerabilities, characterization of strong ground motion from free-field and bridge data monitoring, raising awareness among citizens of Bangladesh through simplified experimental techniques and easily understandable guidelines for earthquake resistant construction, study of other urban disasters such as cyclones, floods, fires and tornadoes, etc. Prof. Ansary is the founder Director of BUET-JIDPUS (Japan Institute of Disaster Prevention and Urban Safety) Institute at BUET. Dr. Ansary is also the founder Secretary General of Bangladesh Earthquake Society. Prof. Ansary is a Director of World Seismic Safety Initiative (WSSI) which is a prestigious international body founded by International Association of Earthquake Engineering IAEE) for earthquake risk reduction of the developing countries. Prof. Ansary is also a member of the Technical Advisory Committee on Disaster Management of the Government of Bangladesh. Prof. Ansary's number of publication in International Journal and Proceedings is around 180.

KEYNOTE SPEECH 4

Title of the Speech: **"**Disaster Risk Reduction in Bangladesh Delta Plan 2100**"**

by Mr. Giasudding Choudhury, Deputy Team Leader, BanDuDeltAS, Bangladesh Delta Plan 2100

Abstract of the Talk

Bangladesh is a disaster-prone country consisting of an area of 147,570 km^2 with a population of about 150 million according to population census in 2011. The country becomes the worst victim of natural calamities causing colossal loss of lives and properties.

Out of many disasters such as floods, cyclones, droughts, river bank and coastal erosion, arsenic contamination in ground water, salinity intrusion and earthquakes etc. the frequency of cyclones and floods are more severe and recurrent. Bangladesh is a global hotspot for tropical cyclones. The floods of 1988, 1998 and 2004 were particularly catastrophic, resulting in large-scale destruction and loss of lives. Estimated that about 5% of the total floodplain of Bangladesh is directly affected by river bank erosion.

The complexity of the Bangladesh delta specially the disaster management necessitates a plan that can adapt to change—a Bangladesh Delta Plan 2100. A long-term, holistic and integrated plan for the Bangladesh delta. Long-term, considering goals for the next fifty to one-hundred years.The problems related to disaster management are numerous, complicated and challenging. The poor are typically worst affected due to water related disasters as they tend to live in vulnerable areas, have least capacity to deal with loss of income and assets, and have limited access to risk sharing mechanisms. As IPCC 5th Assessment report highlights, with a climate change and variability, the frequency and intensity of natural hazards will only increase in future.

Efforts to effectively resolve the disaster management problems require a clear vision of the future conditions and demand new ways of thinking, developing and implementing disaster management programmes and practices. Long-term challenge is the success of paradigm shift from relief and rehabilitation to disaster risk reduction at every step, which largely depends on plan and action of other development ministries and implementing agencies. The magnitude and potential impacts of hazards are likely to be shaped by various external drivers of change including trans-boundary flow, population growth, landuse change, climate change, socioeconomic development and change in governance and institutions. In order to operate an effective and efficient disaster management in the country, establishing a regulatory framework is a must. Bangladesh has now established a structured regulatory framework that provides legal, policy and best practice documents in which the necessary initiatives and activities relating to Disaster Risk Reduction (DRR) and Emergency Response Management (ERM) are managed and implemented.

The long term strategy is to develop new knowledge and tools required for Early Warning of Storm Surge Inundation for the Coastal community of Bangladesh and prepare inundation maps

for pre, during and post disaster management programme. The key activities of the project are: cyclone formation and tracking forecasting, meteorological observation system, hydrological observation system, updating and upgrading of existing cyclone and storm surge model, cyclone and storm surge inundation forecasting in the flood plain at community level, safety of coastal embankments and communities, warning dissemination, and capacity building and technology transfer.

Biography of the Speaker: Mr. Giasuddin Ahmed Choudhury

Giasuddin Choudhury, Deputy Team Leader, BanDuDeltAS, BDP 2100

Mr. Giasuddin Ahmed Choudhury, P.Eng, Deputy Team Leader, Bangladesh Delta Plan (BDP) 2100, is involved in the BDP 2100 Formulation Project since its inception in March 2014. Prior to joining BDP 2100, he held the position of Executive Director of the Center for Environmental and Geographic Information Services (CEGIS) for 8 years after retiring from Bangladesh Water Development Board (BWDB) as an Additional Director General in 2004.

During his career in BWDB, since the 1970s, he was involved with planning, design and implementation of many irrigation, flood control and drainage projects namely; G K Project, Chandpur Irrigation Project, Dutch-aided Early Implementation Projects, Teesta Barrage Project, etc. He had also served as Project Director, Water Management Improvement Project. He conducted feasibility studies for River Bank Protection Project and Gorai River Restoration Project.

He was also appointed by the Government of Bangladesh as a Member of the Indo-Bangladesh Joint Rivers Commission, Bangladesh, where he served for three years (2009 till 2012) and also as the Member of the Executive Committee of Bangladesh Haor and Wetland Development Board till 2012.

He served as a Member of the Executive Committee of Bangladesh Water Partnership of GWP for 15 years. For sometimes he also acted as Regional Coordinator of the Climate Change Initiative of South-Asia Global Water Partnership (SAS-GWP). Presently he holds the position of Regional Member of South Asia Global Partnership.

During his long career, he also served as the Director General of the Water Resources Planning Organization (WARPO), where he was involved in the formulation of the National Water Management Plan, and as the Director General of Bangladesh Haor and Wetland Development Board (BHWDB).

Mr. Choudhury is a graduate in Civil Engineering from the Bangladesh University of Engineering and Technology (BUET) and a Master of Hydraulic Engineering from IHE, Delft, The Netherlands. He has also received extensive local and international training in water resources development and management.

During his tenure in CEGIS, he was involved in the preparation of the Master Plan of Haor Areas and the Agricultural Master Plan for Southern Bangladesh. There are various publications by Mr.

Choudhury on planning and management of the water resources of Bangladesh. Along with being a Fellow of the Institution of Engineers, Bangladesh, he has membership in various Professional Bodies, i.e. the Bangladesh Association of Advancement of Science, the Asiatic Society of Bangladesh. He was a representative in the Bangladesh delegation attending COP 15 in Copenhagen, Denmark, COP 16 in Cancun, Mexico and COP 17 in Durban, South Africa.

Mr. Choudhury is now involved in the preparation of a long term (50-100 years), holistic (integrating various sectors and plans) and adaptive (using various scenarios and tools to prepare for the future) plan for the whole Bangladesh Delta, The Bangladesh Delta Plan 2100, which is led by the General Economics Division of the Planning Commission of Bangladesh and supported by the Embassy of the Kingdom of the Netherlands. Under his guidance 19 Thematic Baseline Studies have been conducted to ensure a holistic resource management approach in future planning. The BDP 2100 is also teaming up with The World Bank to prepare a prioritized list of investments, or the Investment Plan, for the short, medium and long term. The BDP 2100 Project has thus far successfully integrated itself into the upcoming national 7th Five Year Plan and is seen as a paradigm shift in project planning and design.